Innate lymphoid-macrophage crosstalk promotes lung cancer regression in response to IL-12 therapy

Jake Yarren Henry

October 29, 2019

University College London

Cancer Institute, Research Department of Haematology

PhD Supervisors : Professor Sergio A. Quezada, Professor Karl S. Peggs

A thesis submitted for the degree of Doctor of Philosophy

Declaration:

I, Jake Yarren Henry confirm that the work presented in this thesis is my own. Where information has been derived from other sources, I confirm that this has been indicated in the thesis.

Jake Yarren Henry

Abstract

The ability of IL-12 to affect both innate and adaptive immunity positions this cytokine as a promising candidate to overcome the immunosuppressive microenvironment within tumours. Despite its potent activity in experimental models, the clinical use of IL 12 has been thwarted by its reported toxicity in human trials. Intranasal administration of an IL-12-coding lentivirus efficiently transduced alveolar macrophages in tumour-bearing mice, restricting IL-12 expression to the lung parenchyma and promoting rejection of established lung metastases. IL-12 stimulated IFNγ production by innate lymphoid cells (ILC), inducing the activation of interstitial macrophages, whose presence was essential for tumour eradication. These data demonstrates the potent anti tumour activity of local lentiviral IL-12 therapy against metastatic disease in the lung and the critical role played by the innate crosstalk established between ILCs and tissue resident phagocytes within the lung microenvironment.

Impact Statement

Research at the UCL Cancer Institute has produced promising results using immunotherapy to treat lung cancer. Lung cancer is the most common type of cancer worldwide and, in many countries, is the leading cause of cancer associated mortality. In 2012, 1.82 million new cases of lung cancer were diagnosed and was attributed to approximately 1.6 million deaths and a recently concluded 10 year analysis of European lung cancer statistics found poor survival rates of 13% at 5 years from diagnosis.

350,000 cases of melanoma, a type of skin cancer, was diagnosed globally in 2015 and was responsible for 60,000 deaths. Most prevalent in Australia and New Zealand, the incidence of melanoma in the UK has more than doubled since the 1990's. Stage IV melanoma metastasises to major organs including the lungs with an expected 15-20% survival at 5 years.

Under the direction of professors Sergio Quezada and Karl Peggs, a research group at the UCL Cancer Institute have generated pre-clinical data that demonstrates an immune therapy to treat lung cancer. A single dose of this gene therapy is inhaled by the subject and delivers a potent immune activating agent directly to the affected lung. Murine studies have doubled median survival times and increased 100-day survival from 0% to 14% with less than 10% of treated subjects suffering lung disease related mortality. An analysis of the immune system in treated subjects have revealed a complex mechanism of immune activation that has advanced our knowledge of immuno-oncology and may guide the development of novel lung cancer therapies.

Contents

List of Figures

List of Tables

Abbreviations:

Abbreviation	Full name	Abbreviation	Full name
AAV	Adeno-associated virus	ACT	adoptive cellular therapy
Ad	Adenovirus	ADCC	Antibody directed cell cytotoxicity
ADCP	Antibody directed cellular phagocytosis	ANOVA	Analysis of variance
APC	Antigen presenting cell	B-1	Ly-1 B cell
B-2	conventional B cell	BAL	Bronchoalveolar lavage
BCR	B cell receptor	CC	chemokine
CCL2	Chemokine (c-c motif) ligand 2	CCR2	C-C chemokine receptor type 2
CD4eff	CD4+ Effector T Helper cell	cDC1	type 1 conventional dendritic cell
cDC2	type 2 conventional dendritic cell	cDNA	Complementary DNA
CFSE	Carboxyfluorescein succinimidyl ester	CLMF	Cytotoxic Lymphocyte Maturation Factor
CLP	Common lymphoid progenitor	CMP	common myeloid progenitor
CTL	cytotoxic T lymphocyte	CTLA-4	Cytotoxic T-lymphocyte associated antigen 4
DAMP	Damage-associated molecular pattern	DC	Dendritic Cell
DNA	Deoxyribonucleic acid	eGFP	Enhanced Green Fluorescent Protein
Fab	Fragment antigen-binding	FACS	Fluorescence-activated cell sorting
FBS	Fetal bovine serum	Fc	Fragment crystallizable region
FDC	follicular dendritic cell	FFPE	Formalin-fixed paraffin-embedded
Fluc	firefly luciferase	FO B cell	follicular B cell

Abbreviation	Full name	Abbreviation	Full name
FSC	Forward scatter	GATA 3	GATA binding protein 3
GzmB	Granzyme B	HBSS	Hanks Buffered Saline Solution
HIV-1	Human immunodeficiency virus-1	I.N	Intranasal
I.P	Intraperitoneal	I.V	Intravenous
ICOS	Inducible T Cell Costimulator	IFN	interferon
IFNγ	Interferon gamma	Ig	immunoglobulin
IgA	immunoglobulin A	IgG	immunoglobulin G
IgM	immunoglobulin M	IL-	Interleukin
IL-12	Interleukin 12	IL-12R	Interleukin 12 receptor
ILC	Innate lymphoid cell	IMDM	Iscove's modified dulbecco's medium
iNOS	Inducible nitric oxide synthase	IRF	Interferon regulatory factor
JAK2	Janus Kinase 2	KPB6	Kras/P53 mutant lung derived tumour cell line
LB	Lysogeny broth	LTi	Lymphoid tissue initiator cell
LV	Lentivirus	Mϑ	Macrophage
M1	Classically activated macrophage	M2	Alternatively activated macrophage
MAPK	Mitogen-Activated Protein Kinase	MDSC	Myeloid derived suppressor cell
MFI	Mean fluorescent intensity	MHC	Major Histocompatibility Complex
MIIG	Macrophage Insensitive to Interferon Gamma	Mo	Monocyte
NCR	Natural cytotoxicity triggering receptor	NK	Natural Killer cell
NO	Nitric oxide	NS	Not significant

Abbreviation	Full name	Abbreviation	Full name
PAMP	Pathogen-associated molecular pattern	PBS	Phosphate-buffered saline
PCR	Polymerase chain reaction	PD-1	Programmed cell death protein 1
pDC	plasmacytoid dendritic cell	PMN	polymorphonuclear
PRRs	pattern recognition receptors	RAG	Recombination-activating gene
RCF	Relative centrifugal force	RFP	Red fluorescent protein
RNA	Ribonucleic acid	ROR	receptor-related orphan receptor
SFV	Semliki forest virus	SIRPa	signal-regulatory protein alpha
SSC	Side scatter	STAT	Signal Transducer And Activator Of Transcription
T-bet	T-box transcription factor TBX21	TCR	T cell receptor
Tfh	T follicular helper cell	Th	T helper cell
TLR	toll-like receptor	TME	tumour microenvironment
TNF	rumour necrosis factor	TNFα	Tumour necrosis factor alpha
Treg	T regulatory cell	TYK2	Tyrosine Kinase 2
UMAP	Uniform Manifold Approximation and Projection	V(D)J	Variable, Diversity, Joining gene segments

1 Introduction

1.1 The Immune System

The Immune System is a biological network composed of many cell populations that cover a multitude of processes and activities. This network works to protect an organism against diseases arising from foreign pathogens, physiological pathologies and cancer whilst maintaining tolerance for normal tissue. The immune system can be sub-classified into two cooperative compartments known as innate and adaptive immunity.

1.1.1 Innate Immunity

The defining hallmark of the innate immune system is a rapid response to injury or infection, and is considered the host's first line of defense. A disadvantage of this rapid response is an inability to develop specific antigen recognition receptors (such as TCR and BCR) and thus are unable to form immunological memory for previously encountered antigen. Innate cells however are able to sense damage-associated molecular patterns (DAMPs) via expression of a variety of receptors including Toll-like receptors (TLR). Innate cells can also sense exogenous pathogens by pathogen-associated molecular patterns (PAMPs) interaction with expressed pattern recognition receptors (PRRs) [119].

The innate immune system can be sub-categorised into three groups: physical barriers, complement and innate leukocytes. Physical barriers include skin epithelia [277], the blood-brain barrier [197] and mucosal tissues of the gastrointestinal tract, respiratory system, and nasopharynx [65]. As the name suggests, these barriers physically exclude the bulk of pathogens encountered on a daily basis. The complement system is an array of proteins found in blood sera that work together as a biochemical cascade that can recruit leukocytes such as macrophages and neutrophils, direct phagocytosis by antigen opsonisation and form protein complexes that can directed rupture bacterial cell walls [237].

Innate Leukocytes

The majority of innate leukocytes differentiate from common myeloid progenitor (CMP) cells [157]. Innate leukocytes include polymorphonuclear (PMN) granulocytes such as basophils, neutrophils and mast cells and mononuclear cells such as monocytes (Mo), dendritic (DC) cells and macrophages (MΦ) [105]. Granulocyte-derived leukocytes produce cytotoxic agents including cytolytic enzymes, low pH vesicles, reactive nitrogen and reactive oxygen species. These

cytotoxic agents are stored in intracellular granules, and de-granulate upon activation in close proximity to a target pathogen [78].

DC and macrophages are able to engulf pathogens (such as bacteria or virally infected cells), break them down and present pathogen related antigens as a part of the Major Histocompatibility Complex (MHC) to antigen specific components of the adaptive immune system. This process is known as antigen presentation and all cells that can present antigen in such a manner are known as antigen-presenting cells (APC) [77].

In addition to their phagocytic and antigen presentation functions, DC and macrophages are capable of secreting immunomodulatory proteins called cytokines. The cytokine family of proteins include chemokines (CC), interferons (IFN), tumour necrosis factors (TNF), lymphokines and interleukins (of which IL-12 is a member). These proteins are mediators of inflammation and can direct a pro-inflammatory response (eg. IL-1, TNFα, IFNγ and IL-12) or an anti-inflammatory response (eg. IL-4, IL-6, IL-10, TGFβ) [50].

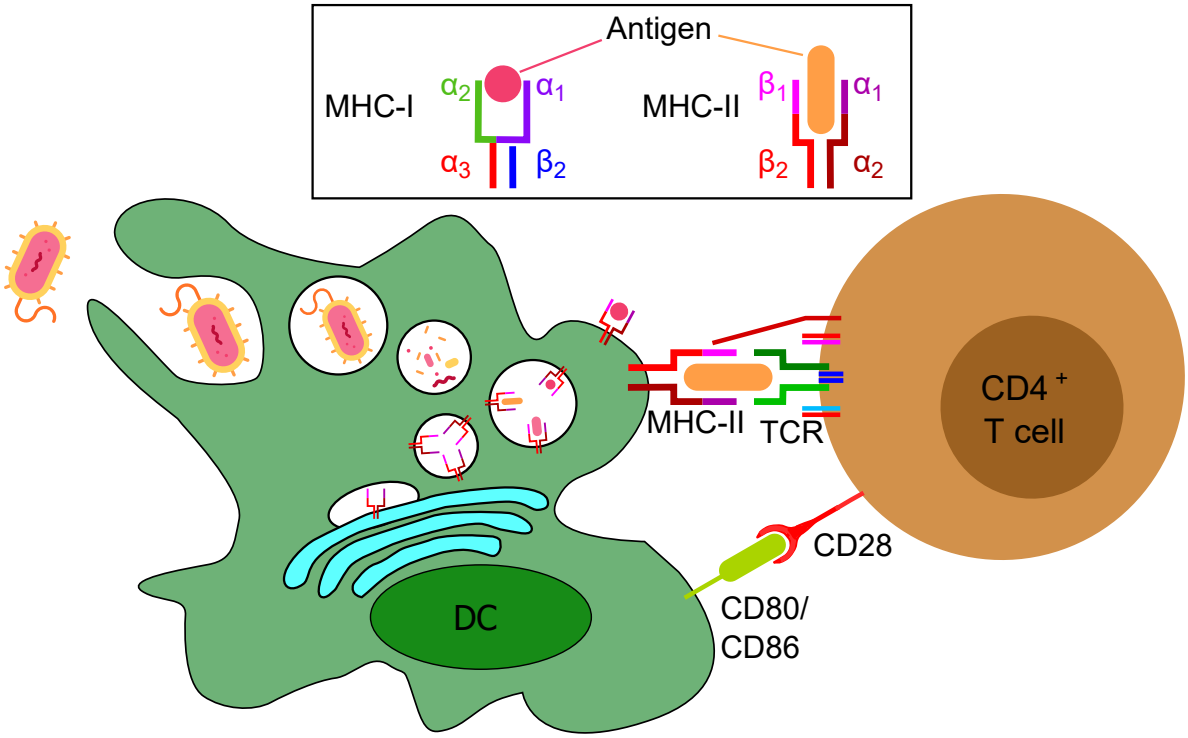

Figure 1: Antigen presentation

Dendritic Cells

Dendritic cells are professional APCs whose purpose is to present antigen to adaptive leukocytes (priming of T cells & B cells) with co-stimulatory ligands (such as CD80, CD86 and 41BB-L) thus mediating a crucial role in the activation of the adaptive immune compartment. DC are commonly found at barrier sites and in the blood, they mature when antigen is encountered and migrate to lymph nodes where T & B cell activation occurs.

There are 3 prevalent sub-populations of dendritic cell: Type 1 conventional DC (cDC1), Type 2 conventional DC (cDC2) and plasmacytoid DC (pDC) [93]. cDC1 (also known as $CD103^+$ DC) are characterised by their primary role sensing viral infection [213] and by cross-presentation of MHC-I associated antigen to $CD8^+$ T cells [91, 217]. They promote natural killer (NK) and type 1 T helper (Th1) responses by expression of Th1 associated cytokines, IL-12 and type III interferons (IFN-λ) [128]. cDC2 (also known as $CD11b^+$ DC) Induce Th1 [131] Th2 [73] and Th17 [190] responses by presentation of MHC-II associated antigen to $CD4^+$ T cells [131]. Plasmacytoid DC (pDC) are a specialised DC subset that respond to viral infection. They detect viral ssRNA / dsDNA by expression of the pattern recognition receptors TLR7 & TLR9. Upon activation, pDC are characterised by high expression of type I interferons (mainly IFNα and IFNβ)

Macrophages

Like DC, macrophages are efficient phagocytes. Capable of engulfing and digesting pathogens, macrophages play a secondary role in priming T cells and B cells with presented antigen [20]. Phagocytic activity of this population is for the purposes of pathogen clearance and removal of necrotic (or apoptotic) cells and cellular debris.

Macrophages were historically thought to differentiate from haematopoeitic stem cells (HSC) via macrophage DC precursors (MDPs) [64] as part of the classically defined mononuclear phagocyte system (MPS) [246]. However, more recent studies using fluorescent reporter lineage mice have shown that many tissue resident macrophages are also derived from embryonic erythromyeloid progenitors (EMP) found in the egg yolk sac and HSC from fetal liver [80]. These fully differentiated resident macrophages have stem-like properties and are capable of self-renewal. Macrophages derived from EMP, fetal liver HSC or adult bone marrow HSC are driven by the PU.1 transcription factor [214] whilst relying upon maturation by macrophage colony-stimulating factor (M-CSF) stimulation.

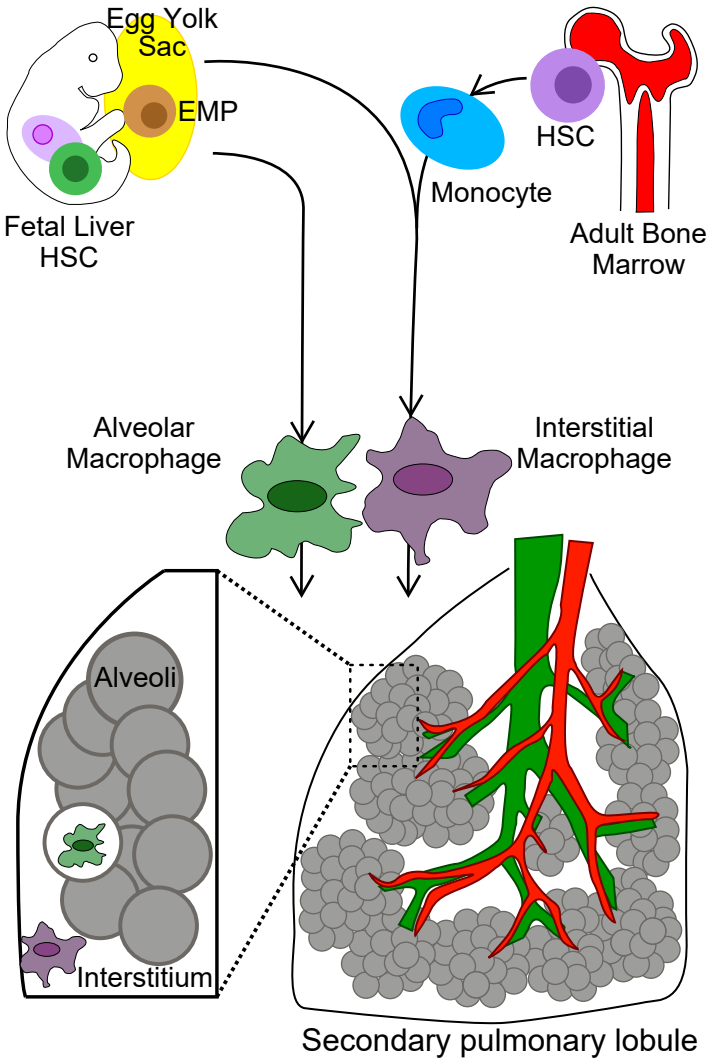

Figure 2: Origins and distribution of pulmonary macrophages

Two distinct pulmonary tissue resident macrophages have been described. Alveolar macrophages (AM) are EMP derived phagocytes that patrol the interior surfaces of pulmonary alveoli where they phagocytose debris and pathogenic organisms. Cytometric analysis characterises murine AM by the co-expression of SiglecF, MHC-II, MerTK, CD64 and f4/80 whilst they lack expression of CD11b, Ly6C, CX3CR1 and CCR2 (the receptor of CCL2, an effective chemotactic chemokine) [215].

Originally thought the be AM pre-cursors, interstitial macrophages (IM) have recently surfaced as a second distinct population of tissue-resident macrophages that originate from EMP / Fetal HSC and may be replenished from $CCR2^{+}$ circulating monocytes-derived macrophages [215]. These macrophages are found in the pulmonary interstitial tissues (including circulatory and pulmonary connective tissues external to alveoli) and play a primary role in pulmonary homeostasis and inflammation. FACS analysis of murine IM has demonstrated a phenotype that is different to AM in the co-expression of CD11b, MHC-II, CX3CR1, f4/80, MerTK

and a mixed expression of CCR2 (possibly reflecting the mixed nature of their lineage) with a notable lack of SiglecF and Ly6C expression.

Tumour-associated macrophages

Tumour-associate macrophages (TAMs) are an abundant population of leukocytes found in most solid tumours [155].

Functionally, TAMs have been shown to be an essential mediator of metastatic tumour cell extravasion [199] and support tumour cell intravasation in the MMTV-PyMT cancer model via an EGF/CSF-1 paracrine loop between tumour cells and TAMs [271]. Analysis of many primary human tumour samples have shown high expression of CSF-1 [138] and CCL2 [244] which correlate with poor prognosis. These cytokines promote macrophage recruitment, differentiation and proliferation. Concurrent expression of TGF-β [84] and IL-6 [167] in the tumour microenvironment exerts immunosuppressive pressure on T cells, NK cells and ensures recruited macrophages adopt immunosuppressive functions whilst eschewing phagocytic or antigen presentation functions associated with normal macrophage function. TAMs have been observed congregating in avascular tumour regions [130] and promoting tumour angiogenesis via secretion of angiogenic factors such as VEGF [134]. TAMs also support tumour progression by expression of ECM remodelling proteases such as MMP-9 [261] and tumour growth by expression proteins such as fibroblast growth factor (FGF) and epidermal growth factor (EGF) [248].

Like other tissue resident macrophages, TAMs may differentiate from HSC derived monocytes [45, 66] or may arise as self-replenishing cells derived from embryonic and fetal progenitors [82]. The mixed ontology of TAMs found in the lung tumour microenvironment resembles that of macrophages found in healthy lung tissues where a recent study in fate-mapping CX3CR1$^{EGFP/+}$ MacBlue mice revealed that EMP derived CCR2^{-}Ly6C^{-} interstitial macrophages seed the lungs and proliferate as the major component of TAM during early tumourigenesis. They are then largely supplanted by CCR2^{+}Ly6C^{high} monocyte derived TAMs as the tumour progresses [149].

TAM immunotherapy

Given their immunosuppressive function in the tumour microenvironment, several trials have focused on depleting TAM where CSF1R inhibition [189] or blockade [177] was combined with PD-1 blockade and the use of CCR2 blockade to reduce recruitment of HSC derived circulating macrophages into the tumour microenvironment [185].

A second approach involves the inhibition of pro-tumoural TAM function by the TGFβ neutralisation [234], Class IIa histone deacetylase (HDAC) inhibition [92] (including HDAC4, a molecule involved in TGFβ signaling [81]) and PI3Kγ inhibition [62].

A third approach promotes anti-tumoural TAM activity by CD40 signaling (application of CD40 agonists or CD40L expressing cells [44]) or release of type I IFN (by application of TLR agonists [109] or activation of the STING pathway [90]). These trials are summarised in a table adapted from Bercovici *et al* [19] (table 2).

Recent studies have indicated that effective control of tumour growth may be dependent upon the interaction of TAM with tumour infiltrating lymphocytes (TIL) wherein depletion of STING activated TAM negatively impacts $CD8^+$ T cell accumulation in the tumour [264] and T cell derived IFNγ was a crucial determinant in NO mediated tumouricidal TAM activity [169].

NO is synthesised by three isoforms of nitric oxide synthase (NOS) where neuronal NOS (nNOS, NOS1) and endothelial NOS (eNOS, NOS3) are responsible for low concentration, calcium dependent NO production and inducible NOS (iNOS, NOS2) generates high levels of NO in a calcium independent manner [5]. The differential expression of NO between NOS1/3 and NOS2 appears to be the deciding factor in the duplicitous role of NO in cancer. Low concentration of NO in the tumour microenvironment promotes tumourigenesis by several mechanisms including modulation of blood flow by regulation of smooth muscle relaxation [140], promotion of cellular proliferation [71] and disruption of apoptotic processes [129].

By contrast, iNOS expression is induced in macrophages by IFNγ signaling and the resultant high expression of NO promotes tumouricidal apoptosis [26]. As a master regulator of tumouricidal macrophage function, IFNγ activated macrophages perform cytotoxic functions via expression of TNFα [282] and antibody directed phagocytosis [23] in addition to NO induced apoptosis.

Macrophage/TIL targets	Clinical phase	Indications	Clinical trial number
Depletion of pro-tumoural TAM			
αCCR2, αCCR5, αPD-1	Phase I	Solid tumours	NCT03184870
αCSF1R, αPD-1	Phase I	Solid tumours	NCT02526017
αCSF1R, αPD-L1	Phase I	Solid tumours	NCT03238027
αCSF1R, αPD-L1	Phase I/II	Solid tumours	NCT02323191
Inhibition of pro-tumoural TAM activity			
αCTLA-4, αPD-L1, OX40L Ig	Phase I	Advanced solid tumours	NCT02705482
αPD-L1, OX40L Ig	Phase I	Recurrent or metastatic solid tumours	NCT02221960
PD1-Fc-OX40L	Phase I	Solid tumours and lymphomas	NCT03894618
TGFbR1 inhibitor, αPD-L1	Phase I	Solid tumours	NCT02937272
TGFbR1 inhibitor, αPD-1	Phase I/II	Solid tumours	NCT02423343
Promotion of anti-tumoural TAM activity			
TLR7/8 agonists, αPD-1	Phase I	Solid tumours	NCT02556463
TLR9, OX40 agonists	Phase I	Solid neoplasms	NCT03831295
TLR4, OX40, ICOS agonists, αPD-1	Phase I	Neoplasms	NCT03447314
STING agonist, αPD-1	Phase I	Solid tumours and lymphomas	NCT03172936
STING agonist, αCTLA-4	Phase I	Solid tumours and lymphomas	NCT02675439
CD40 agonist, αPD-L1	Phase I	Advanced/ metastatic solid tumours	NCT02304393
αCD47, IFN-α2, αPD-1, αPD-L1	Phase I	Solid tumours	NCT02890368
GMCSF, iNEO-Vac-P01	Phase I	Solid tumours	NCT03662815
Ad-IFNγ, TIL adoptive transfer	Phase I/II	Metastatic melanoma	NCT01082887

Table 2: Ongoing clinical trials targeting TAM and TIL in solid tumours. Adapted from Bercovici *et al* [19]

Innate Lymphoid Cells

Recent studies have described a subset of innate cells that, unlike CMP derived innate leukocytes, differentiate from common innate lymphoid progenitor (CILP) cells via fetal liver [272] or bone marrow [274] derived common lymphoid progenitor (CLP) cells [254]. These cells have been classified as Innate Lymphoid Cells (ILC) [225] and include NK cells (owing to their innate function and CLP ancestry).

ILCs express common γ-chain cytokine receptors (IL-2, IL-4, IL-7, IL-9 and IL-21) that are commonly associated with T cell function, however they differ from T cells in that they are *RAG* deficient and as such are unable to generate the T cell receptors (TCR) that confer antigen specificity to all T cells. ILCs are generally thought to display functions that parallel those of the various T helper (Th) subsets [258] and are divided into three classes.

Type 1 ILCs are generally analogous to Th1 cells and are composed of ILC1 and NK cells, they are dependent on the transcription factor T-bet, are IL-12 sensitive and are known to produce IFNγ when stimulated. ILC1 follows a differentiation pathway via CLP, CILP, common helper ILC precursor (CHILP) cells and ILC progenitor (ILCP) cells whereas NK cells are derived from NK progenitor (NKP) cells via CILP [43, 116, 136, 201]. NK cells differ from other ILC by performing functions analogous to cytotoxic $CD8^+$ T cells as well as Th1-analogous functions. NK cells are activated via Ly49, natural cytotoxicity receptors (NCR), Fc-receptors (mediating antibody-dependent cell-mediated cytotoxicity, ADCC) and cytokines (Type 1 IFN, IL-18, IL-15 and IL-12). Upon activation, NK cells directly mediate cytotoxicity by de-granulation of cytotoxic agents (such as granzyme B and perforin) whilst expressing IFNγ and TNFα [255].

Type 2 ILCs (ILC2) are analogous to Th2 cells, they differentiate via the ILCP pathway, are RORα/GATA3 dependent, express IL-7 receptor and secrete IL-4, IL-5 and IL-13 when stimulated.

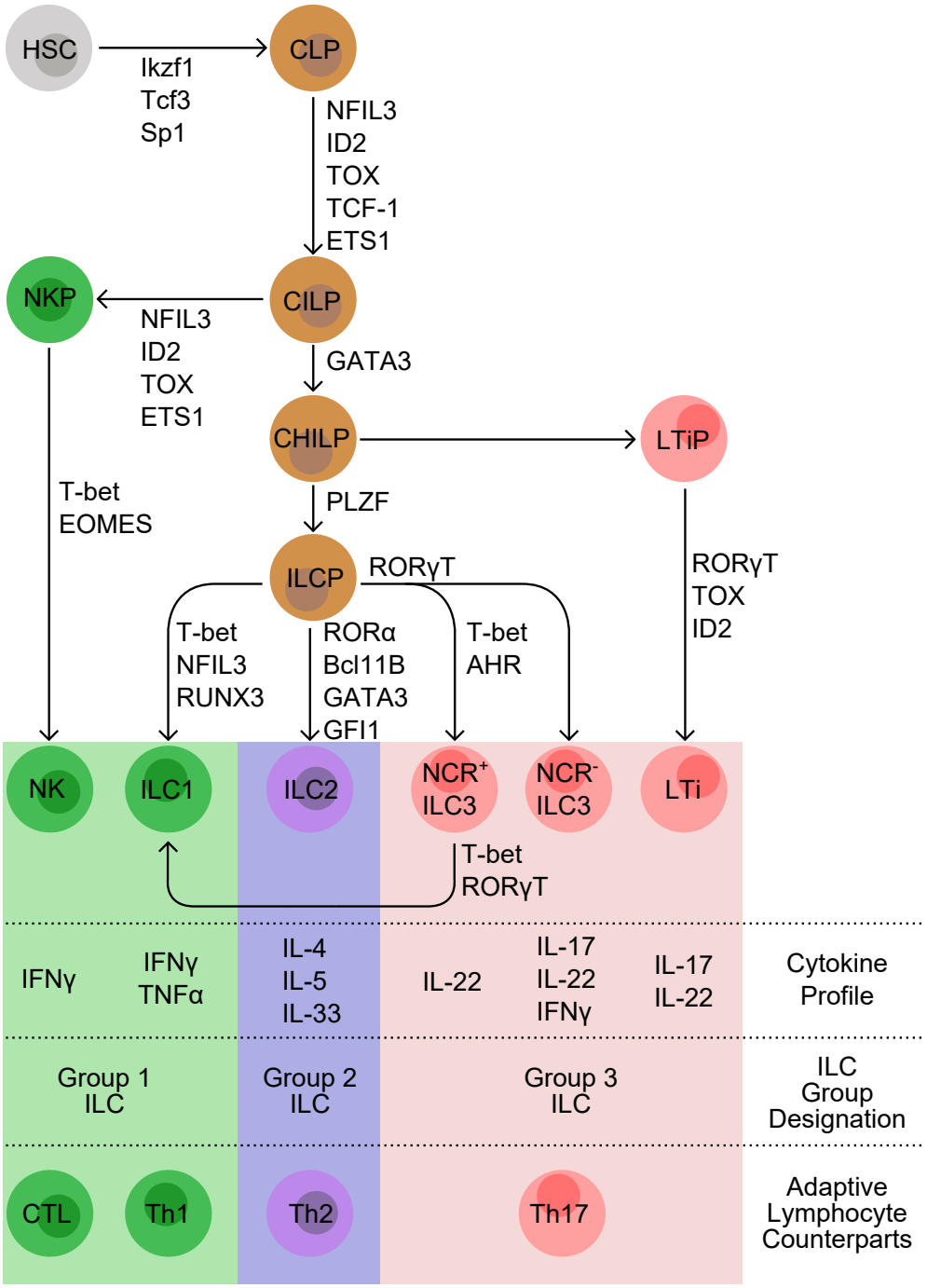

Figure 3: Differentiation and functional schematic diagram of ILC populations A schematic diagram representing the differentiation of ILC populations, important transcriptional elements in their development. ILC are categorised as Group1, 2 and 3 with similarity to T helper subsets. Adapted from Spits *et al* 2013 [225], Walker *et al* 2013 [258] and Vivier *et al* 2018 [254].

Generally characterised as the innate analog to Th17 cells, Type 3 ILCs (ILC3) originate from fetal liver and bone marrow derived CLP. Best described in the context of gut immunity [269], ILC3 cells are predominantly found at mucosal barriers including lung. There are generally considered to be three distinct ILC3

sub-populations: ILCP derived NCR$^+$ILC3, NCR$^-$ILC3 and LTiP derived LTi cells (refer to figure 3) and are defined by expression of the transcriptional element RORγt.

Lymphoid tissue inducer (LTi) cells were the first population of ILC identified (predating ILC nomenclature) [164] and in the context of gut immunity, these cells were found to be required for the development of gut-associated lymphoid tissue (GALT) [59]. Generally found at lymphoid follicle sites including cryptopatches, LTi cells regulate immune responses to infection and disease by release of Th17 associated cytokines such as IL-17 and IL-22.

Following the examples of gut related LTi cells, ILCP derived NCR$^+$ and NCR$^-$ ILC3 cells are predominantly found in the lamina propria region of the small intestine [211] and the colon [269]. Both of these cells are described to express IL-22, IL-17 and IFNγ [209] in response to IL-1, IL-18 and IL-23 activation [281].

IL-22 helps maintain the mucosal barrier where IL-22 and lymphotoxin-α are important in the fucosylation of intestinal epithelia in cooperation with lymphotoxin [85, 191]. IL-17 and IL-22 induce gut epithelial cells to produce anti-microbial peptides (including peptides of the RegII family) [135, 285] and chemokines such as CXCL1 which actively attract neutrophils to sites on infection [4, 180]. These cytokines also play a role in autoimmune pathologies such as crohn's disease [270], psoriasis [32] and asthma [163].

NCR$^+$ILC3 cells have been shown to express IFNγ both independently of IL-12 activation [209] and as a consequence of IL-12 induced T-bet overexpression, RORγt loss and a conversion to an ILC1 phenotype that has been described as ILC plasticity [257] or and 'Ex-ILC3' phenotype [21].

1.1.2 Adaptive Immunity

Considered the host's second line of defense, the adaptive immune system is characterised by its ability to recognise specific antigens and to form immunological memory. When compared to the innate compartment, the adaptive immune system is characteristically slow to respond to an initial exposure to a pathogen. Its ability to recognise antigen and form memory, however, allows the adaptive immune compartment to rapidly mount responses to subsequent exposures with a far greater persistence than the innate compartment.

The adaptive immune system can be broadly classified into two cellular compartments, T cells and B cells, both of which present antigen recognition receptors called T cell receptor (TCR) and B cell receptor (BCR) respectively. These cells are host to a process of genetic recombination called V(D)J recombination and is driven by recombination-activating genes (*RAG*) [53]. This process generates

the TCR/BCR/antibody hyper-variability,that allows them to recognise virtually all possible antigens (akin to a kind of antigenic pattern prediction).

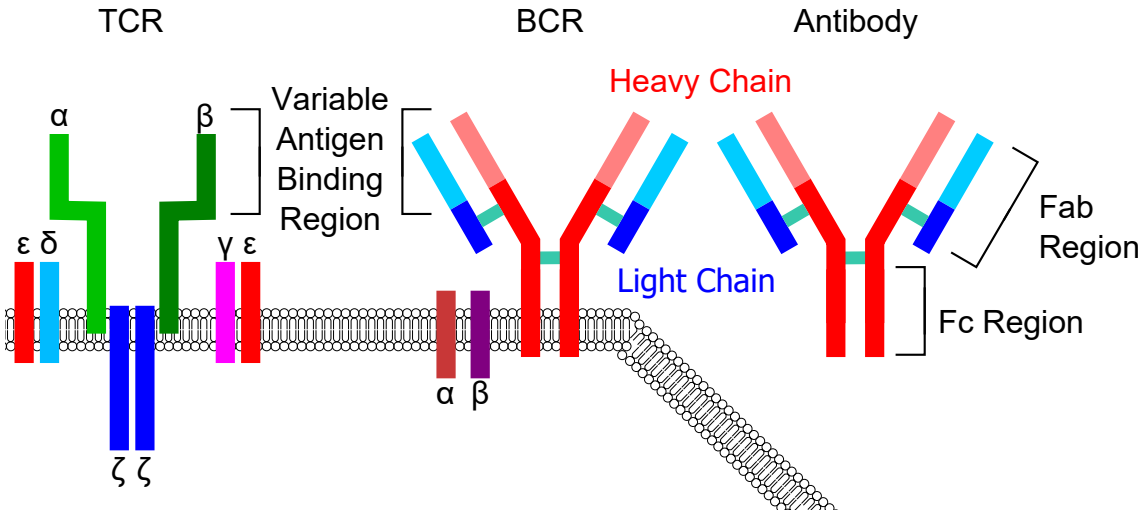

Figure 4: Antigen Receptors

T cells

So called as they mature in the thymus, T cells fall into two major sub-groups, $CD4^+$ T cells and $CD8^+$ T cells. $CD4^+$ T cells can be further categorised into three broad sub-groups, $CD4^+$ T Helper cells (Th, $CD4^+$ effector), $FoxP3^+$ T regulatory cells (Treg) and $CD4^+$ Cytotoxic T Lymphocytes ($CD4^+$ CTL). $CD4^+$ T cells recognise target antigen when presented as part of the Major Histocompatibility Complex II (MHC-II), commonly expressed on the surface of antigen presenting cells such as dendritic cells (DC).

Upon antigen recognition, Th cells generate cytokines that support further immune functions such as B cell maturation, activation of $CD8^+$ Cytotoxic T cells and macrophages. The array of cytokines produced by T helper cells fall into three groups [97, 173]. Type 1 T helper cells (Th1) secrete IL-2, Tumor Necrosis Factor alpha ($TNF\alpha$) and Interferon gamma ($IFN\gamma$). Type 2 Th cells (Th2) express IL-4, IL-5, IL-6, IL-10 and IL-13 upon activation, and T helper 17 (Th17) cells secrete IL-17 when stimulated [16, 208].

$CD8^+$ T cells recognise target cells via antigen expressed as part of the Major Histocompatibility I (MHC-I) complex displayed on all nucleated cells, upon which the $CD8^+$ T cell may destroy target cells via the release of cytolytic molecules Granzyme B (GzmB) and perforin as well as the cytokines $TNF\alpha$ and $IFN\gamma$. For this reason they are commonly referred to as $CD8^+$ Cytotoxic T Lymphocytes ($CD8^+$ CTL) [57].

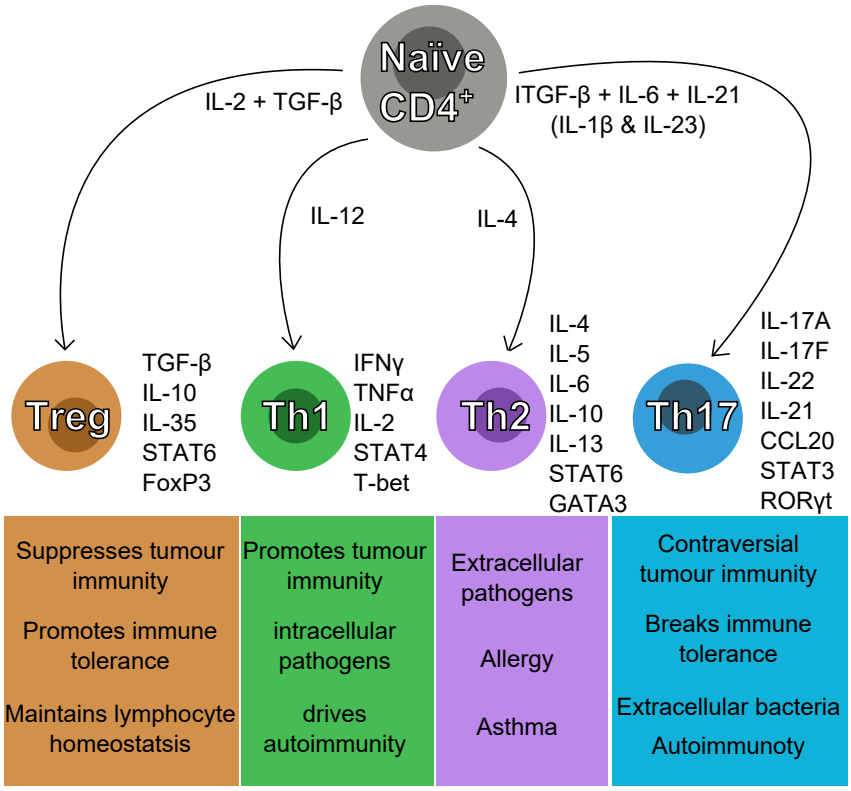

Figure 5: CD4⁺ T helper (Th) cell sub-populations

B cells & Antibodies

B cells mature in bone marrow and generally migrate to secondary lymphoid organs (such as lymph nodes and spleen). Within these lymphoid tissues, B cells form germinal centres where they produce antibodies in response to antigen exposure.

Follicular (FO) B cells (otherwise known as B-2 cells) are the most frequent type of B cell, they migrate to secondary lymphoid organs (eg. lymph nodes) and form lymphoid follicles within germinal centres. Here, FO B cells interact with follicular helper T cells (Tfh) and follicular dendritic cells (FDC) to generate high-affinity antibodies in response to antigen exposure. B-1 cells are predominantly found in the peritoneal and pleural cavities, protect again mucosal pathogens and exhibit T-cell independent activation [184]. Memory B cells circulate throughout the body and lay dormant, they are capable of mounting a rapid secondary antibody response when activated. Plasma cells (otherwise known as Effector B cells) are circulating, non-proliferative B cells with great longevity and produce high quantities of antibody [123].

Also known as immunoglobulins (Ig), antibodies are small proteins that specifically bind to antigen. With a Y-shaped conformation, antibodies are composed of two heavy chains and two light chains bound by di-sulphide bridges. The interaction of heavy and light chains form variable, antigen binding areas known and Fab regions where the opposite (tail end) heavy chains form constant, Fc regions (Figure 4). Antibody units may form complexes that can be monomeric (eg. IgG), dimeric (eg. IgA) and pentameric (IgM) complexes. Functionally, immunoglobulins can mediate pathogen neutralisation by blocking pathogens from interacting with other cells and may trigger a complement cascade activation. Antibodies may agglutinate or precipitate antibody/pathogen complexes for phagocytosis by ADCP, direct ADCC by connecting pathogens with Fc-receptor expressing NK cells.

1.2 Cancer Immunotherapy

For more than 100 years, efforts have been made to harness the cytotoxic capacity of the immune system and direct it not towards foreign pathogens; but to cancerous malignancies arising from the hosts own cells.

An initial milestone over this period include the first cancer vaccine in 1891 by William Coley. During a review of 90 sarcoma cases, Coley identified a single case of spontaneous tumour regression in a sarcoma that had been incompletely excised and subsequently recurred four times. Upon a fifth recurrence, the tumour was partially resected and an accidental *Streptococcus* infection resulted in erysipelas of the surgical area and an acute fever. Within two days of this infection, the remaining tumour spontaneously regressed and the patient was found alive and well seven years thereafter.

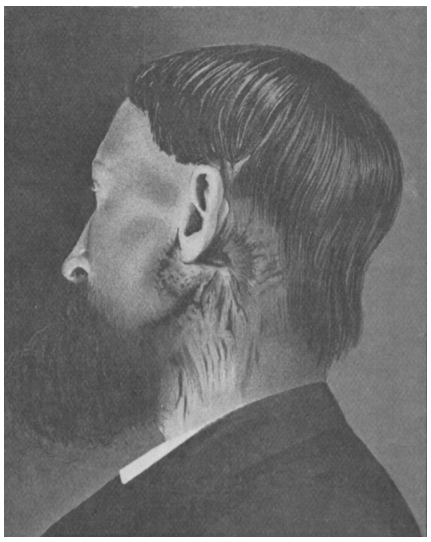

Figure 6: Recurrent round-celled sarcoma. Spontaneous recovery following accidental erysipelas
Photograph taken seven years after cure. From Coley WB [41]

Following a review of this case, Coley then attempted to induce erysipelas in sarcoma patients by inoculation with live *Streptococcus pyogenes* and *Serratia marcescens* that had been cultured from erysipelas patients. Variable results led to the development of Coley's toxins whereby microbial endotoxins were extracted from heat-killed cultures of *Streptococcus pyogenes*, *Serratia marcescens* and *Bacillus prodigiosus* [41]. The use of Coley's toxins in sarcoma patients was met with a modicum of success although complete tumour regression was rarely observed and this therapy eventually fell out of favor as radiation and chemotherapy gained popularity [160].

It was later found that the primary endotoxin responsible for the acute fever associated with Coley's toxin was lipopolysaccharide (LPS) [266]. It is thought that at least part of the efficacy of Coley's toxin may be attributed to this source of LPS which in turn induces IL-12 leading to subsequent activation of cytotoxic NK and T cells [243].

Recent advances in cancer immunotherapy have delivered some major successes in the development of monoclonal antibodies directed against inhibitory receptors expressed by T cells (such as PD-1 [74] and CTLA-4 [263]). Activated leukocytes have been known to turn against their host, attacking healthy cells and causing pathologies such as lupus, multiple sclerosis and type 1 diabetes. The immune system has evolved over time to develop self-regulatory mechanisms in order to suppress potentially pathological immune responses, one such mechanism involves the expression of the programmed cell death protein 1 (PD-1) on activated T cells.

The interaction of PD-1 with the PD-1 ligands (PD-L1 & PD-L2) has been shown

to induce inhibitory signaling in T cells, reducing their activity [67]. One method in which cancer evolves to escape immune surveillance [96] is to over-express PD-L1 on malignant cells and associated antigen presenting cells (APC) [236]. PD-1 ligation on T cells by PD-1 ligands results in T cell inhibition by the suppression of T cell receptor (TCR) signaling and promotion of apoptosis by the down-regulation of anti-apoptotic factors [99]. The anti-PD1 monoclonal antibodies Nivolumab and Pembrolizumab were developed to block the PD-1/PD-L1 axis, thus restoring normal T cell function in the tumour microenvironment.

Cytotoxic T-lymphocyte associated protein 4 (CTLA-4) was discovered by Brunet *et al* in 1987 [27] and was so named as it was highly expressed on activated cytotoxic T cells. Subsequent studies showed that CTLA-4 is an immunosuppressive molecule where genetic ablation of CTLA-4 led to fatal immunopathology in CTLA-4 knockout mice [262]. The primary method that CTLA-4 exerts immunosupressive pressure on T cells is via its high affinity for the co-activatory ligand B7 which, upon ligation does not relay an activatory signal within the T cell (Figure 7b) such as is observed by the interaction of B7 with CD28 (Figure 7a) [141]. By virtue of it's greater affinity for B7, CTLA-4 effectively sequesters B7 from CD28 and causes T cell anergy. This suppression can occur in cis (T cells expressing their own CTLA-4) or more effectively in trans, where T regulatory (Treg) cells overexpress CTLA-4 [101], sequestering B7 (Figure 7d) [207] and suppressing local T cells via additional means such as IL-2 sequestration [36] via overexpression of CD25 and expression of immunosuppressive cytokines such as IL-10 and TGF-β.

It has been recently demonstrated that the application of anti CTLA-4 (αCTLA-4) monoclonal antibodies effectively blocks the CTLA-4/B7 interaction thus restoring T cell activation via CD28 signaling (Figure 7c) [122]. Additional αCTLA-4 activity may also be attributed to the depletion of immunosuppressive Tregs via αCTLA-4 antibody mediated cytotoxicity (ADCC) (Figure 7f) or antibody mediated cellular phagocytosis (ADCP) (Figure 7e) [221]. This restoration of T cell function promotes tumouricidal activity and the development of anti-human CTLA-4 mAbs (ipilimumab and tremelimumab) have met FDA approval [142] having been successfully deployed to treat a range of solid cancers.

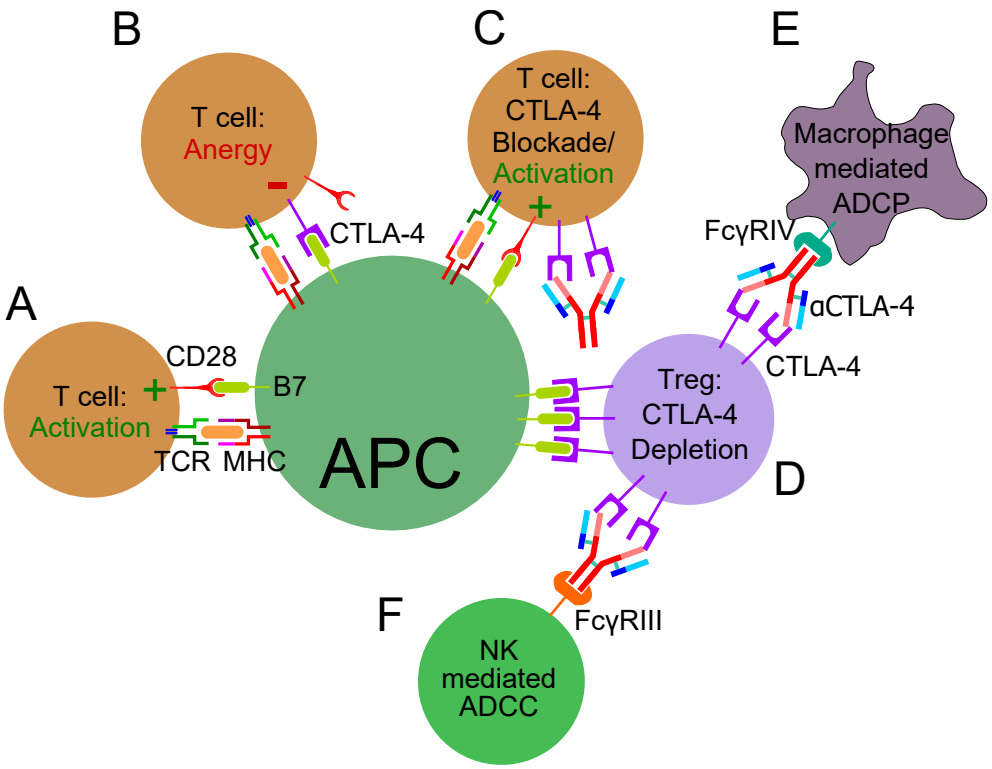

Figure 7: CTLA-4 blockade
CD28 is displaced as the main receptor of B7 when T cells express CTLA-4 (a/b) while Treg overexpression of CTLA-4 further sequesters available B7 (d). CTLA-4 blockade promotes T cell activation by restoration of CD28 (c) signaling and Treg depletion (e/f).

CTLA-4 and PD-1 blockade both present a mechanism to alleviate suppression of the adaptive immune response in the tumour microenvironment. Another approach to immunotherapy involves direct stimulation of immune cells via their expressed activatory receptors (such as CD28, ICOS and 4-1BB). Monoclonal antibodies have also been used in this capacity to stimulate immune responses, most notably in a 2006 phase I trial of an agonistic CD28 antibody known as TGN1412 [228]. The trial was a failure as the drug caused systemic activation of the T cell compartment, leading to severe immune associated toxicities in trial subjects via a phenomenon known as cytokine release syndrome (CRS).

Given their importance in immune signaling, cytokines have long been considered as prime candidates for the application of immunotherapy in cancer, however the pleiotropic nature of many immunomodulatory cytokines hampers their adoption as immunotherapies as their application may lead to unpredictable results ranging from immunosuppression to CRS.

Interleukin 2 (IL-2) is a prime example of a cytokine that has found success in the clinic where a nine-year study between 1985 and 1993 trialed the application of a large bolus of IL-2 (600,000 or 720,000 IU/kg) every 8 hours for 14 consecutive days to patients with metastatic melanoma. This study returned an overall

objective response rate of 16% and complete responses in 6% of patients [11]. The results of this and proceeding studies indicate that although IL-2 may hold promise as an immunotherapeutic compound, it is significantly hampered by two major factors associated with many cytokine therapies. The first being that the pleiotropic nature of IL-2 leads to activation of not only cytotoxic T cells (CTL), but also immunosuppressive Tregs. An overexpression of CD25 (the high affinity IL-2 receptor) on Tregs in the tumour microenvironment (a Treg enriched environment) may even lead to selective expansion of Tregs over effector T cells and attenuation of any cytotoxic effect (Figure 8a). Additionally, the systemic nature of IL-2 delivery in these trials have lead to severe peripheral toxicities that restrict tolerable dosages and reduces therapeutic efficacy (Figure 8b). These toxicities are not restricted to IL-2, but other relevant cytokines used in clinic such as interferon gamma (IFNγ) [29] and interleukin 12 (IL-12) [12]. We hypothesise that tumour restricted immunosuppression may be avoided by use of IL-12, a cytokine that may not favor Treg expansion [284] in the tumour whilst peripheral toxicity may be avoided by use of a local delivery method.

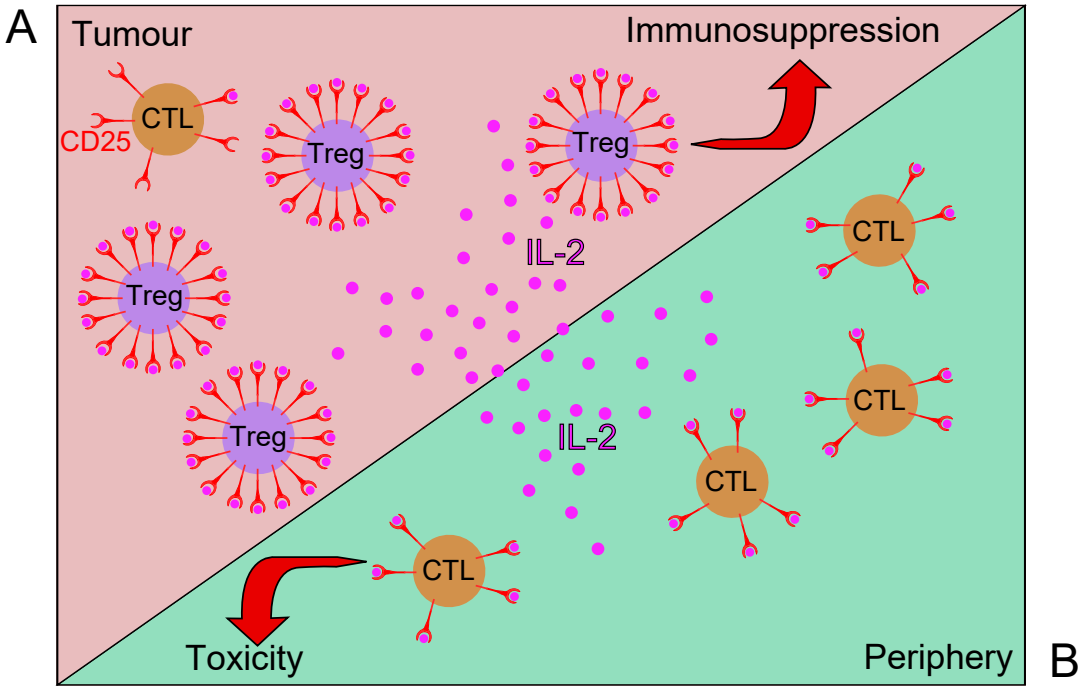

Figure 8: The dual caveats of IL-2 cytokine therapy

1.3 IL-12

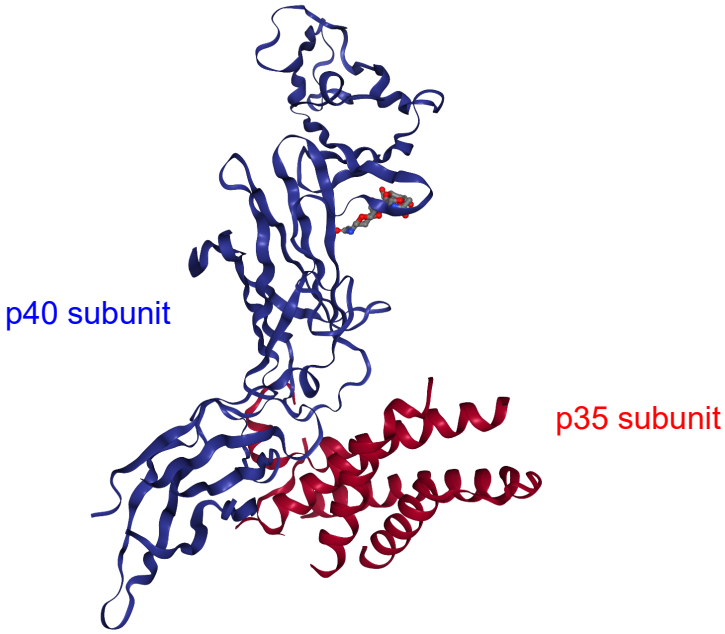

Protein Data Bank (www.rcsb.org/structure/1F45), 2019

Figure 9: Human IL-12 crystal structure

Interleukin 12 (IL-12) is a heterodimeric cytokine composed of two disulphide-bonded glycoprotein subunits, p35 and p40 (encoded by *IL-12A* and *IL-12B* genes respectively). Containing an arrangement of four α-helical chains, IL-12 is classified as a type I cytokine and is predominantly secreted by monocytes, macrophages, neutrophils and dendritic cells [95, 241]. Previously known as Cytotoxic Lymphocyte Maturation Factor (CLMF), this cytokine was given an interleukin designation in 1991 [89] as it displayed immunoregulatory properties similar to that of other interleukin cytokines.

1.4 IL-12 Receptor Signaling

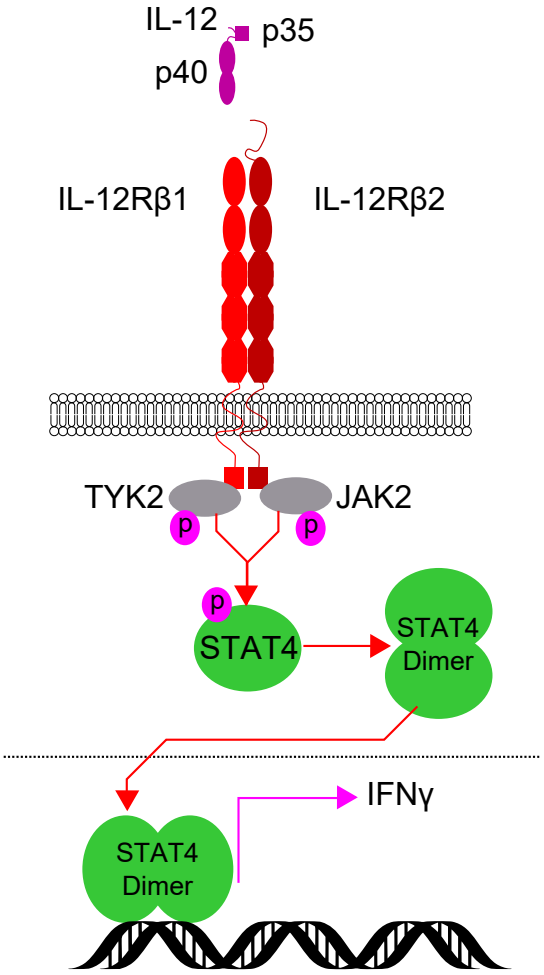

Figure 10: IL-12 Receptor Signaling

The IL-12 receptor (IL-12R) is a type I cytokine receptor comprised of two transmembrane subunits, IL-12Rβ1 and IL-12Rβ2. It is expressed on T cells, NK cells [48, 88] and ILC [70]. IL-12R signaling induces tyrosine phosphorylation of JAK2 and TYK2 janus family kinases [14], which in turn activates STAT4 via phosphorylation of tyrosine [15, 106] and serine [253] residues. Serine phosphorylation of STAT4 is mediated by p38 mitogen-activated protein kinase (MAPK) and responsible for STAT4 mediated IFNγ production [253]. IL-12 mediated activation of the phosphatidylinositol 3-kinase (PI3K)/Akt pathway has been shown to stimulate cellular proliferation; but not IFNγ production [278].

1.5 IL-12 : Clinical Applications for Cancer Immunotherapy

Given it's immunomodulatory activity, IL-12 has been considered a potentially valuable immunotherapeutic tool and has been shown to mediate tumour regression in pre-clinical models of cancer.

A 1993 study published by Brunda *et al* [25] investigated the effects of systemic (intra-peritoneal) administration of recombinant IL-12 (rIL-12) in B16.F10 melanoma bearing mice, both in models of subcutaneous tumour growth and by use of the intravenously delivered 'experimental lung metastasis' model. The results of this study indicated that a 1μg dose of rIL-12 was well tolerated whereas a 5μg dose resulted in toxicity (as evidenced by observed murine lethargy). A single 1ug dose of rIL-12 was shown to reduce the number of pulmonary lesions in the intravenous model whilst subcutaneous tumour progression was reduced. A significant survival advantage was measured in subcutaneously grown tumours treated with rIL-12 on alternating days (although no complete responses were recorded). Interestingly, the efficacy of rIL-12 was not impacted in mice that had been depleted of NK and $CD4^+$ T cells. $CD8^+$ T cell depletion however resulted in a partially reduced tumouricidal effect. This study showed that systemic rIL-12 therapy can slow tumour progression and that the mechanism of action is partially attributed to cytotoxic $CD8^+$ T cell activity although unidentified secondary mechanisms may be at play.

A second study in 1994 from Nastala *et al* [175] added to the Brunda story by testing systemic and intra-tumoural (local) delivery of rIL-12 in subcutaneously grown tumours. Tumours were rejected and significant survival benefits were measured regardless of systemic or local delivery of rIL-12. Mechanistic analysis demonstrated that both $CD4^+$ and $CD8^+$ T cells were required to mediated tumour rejection as was the presence of IFNγ (possibly relating to the secondary mechanism aluded to in the Brunda study).

Therapeutic modality	Route of IL-12 (or IL-12 vaccine) administration	Tumour
Combined treament		
Trastuzamab	i.v.	Breat, pancreas, cervical cancer
Trastuzamab and paclitaxel	i.v. or s.c.	Breast, colon, and other cancers
Rituximab	s.c.	Non-Hodgkin's lymphoma
Peptide vaccine with adjuvant[a]	IL-12 + alum or GM-CSF, s.c. at vaccine injection site	Melanoma
Peptide vaccine with adjuvant[b]	i.d. at vaccine injection site	Melanoma
Idiotype vaccine $\mp$ GM-CSF	s.c.	Mutiple myeloma
Peptide-loaded PBMCs[c]	s.c. adjacent to immunization site	Melanoma
Pegylated liposomal doxorubicin	s.c.	AIDS-associated Kaposi sarcoma
IL-2	i.v.	Melanoma, renal cancer
IFNα	i.v. or s.c.	Melanoma, renal cancer, and other cancers
Gene Therapy		
IL-12-transduced autologous fibroblasts	Peritumoural	Melanoma and other cancers
Adenovirus encoding IL-12	Intratumoural	Lover, colorectal, pancreatic cancer
Autologous dendritic cells transfected with adenovirus encoding IL-12 gene	Intratumoural	Gastrointestinal carcinomas
IL-2 gene modified autologous melanoma cells	s.c.	Melanoma
Canarypox virus expressing IL-12	Intratumoural	Melanoma
Canarypox expressing IL-12 + expressing B7.1	Intratumoural	Melanoma

[a] Peptides: $gp100_{209\text{-}217}$ (210M), $MART\text{-}1_{26\text{-}35}$ (27L), $tyrosinase_{368\text{-}376}$ (370D), adjuvant: Montanide ISA 51

[b] Peptides: $gp100_{209\text{-}217}$ (210M), $tyrosinase_{368\text{-}376}$ (370D), adjuvant: Montanide ISA 51

[c] Peptide: $Melan\text{-}A_{27\text{-}35}$

Table 3: Summary of clinical studies on the antitumour effects of IL-12-based treatment in combination therapies or gene therapy. Reproduced from Lasek *et al* [127]

Clinical trials of IL-12 as a cancer immunotherapy followed these successful preclinical studies and were based at the University of Pittsburgh (PA, USA) [147], the Genetics Institute (MA, USA) [133] and Hoffman La Roche (NJ, USA) [194]. These phase I trials utilised differing methods of delivering rIL-12 (subcutaneous, intra-peritoneal and intravenous) or autologous fibroblasts engineered to express IL-12 [147] with differing schedules (daily, triweekly or weekly). The Genetics Institute utilised the highest dose/frequency method and a maximal tolerated intravenous dose of 500ng/kg/day was recorded, however a subsequent phase II trial had to be halted when this therapeutic regimen resulted in severe toxicities in 12 of 17 patients (including 2 fatalities) [107]. A comparative examination of these two trials showed that lower toxicities were encountered in the phase I trial when an initial 'priming' dose of IL-12 was used prior to daily rIL-12 dosing [40]. This priming strategy was employed in subsequent trials, however result were underwhelming as patients appeared to develop acquired resistance to IL-12 therapy [195]. More recent studies have focused on combining IL-12 with existing chemotherapies, immunotherapies or the development of locally delivered IL-12 gene therapies as summarised in table 3 (reproduced from Lasek *et al* [127])

1.6 Strategies for the local delivery of IL-12

High toxicity associated with systemic administration of IL-12 has lead to the development of a variety of methods to deliver IL-12 directly to the tumour microenvironment. These methods broadly fit into two categories: (1) delivery of recombinant protein or (2) genetic therapy. The first category involves intra-tumoural administration of recombinant or fusion IL-12 protein [256] either alone or encapsulated in a slow release system such as biodegradable polymers or microspheres [60]. The second category involves the use of genes encoding IL-12 as an *ex vivo* or *in vivo* gene therapy. Several methods have been developed to facilitate this including genetic vaccination via gene gun [179], *in vivo* electroporation of IL-12 plasmid DNA [145] and an array of IL-12 encoding viral vectors.

IL-12 encoding viruses have been used both for *ex vivo* and *in vivo* therapies. *Ex vivo* transduction strategies have involved the manipulation of autologous tumour [233], fibroblasts [113], dendritic cells [186] and modified T cells [114] to be used as an adoptive cellular therapy (ACT). Viral vectors have been edited to reduce immunogenicity [259], pathogenicity, to remove their replicative capacity [286] and to increase space for genome incorporation. Adenoviruses (Ad) encoding IL-12 have been used in preclinical studies to treat melanoma [37], colorectal carcinoma [159] and glioma [238]. IL-12 encoding Adeno-associated viruses (AAV) have been studies in models of hepatic colorectal metastasis [250]. The positive-strand RNA alphavirus, Semliki Forest virus (SFV) has been used to deliver IL-12

in models of melanoma [10] and glioma [273].

1.7 Lentiviral vectors for gene therapy

The human immunodeficiency virus (HIV) is a member of the lentivirus genus of retroviruses. HIV-1 is the most well studied of the lentiviruses and, like all retroviruses, is able to insert a copy of its genome directly into the genome of the host [223]. The expression of gp120 on the surface of HIV-1 allows the virus to interact with CD4 [47] and chemokine receptors CCR5 & CXCR4 [6] on $CD4^+$ T cells and some macrophages [39]. This interaction directs viral tropism to these cells and allows infection and stable transduction of the hosts immune cells that may lead to an eventual collapse of the immune system known as acquired immunodeficiency syndrome (AIDS) [265].

A single-stranded RNA virus, the HIV-1 genome contains several important structures (Figure 11) [121] where the 3 genes that encode structural proteins are known as *gag*, *pol* and *env*. *Gag* encodes the matrix (MA), capsid (CA) and neucleocapsid (NC) core proteins [125]. *Pol* encodes three essential enzyemes: viral protease (PRO), reverse transcriptase (RT) and integrase (IN)[104]. *Env* encodes viral surface glycoprotein gp160, during viral maturation, gp160 is cleaved into gp41 transmembrane (TM) and gp120 surface (SU) proteins [31]. Gp120 is essential for binding of the virus to CCR5 and CD4 thus allowing pseudo-specific infection of $CD4^+$ T cells and some macrophages.

The HIV-1 genome includes 2 regulatory genes known as *tat* [203]and *rev* [279] where *tat* encodes trans-activators required for viral transcription and *rev* encodes proteins required for splicing and export of viral transcripts. Flanking long terminal repeats (LTR) are required for viral transcription, reverse transcription and genome integration[227]. Ψ, (found between the 5'LTR and *gag*) is an essential signal for genome dimerization and packaging while *vif*, *vpr*, *vpu* and *nef* are characterised as non-essential accessory genes[154] .

The ability to stably transduce cells combined with tropism conferred by the viral envelope makes HIV-1 an attractive concept as a genetic vector that researchers and clinicians may be able to exploit as a gene therapeutic tool [121].

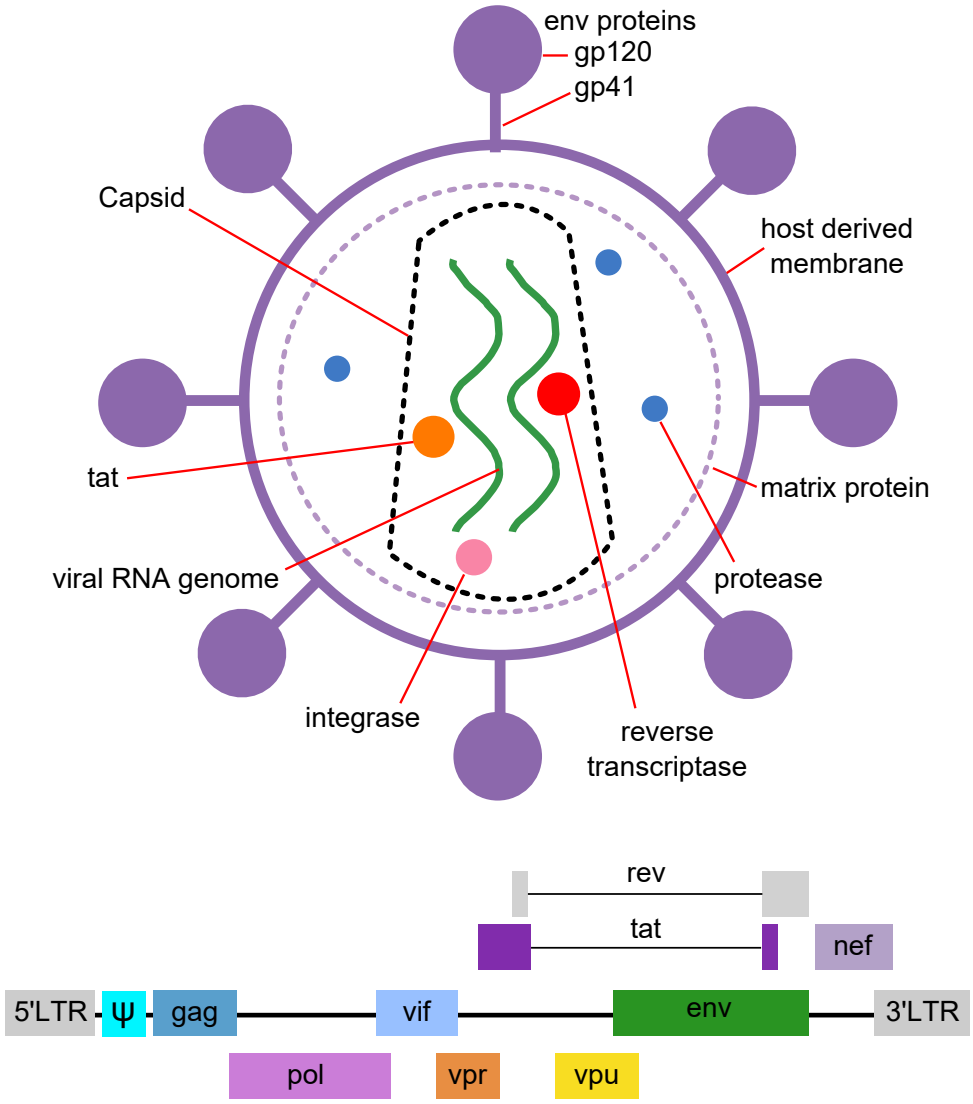

Figure 11: Structure of HIV-1 and viral genome
Adapted from Kotterman *et al* [121]

Three subsequent generations of replication incompetent lentiviral vectors have been developed, with each generation introducing features that improve the biosafety of these genetic vectors.

The first generation of lentiviruses separated the viral genome into 3 separate plasmids [174]. The packaging plasmid contained a majority of the original HIV-1 genome under a CMV promoter with the exception of the viral envelope, LTRs and Ψ. An envelope plasmid with CMV promoter replaced the original *env* gene with a viral envelope of choice, a commonly used envelope was the vesicular stomatitis virus G (VSV-G) protein that allows viral infection of a wide variety of cell types. The third plasmid contains CMV promoter, LTRs, Ψ and the transgene of choice (Figure 12a). The components of this third plasmid are the only viral components that are integrated into the hosts genome, thus removing the replicative capacity of the vector.

The use of first generation lentiviral vectors raised biosafety concerns regarding the inclusion of the accessory genes *vif*, *vpr*, *vpu* and *nef.* These genes are important for in vivo viral replication and pathogenesis, are not desirable features for a non-replicative genetic vector and were subsequently removed in what became known as the second generation lentivirus system [287] (Figure 12b).

Further safety improvements resulted in the development of third generation self-inactivating (SIN) lentiviruses as *rev* was separated from the packaging plasmid whilst *tat* and the U3 promoter/enhancer region of the LTR were deleted and their transactivator/promoter functions were replaced with a strong (CMV) promoter [54] (Figure 12c).

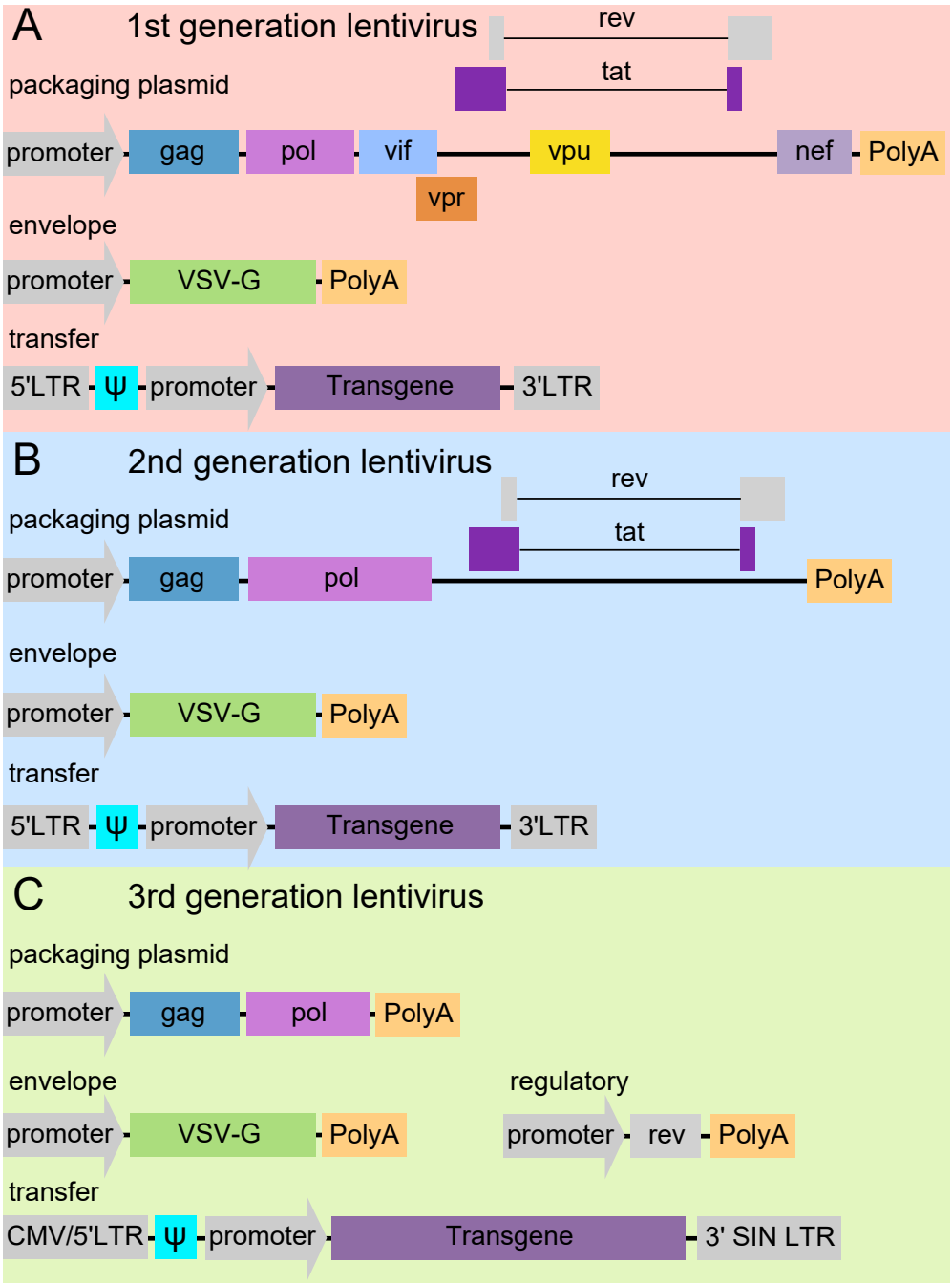

Figure 12: Development of replication incompetent lentiviral vectors.

Lentiviruses have been used as an immunotherapeutic agent in a variety of models. Subcutaneous vaccination with an antigen encoding lentivirus transduces DC, promoting efficient antigen presentation [83], cross-presentation [102] and T cell activation. Lentiviral delivery of immunomodulatory cytokines (such as IL-7 [251]) promote T cell activation whilst lentiviral CRISPR/Cas9 constructs effectively disrupt PD-1 expression on T cells protecting them from PD-1 associated apoptosis [205]. Lentiviruses are routinely used in the production of chimeric antigen receptor (CAR) T cells [158] such as the CD19 restricted CAR T cells that have shown much promise in recent clinical trials [111].

Patient studies utilising retroviruses (Table 4, reproduced from Kotterman *et al* [121]) thus far have been restricted to *ex vivo* manipulation of autologous patient materials due to continuing safety concerns regarding off-target associated indel events, and have been used to correct genetically defective immune populations as well as CAR-T cell production to treat leukemia. Adeno-associated viral (AAV) vectors are non-integrating viral vectors that have been developed as a safer alternative to retroviral systems. Unlike retroviruses, AAV have been successfully utilised as in vivo gene therapeutic tools in a number of clinical trials to treat a range of diseases including haemophilia, cystic fibrosis, muscular dystrophy and Parkinson's disease (Table 5, reproduced from Kotterman et al [121]).

Vector Type	Transgene	Clinical phase	Route of administration	Clinical trial identifier
Adenosine deaminase deficiency-severe combined immunodificiency				
MLV retrovirus	ADA	NA	Ex vivo to T cells	NA
MLV retrovirus	ADA	NA	Ex vivo to HSCs	NA
MLV retrovirus	ADA	Phase I/II	Ex vivo to HSCs	NCT00598481 NCT00599781
X-linked severe combined immunodeficiency (X-SCID)				
MLV retrovirus	γc	Phase I	Ex vivo to HSCs	NA
β-Thalassemia				
SIN lentivirus	β-globin	Phase I/II	Ex vivo to HSCs	NA
X-linked adrenoleukodystrophy (ALD)				
SIN, VSV-G lentivirus	ABCD1	Phase I	Ex vivo to HSCs	NA
Wiskott-Aldrich Syndrome (WAS)				
SIN, HIV-derived lentivirus	WAS	Phase I/II	Ex vivo to HSCs	NCT01515462
Metachromatic leukodystrophy (MLD)				
SIN, VSV-G lentivirus	Arylsulfatase A gene	Phase I/II	Ex vivo to HSCs	NCT01560182
Chronic lymphocytic leukemia (CLL)				
SIN lentivirus	Chimeric antigen receptors	Phase I	Ex vivo to T cells	NCT01029366 NCT00466531
B-cell acute lymphoblastic leukemia (ALL)				
SIN lentivirus	Chimeric antigen receptors	Phase I	Ex vivo to T cells	NCT01044069

Abbreviations: γc, gamma-chain protein of interleukin receptor; HSCs, hematopoeitic stem cells; MLV, murine leukemia virus; NA, not applicable; ABCD1, adenosine triphosphate (ATP)-binding cassette, subfamily D (X-linked adrenoleukodystrophy), member 1; SIN, self-inactivating; VSV-G, G-protein of the vesicular stomatitis virus.

Table 4: Summary of clinical trials using retroviruses by disease. Reproduced from Kotterman *et al* [121]

AAV Serotype	Transgene	Clinical phase	Route of administration	Clinical trial identifier
Heomophilia B				
AAV2	Factor IX	Phase I/II	Intramuscular	NCT00076557
		Phase I	Hepatic	NCT00515710
AAV8		Phase I/II	Intravenouse	NCT00979238
Rheumatoid arthritis				
AAV2	TNF receptor-antibody fusion	Phase I/II	Intraarticular	NCT00617032 NCT00126724
Cystic Fibrosis				
AAV2	CFTR	Phase I/II	Aerosol	NCT00004533
Lipoprotein lipase deficiency				
AAV1	LPL	Phase I/II/III	Intramuscular	NCT01109498 NCT00891306
Leber's congenital amaurosis				
AAV2	RPE65	Phase I/II	Subretinal	NCT00516477 NCT00643747 NCT00481546
Choroideremia				
AAV2	REP1	Phase I/II	Subretinal	NCT01461213
Canavan's disease				
AAV2	Aspartocyclase	Phase I	Intracranial	NA
Muscular Dystrophy				
AAV1/AAV2 chimera	Microdystrophin	Phase I	Intramuscular	NCT00428935
AAV1	α-Sarcoglycan	Phase I	Intramuscular	NCT00494195
α-1-Antitrypsin deficiency				
AAV2	α-1-Antitrypsin	Phase I/II	Intramuscular	NCT00377416
AAV1				NCT00430768
Severe heart failure				
AAV1	SERCA2a	Phase I/II	Coronary artery infusion	NCT00454818
Parkinson's disease				
AAV2	GAD	Phase I/II	Intracranial	NCT00195143 NCT00454818
	Neurturin	Phase I/II		NCT00252850 NCT00400634
	AADC	Phase I		NCT00229736
Wet age-related macular degeneration				
AAV2	anti-VEGF	Phase I/II	Subretinal	NCT01494805
		Phase I	Intravitreal	NCT01024998

Abbreviations: AADC, L-amino acid decarboxylase; CFTR, cystic fibrosis transmembrane conductance regulator; GAD, glutamic acid decarboxylase; LPL, lipoprotein lipase; NA, not applicable; REP1, Rab1 escort protein; RPE65, retinal pigment epithelium-specific protein 65 kDa; SERCA2a, sarcoplasmic reticulum calcium ATPase 2a; TNF, tumour necrosis factor; VEGF, vascular endothelial growth factor.

Table 5: Summary of clinical trials using adeno-associated virus (AAV) by disease.
Reproduced from Kotterman *et al* [121]

1.8 Local delivery of IL-12 to treat pulmonary metastasis

The lung is a common anatomical site for both primary and metastatic malignancies [30, 230]. Based on the complexity of the lung microenvironment and the multiplicity of targets downstream of IL-12, we sought to determine whether local delivery of IL-12 to the lung microenvironment would induce a potent and multi-cellular response against established lung metastasis, and to characterize the key components linked to anti-tumour activity. We decided to exploit the previously described tropism of lentivirus for alveolar macrophages [152] to allow sustained IL-12 release within the lung tumour microenvironment.

We demonstrate that local delivery of a lentiviral vector encoding IL-12 (IL-12 LV) promotes regression of established lung metastases. Despite concomitant activation of the adaptive T cell response, anti-tumour activity relied upon production of IFNγ by ILCs within the tumour, prompting direct activation of interstitial macrophages and tumour eradication. These data underscore the potency of IL-12 LV in the lung microenvironment and the plasticity of the innate lymphoid and myeloid compartments in anti-tumour responses within the lung.

2 Materials and Methods

2.1 Cell lines

Human embryonic kidney 293-T (HEK293T) cells and B16.F10 murine melanoma cells were cultured in 10% FBS-supplemented iscove's modified dulbecco's medium (IMDM) and RPMI-1640 (RPMI), respectively. To generate the B16.F10-FLuc.eGFP (B16.eGFP) cell line, B16.F10 cells were transduced with a bicistronic lentiviral vector encoding firefly luciferase (FLuc) and enhanced green fluorescent protein (eGFP), which were kindly gifted by M. Pule (pSew-FLuc.A2.eGFP; UCL, London). Highly-expressing $eGFP^{+}$ cells (B16.F10.eGFP) were sorted to >99% purity using a FACSAriaIII cell sorter (Becton Dickinson, BD).

The KPB6.F1 mouse lung adenocarcinoma cell line was generated by intransal administration of a Cre-recombinase expressing adenovirus was to *K-ras/P53* mice in order to induce carcinogenesis as previously described [56]. Tumour bearing lungs were harvested, disaggregated and cultured in RPMI+10% FBS to generate the KPB6.F0 cell line. KPB6.F0 cells were then administered to C57BL/6 mice via the intravenous route, and lungs were recovered 21 days post tumour challenge. Disaggregated lungs were cultured, tumour cells were cultured and the KPB6.F1 cell line was established. Cells were trypsinized, washed and resuspended in PBS for injection.

2.2 Animals

4-6 week old female C57BL/6J mice were obtained from Charles River Laboratory (Surrey, UK). C57BL/6.*Rag1*$^{-/-}$ (*Rag1*$^{-/-}$) and C57BL/6.*CCR2*$^{-/-}$ (*CCR2*$^{-/-}$) mice were a kind gift from Prof. Derek Gilroy (UCL, London). Macrophage Insensitive to IFN-Gamma (MIIG) mice were kindly donated by Michael B. Jordan (University of Cincinnati, OH). The *K-ras*$^{LSL\text{-}G12D/+}$*;p53*$^{fl/fl}$ (*K-ras/P53*) Cre-inducible transgenic mice (developed on a C57BL/6 background) were a kind gift from Tyler Jacks (Massachusetts Institute of Technology, Cambridge, Massachusetts, USA). All experiments were performed with approval of the UCL ethics committee and the Home Office of the United Kingdom.

2.3 Molecular Biology

2.3.1 PCR amplification of DNA

Polymerase chain reaction (PCR) was performed to amplify DNA for plasmid construction. PCR master mixes were made as per table 6 below with details of primers and template DNA specified in section 3.1.

Component	Final concentration	Volume (μl)
Phusion DNA Polymerase (NEB)	1 U/50μl	0.6μl
5x HF Buffer (NEB)	1x	12μl
10mM dNTPs	200μM	1.2μl
Template DNA as specified	< 250ng	variable
25μM forward primer*	0.5μM	3μl
25μM reverse primer*	0.5μM	3μl
DNAse free water		up to 60μl total volume

Table 6: PCR reaction mixture recipe
*Please refer to Appendix Figure 63 for primer designs

PCR was performed using the following PCR cycler program (Table 7) on a Bio-Rad C1000 thermal cycler.

Step	Phase	Temperature	Time
1	Initial Denaturation	98℃	30 sec
2	Denaturation	98℃	10 sec
3	Annealing	65℃*	40 sec
4	Extension	72℃	1 min per Kb DNA
5	Loop steps 2-4, 35x		
6	Final Extension	72℃	10 min
7	Hold	4℃	-

Table 7: PCR cycler program
* Primers designed for optimal 65℃ annealing temperature using Primer3 [245]

2.3.2 Restriction digestion

Digestion of DNA was performed by use of restriction enzymes for restriction analysis of DNA as well as digestion of DNA for cloning and ligation. Digestion reaction mixes were made up as per table 8 using restriction enzymes and buffers as described in section 3.1. DNA was digested at 37℃ for 1hr.

	Analysis	Digestion for Cloning
DNA (1mg/ml)	1μl	10μl
DNAse free water	16μl	15μl
Buffer	2μl	3μl
Enzyme 1	0.5μl	1μl
Enzyme 2	0.5μl	1μl

Table 8: Restriction digest reaction mix recipes

2.3.3 DNA ligation

Digested DNA fragments (insert) was ligated into digested viral plasmids (refer to section 3.1) by use of T4 DNA ligase (NEB). Ligation reaction mix was made as per table 9 and incubated at room temperature for 15min, after which ligated DNA was used to transform competent bacteria (as per section 2.3.4).

Component	Volume
Insert DNA (1mg/ml)	4μl
Viral plasmid DNA (1mg/ml)	4μl
T4 DNA Ligase	1μl
10x T4 Ligase Buffer	1μl

Table 9: DNA Ligation reaction mix recipe

2.3.4 Transformation of competent bacteria

Plasmid DNA was amplified by transformation of competent bacteria as follows. An aliquot of DH5α *E. coli* (NEB) was thawed on ice for 20min. DNA was added to the bacteria (1mg of plasmid DNA or 5ul of ligation mix as per section 3.1) and incubated for 30min on ice. Bacteria was heat shocked at 37℃ for 2min and then incubated on ice for 2min. Transformed bacteria was streaked onto LB agar plates (containing 50μg/ml ampicillin). Agar plates were incubated overnight at 37℃ (5% CO2), single colonies were picked and inoculated into LB broth media (containing 50μg/ml ampicillin). Broth cultures were incubated at 37℃ (5% CO2) and plasmid DNA was extracted either by mini-prep or midi-prep (Qiagen, as per manufacturers instructions) depending on culture volume.

2.3.5 Lentivirus Production and Titration

Prepared Reagents:

- Complete IMDM (containing 10% FBS, 100U penicillin, 100ng streptomycin and 2mM L-glutamine)

- TE buffer : 1ml Tris-HCl (1M, pH 8.0) + 0.2ml EDTA (0.5M, pH 8.0), top up to 100ml with de-ionised water.
- 20% Sucrose cushion: 50ml Hanks Buffered Saline Solution (HBSS) + 10g sucrose. Sterilise by 0.22μm syringe filtration.

Method:

Lentivirus was produced for *in vivo* studies as follows. A 15cm^2 dish of confluent HEK293T cells (less than 12 passages) were split into 3x 15cm^2 plates in complete IMDM. Cells were incubated overnight at 37℃ with 5% CO2 (and confirmed 80-90% confluent before transfection). Plasmid DNA mix was prepared as per table 10, transfection reagent was prepared as per table 11, the plasmid DNA mix was carefully added to the transfection reagent (yielding a total volume of 582.5μl per plate) and incubated at room temperature for 15min.

Component	Quantity
pCMV8.91 (gag, pol, rev, tat)	2.5μg
pMD-G (VSV-G envelope)	2.5μg
pSIN-IL12Fc (or pSIN-FcTag)	3.75μg
TE buffer	make up to 37.5μl

Table 10: Plasmid DNA mix

Component	Volume
Fugene-6 (Roche)	45μl
Optimem	500μl

Table 11: Transfection reagent

Cell cultures were aspirated and 18ml of fresh complete IMDM was added to each plate. 582.5μl of the DNA transfection mix was pipetted drop-wise onto each plate of cells and incubated for 24hr at 37℃ (with 5% CO2). Cell cultures were aspirated, 18ml of fresh complete IMDM was added to each culture plate and incubated for a further 48hr. Viral supernatant was collected from each culture plate 72hr post transfection, and cellular debris was removed by 0.45μm syringe filtration. Viral particles were concentrated by ultracentrifugation of viral supernatant over a 20% sucrose cushion for 2hrs, 4℃ at 22000rpm. Viral pellets were resuspended in 50μl HBSS (per 33ml of viral supernatant), aliquoted and stored at -80℃ either for estimation of viral titre (as follows) or *in vivo* use (following viral titre estimation).

Viral titre was estimated as follows. 2x10^5 HEK293T cells (in 500μl complete IMDM) were dispensed into multiple wells of a 24-well plate and incubated for 2hrs at 37℃ (until cells had attached to the wells). An aliquot of frozen lentivirus

was thawed and serial dilutions (1:5, 1:25, 1:125, 1:625 and 1:3125 dilutions, 30μl per dilution) were made in complete IMDM. 25μl of each dilution was added to separate wells of HEK293T cells (media alone was added to 2 wells for non-transduced controls) and incubated for 6hrs at 37℃ (5% CO2). 1ml of complete IMDM was added to each well, cells were incubated for 72hrs and expression of IL-12p40 (for IL-12 LV titre or IgG for control FcTag LV titre) was measured by flow cytometry (see section 3.2). The viral dilution that yielded approximately 30% IL-12p40 (or IgG) expression was used to calculate viral titre. Infectious units per millilitre (IU/ml) viral titre was calculated as follows : IU/ml = (200,000 cells x % transduced x dilution factor x 1000) / 25. Viral stocks of titre between 34 IU/ml and 55 IU/ml ($1.7x10^7$ IU per 30-50ul) were kept for *in vivo* use.

2.4 *In Vivo* Tumour models and therapeutic interventions

For the generation of pulmonary metastasis models, mice were injected with 1.5 x 10^5 B16.F10, B16.F10.eGFP or KPB6.F1 cells (suspended in 200μl PBS) by intravenous injection (day 0). Pulmonary tumour lesions are well established by day 11 [268], and at this time 1.7 x 10^7 IU of IL-12 LV, FcTag LV or eGFP LV were delivered by inhalation (typical volume 30-50 μl) under anesthesia (ketamine 100 mg/kg and xylazine 10 mg/kg). For cell depletion experiments, 200 μg of the following antibodies were administered by intraperitoneal (IP) injections 24 hours before lentiviral therapy and continued every third day for the duration of the experiment: anti-CD8a (2.43), anti-NK1.1 (PK136), anti-CD90 (T24/31), anti-IFNγ (XMG1.2) (BioXcell). Experiments were typically terminated at day 21, when tissues were harvested and processed for flow cytometry or immunohistochemistry. For survival experiments, mice were monitored every 48 hours and sacrificed upon signs of distress, which included >10% weight loss, breathing difficulty, abdominal swelling, paralysis or palpable tumours.

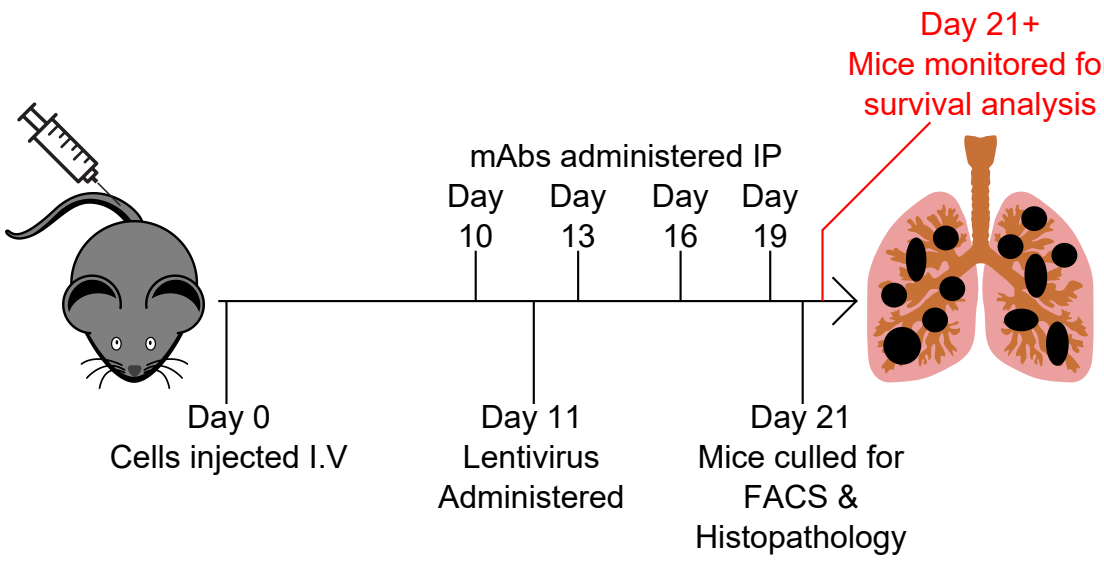

Figure 13: *In Vivo* model therapeutic schedule

2.5 Histopathology

Lungs for histopathology analysis were harvested and fixed in 10% Formalin for 24 hours at 4℃. Fixed lungs were then washed with cold PBS and transported in PBS to UCL core pathology services. Core pathology staff then embedded the fixed lungs in paraffin (Formalin-Fixed Paraffin-Embedded, FFPE) and 2μm serial sections were cut and mounted on negatively charged, lysine coated glass microscope slides. Mounted sections were stained with eosin & haematoxilin and imaged using a Hamamatsu nanozoomer slide scanner.

Images were analysed using the NDP View 2 software package (Hamamatsu), where 3 metrices were recorded: total lung area, total area of metastatic lesions (metastasis area) and total number of metastatic lesions. Triplicate sections from each mouse were recorded and average metrices per mouse were used to calculate metastasis index and metastatic number index as previously described [199]. Metastasis index was calculated as the metastatic area divided by total lung area and metastasis number index was calculated as the number of metastatic lesions divided by the total lung area.

2.6 Bronchoalveolar Lavage

Bronchoalveolar lavage (BAL) was performed as described previously [232] (with modification) to collect bronchoalveolar aspirants for cytometric analysis. Mice were culled by i.p injection of pentobarbitol and dissection was performed to expose the heart, lungs and trachea. A nylon thread (approximately 10cm in length) was passed beneath the trachea and a 22G intravenous canula was inserted into

the trachea. The rigid needle was removed from the canula and the nylon thread was tied off thus fastening the trachea to the canula. A 1ml syringe was loaded with 500μl PBS and inserted into the canula. PBS was slowly injected into and aspirated from the lungs four times after which recovered lavage fluids were expelled into a 1.5ml eppendorf tube for flow cytometric analysis.

2.7 Flow Cytometry

2.7.1 Tissue processing

Lungs were homogenized using a Gentlemacs dissociator (Miltenyi) and digested with Liberase TL (Roche; 1 mg/ml), DNAse (Roche; 0.2 mg/ml) in serum-free RPMI for 30 minutes at 37℃ and the cell suspension was then passed through a 70μm cell strainer. For tumour quantification, sample volumes were homogenized and a 200μl aliquot of cells was taken from each sample for flow cytometric analysis of eGFP$^+$ tumour cells (as per section 2.7.4). Absolute number quantification was performed by ratio-metric enumeration of samples that had been spiked with 5000 fluorescent cell sorting set-up beads (Life Technologies, C16506), a method previously described as single bead-enhanced cytofluorometry [172]. Leukocytes in remaining cell suspensions were enriched by density gradient centrifugation with Histopaque 1119 (Sigma), the interphase collected and resuspended in FACS buffer for flow cytometric analysis (as per section 2.7.5).

2.7.2 FACS Buffers & Reagents

Refer to table 13 of the Appendex (section 7.1)

2.7.3 Antibodies:

- T Cell Panel Antibodies : Refer to table 14 of the Appendix (section 7.1)
- IFNγ / ILC Panel Antibodies : Refer to table 15 of the Appendix (section 7.1)
- Myeloid Phenotype Panel Antibodies : Refer to table 16 of the Appendix (section 7.1)
- Myeloid Function Panel Antibodies : Refer to table 17 of the Appendix (section 7.1)
- IL-12 LV viral titration : IL-12/IL-23p40 (Clone C17.8, PerCP-Cy5.5, Thermo)
- FcTag LV viral titration : Goat polyclonal anti-mouse IgG (APC, Thermo)

2.7.4 FACS quantification of eGFP$^+$ tumour cells

200μl aliquots of disaggregated lung suspension (as described in section 2.7.1) were centrifuged (800 RCF, 2min at 4℃), aspirated and resuspended in amine reactive viability dye (APC eFluor 780, Thermo) diluted 1:1000 in PBS. Cells were incubated for 30min, covered on ice and then washed 3x (centrifugation, aspiration and resuspension in 180μl PBS). Cell were finally resuspended in 150μl PBS and transferred to titre tubes with 50μl of PBS containing 5000 fluorescent counting beads. Total numbers (count) of eGFP$^+$ tumour cells and counting beads were identified cytometric analysis of stained cells on a LSR II Fortessa flow cytometer (BD). eGFP$^+$ tumour burden was calculated as the number of eGFP$^+$ cells recovered per counting bead, multiplied by total counting beads spiked into the sample (5000) and the dilution factor of the original sample (200μl of 3ml, 15x).

2.7.5 Leukocyte Staining

Leukocyte enriched cell suspensions (as described in section 2.7.1) were isolated and resuspended in FACS buffer at 200μl per antibody panel. Staining of extracellular surface antigens was performed by transferring 200μl of enriched leukocyte suspension to a 96-well plate, followed by centrifugation (800 RCF, 2min at 4℃). Cells were aspirated and resuspended in 50μl of extracellular master-mix and incubated for 30min covered on ice and then washed 3x (centrifugation, aspiration and resuspension in 180μl PBS). Cells were then either resuspended in 150μl FACS buffer for FACS analysis, or passed onto intracellular/intranuclear staining protocols as required.

For the detection of cytoplasmic antigens (and not intranuclear antigens), intracellular permeabilization was performed using the BD Cytofix/Cytoperm kit as per the manufacturers instructions. For the detection of intranuclear antigens (or intranuclear and intracellular antigens), intracellular/inctranuclear permeabilization was performed using the Thermo FoxP3 permeabilization kit as per the manufacturers instructions. Cells were resuspended in 50μl of intracellular or intranuclear master-mix and incubated on ice for 30min followed by centrifugation. Cells were washed 3x with appropriate Wash buffer and finally resuspended in 150μl FACS buffer. Cells were transferred to titre tubes with 50μl of PBS containing 5000 fluorescent counting beads and analysed using an LSR II Fortessa flow cytometer (BD).

For analysis of IFNγ, cells were re-stimulated with phorbol myristate acetate (20 ng/ml) and ionomycin (1 μg/ml) for 4 hours at 37 ℃, and Golgi Plug (BD) was added during the last 3 hours. Staining was then performed as described above.

2.7.6 Compensation controls

1μl of each fluorescent antibody was was incubated with 1 drop of Ultracomp (pan-species anti-Fc beads) compensation beads (Thermo) for 5min at room temperature, and then topped up to 200μl with FACS buffer. 1μl of the Viability dye (APC eFluor 780, Thermo) was incubated with ArC amine reactive compensation beads (Thermo, as per the manufacturers instructions)

2.7.7 Analysis of cytometry data; manual analysis

Cytometry data (FCS files) were analysed using the FlowJo flow cytometry analysis software (FlowJo LLC.), basic live leukocyte gating strategy consisted of biaxial plotting FSC-A/SSC-A (cells) → FSC-A/FSC-H (single cells) → FSC-A/Viability (Live, viability dye low cells) (Figure 14). Beyond live cell identification, gating strategies varied (refer to results chapters). Fluorescent counting beads were identified on ungated FCS data (FSC-A/v450 channel) for ratio-metric quantification of gated cell populations.

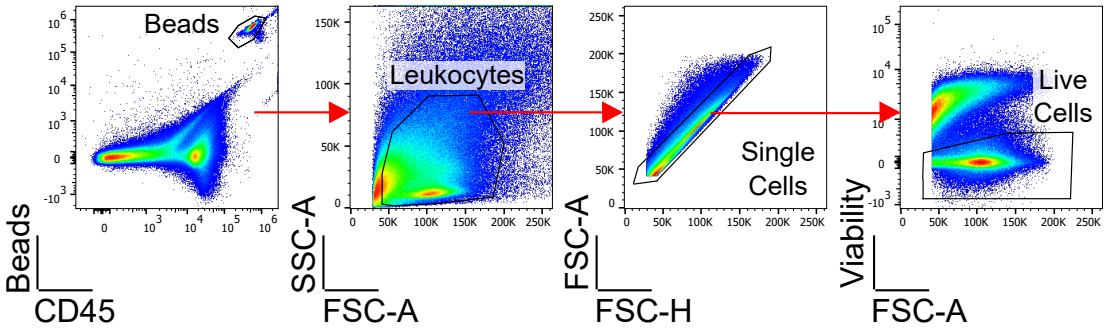

Figure 14: Example basic live FACS gating strategy

2.7.8 Analysis of cytometry data; automated analysis

High-dimension cytometry data sets were anlysed using a custom analysis pipeline, Cytofpipe [42], (Lucia Conde, UCL Bill Lyons Informatics Centre), developed for the automated analysis of flow and mass cytometry data, comprising cytofkit [35], SCAFFOLD [226] or CITRUS [24] R packages. For this analysis, marker expression values were transformed using the autoLgcl transformation from cytofkit, a fixed number of cells were then randomly sampled without replacement from each file and merged for analysis (<100,000 cells total sub-sampled). Cell populations were identified using FLowSOM [247] clustering based on expression of markers of interest using k=20 predefined numbers of clusters. To ensure reproducibility, FlowSOM clustering was repeated 50 times and results from the 50 iterations

were combined to filter out low frequency or non-consistent clusters. Median intensity values per cluster were used to generate heatmaps and these expression profiles were used to infer the identity of each cluster. UMAP [17] dimension reduction was applied to the same expression data and UMAP coordinates were used to visualise the cell populations with colours based on identified clusters and marker expression.

2.8 Statistical analysis

Numeric and statistical analysis was calculated using Prism 6.0 (GraphPad Software Inc.). D'Agostino & Pearson normality test was applied to all data sets containing two or more comparisons. Unpaired t-test was applied to data containing only one comparison. 1-way ANOVA with Tukey's post test was then applied to all sets of parametric data and Kruskal-Wallis tests with Dunn's post correction was applied to all non parametric data sets. 2-Way ANOVA was applied to data sets containing two independent categorial variables, with Tukey's post testing applied to parametric data sets and Sidak post testing applied to non-parametric data sets. Survival data was presented as a Kaplan-Meier plot and statistical analysis was performed using the Log-rank (Mantel-Cox) test. Gray's K-sample test [86] was applied to competing risk data sets. All experiments were repeated 2-6 times as indicated.

Results

3 IL-12LV production and tumouricidal effect

IL-12 is an immunomodulatory cytokine that is capable of driving robust Th1, CTL and NK responses against cancer [25, 175]. Systemic administration of recombinant IL-12 has been trialled as a cancer therapy, though it's efficacy was hampered by severe toxicity [12, 132, 133, 194].

A number of groups have recently sought to develop methods of delivering IL-12 directly to the tumour in an effort to limit the toxic effects of systemically delivered IL-12 whilst restricting it's potent immunomodulatory activity to the tumour microenvironment. One such group, headed by Prof. Burkhard Becher, have developed an Fc stabilised IL-12 fusion protein that has displayed potent anti-tumour effects in several models of solid cancer including the historically treatment resistant B16 melanoma [61] and GL261 glioma othotopic [256] models.

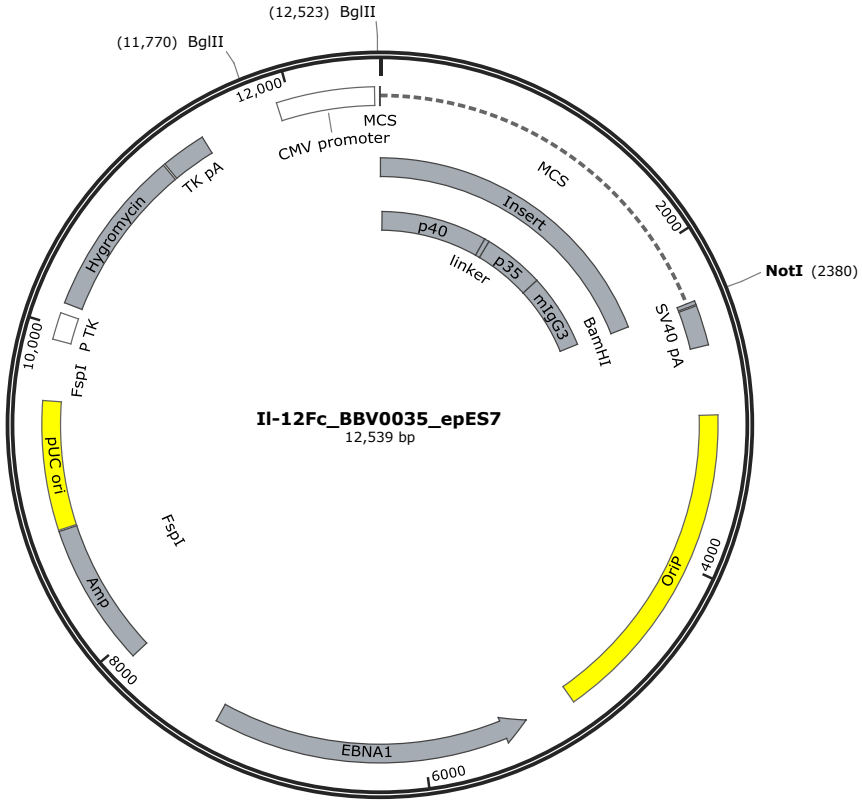

Figure 15: IL-12Fc Vector Map

At the time that this study was initiated, the Becher team had been unable to effectively control lung metastases using their established method of intratumoural delivery of IL-12Fc protein. We hypothesised that a large bolus of therapeutic

agent (such as IL-12Fc) delivered to a site of disseminated disease (such as pulmonary metastases) may diffuse out of the pulmonary compartment before a therapeutic effect can be measured. In this case, an alternative delivery method may be desirable.

A previous study by Douglas MacDonald [152] had found that a second generation lentivirus [168] can be engineered to express influenza viral peptides. When delivered intranasally, this engineered lentivirus was able to transduce alveolar macrophages *in situ* and re-program them to persistently express the influenza peptides as intended. This method effectively vaccinated mice against influenza and was able to protect vaccinated mice from subsequent influenza infection.

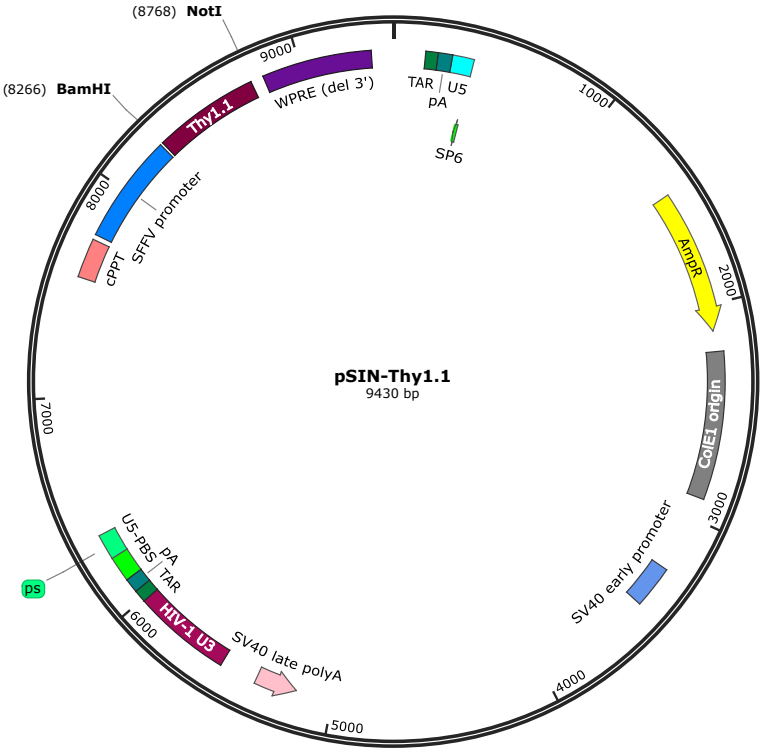

Figure 16: pSIN-Thy.1. Vector Map

We reasoned that this ability to deliver a peptide based therapeutic in a persistant manner directly to the pulmonary compartment would serve as an ideal method to deliver IL-12Fc to treat established pulmonary metastases. With generous donations of IL-12Fc construct plasmid (from Prof. Burkhard Becher) and lentiviral constructs (from Prof. Mary Collins) we embarked to clone an IL-12Fc expressing lentivirus and test this construct in models of metastatic lung cancer.

3.1 Lentivirus Cloning

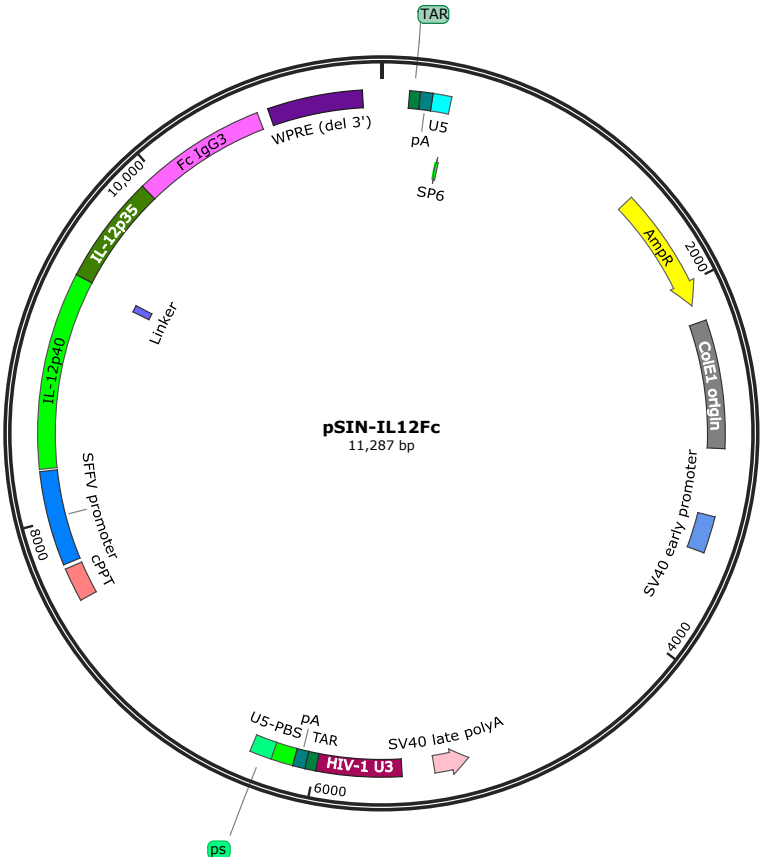

Figure 17: pSIN-IL12Fc (IL-12 LV) Vector Map
A schematic representation of the pSIN-IL12Fc lentiviral plasmid presenting the murine IL-12.IgG3Fc expression cassette under the SFFV promoter.

The lentiviral vector expressing eGFP (eGFP LV) under the control of spleen focus forming virus promoter (pCGSW eGFP LV) was donated by Mary K. Collins [7] . The IL-12 Fc (Figure 15) and FcTag (Appendix Figure 61) expression plasmids were a gift from Burkhard Becher (University of Zurich, Institute of Experimental Immunology). The IL-12 Fc construct consists of a fusion of the murine *IL12a* (p40) and *IL12b* (p35) subunits with the constant region of murine IgG3 (IL-12Fc) [61].

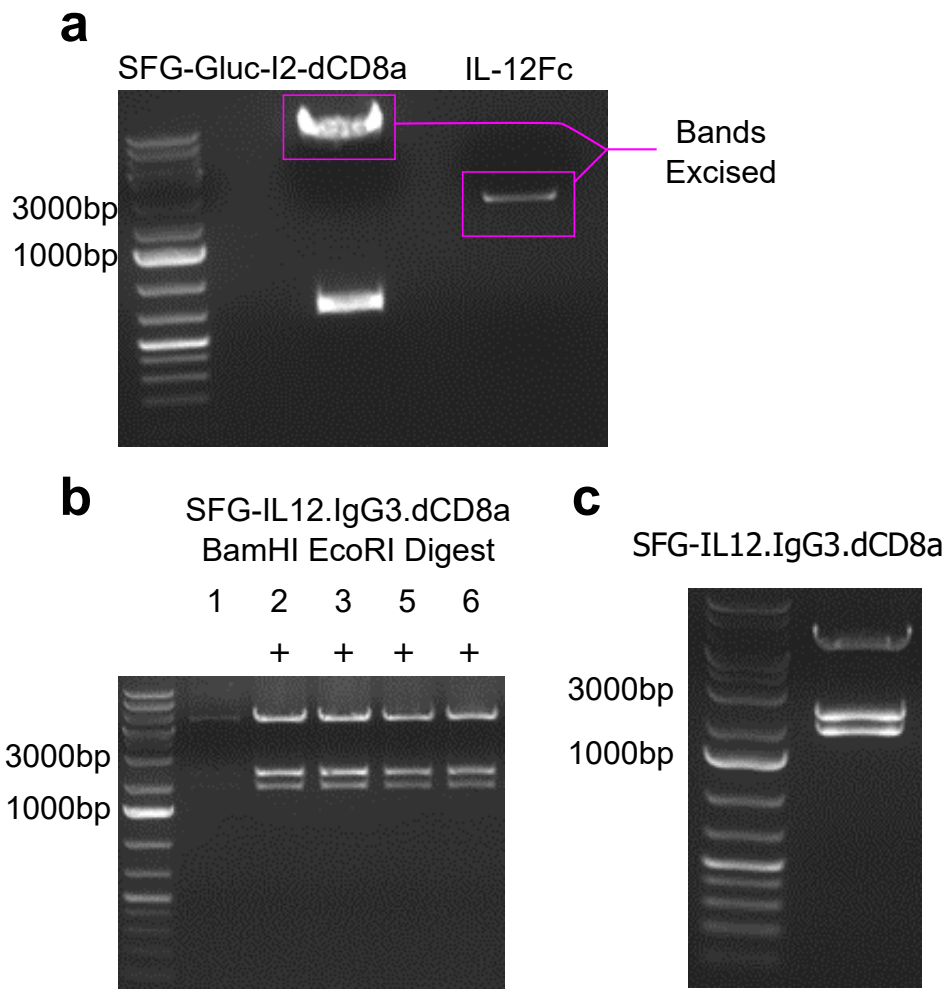

Figure 18: Construction of SFG-IL12.IgG3.dCD8a vector

An IL-12 Fc expressing retrovirus (SFG-IL12.IgG3.dCD8a) was produced as follows. The IL-12Fc sequence was cloned out of the IL-12Fc vector by PCR and SalI/MluI restriction sites were added (as per section 2.3.1, with p40_FW_SalI and Fc_RV_MluI primers as per Appendix Figure 63). 10ug of both the retroviral template (SFG-Gluc-I2-dCD8a) and IL-12Fc PCR product were digested with SalI and MluI restriction enzymes (as per section 2.3.2, using NEB buffer 3). Both digests were visualised on a 1% agarose gel (Figure 18a), DNA bands were excised and purified using Qiagen Gel extraction kits (as per manufacturer's instructions). The digested IL-12Fc insert was ligated into the digested SFG retroviral template (as per section 2.3.3). Ligated DNA was amplified by transformation of competent bacteria, 6 bacterial colonies were picked and mini-prepped (as per section 2.3.4). Extracted plasmid DNA from the 6 clones was analysed by restriction digestion (Figure 18b) with BamHI and EcoRI restriction enzymes (as per section 2.3.2, using NEB buffer 2). Clone 6 was selected, midi-prepped and BamH1/EcoR1 restriction analysis confirmed presence of the IL-12Fc insert (Figure 18c).

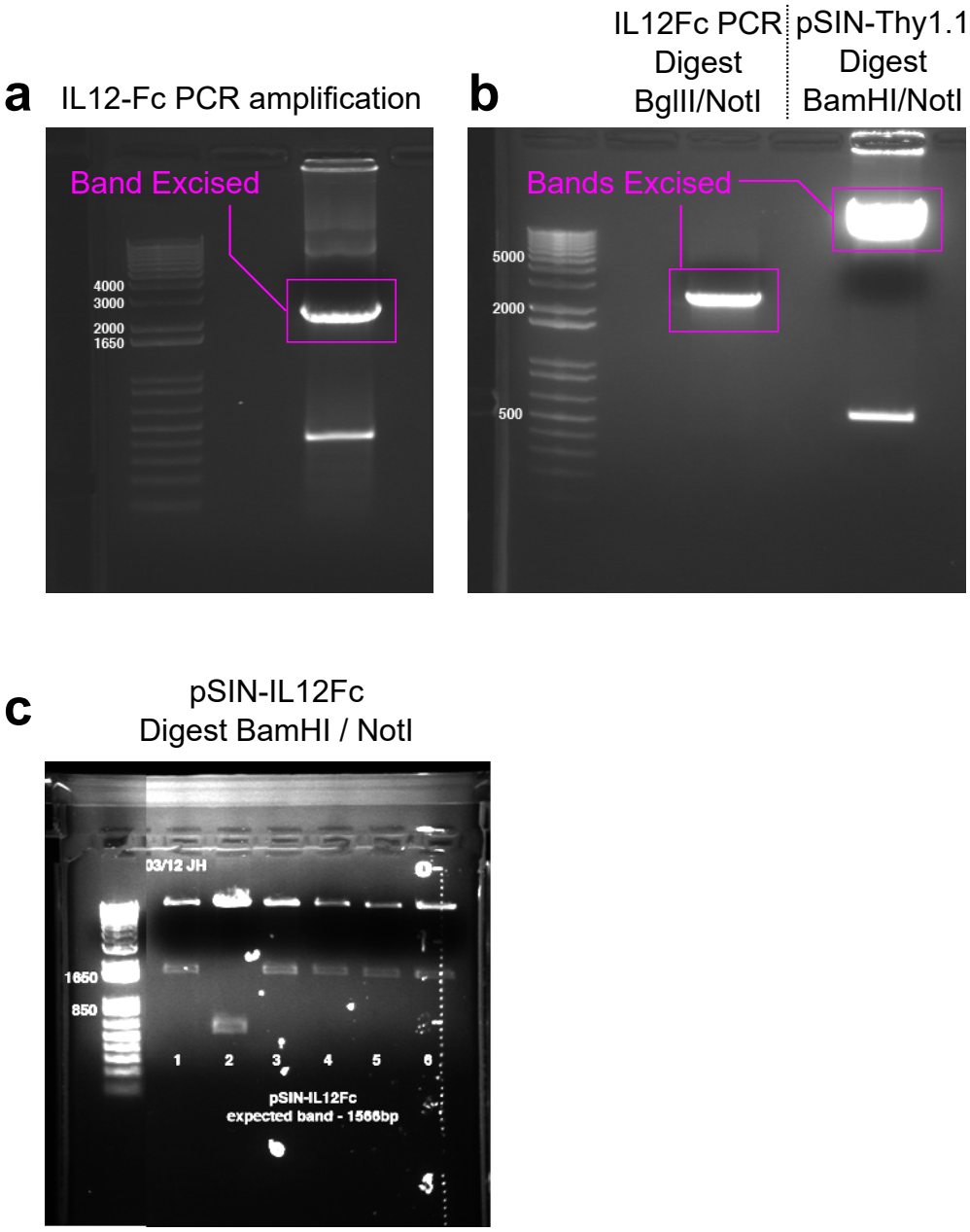

Figure 19: Construction of pSIN-IL12Fc (IL-12 LV) vector

Once the SFG-IL12.IgG3.dCD8a plasmid was created, the IL-12 Fc insert was then cloned into a lentiviral backbone (pSIN) as follows. Using the SFG-IL12.IgG3.dCD8a vector as a template, the IL-12Fc sequence was amplified via PCR (as per section 2.3.1, with p40_FW_BglII and Fc_RV_NotI primers as per Appendix Figure 63) and PCR products were visualised on a 1% agarose gel (Figure 19a), a DNA band (IL-12Fc insert) was observed at approximately 2000bp and excised. The IL-12Fc insert was digested with BglII & NotI restriction enzymes (as per section 2.3.2 using NEB buffer 3), and a pSIN-Thy1.1 lentivirus template (Figure 16) was digested with BamHI & NotI restriction enzymes (as per section 2.3.2 using NEB buffer 3). These digests create compatible cohesive ends that will allow ligation of the IL-12Fc insert into the digested pSIN template. Both digest products

were visualised on a 1% agarose gel and expected bands were observed and excised at approximately 2000bp (IL-12Fc) and >5000bp (pSIN) (Figure 19b). The pSIN-IL12Fc lentiviral (Figure 17, IL-12 LV) vector was finally created by ligating the digested IL-12Fc insert into the digested pSIN template (as per section 2.3.3). Competent bacteria was transformed with ligated DNA (as per section 2.3.4) and 6 colonies were midi-prepped and analysed via BamHI/NotI restriction digestion (as per section 2.3.2, using NEB buffer3). Visualisation of DNA digests confirmed the presence of the IL-12 FC insert at approximately 1650bp (Figure 19c) in 5 colonies, and colony 6 was kept for future use.

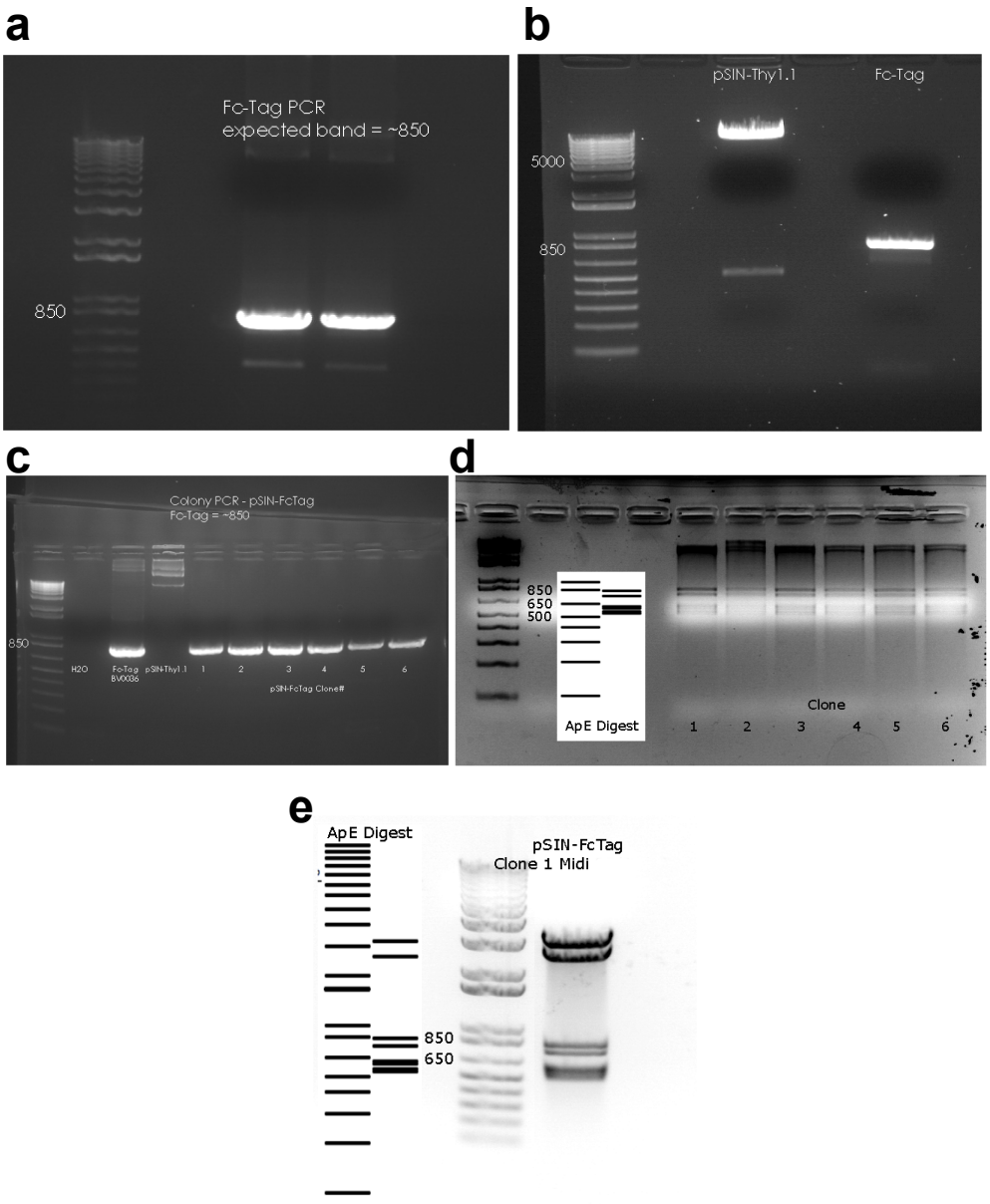

Figure 20: FcTag Gel-dock images

The control FcTag sequence was cloned out of the original expression plasmid

(also gifted from Burkhard Becher, Appendix Figure 61) via PCR with addition of BglII and NotI restriction sites (as per section 2.3.1). PCR products were isolated on a 1% agarose gel and FcTag insert DNA was observed at ~850bp (Figure 20a) and extracted (using Qiagen gel extraction kits as per the manufacturers instructions). Template pSIN-Thy1.1 plasmid was digested with BamH1 & NotI restriction enzymes (as per section 2.3.2, using NEB buffer 3) while the FcTag PCR fragment was digested with BglII & NotI restriction enzymes (as per section 2.3.2, using NEB buffer 3). Both DNA digests were isolated on a 1% agarose gel, expected bands were observed and excised at >5000bp and ~850bp respectively (Figure 20b). The digested FcTag fragment was then ligated into the digested pSIN plasmid using T4 DNA ligase (as per section 2.3.3) and competent bacteria was transformed with the ligated DNA (as per section 2.3.4). Bacterial colonies were isolated and PCR was performed to confirm presence of FcTag insert (Figure 20c). Restriction analysis was performed on each clone by digestion with HindIII restriction enzyme (as per section 2.3.2, using 2ul of HindIII enzyme only and NEB buffer 2), and predicted bands were observed in each clone (Figure 20d). Clone 1 was selected for use, was midi-prepped and a final HindIII restriction analysis was performed with expected bands observed (Figure 20e) confirming integrity of the pSIN-FcTag (FcTag LV) plasmid (Appendix Figure 62).

3.2 Cytometric evaluation of viral titre

IL-12 LV and FcTag LV lentiviruses were titrated onto HEK293T cells (as per section 2.3.5) for the estimation of viral titre. Transduced cells were incubated with brefeldin-A (BD Golgi Plug, 1μl per well) for 4 hours at 37 ℃. Cells were harvested, transferred to 1.5ml eppendorf tubes and pelleted by centrifugation (450 RCF, 5min, 4℃). Cells were then resuspended in 200μl FACS buffer and transferred to 96-well plates for intracellular staining.

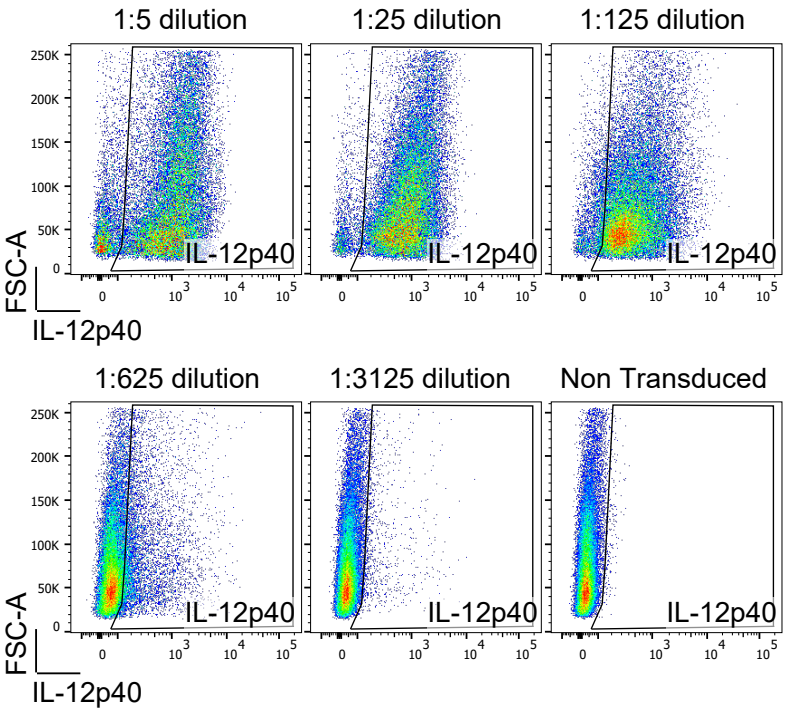

Figure 21: IL-12 LV transduction of HEK293T cells
Example of lentiviral vector titration by transduction of HEK293T cells with a serial dilution of IL-12 LV. Quantification of transduced, IL-12p40 expressing, cells was measured by flow cytometry and viral titre was calculated.

Intracellular detection of IL-12p40 (Figure 21) or mouse IgG (Figure 22) (for IL-12 LV or FcTag LV transduced cells respectively) was performed by resuspension of cells in 100µl BD Fixation/Permeabilization buffer (Perm buffer) and incubated covered on ice for 30min followed by centrifugation. Cells were resuspended in 50µl of 1x BD Perm Wash containing anti-IL-12p40/anti-IgG (refer to section 2.7.2) and incubated on ice for 30min followed by centrifugation. Cells were washed 3x with 1x BD Perm/Wash and resuspended in 200µl FACS buffer for analysis on an LSR II Fortessa flow cytometer (BD).

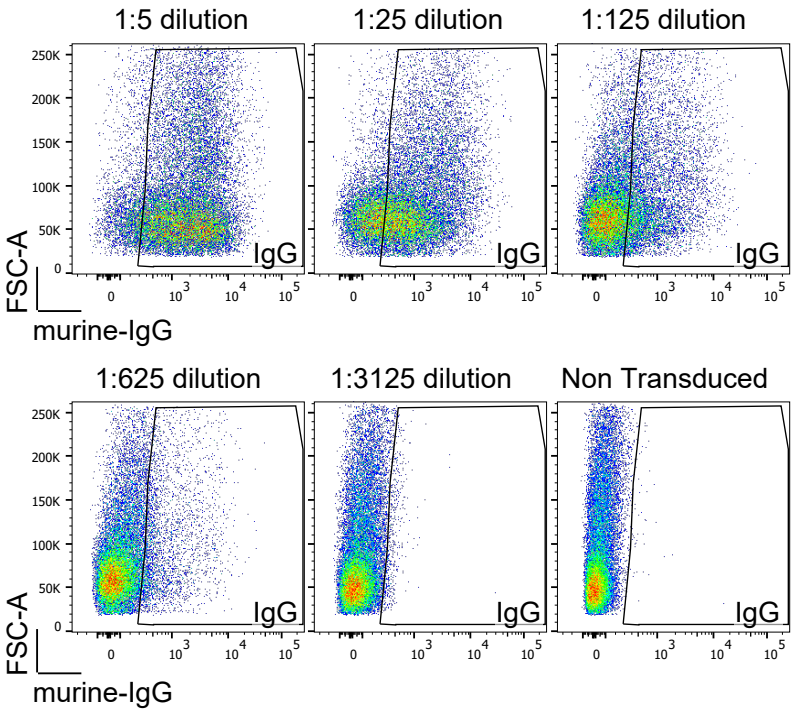

Figure 22: FcTag LV transduction of HEK293T cells

3.3 Lentiviral vectors transduce alveolar macrophages *in vivo*

MacDonald *et al* have previously demonstrated effective in vivo lentiviral transduction [152]. In this study an influenza peptide encoding lentivirus was intranasaly administered to naïve C57BL/6 mice. Effective *in vivo* transduction of alveolar macrophages produced an *in situ* influenza peptide vaccine that protected these mice from subsequent influenza infection. Given the reported high toxicity of systemically administered IL-12, we hypothesised that intranasal administration of an IL-12 encoding lentiviral vector could deliver IL-12 to the lung tumour microenvironment in a similar fashion.

To assess the efficacy of locally delivered lentivirus, IL-12 LV and a reporter eGFP LV was delivered via intranasal injection (i.n) 11 days post intravenous administration of 1.5 x 10^5 B16.F10 melanoma cells. Eight days after lentiviral administration (Day 19), bronchoalveolar lavage (BAL) was performed, aspirates collected and lungs were harvested. Identification of eGFP expressing cells in isolated pulmonary leukocytes was performed by flow cytometry (FACS). The following populations were identified: T cells ($CD3^+$), Alveolar macrophages (Alveolar MΦ, $CD45^+CD11c^{high}CD11b^{int/low}$), $CD11b^{hi}$ (including macrophages, $CD11b^+$ DCs and monocytes), $CD11b^{int}$ (including NK cells), $I\text{-}Ab^+CD11b^-$ (including B cells and $CD103^+$ DCs), $I\text{-}Ab^-CD11b^-$ and $CD45^-$ cells (including epithelia) (Figure 23a).

In vivo lentiviral transduction was restricted to alveolar macrophages with 21%

(figure 23c) & 25% (figure 23d) transduction (in BAL and Lung respectively) when treated with eGFP LV alone. Combination of eGFP LV and IL-12 LV resulted in transduction efficiencies of 6% (figure 23c) and 19% (figure 23d) in BAL and Lung derived alveolar macrophages, a significant decrease when compared to single eGFP LV administration that may be due to viral competition as described by Pinky & Dobrovolny [192].

These data support the use of lentivirus and their preferential transduction of alveolar macrophages for the localized delivery of payload (i.e. IL-12) into the lung microenvironment.

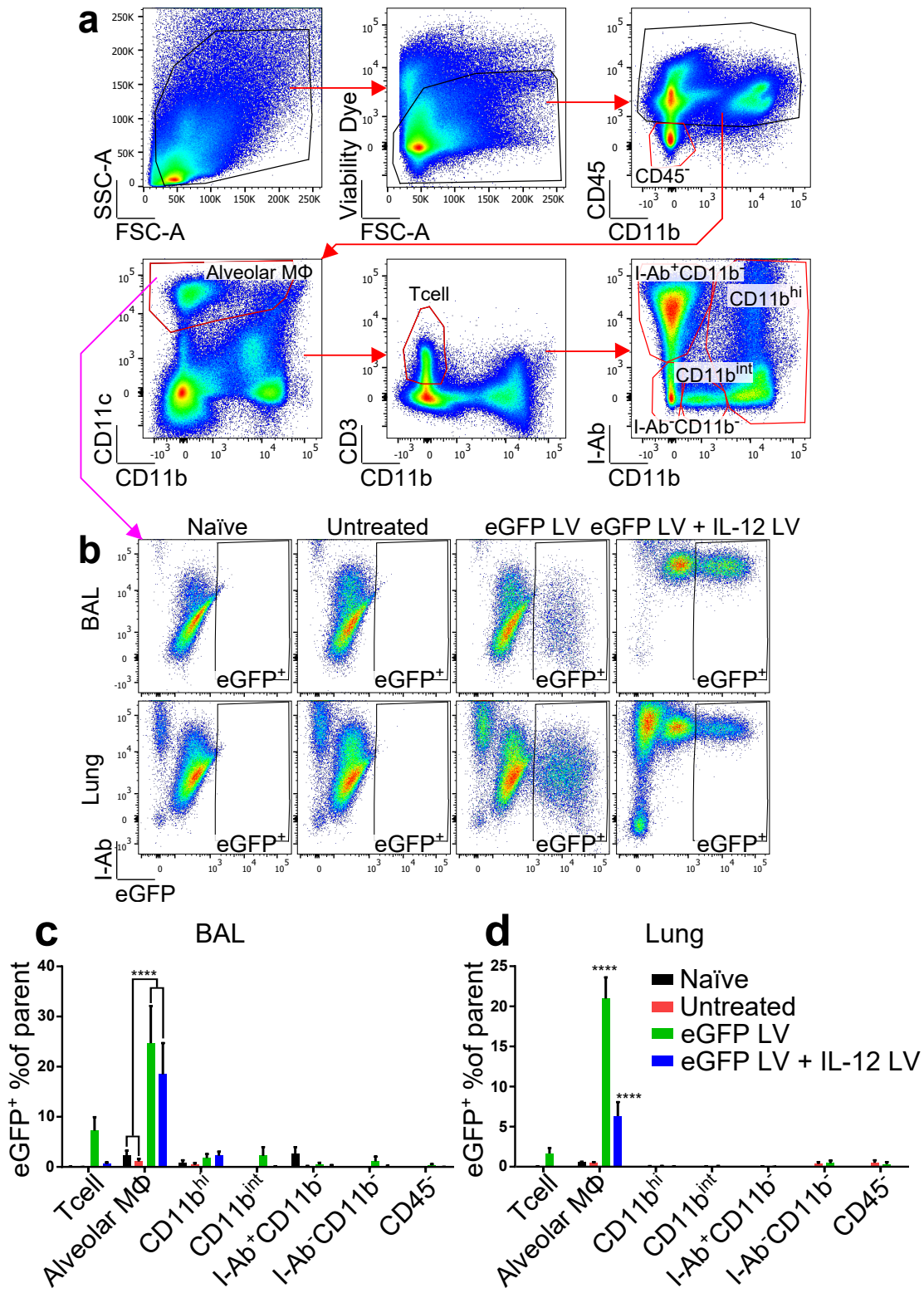

Figure 23: Lentiviruses transduce Alveolar Macrophages *in vivo*
Tumour bearing mice received GFP LV +/- IL12 LV. Bronchoalveolar lavage (BAL) and lungs were collected on day 19. (a) FACS analysis identifies cell subpopulations including Alveolar Macrophages (MΦ, b). Transduction of each population was measured as eGFP expression, and transduction of Alveolar MΦ was observed in BAL (b,c) and lungs (b,d). ****p<0.0001, 2-Way ANOVA with Tukey's post. n=6

3.4 IL-12 LV promotes rejection of established metastatic melanoma

We evaluated whether local delivery of IL-12 LV could mediate tumour rejection in a model of metastatic melanoma. We used the poorly immunogenic B16.F10 melanoma model, which is known to grow aggressively in the lung after intravenous (i.v.) injection into C57BL/6 mice [196]. In order to accurately quantify tumour burden, we used a firefly luciferase-eGFP-expressing B16.F10 cell line (B16.F10.eGFP), allowing enumeration of $eGFP^+$ tumour cells by flow cytometry. This cell line was used in all subsequent experiments involving cytometric evaluation of tumour burden.

IL-12 LV and a control FcTag LV was administered 11 days post tumour challenge and lungs were harvested for tumour burden analysis on day 21 (Figure 24).

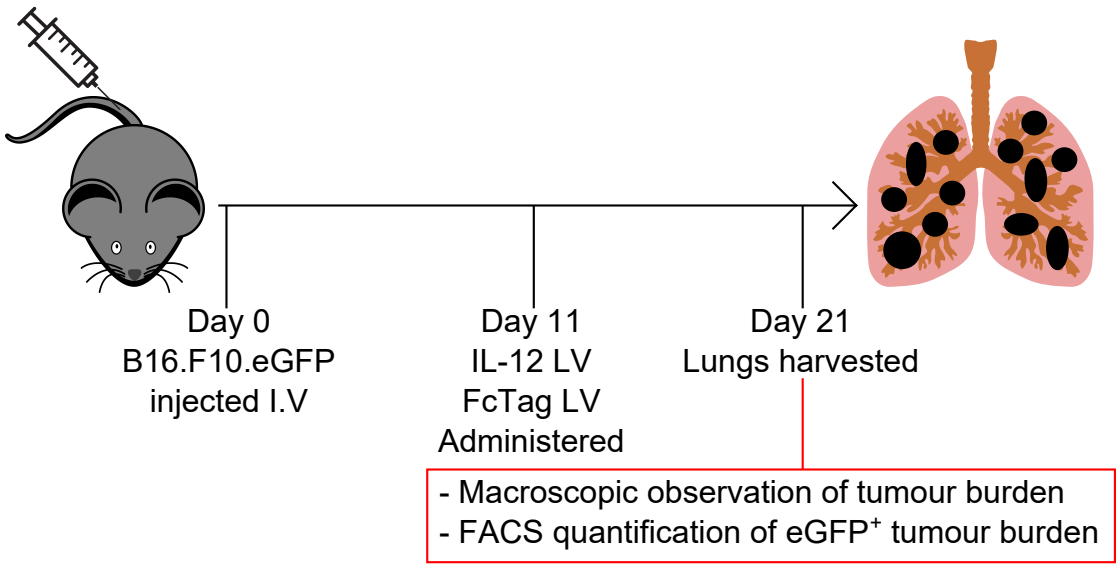

Figure 24: Lentivirus Therapeutic schedule

A striking reduction of metastasis was macroscopically observed in IL-12 LV treated mice and not FcTag LV treated mice (Figure 25a). Lungs were disaggregated and tumour burden was measured by flow cytometric analysis of eGFP expressing tumour cells (Figure 25b), the quantification of which (Figure 25c) showed that IL-12 LV therapy significantly reduced $eGFP^+$ tumour burden to levels not significantly higher than non-tumour bearing naïve controls.

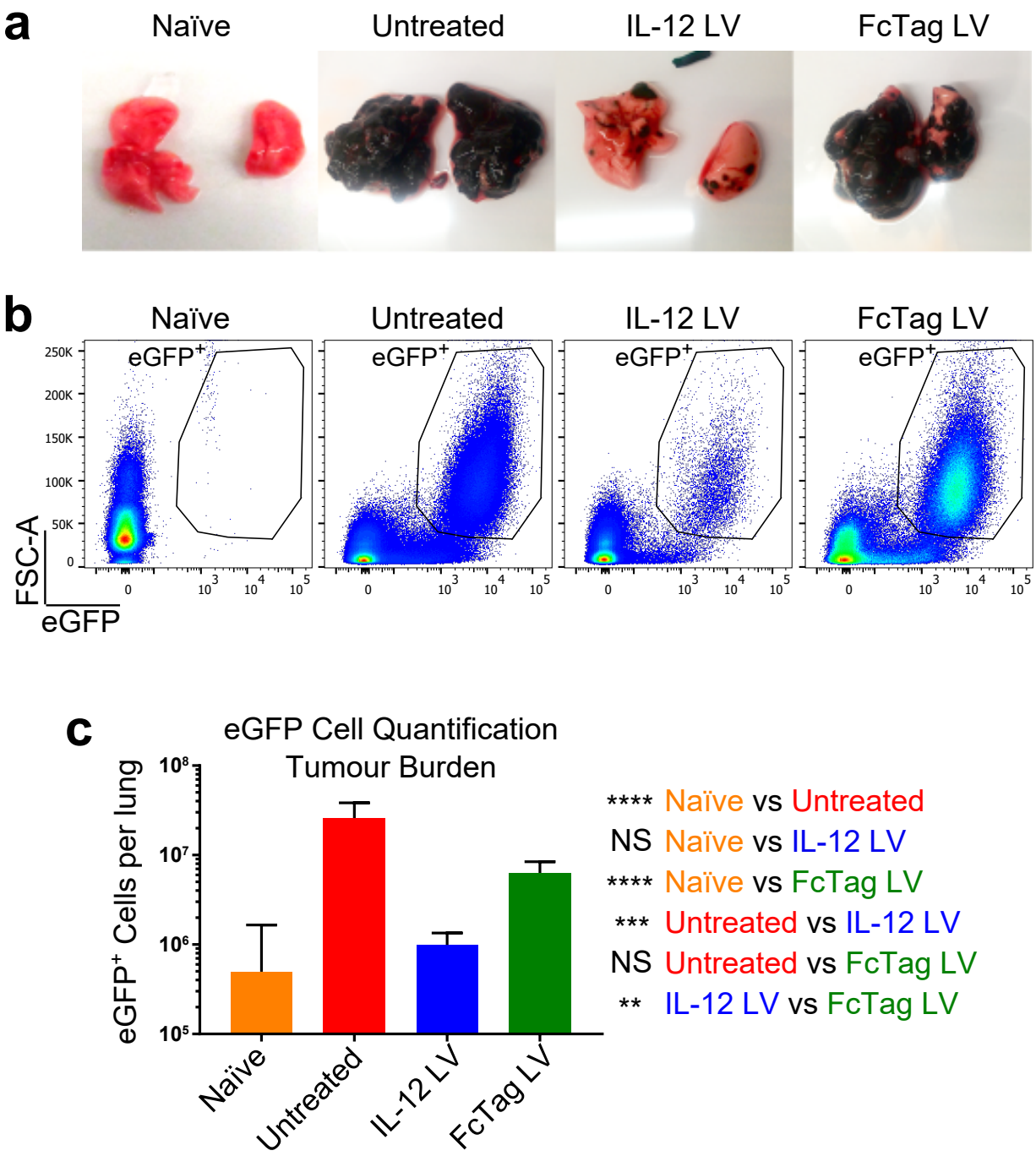

Figure 25: Locally delivered IL-12 LV eradicates established lung metastases Macroscopic observation (a), flow cytometric identification and (b) quantification ± S.E.M (c) of eGFP⁺ tumour cells from lungs treated of naïve [n=20], untreated [n=36], IL-12 LV treated [n=39] and FcTag LV treated [n=19] mice. NS p>0.05m **p<0.01, ***p<0.001, ****p<0.0001. Kruskal-Wallis test of non-parametric data with Dunn's test multiple comparisons from 9 independant experiments.

3.5 IL-12 therapy rejects parental B16.F10 cell line and KPB6.F1 lung carcinoma metastases

To confirm that the tumouricidal activity of IL-12 LV therapy was not restricted to the B16.F10 model or a function of GFP immunogenicity [72, 222], we repeated IL-12 LV therapy in mice challenged with the parental B16.F10 cell line (from which the B16.F10.eGFP cell line was produced) and in mice challenged with the KPB6.F1 tumour cell line derived from lung tumours induced in *K-ras*$^{LSL\text{-}G12D/+}$;*p53*$^{fl/fl}$ mice [56] (see methods section 2.1).

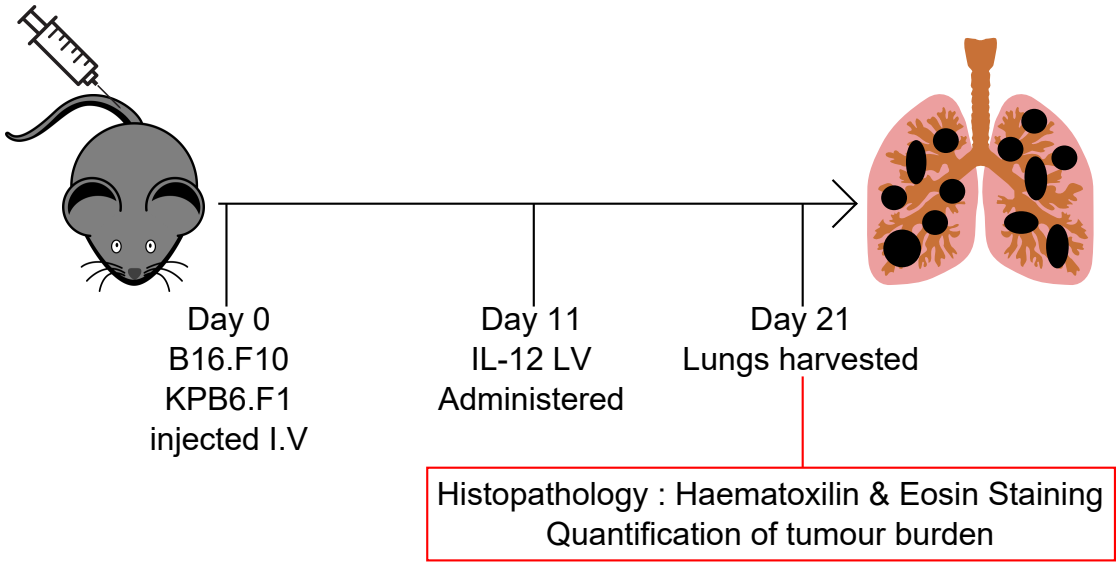

Figure 26: Therapeutic Schedule for Histopathology

Mice were culled on day 21 (as per Figure 26), lungs were harvested and processed for histopathology as described in section 2.5. Analysis of high resolution scanned H&E slides reveals a marked decrease in the number of tumour lesions, the size of each tumour lesion and the average tumour area (both gross and as a proportion of whole lung) in B16.F10 or KPB6.F1 bearing IL-12 LV treated mice when compared to untreated mice (Figure 27a). The average tumour-to-whole lung area ratio was calculated from 3 slides collected from each mouse and summarised as a Metastasis Index (Figure 27b) with the number of metastatic lesions forming the base of the Metastatic Number Index (Figure 27c), both indices (as originally described by [199]) displayed a significant decrease in tumour burden. These data recapitulates the previously presented eGFP^{+} tumour burden data in 2 tumour models that do not express eGFP.

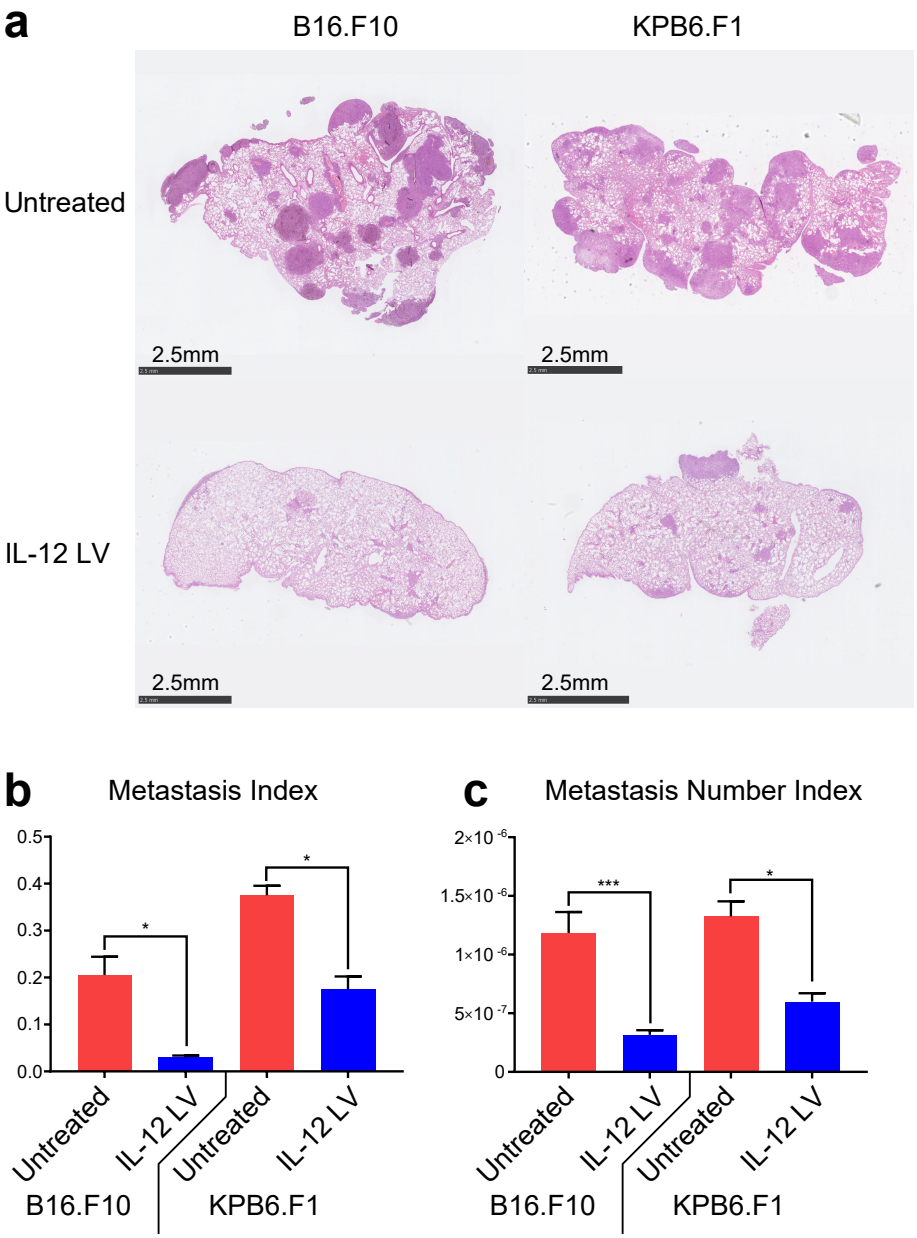

Figure 27: IL-12 LV eradicates established B16.F10 and KPB6.F1 metastases Representative heamatoxilin & eosin stained lung sections (a) from untreated and IL-12 LV treated mice bearing B16.F10 or KPB6.F1 pulmonary metastases. Bar graphs show average (± S.E.M) metastasis index (b) and metastasis number index (c) for each condition . *p<0.05,***p<0.001, n=6, Kruskal-Wallis test of non-parametric data with Dunn's test multiple comparisons, n=3.

3.6 Intranasal IL-12 LV mediates local protection from pulmonary metastases and long-term survival

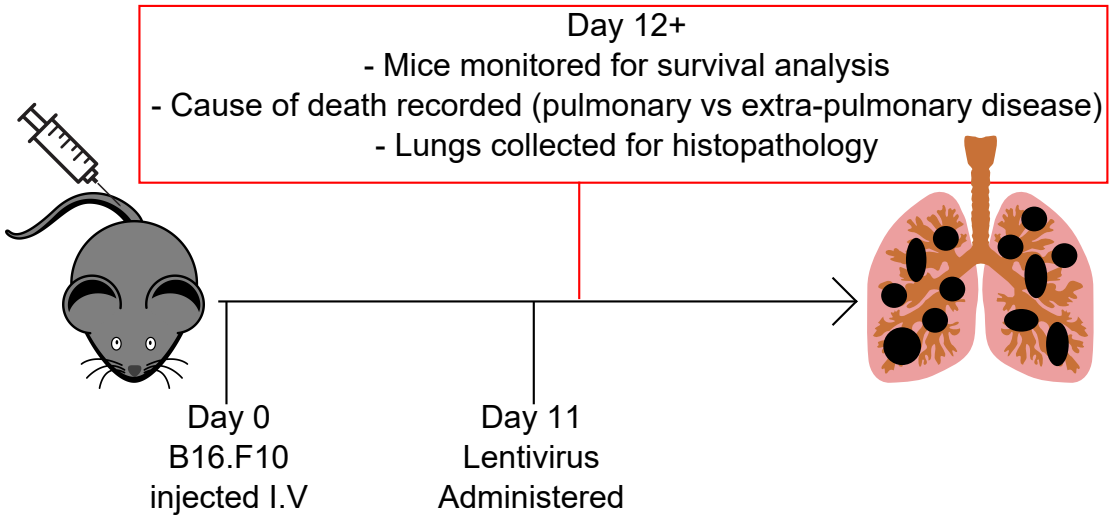

Figure 28: IL-12 LV survival experimental schedule

To determine the long-term impact of IL-12 LV treatment on tumour bearing mice we monitored survival over time. Median survival increased from 26 days in untreated mice to 49 days in IL-12 LV-treated mice (Figure 29a). 13.8% of IL-12 LV treated mice survived to day 100 whereas 100% mortality of untreated mice was observed by day 35 after tumour challenge. Although treated mice survived longer and their lungs remained tumour-free (Figure 29d), they eventually succumbed to extra-pulmonary disease, usually manifested as intra-abdominal or base-of-tail tumours. Cause of death was determined by macroscopic observation of lung tumour burden. Mice that were culled due to imminent respiratory failure, with a high observed tumour burden (for example, Figure 29c) were recorded as death by pulmonary disease. When mice were culled due to a poor clinical score (as described in section 2.4), and displayed little-to-no pulmonary disease (for example, Figure 29d) advanced distal metastases were observed and death was attributed to extra-pulmonary disease. In order to quantify these observations, analysis of competing risks [216] was performed and the probability of pulmonary associated mortality was significantly decreased in IL-12 LV mice (Figure 29b). In addition to the potency of the therapy, these data suggests that protection mediated by i.n delivery of IL-12 LV is restricted to the lung microenvironment.

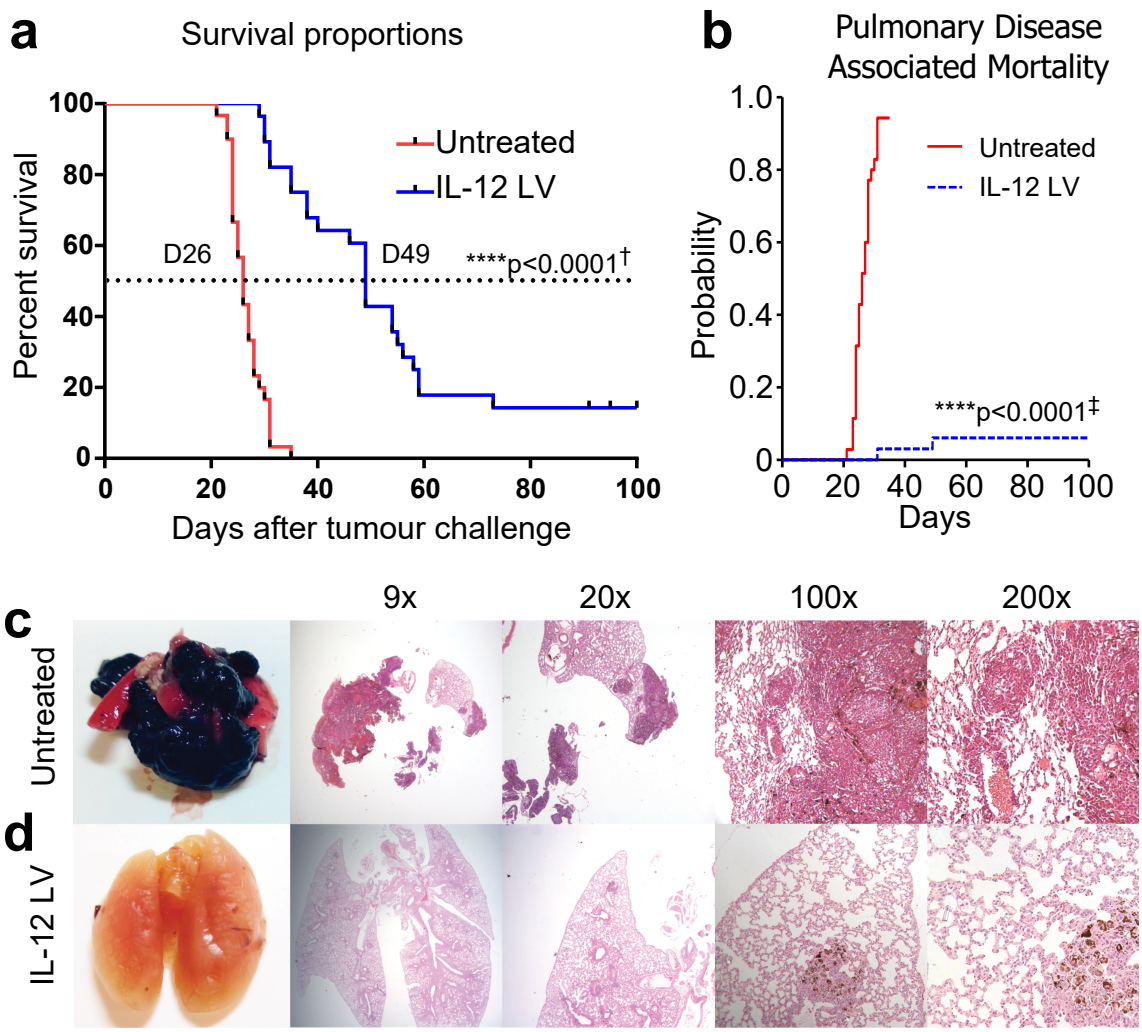

Figure 29: IL-12 LV therapy significantly improves long term survival Survival of untreated and IL-12 LV treated mice is presented as a Kaplan-Meier plot (a), with an analysis of competing risks from pulmonary disease associated mortality (b). Macroscopic and immunohistochemical examination of representative lungs taken from mice culled on respective median survival timepoints (c). ****p<0.0001†, Log-rank test, ****p<0.0001‡, Gray's *K*-sample test[86], n=30 from 6 independent experiments.

3.7 Results Section 3 Discussion

The results presented in this chapter demonstrate the successful integration of the IL-12Fc expression vector into the pSIN lentivirus plasmid thus creating the pSIN-IL12Fc construct, whilst simultaneously constructing a control pSIN-FcTag lentiviral vector.

Following lentiviral production, we validated the integrity of these new constructs by titration of concentrated lentiviral particles onto HEK293T cells. Flow cytometric (FACS) analysis of virally transduced HEK293T cells confirmed overexpression of IL-12p40 and murine IgG on IL-12 LV and FcTag LV transduced cells respectively.

Once competent lentivirus had been made, we demonstrated that lentiviruses may transduced Alveolar Macrophages (AM) in situ. This was achieved by FACS analysis of the lung microenvironment and bronchoalveolar aspirants (BAL) of tumour bearing mice that had received intranasally delivered eGFP expressing and IL-12 expressing lentiviruses.

Previous work has shown that when 500ng/kg of recombinant IL-12 is administered intravenously to patients, serum concentrations peak at approximately 10ng/ml and drop 10-fold over a 24-hour period [12]. The ability to target the pulmonary tumour microenvironment coupled with the persistent nature of lentiviral transduction may provide better bio-distribution of IL-12 than the administration of recombinant (or fusion) IL-12, making this approach an attractive one for clinical evaluation.

Alveolar Macrophage activation was observed in IL-12 LV treated mice (as evidenced by increased I-Ab expression) and confirms results previously published by MacDonald *et al*. This effect was restricted to therapeutic conditions that included IL-12 LV (and not GFP LV alone), indicating AM activation as a consequence of payload expression (in this case IL-12), and not in direct response to lentiviral transduction.

Further investigation of this model would ideally include the *ex vivo* analysis of IL-12 production by IL-12 LV transduced AM and would involve isolation of AM from IL-12 LV transduced pulmonary suspensions and BAL with subsequent ELISPOT assay or intracellular FACS detection of IL-12p40. FACS characterisation of AM would be improved by the addition of SiglecF to the FACS panel and as such there is a possibility that the existing AM gate as defined in figure 23a may contain contaminating $CD11c^{+}$ dendritic cells (DC). Evidence of $CD11c^{+}$DC contamination in

this gate may be present in figure 23b (lower panel) where two populations of I-Ab^{+}eGFP^{-} cells are observed and autofluorescent AM may be distinguished from non-autofluorescent CD11c^{+}DC (read as eGFP intermediate and negative populations respectively). It could be postulated that that such a refinement would eliminate contaminating CD11^{+}DC from the AM gate and consequentially may increase the measured relative frequency of eGFP transduced AM.

Having demonstrated that our IL-12 LV construct may generate competent viral particles, that such viral particles force IL-12 expression in transduced cells and that the lentivirus is capable of transducing AM *in vivo*, we then characterised the therapeutic efficacy of IL-12 LV in three models of pulmonary metastasis.

The first model established pulmonary metastases via intravenous (iv) injection of eGFP^{+} B16.F10 melanoma cells. Here we establish a model of pulmonary metastasis that can be rapidly evaluated by FACS analysis using less than 2% of the pulmonary lung suspension whilst the remaining 98% of lung suspension may be used for immunophenotypic FACS analysis. The relative strength of this output led us to use this model in subsequent mechanistic analyses.

Previous studies have discussed the immunogenicity of GFP in murine models [231], and eGFP tolerence in C57BL/6 mice (compared to BALB/c mice) [222]**.** Forced expression of eGFP by our tumour cell line B16.F10 had no apparent effect on tumour growth kinetics where intravenous injection of wild type B16.F10 or B16.F10.eGFP cells in treatment naïve mice resulted in pulmonary failure within 26 days.

Tumouricidal responses in this first model may be directed toward tumour cells expressing exogenous eGFP antigen. To control for this effect, we established a second experimental B16 metastasis model using the parental wild type B16.F10 cell line that does not express eGFP. A histopathology method of tumour burden quantification (as previously described by Qian *et al* [199]) was employed as cytometric enumeration of tumour burden was not possible without a reporter (such as eGFP). This method of tumour quantification retains the architecture of the lung and allows determination of factors that cannot be measured by FACS such as the number of discreet metastatic lesion as well as the absolute size of the tumour mass and it's relative size in relation to the gross size of the entire lung. This model of tumour growth was additionally employed to generate the long term survival data presented in this study.

Finally, a third model was established in parallel to the second model described above. This third model involves the intravenous injection of the KPB6.F1 cell line as established in the Quezada group. This cell line is derived from tumours induced by intranasal application of cre-recombinase expressing adenovirus to *K-ras$^{LSL\text{-}G12D/+}$;p53$^{fl/fl}$* (K-ras/P53) mice. Over an 8 week period, these mice went on

to develop lungs tumours which were then isolated and passaged to establish the KPB6.F0 line from which the KPB6.F1 cell line was derived. The efficacy of IL-12 LV in this model was also evaluated by histopathology methods as described above and the results of which are presented in section 3.5. We found that IL-12 LV effectively controls pulmonary metastases in these three models and confers a significant survival advantage in the B16.F10 model.

The 'experimental metastasis' model of intravenously injected tumour cells as previously described by Talmudge and Fidler [235] was selected for this study on the basis of reliability, reproducibility and fast tumour growth kinetics. These features lead to rapid and reproducible experimental outcomes in this study. The disadvantage of such a system is that it does not model tumour extravasation from the site of primary disease, an integral feature of cancer metastasis. Nor does it accurately model the slow rate (and associated angionegenesis/fibroblast integration) that would be observed in a higher-fidelity model. An interesting addition to these experiments may be a time course model to determine the kinects of tumour growth under IL-12 LV, though may prove difficult given the small therapeutic window presented in this model.

The 4T1 metastasis model (as described by Yang *et al* [275]) may be an ideal addition to the models described above as it involved extravasion of tumour cells from the site of implantation (mammary fat pad) to the lungs. This model is often combined with surgical resection of the primary tumour so that long term treatment of secondary lung metastases may be studied. It could be argued however that either the intravenous or 4T1 methods discussed here are appropriate models for this study as the nature of our IL-12 LV therapy is restricted to the pulmonary compartment for the treatment of established pulmonary metastases regardless of their source. This argument is, however, predicated on the assumption that intranasally delivered IL-12 LV restricts IL-12 expression to the pulmonary compartment. An interesting benefit of the 4T1 metastasis model would additionally allow observation of IL-12 LV responses to primary tumour and secondary metastases where not only would both sites of malignancy be analysed for mechanistic determinants and viral transduction, but blood sera would be collected for analysis of soluble IL-12.

Although not included in this study, orthotopic lung cancer models would be an ideal addition as the kinetics of primary pulmonary tumour growth drastically differ from the metastatic model employed in this study. Appropriate models would include orthotopic implantation (via intrapulmonary injection) of KPB6.F1 tumour cells or other established primary lung cancer cell lines (such as Lewis Lung Carcinoma). Alternatively, models of genetically induced primary pulmonary tumour growth may be pursued such as K-ras/P53 model as described above, however experimental data from a separate pilot study indicated that tumour growth kinet-

ics in this model was too variable and slow to be able to fully evaluate the efficacy of IL-12 LV and elucidate it's mechanism of action whilst requiring the use of specialised in vivo imaging equipment (eg. PET-CT) to monitor tumour growth.

It is important to note that while i.n. IL-12 LV promotes potent tumouricidal activity within the lung microenvironment, we did not observe similar effects outside of the targeted organ. IL-12 LV conferred a significant survival benefit to B16.F10 bearing mice, with <20% of mice surviving the 100-day duration of the experiment (Figure 29a) and tumouricidal activity appeared to be restricted to the pulmonary microenvironment (Figure 29b).

This observation likely reflects the local aspect of IL-12 LV therapy, as mice are protected from pulmonary disease long enough to allow additional metastatic lesions to establish at distal sites. Metastatic involvement at these sites is likely a consequence of the site of injection of tumour cells in this model near the site of injection and the draining nodal system (base of tail and within the abdominal cavity). These sites may be less significant in clinical practice, though distal sites of primary disease in patients with lung metastases may require additional therapeutic interventions.

Characterisation of extra-pulmonary metastases may be performed by flow cytometric assessment of leukocyte infiltration, activation and suppression. Whole exome sequencing of pulmonary and extra-pulmonary metastases from IL-12 LV treated (and untreated) mice may give insight into tumour heterogeneity & evolution [79], neoantigen expression [161] and immunoediting [103]. These insights may reveal therapeutic targets that could be exploited in combination with IL-12 LV.

Possible combination therapies may involve clinically relevant systemic immunotherapies targeting the adaptive immune compartment such as PD-1/PD-L1 blockade [46], CTLA-4 blockade/depletion [8, 221] and CD25 depletion [9]. Targeting the innate compartment may synergise with IL-12 LV mediated activation of macrophages and could include the use of TLR agonists [28] and CD47 blockade [242].

This section concludes with a finding that IL-12 LV is an effective therapy for the control of established lung metastases and confers a significant survival advantage with durable protection of the pulmonary compartment. The following results chapters will seek to resolve the mechanism of action through which IL-12 LV mediates tumour rejection via modulation of the pulmonary immune niche.

4 Investigating IL-12 responsive cytotoxic effector cells

The results presented in chapter 3 show the successful production of an IL-12 expressing lentivirus and a significant therapeutic benefit observed when used to treat established pulmonary metastases. We next sought to determine the mechanism by which IL-12 LV mediates tumouricidal activity in the lung tumour microenvironment.

Previous studies have shown that IL-12 exerts immunomodulatory effects either directly on cytotoxic lymphocytes ($CD8^+$ CTL and NK cells [143]) or via Th1 polarisation of lymphocytes and subsequent expression of IFNγ [106].

In this chapter we explore the cytotoxic and proliferative potential of $CD8^+$ CTL and NK cells in IL-12 LV treated mice. We then dissect the contribution of T cell and NK compartments to IL-12 LV tumouricidal activity via the use of cellular depletion strategies and genetically modified mice. We finally investigate the role of IFNγ and identify IFNγ express leukocytes in this model of IL-12 LV therapy.

4.1 IL-12 LV increased T cell and NK proliferation, potentiates cytotoxic activity in CD8+ T cells and NK cells.

Previous studies have shown that IL-12 mediates tumour destruction via activation of cytotoxic T cells [33] and NK cells [68]. We performed cytometric analysis of the T cell and NK compartments in order to determine whether the proliferative and cytotoxic capacity of NK and T cells had been affected by IL-12 LV therapy.

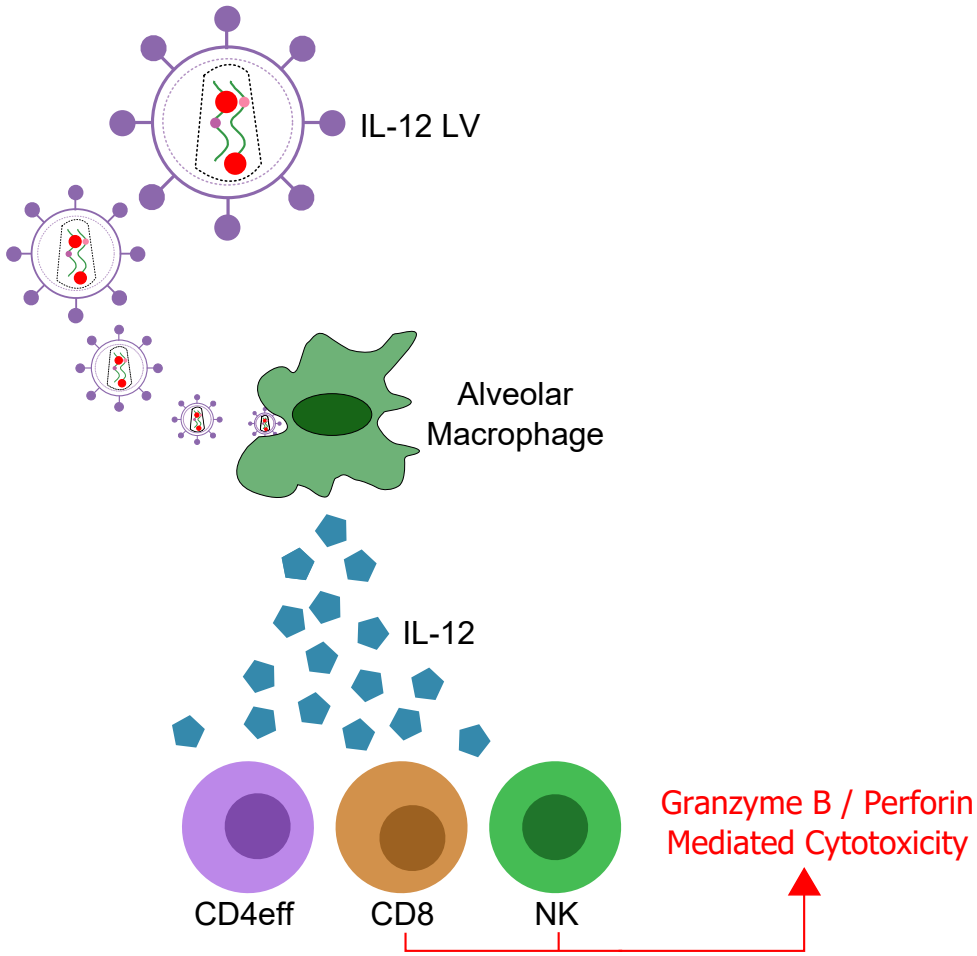

B16.eGFP cells were administered via intravenous injection to mice and IL-12 LV or FcTag LV was applied via intranasal injection 10 days post challenge. A subset of non-tumour challenged mice were kept as a naïve control. On the 21st day post tumour challenge (10 days post therapy), lungs were harvested for cytometric evaluation of NK cells ($CD3^{-}NK1.1^{+}$), $CD8^{+}$ T cells ($CD3^{+}NK1.1^{-}CD8^{+}CD4^{-}$), CD4 effector cells (CD4eff, $CD3^{+}NK1.1^{-}CD8^{-}CD4^{+}FoxP3^{-}$) and T regulatory cells (Treg, $CD3^{+}NK1.1^{-}CD8^{-}CD4^{+}FoxP3^{+}$) (Figure 30a). Expression of Ki67 (a marker of proliferation) was measured on each effector sub-set (Figure 30b). Expression of the cytotoxic molecule granzyme B (GzmB) was also measured (Figure 30b) on each population as GzmB de-granulation in conjunction with perforin a primary mechanism of NK & T cell mediated cytotoxicity [239]. CD4eff, CD8 and NK cell proliferation increased under IL-12 stimulation as evidenced by and expansion of each population as a proportion of live cells (Figure 31a), by total cell enumeration of each population (Figure 31b) and by Ki67 expression (Figure 31c). GzmB expression was also significantly increased (Figure 31d) on the NK and $CD8^{+}$ T cell cytotoxic sub-populations (cf. naïve, untreated and FcTag LV controls).

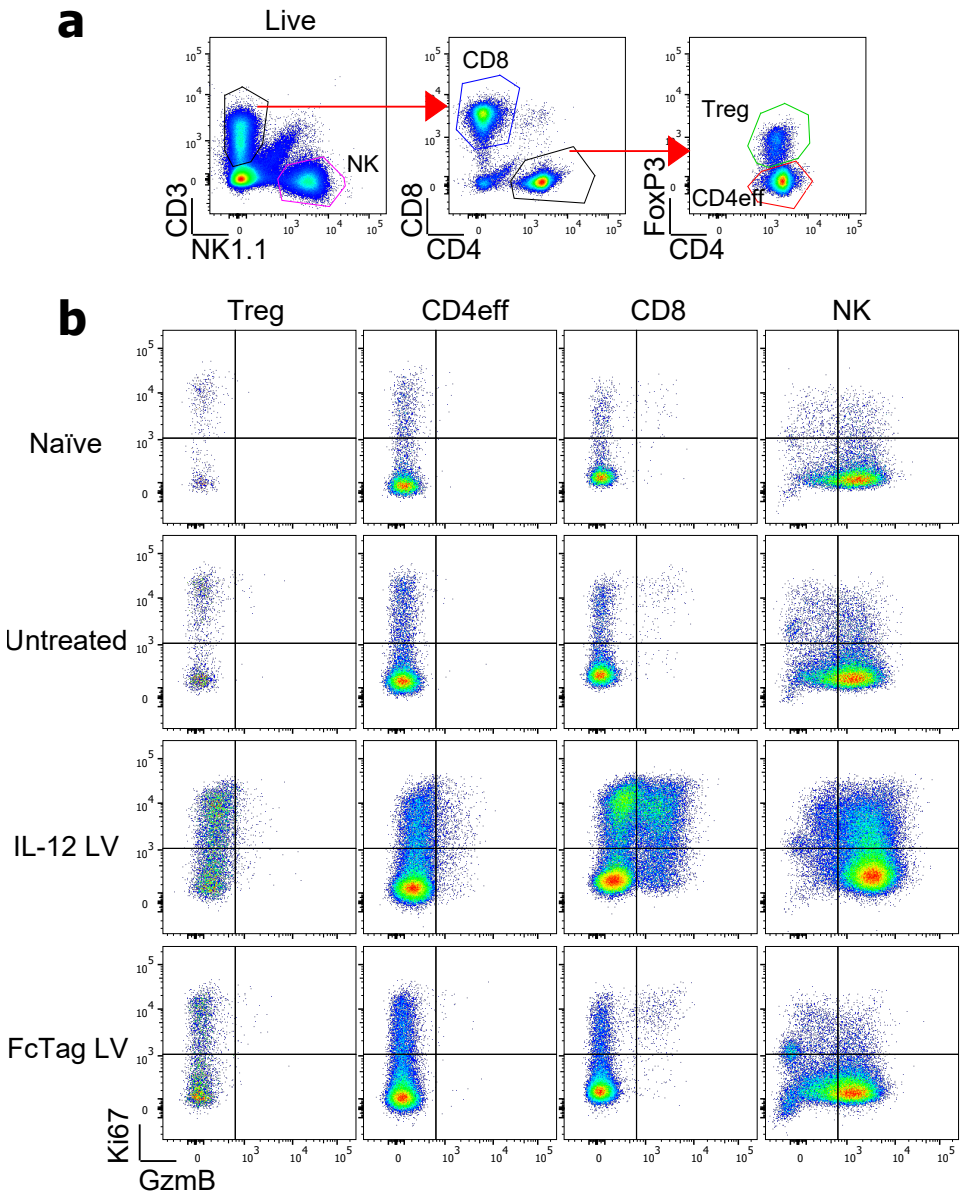

Figure 30: IL-12 LV therapy promotes T cell / NK proliferation & cytotoxic function. NK, CD8, Treg, and CD4 effector (CD4eff) T cells were identified via FACS analysis (a). Expression of the cytotoxic molecule Granzyme B (GzmB) and the proliferation marker Ki67 was measured on each cell population (b) from non-tumour bearing mice (Naïve), untreated mice and mice treated with IL12 LV or the FcTag LV control lentivirus.

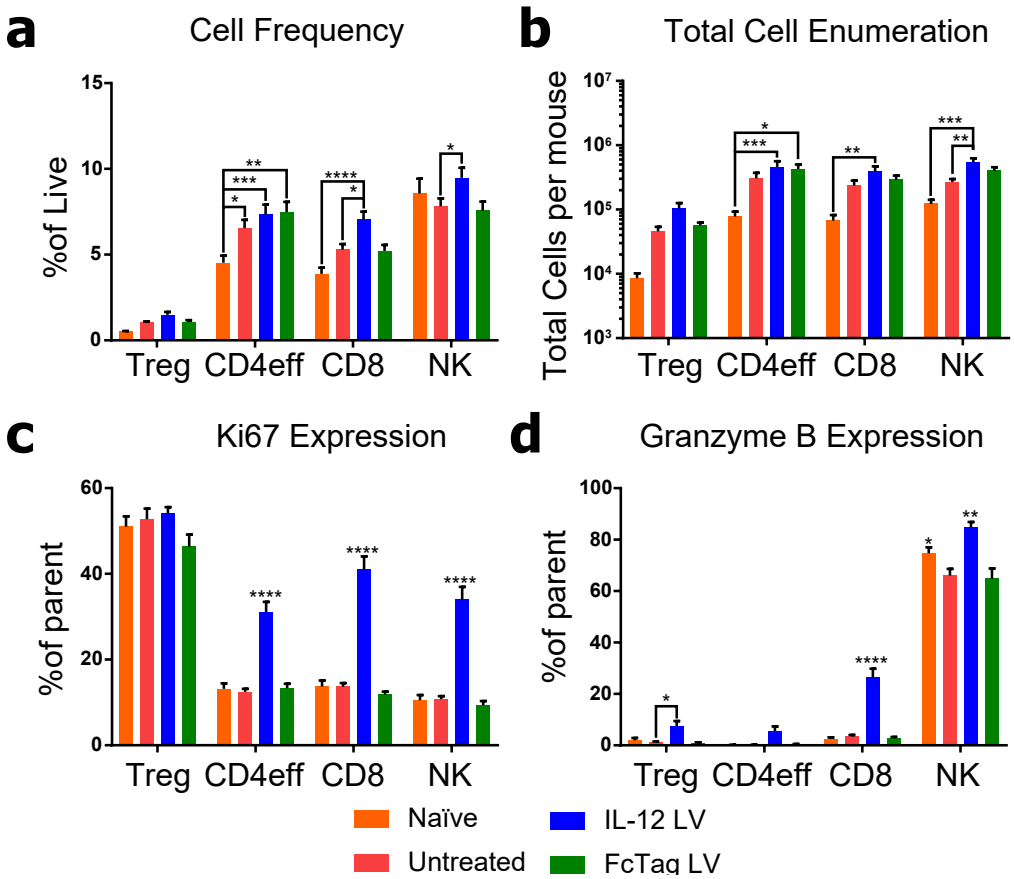

Figure 31: IL-12 LV significantly increases T cell/NK proliferation & cytotoxic function
FACS quantification of Treg, CD4eff, CD8 and NK cells was measured by percentage of total live leukocytes (a) and total cell enumeration (b). Proliferative and cytotoxic capacities of each population were measure by cytometric analysis of Ki67 (c) and Granzyme B (GzmB) (d) expression respectively. ****p<0.0001, ***p<0.001, *p<0.05, 2-Way ANOVA with Tukey post-testing, Naïve [n=14] Untreated [n=32], IL12 LV [n=29], FcTag LV [n=16] from 4 independent experiments. Error bars represent S.E.M

4.2 Tumouricidal activity of IL-12 LV is not mediated by T cells or Natural Killer cells

IL-12 is a bona fide activator of $CD8^+$ T cells and NK cells [143]. Having observed similar activation in this model of IL-12 LV therapy, we hypothesised that the absence of such cells would abrogate the observed tumouricidal activity of this therapy with an expected increase in pulmonary tumour burden in IL-12 LV treated mice.

To test this hypothesis, we performed the same experiment in T cell / B cell deficient *Rag*$^{-/-}$ mice, in which NK cells were depleted with an anti-NK1.1 (αNK1.1)

antibody (Figure 32a). Absence of lymphocytes and NK cell ablation were confirmed by flow cytometry (Figure 33a-e).

Macroscopic evaluation of gross tumour burden revealed that, IL-12 LV appeared to robustly reject established metastases in both the wild type and the T cell / NK deficient *Rag*$^{-/-}$ αNK1.1 mice (Figure 32b). This result was verified and quantified by cytometric enumeration of eGFP^{+} tumour cells isolated from disaggregated lungs, with a significant decrease in tumour burden measured in both IL-12 LV treated wild type and *Rag*$^{-/-}$ αNK1.1 mice (Figure 32c,d).

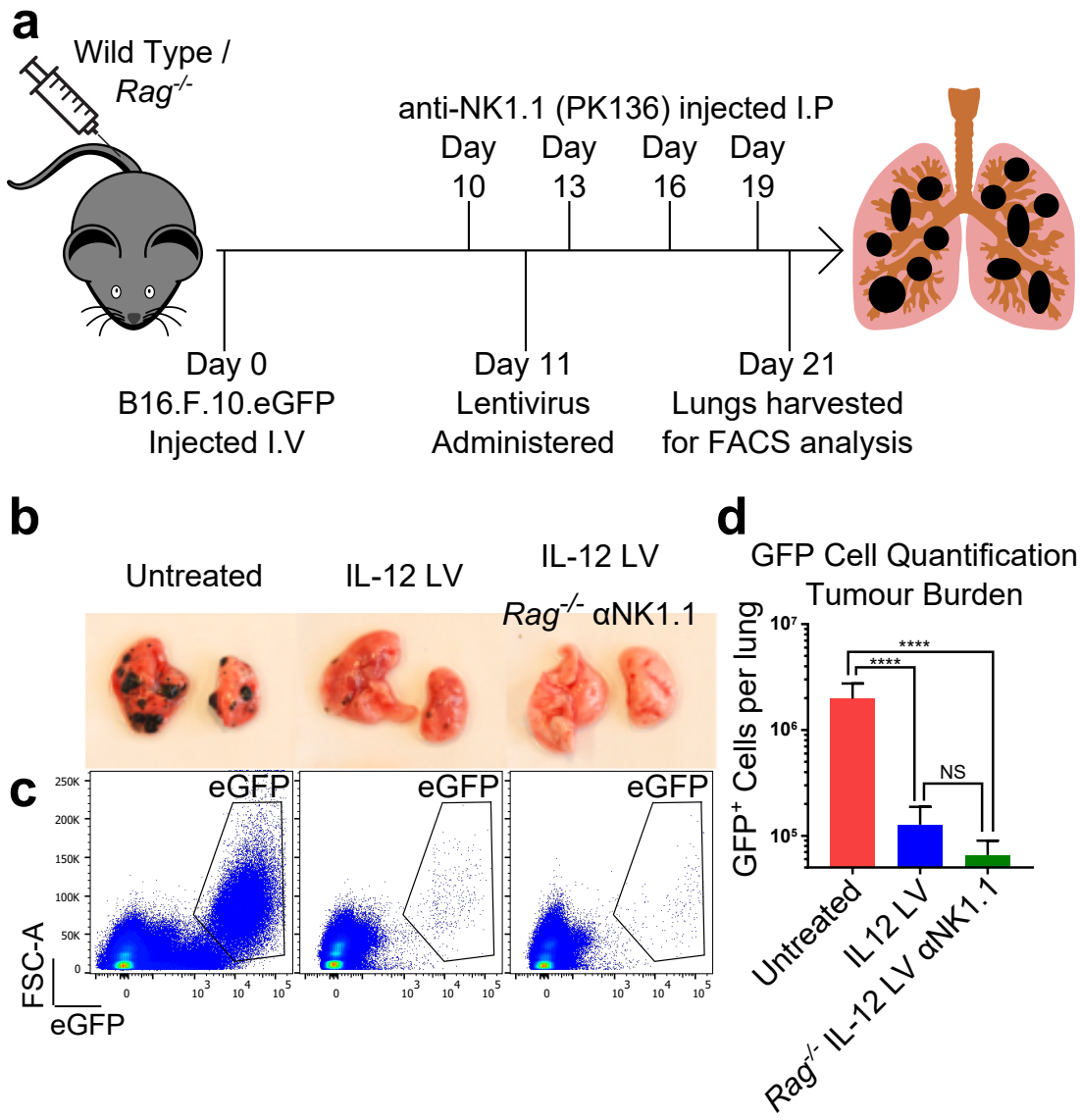

Figure 32: IL-12 LV mediates NK and T cell independent cytotoxic activity
IL-12 LV therapy was repeated in wild type and NK depleted *Rag*$^{-/-}$mice (a). Macroscopic observation (b) and cytometric (c) quantification (d) of eGFP^{+} tumour cells (± S.E.M). NS $p>0.05$, ****$p<0.0001$, Kruskal-Wallis test of non-parametric data with Dunn's post test, n=15 from 3 independent experiments.

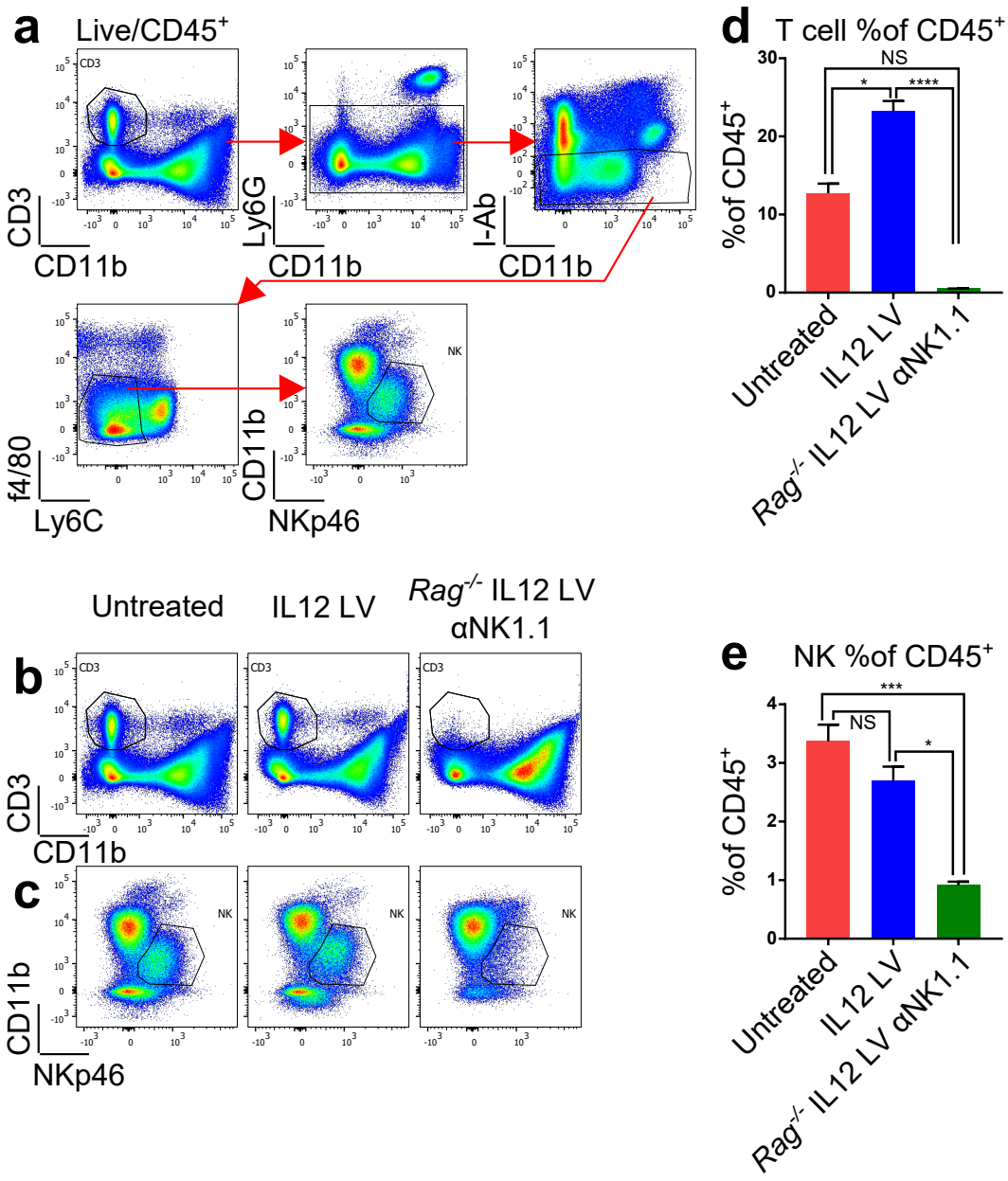

Figure 33: Confirmation of T cell/NK ablation in IL-12 LV treated mice FACS analysis (a) of the leukocyte compartment identified ablation of T cells ($CD45^+CD3^+CD11b^-$) (b,d) and NK cells ($CD45^+CD3^-Ly6G^-I\text{-}Ab^-f4/80^-Ly6C^-CD11b^{int}NKp46^+$) (c,e) in IL12 LV treated NK depleted *Rag*$^{-/-}$ mice. NS $p>0.05$, *$p<0.05$, ***$p<0.001$, ****$p<0.0001$. Kruskal-Wallis test of non-parametric data with Dunn's post test, n=15 from 3 independent experiments. Errors bars represent S.E.M.

4.3 IFNγ mediates tumouricidal activity of IL-12 LV therapy

Two primary functions of IL-12 have previously been described as an enhancement of NK & $CD8^+$ T cell cytotoxicity and the production of IFNγ by Th1 effector T cells [240]. Having precluded NK and T cells as the main contributors to cytotoxicity in this model of IL-12 LV therapy, we next sought to investigate the role of IFNγ in mice lacking cytotoxic $CD8^+$ T cells and NK cells. CD8/NK depletion and IFNγ neutralisation was acheived by co-administration of anti-IFNγ (αIFNγ, clone XMG1.2), anti-CD8 (αCD8 clone 2.43) and anti-NK1.1 (αNK1.1, clone PK136) monoclonal antibodies (Figure 34a). Macroscopic observation (Figure 34b) and FACS quantification (Figure 34c) of $eGFP^+$ tumour cells revealed a significant reduction of tumour burden in IL-12 LV treated mice (Figure 34d) regardless of the presence of $CD8^+$ or NK cells (recapitulating the previous result in a different model). A striking increase in tumour burden was macropscopically observed (Figure 34b) when IFNγ was neutralised in IL-12 LV treated, CD8/NK depleted mice. This results was quantified by cytometric enumeration of $eGFP^+$ tumour cells (Figure 34c) where tumour burden was significantly increased in IFNγ neutralised mice (Figure 34d)**.**

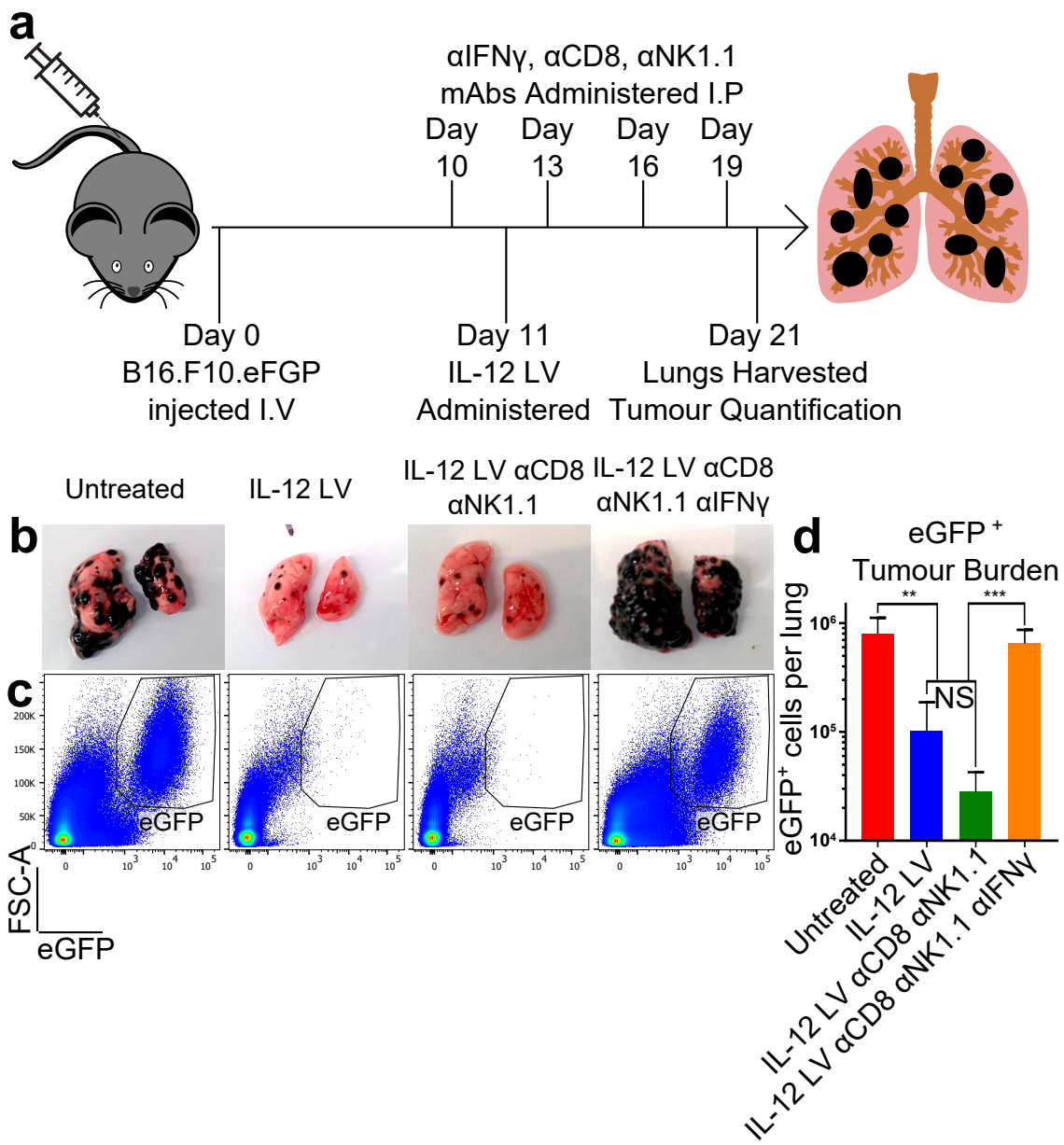

Figure 34: IFNγ neutralisation abrogates the tumouricidal activity of IL-12 LV therapy

Mice were treated with a combination of IL-12 LV, IFNγ neutralising and CD8/NK1.1 depleting monoclonal antibodies (a). Macroscopic evaluation (b) and cytometric (c) quantification (± S.E.M) of eGFP$^+$ tumour cells. **p<0.01, ***p<0.001, Kruskal-Wallis test of non-parametric data with Dunn's multiple comparison post-tests, n=15 from 3 independant experiments.

4.4 Identification of IFNγ expressing leukocytes in IL-12 LV treated mice.

Having demonstrated that IFNγ is an essential mediator of tumouricidal activity following IL-12 LV therapy, the canonical concept was that IL-12 receptor expressing T cells and NK cells were responding to IL-12 stimulation and producing IFNγ that in turn would mediated tumouricidal activity in our model. This is a well-defined pathway that presents an intriguing question in the context of our previous data, namely, which population (or populations) of cells express IFNγ in a T cells and NK deficient model of IL-12 stimulation?. We therefore performed flow cytometric analysis of tumour infiltrating leukocytes in order to identify the subpopulations of cells that express IFNγ in our model of IL-12 LV therapy.

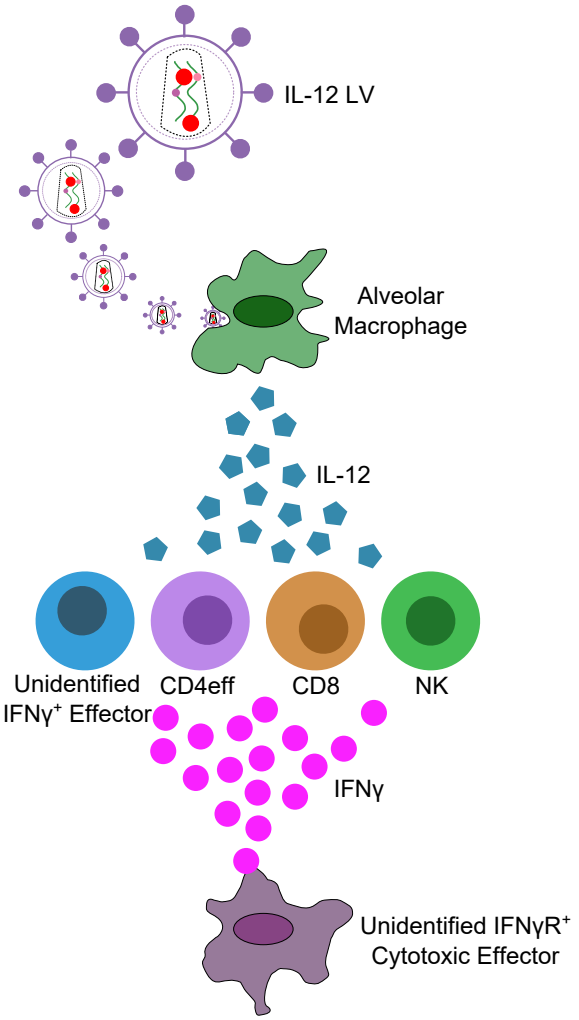

4.5 IL-12 LV induces IFNγ expression in NK, T cells and Lin$^-$NK1.1$^-$ cells

Tumour bearing mice were treated with IL-12 LV (untreated and FcTag LV conditions were used as negative controls) and lungs were harvested 21 days post challenge (Figure 35a). FACS analysis of Lin$^+$(CD3/CD19$^+$) CD90$^+$CD4$^+$ T cells, Lin$^+$CD90$^+$CD4$^-$ T cells, Lin$^-$NK1.1$^+$ NK cells and Lin$^-$CD90$^+$NK1.1$^-$ cells (Figure 35b) revealed IL-12 LV induced expression of IFNγ in all four populations (Figure 35c). IFNγ was co-expressed as a sub-population of T-bet$^+$ cells in each population. The frequency of IFNγ^+ cells within each population was significantly increased under IL-12 LV therapy (average 16% increase across populations and control groups)(Figure 36a) whilst the density of IFNγ expression (as measured by mean fluorescent intensity) was significantly increased in T cells and CD90$^+$NK1.1$^-$ cells, but not NK cells (Figure 36b). In order to ensure that no other sources of IFNγ were missed in this analysis, we re-analysed the data using an IFNγ-centric gating strategy. IFNγ^+ cells were gated from the total live population, T cell, NK and CD90$^+$NK1.1$^+$ cells were identified therein (Figure 36c). This gating strategy captured approximately 90% of all IFNγ^+ cells (Figure 36d).

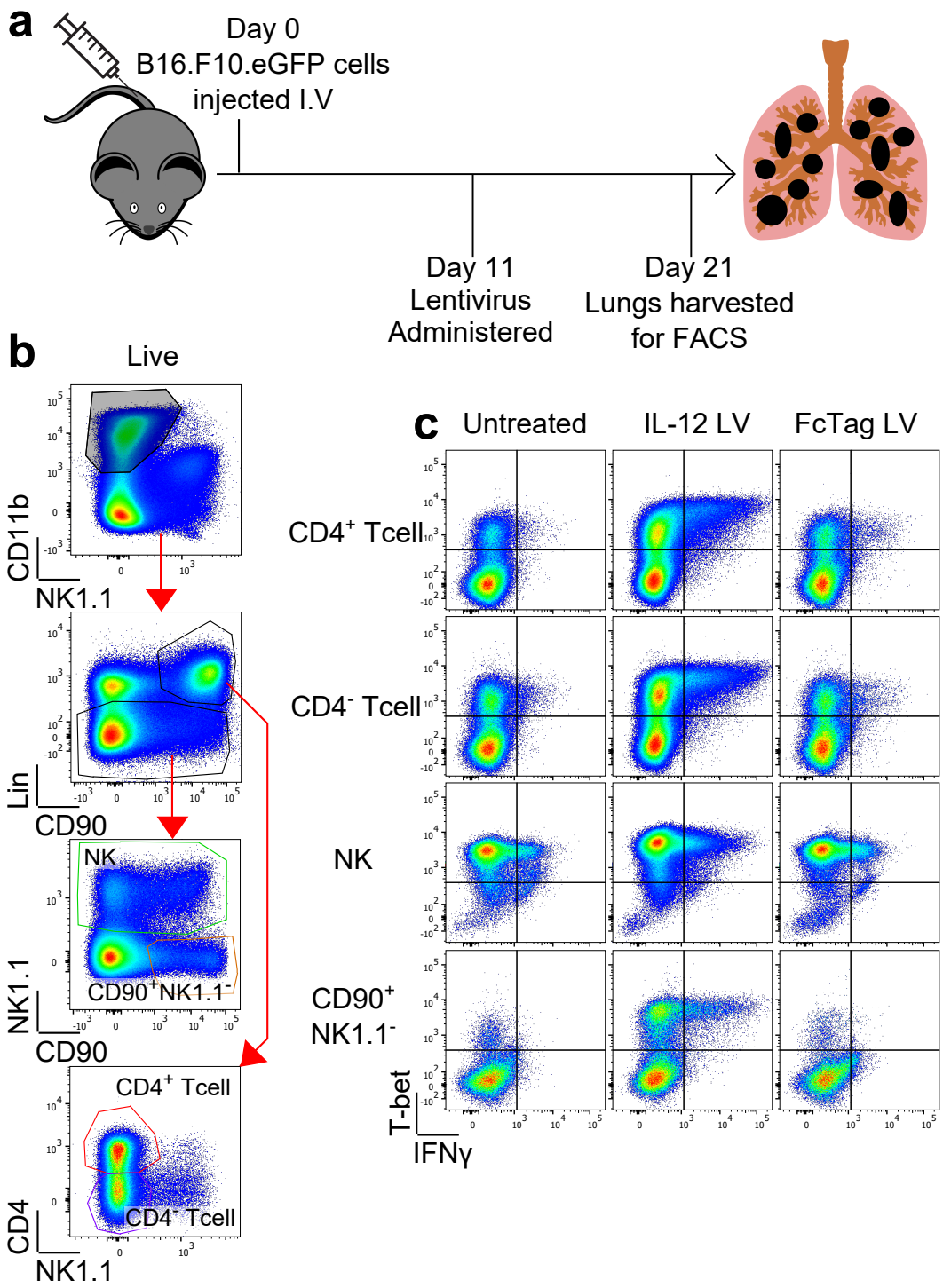

Figure 35: IL-12 LV therapy induces IFNγ & T-bet by T cells, NK cells and Lin$^-$CD90$^+$NK1.1$^-$ cells

B16.F10.eGFP bearing mice were treated with IL-12 LV (or control FcTag LV) and lungs were harvested for analysis (a). FACS analysis of CD11b^{int}/CD11b$^-$ cells identified CD3/CD19(Lin)$^+$CD90$^+$CD4$^+$/CD4$^-$ T cells, Lin$^-$NK1.1$^+$ NK cells and Lin$^-$CD90$^+$ cells (b). Expression of IFNγ was measured on these four populations of cells (CD4$^+$ T cells, CD4$^-$ Tcells, NK and CD90$^+$NK1.1$^-$ cells) where IFNγ was co-expressed with the transcription factor T-bet (c).

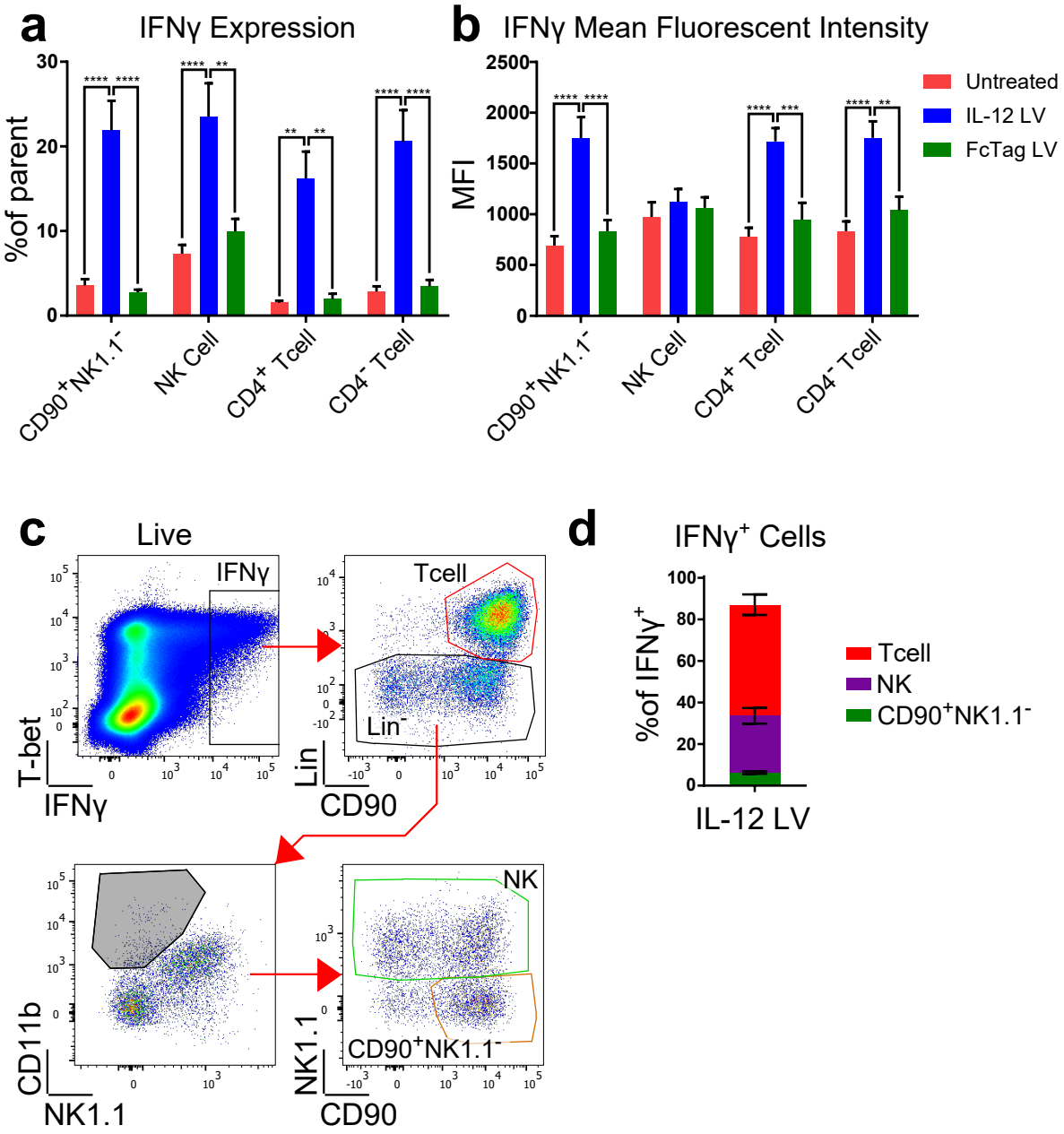

Figure 36: IL-12 LV induces IFNγ in T cells, NK cells and Lin$^-$CD90$^+$NK1.1$^-$ cells Bar plots (± S.E.M) present IFNγ expression measured as a percentage of CD90$^+$NK1.1$^-$ cells, NK cells, CD4$^+$ and CD4$^-$ T cells (a) and by mean fluorescent intensity (MFI) (b). IFNγ-centric re-analysis of FACS data (c) demonstrates that 90% of IFNγ$^+$ cells are captured by T cell, NK and CD90$^+$NK1.1$^-$ gating strategies. **p<0.01, ****p<0.0001, 2-Way ANOVA with Tukey's test of multiple comparisons, n=15 from 3 independent experiments.

4.6 IFNγ^+ Lin$^-$CD90$^+$NK1.1$^-$ cells present a plastic ILC phenotype

Our previous experiments identified IL-12 induced IFNγ expression via canonical IFNγ expressing T cells and NK cells. However, we also identified a third population of cells that appear to be induced by IL-12 stimulation and express IFNγ. These cells do not express markers associated with most haematopoietic lineages (CD3, CD11b, CD19, NK1.1) and may represent a population of recently described innate lymphoid cells (ILC) [225].

ILCs are innate immune cells that are derived from a common lymphoid progenitor (CLP), they lack expression of recombination activating gene (*RAG*) and are implicated in serving an important role in immunity, tissue homeostasis, inflammation [58], lymph node organogenesis [34] , and functionally resemble helper T cells in their expression of various cytokines. Three major categories of ILC have been described that are analogous to Th1, Th2 and Th17 T cells.

These three categories can generally be defined by their expression of the transcription factors T-bet (Th1-like Type 1 ILC / ILC1), GATA3 (Th2-like Type 2 ILC / ILC2) and RORγt (Th17-like Type 3 ILC / ILC3). IFNγ expression has been attributed to ILC1 cells, NK cells (having recently been re-classified as Type 1 ILCs) and NKp46 expressing NCR$^+$ILC3 cells. Here we sought to phenotypically characterise the Lin$^-$CD90$^+$NK1.1$^-$ cells observed in our model of IL-12 LV therapy and to discern if they are ILC1 or ILC3 cells.

Tumour bearing mice were treated with IL-12 LV (as per Figure 35a), cytometric analysis of pulmonary leukocytes identified populations of T cells, NK cells and CD90$^+$NK1.1$^-$ ILCs (Figure 37a). Expression of T-bet, RORγt, IFNγ and NKp46 was measured on T cells, NK cells and CD90$^+$NK1.1$^-$ cells (Figure 38a-c) where CD90$^+$NK1.1$^-$ cells significantly increased expression of T-bet (Figure 39a) (and proportionally decreased RORγt expression (Figure 39b)), NKp46 (Figure 39c) and IFNγ (both by proportion of total cells (Figure 39d) and by density of IFNγ production per cell (Figure 39e)). Both NK and T cells increased expression of IFNγ (Figure 39d,e) whilst NK cells did not significantly alter their expression of T-bet, RORγt or NKp46 (Figure 39a,b,c) and T cells increased their expression of T-bet (with a proportional decrease in RORγt expressing cells) (Figure 39a,b).

These data present a population of ILCs that display characteristics of both ILC1 (T-bet$^+$RORγt$^-$) and NCR$^+$ILC3 (NKp46$^+$CD90$^+$) and may represent a transitional phenotype previously described as 'Ex-ILC3' [21] herein after referred to as 'IFNγ^+ILCs'.

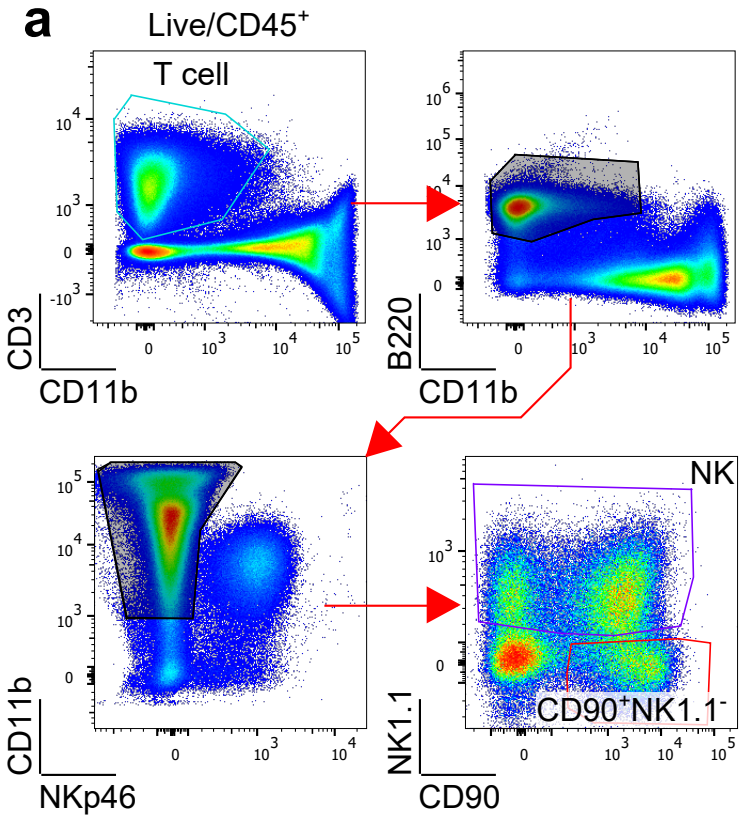

Figure 37: Identification of CD90$^+$NK1.1$^-$ ILC in IL-12 LV treated mice
Cytometric analysis of pulmonary CD45$^+$ leukocytes from IL-12 LV mice identified T cells (CD3$^+$CD11b$^-$), NK cells (CD3$^-$B220$^-$CD11b^{int}NK1.1$^+$) and CD90$^+$NK1.1$^-$ ILC (CD3$^-$B220$^-$CD11b$^-$CD90$^+$NK1.1$^-$) cells.

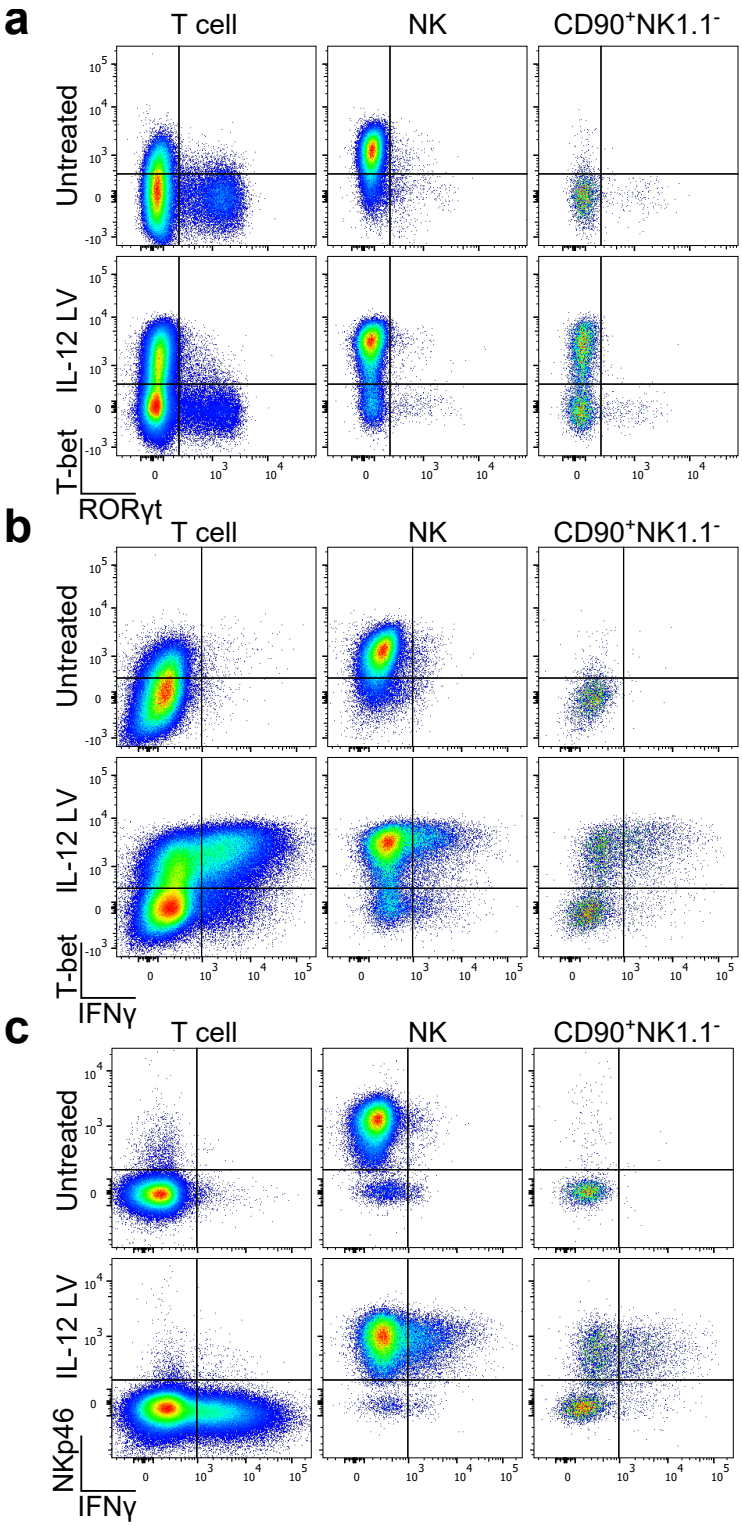

Figure 38: ILC plasticity in IL-12 LV treated mice
Representative FACS plots of gated T cells, NK and CD90$^+$NK1.1$^-$ cells from Untreated and IL-12 LV treated mice illustrate co-expression of T-bet/RORγt (a), T-bet/IFNγ (b) and NKp46/IFNγ (c).

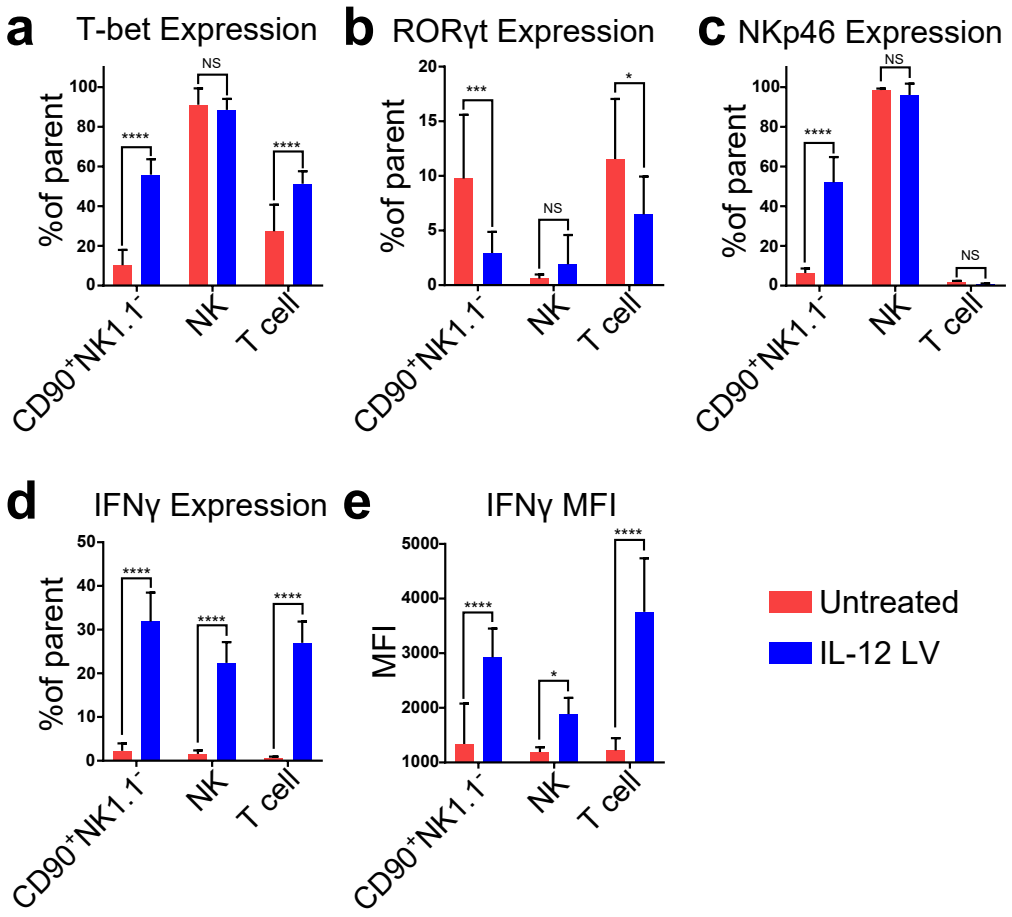

Figure 39: ILCs expressing IFNγ under IL-12 LV therapy exhibit ILC1 and ILC3 phenotypic features

Bar plots present expression of T-bet (a), RORγt (b), NKp46 (c) and IFNγ as a percentage of $CD90^{+}NK1.1^{-}$ cells, NK and T cells (d). IFNγ was also measure by mean fluorescent intensity (MFI) (e). Error bars represent S.E.M. NS $p>0.05$, *$p<0.05$, **$p<0.01$, ***$p<0.001$, ****$p<0.0001$. 2-Way ANOVA with Sidaks multiple comparison post-testing. n=10 from 3 independent experiments.

4.7 IFNγ⁺ILCs support IFNγ dependent, IL-12 LV mediated cytotoxicity

IFNγ⁺ILCs represent a relatively small population of IFNγ expressing cells when compared to the NK and T cell compartments. In order to determine the impact this population may have in the model of IL-12 LV mediated cytotoxicity, we designed an experiment that ultimately ablates ILC (as described by Kirchberger et al [115]) to elucidate the minimum components of IFNγ expressing cells required to drive tumouricidal activity.

IL-12 LV was replicated in tumour bearing mice under the following conditions: wild type (T cell, NK IFNγ⁺ILC replete), *Rag*$^{-/-}$ (T cell deficient), *Rag*$^{-/-}$ αNK1.1 (T cell deficient, NK depleted) and *Rag*$^{-/-}$ αNK1.1 αCD90 (T cell deficient, NK / CD90 depleted). These conditions were selected to remove populations of IFNγ expressing cells in order of abundance with the smallest population of CD90⁺NK1.1⁻ IFNγ⁺ILCs being removed last.

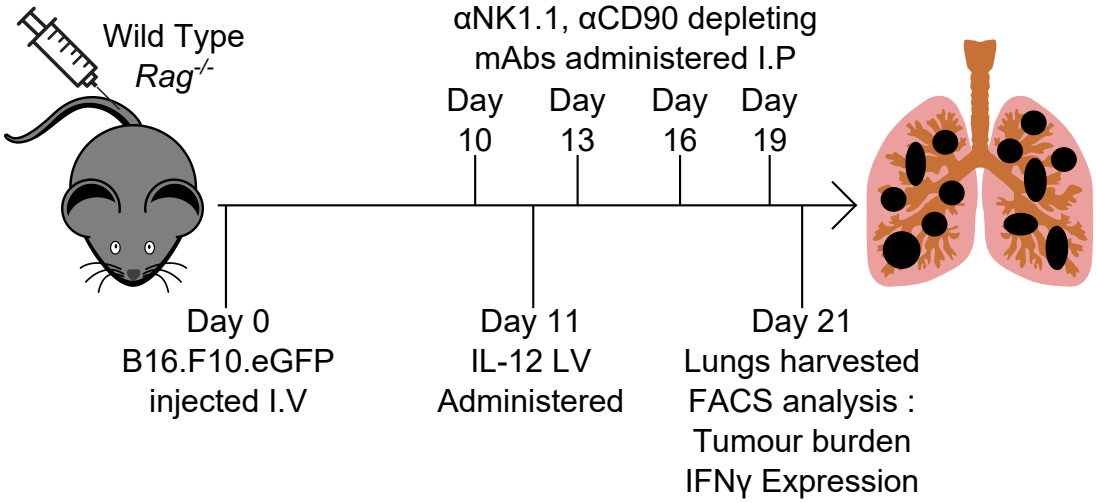

Figure 40: IFNγ minimum components experimental design

Tumour bearing mice were treated, with IL-12 LV and NK1.1/CD90 depleting antibodies as per Figure 40. Lungs were harvested and eGFP⁺ tumour burden was measured by flow cytometry (Figure 41a). IL-12 LV therapy significantly reduced pulmonary tumour burden in all conditions with the exception of mice that were T cell, NK and IFNγ⁺ILC deficient (Figure 41b). Ablation of IFNγ⁺ T cells in *Rag*$^{-/-}$ mice (Figure 42a,b), IFNγ⁺ NK cells in NK1.1 depleted mice (Figure 42c) and the remaining CD90⁺ IFNγ⁺ILCs in CD90 depleted mice (Figure 42d) was confirmed by ratiometric quantification of cell populations.

This series of data demonstrates that not only is IFNγ a key intermediary in IL-12 LV mediated cytotoxicity; but that the threshold for IFNγ requirement is low enough to be supported by a relatively infrequent population of IFNγ⁺ILCs.

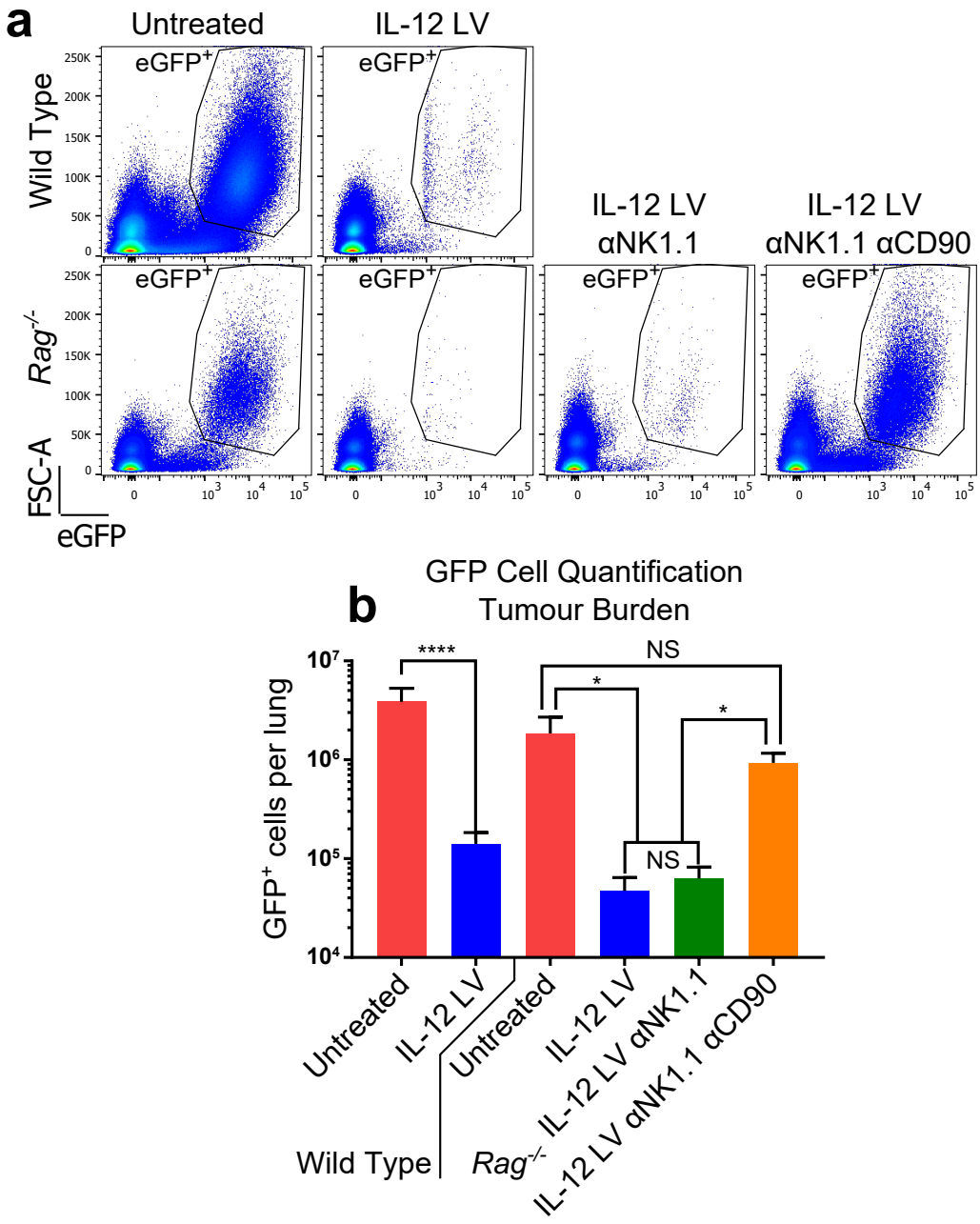

Figure 41: NK, T cells and ILC support IFNγ mediated cytotoxicity
Tumour burden measured by FACS analysis of eGFP+ tumour cells isolated from lungs of wild type and *Rag*$^{-/-}$ mice under IL-12 LV therapy and *Rag*$^{-/-}$ mice under addition NK1.1 and CD90 depletion under IL-12 LV therapy (a). Bar plots represent quantification of eGFP+ tumour burden (± S.E.M) from each condition. NS $p>0.05$, *$p<0.05$, ****$p<0.0001$, Kruskal-Wallis analysis of non-parametric data with Dunn's multiple comparison post testing. n=9 from 3 independent experiments.

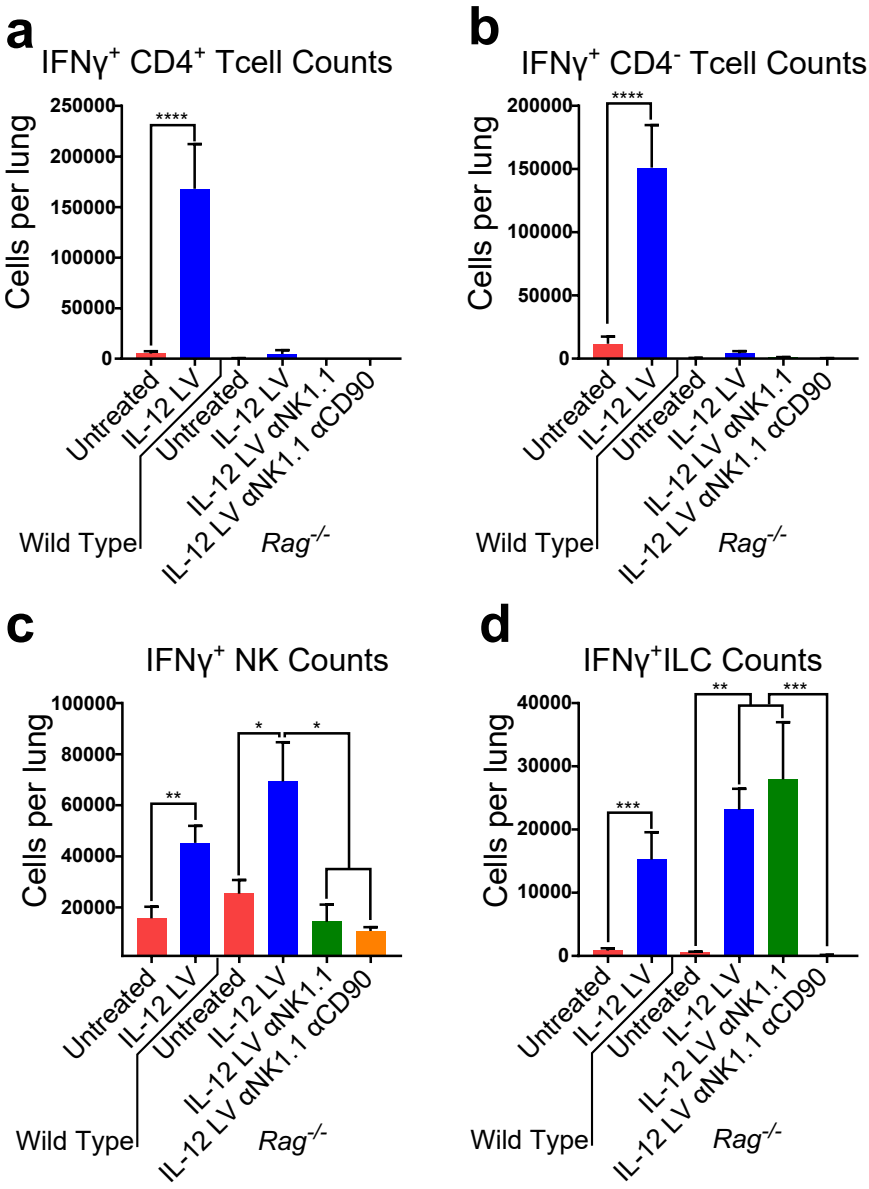

Figure 42: Depletion of IFNγ T cells, NK cells and ILCs in IL-12 LV mice
Total numbers of IFNγ expressing CD4+ T cells (a), CD4- T cells (b), NK cells (c) and IFNγ+ILCs (d) were enumerated from lungs of mice as described in Figure 41. *p<0.05, **p<0.01, ***p<0.001, ****p<0.0001, Kruskal-Wallis analysis of non-parametric data with Dunn's multiple comparison post testing. n=9 from 3 independent experiments.

4.8 Results Section 4 Discussion

IL-12 is known to mediate cytotoxicity via two well documented pathways: induction of cytotoxic activity in NK & T cells [204, 283], and the expression of IFNγ by Th1 effector T cells [253]. Interestingly, our data indicates that the former is not an essential element of this model whilst the latter is indispensable.

Initially, we observed significant cytotoxic $CD8^+$T cell and NK responses to IL-12 LV in the form of increased proliferation (indicated by elevated Ki67 expression, Figures 30b & 31a) and expression of the cytotoxic molecule granzyme b (GzmB, Figures 30b & 31b).

It is important to note that discrepancies may arise within this body of work when comparing results generated from differing experimental modalities and designs. One such discrepancy exists where figure 31 indicates that NK cells expand under IL-12 LV therapy whereas figure 33 presents NK cells as a population that contracts under IL-12 LV therapy. This discrepancy may have arisen as the statistics presented in either figure are resultant of differing FACS gating strategies and enumeration methods.

The FACS gating strategy employed in figure 31 involves defining NK cells as expressing NK1.1 and results in a well-defined NK population. A different gating strategy was used in the generation of figure 33 as αNK1.1 antibodies were used to deplete NK cells from mice *in vivo*. Subsequent FACS analysis of NK cells could not then use NK1.1 as a phenotypic marker as NK1.1 present on any residual NK cell may be occupied by the depleting antibody, thus blocking any fluorescently labelled NK1.1 antibody used for analysis. In these experiments, NK cells were defined as expressing the natural cytotoxicity receptor (NCR, NKp46) instead of NK1.1. It should be noted that NKp46 appeared to by expressed at lower density than NK1.1 and that NKp46 is not entirely restricted to NK cells (is a hallmark feature of some ILC populations).

In addition to these differing FACS gating strategies, figures 31 and 33 used differing methods of cell quantification where figure 31 measures the total number of NK cells per sample as per the ratio-metric quantification method presented in section 2.7.4 and figure 33 measures the relative abundance of NK cells within the $CD45^+$ leukocyte compartment.

The ratio-metric enumeration method has an advantage over measuring relative abundance (% of $CD45^+$ cells) as the latter cannot not use a fixed reference population and is in turn affected by expansion and contraction of all other $CD45^+$ leukocytes in the sample whereas the former introduces a fixed population (ie. fluorescent counting beads) and is an attempt to calculate the absolute number of cells in any given sample.

The main disadvantage of using this enumeration method is that the resulted number is extrapolated from the analysis of a fraction of the original sample that has undergone a lot of manual processing in the interim. Although described in the literature as a method to enumerate the total number of cells in a sample, it's our belief that this number, whilst comparable across samples and data sets, is most likely an underestimation of the actual total number of cells in any given sample. Evidence of this underestimation may be inferred from data presented in Figure 34 where macroscopic observation of lungs from untreated and IFNγ neutralised lungs present with a heavy metastatic burden and matched FACS derived quantification estimates the number of tumour cells present in that lung to be approximately 1x10^6 cells. Such a cell number in reality would account for a small fraction of cells observed macroscopically. Potential explanations for this discrepancy may include the loss tumour cells during physical processing and exclusion of tumour cells in FACS analysis by size (tumour cells present a diverse range of cell sizes), viability (a large percentage of tumour cells may have died during processing) or GFP gating (possible attenuation of eGFP expression).

Given the observed increase in CD8$^+$ CTL and NK cytotoxic potential, we hypothesized that ablation of the T cell and NK compartments would result in a correlating loss of tumouricidal activity. Subsequent experiments replicating IL-12 LV therapy in NK / T cell (as well as B cells by use of *Rag*$^{-/-}$ mice) had no impact on tumouricidal activity (Figure 32). Although these data do not infer that CD8$^+$T cell and NK cytotoxicity play no role in this model. Our data shows that IL-12 LV therapy upregulates expression of Granzyme B (GzmB) on CD8$^+$ T cells and NK cells (see section 4.1). GzmB is a serine protease that induces apoptosis (via caspase activity) in target cells [3], and as a member of the Granzyme family of proteases is considered a classical mediator of NK and T cell cytotoxicity [108].

Further characterisation of cytotoxic T cell and NK activity in our model would involve measurement of perforin expression. Perforin is a pore forming protein that binds to a targets cell's membrane, increasing its permeability allowing Granzyme B to enter the cells and induce apoptosis [148]. This could be measured much as Granzyme B was (in section 4.1) by intracellular flow cytometry.

The process by which Granzyme B and perforin is expressed by cytotoxic lymphocytes (CTL) is known as de-granulation [252]. This can be measured by ELISPOT detection of soluble Granzyme B and perforin when activated CTL are co-cultured with target tumour cells *in vitro* [218]. De-granulation can also be measured by flow cytometric detection of CD107a (LAMP-1), a protein that lines the interior of lytic granules and is expressed on the CTL cell surface during granule exocytosis [146] (Figure 43).

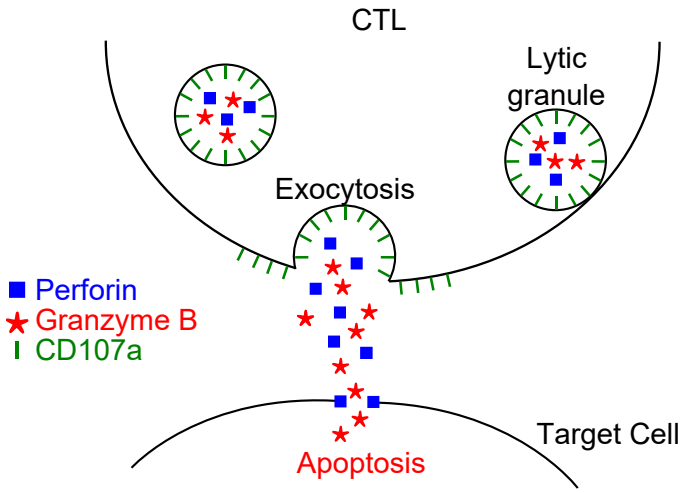

Figure 43: CTL de-granulation

Finally, direct cytotoxic function in IL-12 LV activated CTL could confirmed by in vitro cytotoxicity assays where CTL are isolated from IL-12 LV treated mice and co-cultured with CFSE labelled B16.F10 tumour cells. Cytometric analysis of $CFSE^+$ cells would then be used to measure CTL directed lysis of target tumour cells [200].

Having demonstrated that T cells and NK cells were dispensable populations in this model of IL-12 mediated cytotoxicity, we then focused on investigating the role of IFNγ as a powerful immunomodulatory cytokine that is known to be induced by IL-12 [253]. Neutralisation of IFNγ in IL-12 LV treated mice effectively negated the tumouricidal activity of IL-12 thus proving an essential role of IFNγ in this mechanism (Figure 34).

In light of our experiments using NK and T cell depleted mice, an interesting question was raised regarding the source of IFNγ in such mice as T cells and NK cells are the canonical producers of IFNγ under IL-12 stimulation [126]. Analysis of leukocytes isolated from IL-12 LV treated mice revealed IFNγ expression restricted to T cells, NK cells (as defined by NK1.1 expression and intermediate expression of CD11b) and a relatively small population of $CD45^+$cells that do not express the lineage markers CD3, CD11b or NK1.1 (Figure 35).

Further analysis of these lineage negative cells revealed that they express CD90 (Thy-1, a T cell associated surface antigen that may facilitate TCR independant activation [94]), the Th1 associated [2] transcription factor T-bet, the natural cytotoxicity triggering receptor 1 (NCR1, NKp46, CD335) and lack expression of the Th17 associated transcription factor RORγt (Figure 38a). Given the lack of TCR, CD11b, NK1.1 (and the pan NK marker CD49b) we believe that this population of cells represent a population of innate lymphoid cells.

This population of $IFN\gamma^+$ ILCs display hallmarks of two distinct ILC sub-populations

[225]. The expression of T-bet, IFNγ and the absence of RORγt is commonly associated with ILC1 cells [254], whereas expression of NKp46, CD90 and RORγt (with a corresponding absence of T-bet) are associated with ILC3 cells [254]. As ILCs observed in this study display elements of both sub-populations, they resemble previously described 'ex-ILC3' cells [21]. In response to IL-12, these semi-plastic ILC3 cells differentiate into an ILC1 phenotype, characterized by the loss of CD127 and RORγt and the gain of T-bet and IFNγ expression [21, 257].

Further characterisation of ILC plasticity within the context of IL-12 LV therapy would ideally include expanded single-cell analysis methods including high-parameter flow or mass cytometric panels that include a full transcription factor profile and hallmark features of all types 1, 2 and 3 ILC. An ideal method to fully characterise these cells would involve sorting $Lin^{-}CD90^{+}$ ILCs from IL-12 LV treated lung suspensions and then passing them on to a single-cell RNA sequencing (scRNAseq) platform (such as Chromium 10x) coupled with oligo-conjugated antibody staining and detection of surface antigens (such as CITE-Seq).

This method would generate complete transcriptomic profiles and matched protein expression data with single-cell resolution and would allow classification of our 'IFNγ^{+}ILC' population as one the defined ILC populations, a transitional population (plastic) or the development of a novel population that does not fit into any of the existing pre-defined phenotypes.

Development of ILCs and ILC plasticity has been previously studied by use of fate-mapping mice where a gene of choice (eg. RORγt) drives expression of Cre, CreER or the Tet-transactivator (tTA) which in turn activates expression of a reporter gene (eg. GFP) that is stably expressed regardless of the initial triggering gene [183]. These systems may be employed to fluorescently label all ILCs that develop under the PLZF transcription factor [43] and ILC plasticity may be mapped via use of RORγt [183] or IL-5 [182] fate-mapping mice where ILC3 and ILC2 (respectively) may be tracked as they acquire T-bet and convert into ILC1 cells. These fate-mapping experiments may be combined with FACS or scRNAseq analysis as described above.

In section 4.7, we explorer the contribution of ILC to IFNγ dependant activity through the use of *Rag2*$^{-/-}$ mice. An expansion of this experimental design may employ addition knock-out models such as *Rag2*$^{-/-}$*IL2r*$\gamma^{-/-}$ mice to genetically ablate ILC (including NK cells) as well as T cells [206] while *Rag2*$^{-/-}$*ROR*(γt)$^{-/-}$ mice could be used to dissect the contribution of ILC3 [211].

It should be noted that these knock-out models may overstate the roles of remaining populations as they expand to fill the niche left by genetically ablated populations and it has previously been reported that ILC3 cells expand in the intestines of *Rag*$^{-/-}$ mice (relative to WT controls) [120, 211]. This observation

is supported by data presented in figure 42 where a non-significant increase in IFNγ^+ILC counts was measured in IL-12 LV treated *Rag*$^{-/-}$ mice (cf. IL-12 LV treated wild type mice).

5 Downstream effects of IL-12 LV mediated IFNγ production

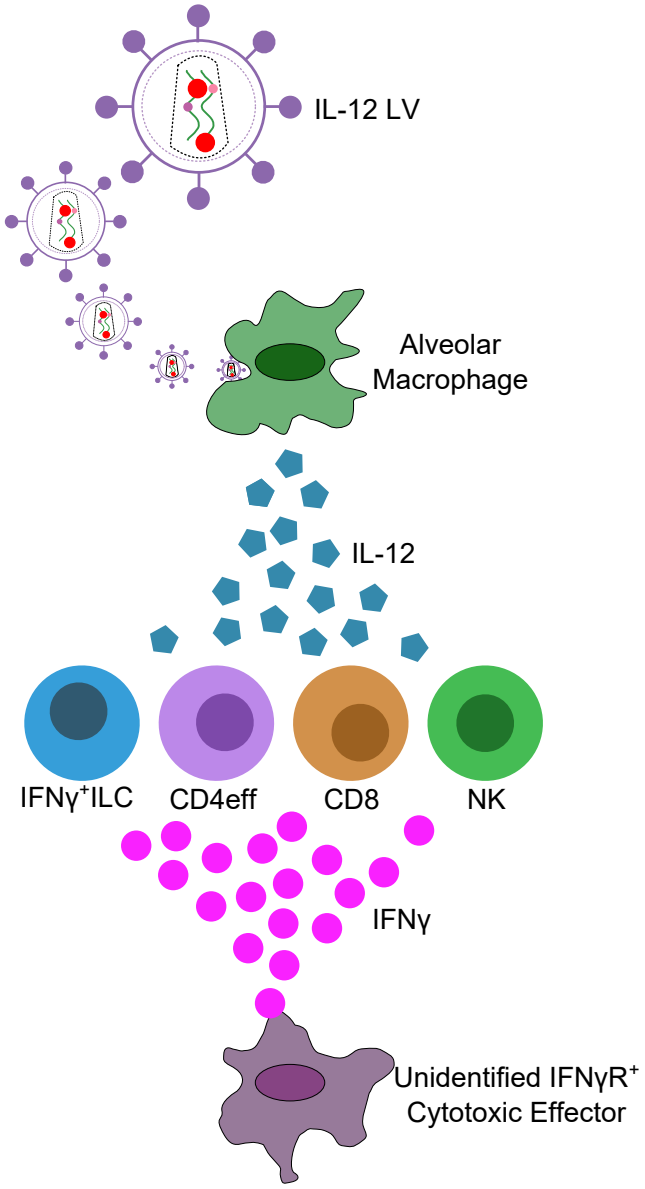

The data presented thus far identified alveolar macrophages as primary targets of in vivo transduction by lentiviral particles and serve as a source of IL-12 when transduced by IL-12 LV. We have observed (dispensable) induced cytotoxic potential in T cells and NK cells and have identified that IFNγ (secreted by T cells, NK cells and IFNγ+ILCs) is an indispensable mediator of IL-12 LV induced tumouricidal activity.

IFNγ exerts many direct effects on tumour and stroma where IFNγ halts mammary carcinoma cell cycle by upregulation of the cell cycle inhibitor protein p27Kip [98], induces apoptosis via expression of mitochondrial derived reactive oxygen species (ROS) in colorectal cancer cells [260], stimulates adaptive immune responses via upregulated expression of MHC-I and MHC-II [198] and effects tu-

mour associated epithelia, resulting in regression of tumour vasculature and subsequent tumour ischemia [112].

In addition to IL-12, IFNγ is considered a canonical Th1 associated cytokine and as such exerts broad stimulatory functions within multiple compartments of the immune system. IFNγ has been shown to module APC function by upregulation of CD86, IL-12, IL18 and MHCI/II [124] whilst IL-12 and autocrine IFNγ stimulation are required for optimal NK cell cytotoxic function [103]. IFNγ has been shown to alleviate immunosuppression via inhibition of Treg function [187], triggers Bcl2a1 mediated apoptosis of MDSC [165]] and as an important modulatory of macrophage plasticity.

Macrophage plasticity describes a fluid array of functional states that has classically been bifurcated into two polar functional types: M1 and M2 macrophages [220].

Classically activated (M1) macrophages were first described in 1962 when macrophage activation was observed in response to *Listeria monocytogenes* infection [153]. Subsequent *in vitro* studies recapitulated these finding using combinations of lipopolysaccharide (LPS) and IFNγ [170]. Later *in vivo* studies observed M1 polarisation driven by Th1 lymphocyte derived IFNγ [176]. M1 macrophages express Th1 associated pro-inflammatory cytokines such as IFNγ, IL-23 and IL-12 [156]. They effectively destroy pathogens by phagocytosis [13] and by the expression of cytotoxic chemicals such as reactive oxygen species (ROS) and reactive nitrogen species (RNS), the latter of which are derived from NOS synthesised nitric oxide (NO) [110, 249].

Excessive over-activation of M1 macrophages may lead to disruption of tissue homeostasis, may contribute to inflammatory immunopathology [69] and cytokine release syndrome [181]. This pathological activity may be balanced by anti-inflammatory polarisation of macrophages to what has become known as alternatively activated macrophages (M2).

M2 macrophages were later identified as macrophages activated by anti- inflammatory Th2 cytokines such as IL-4, IL-10 and IL-13 [51, 229]. Once polarised, these macrophages downregulate expression of inflammatory cytokines and upregulate expression of the scavenging macrophage mannose receptor (MMR, CD206) [229]. The M2 compartment is further divided into 4 subtypes as described in table 12.

Phenotype	Stimuli	Cell expression markers	Cytokines, chemokines, and other secreted mediators	Functions
M1	IFNγ, TNFα, LPS	CD80, CD86, CD68, MHC-II, IL-1R, TLR2, TLR4, iNOS, IL-10 low, IL-12 high	TNFα, IL-1β, IL-6, IL-12, IL-23, IL-27, CXCL9, CXCL10, CXCL11, CXCL16, CCL5, Arg-2 (mouse), iNOS (mouse), ROS	Pro-inflammatory Th1 response, tumour resistance
M2a	IL-4, IL-13	Human: CD206, IL-1Ra, IL-1R II. Mouse: Arg-1, FIZZ1, Ym1/2	IL-10, TGFβ, CCL17, CCL18, CCL22, CCL24	Anti-inflammatory, tissue remodeling
M2b	Immune complexes, TLR ligands, IL-1β	IL-10 high, IL-12 low, CD86	TNFα, IL-1β, IL-6, IL-10, CCL1	Th2 activation, immunoregulation
M2c	IL-10, TGFβ, glucocorticoids	Human: CD206, TLR1, TLR8. Mouse: Arg-1	IL-10, TGFβ, CCL16, CCL18, CXCL13	Phagocytosis of apoptotic cells
M2d	TLR ligands, adenosome receptor ligands	VEGF, IL-12 low, TNFα low, IL-10 high	IL-10, VEGF	Angiogenesis, tumour progression

Table 12: Differing Biological and physiological features of M1 and M2 macrophages
Reproduced from Shapouri-Moghaddam *et al* [219]

It is important to note that these M1/M2 subtypes generally do not exist within the strict bounds of their reported phenotypes/functions but on a continuum of M1"like"-M2"like" where multiple stimuli from across the polarisation range (as described in table 12) may lead to mixed or continually changing functional and phenotypical profiles.

Given that IL-12 LV mediated cytotoxicity is not dependant on cytotoxic components of the adaptive immune response (T cells and NK cell), this final results chapter investigates the effect of IL-12 LV induced IFNγ on the innate compartment with particular focus on the role of tissue resident macrophages in this model of IFNg mediated tumouricidal activity. This results chapter will utilise two genetically modified murine models in an attempt to identify the activation stimuli, cy-

totoxic contribution and ontogeny of macrophage populations that expand under IL-12 LV therapy.

The *CCR2* knockout (*CCR2*$^{-/-}$) murine model was kindly donated by Prof. Derek W. Gilroy and lack expression of C-C chemokine receptor 2 (CCR2). This receptor is instrumental in the recruitment of HSC derived Ly6C^{+} monocytes from the periphery into CCL2 expressing tissues and ablation of CCR2 effectively traps these monocytes in the bone marrow [178]. Application of IL-12 LV in this model will help dissect the contribution of the remaining CCR2^{-} embryonically derived macrophage compartment to IL-12 mediated tumouricidal activity.

The second genetically modified murine model used in this chapter is called "macrophages insensitive to interferon gamma" (MIIG) and was a generous gift from Prof. Michael B. Jordan. The MIIG transgene was constructed by cloning a truncated IFNγR (lacking the intracellular signaling domain), known as a dominant-negative IFNγR (dnIFNγR) [49], downstream of a genomic DNA fragment containing the 5' region and intron 1 of the human CD68 gene [137]. When stably expressed in a murine model, this gene restricts overexpression the dnIFNγR to CD68^{+} macrophages thus rendering them insensitive to IFNγ stimulation. This macrophage restricted insensitivity to IFNγ will help establish the role of macrophages in the tumouricidal response to IL-12.

5.1 IL-12 LV therapy mediates expansion of interstitial macrophages and Ly6C$^-$ monocytes

A pulmonary myeloid phenotyping panel and gating strategy was designed and implemented based as previously described by Misharin *et al* [171]. From the CD45$^+$CD3$^-$ CD19$^-$NK1.1$^-$ myeloid compartment, this panel identified CD11c^{hi} alveolar macrophages, CD103$^+$ DCs, CD11b$^+$ DCs, neutrophils, eosinophils, Ly6C$^+$ monocytes/macrophages, Ly6C$^-$ monocytes/macrophages and interstitial macrophages (Figure 44a). Ratiometric quantification of each populations revealed expansion of MHC-II$^+$ (I-Ab$^+$) interstitial macrophages (but not I-Ab$^+$ CD11b$^+$ DC) and MHC-II$^-$ Ly6C$^-$ monocyte/ macrophages in IL-12 LV treated mice (cf. untreated and FcTag LV controls) (Figure 45a).

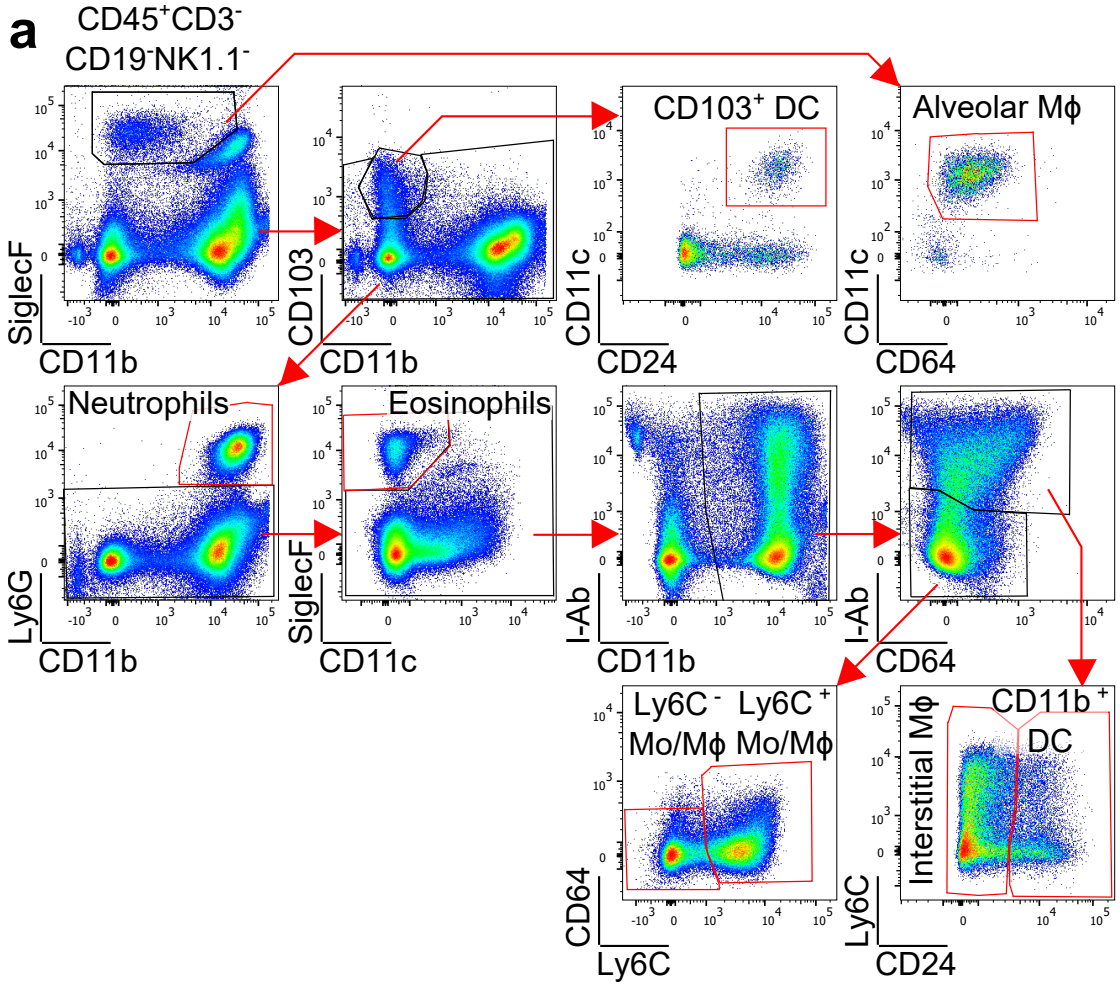

Figure 44: FACS identification of pulmonary myeloid leukocytes
Cytometric analysis of the pulmonary myeloid compartment reveals populations of CD103$^+$ DC, CD11b$^+$ DC, eosinophils, neutrophils, alveolar macrophages, Ly6C$^+$ & Ly6C$^-$ monocytes/macrophages and MHC-II$^+$ (I-Ab$^+$) interstitial macrophages.

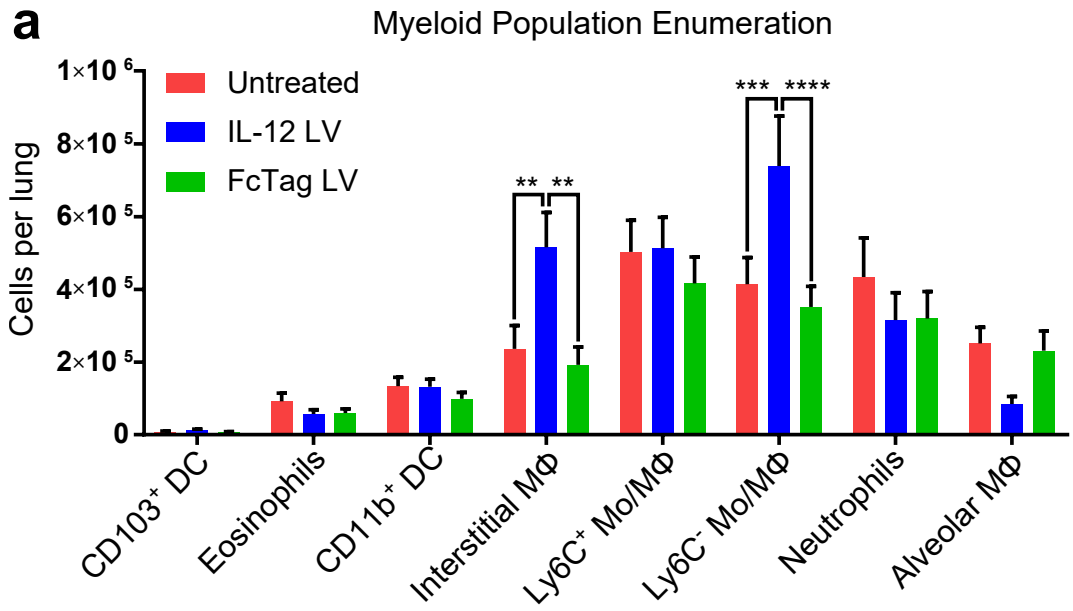

Figure 45: IL-12 LV therapy promotes expansion of interstitial macrophages and monocytes
Bar plots represent quantification (± S.E.M) of myeloid populations as identified in Figure 44. **p<0.01, ***p<0.001, ****p<0.0001. 2-Way ANOVA with Tukey multiple comparison post testing. n=15 from 3 independent experiments.

These multi-parametric cytometry data was then analysed using a custom machine learning pipeline (cytofpipe),where application of the FlowSOM clustering algorithm (50x iterations, k=20 clusters), recapitulated previous manual gating results by identification of all expected populations by super-clustering of relative marker expression (Figure 46a), the frequency of which (of a proportion of the myeloid compartment) was plotted (Figure 46b). Interestingly, an unidentified population of SSC-A^{high}CD24/FiTC^{high} cells appeared to be diminished in IL12 LV treated mice, subsequent manual gating of this population suggests the presence of eGFP^{+} tumour cells in the FACS data.

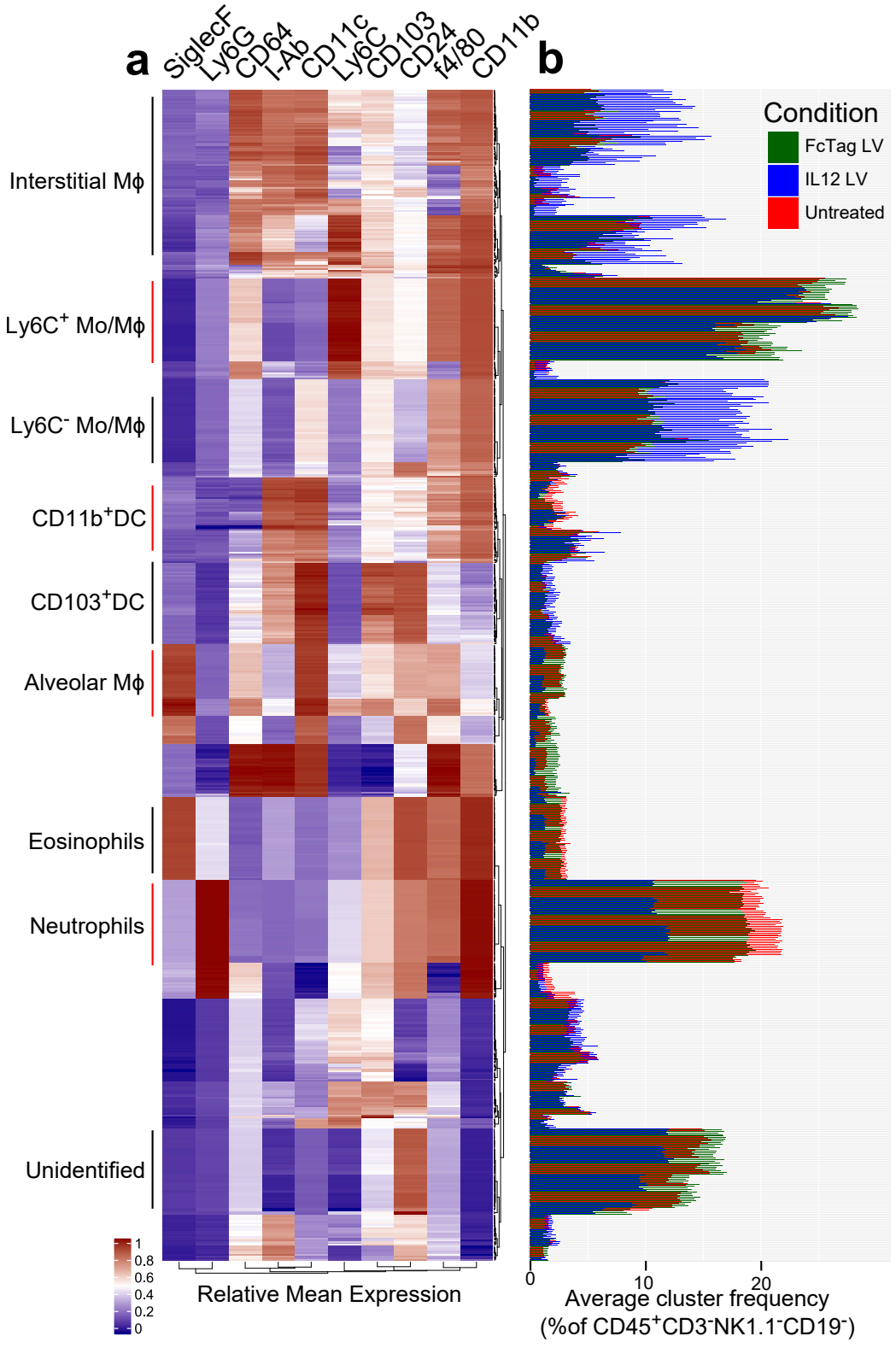

Figure 46: Unbiased identification of pulmonary myeloid leukocytes
Relative mean marker expression from 50x FlowSOM iterations is presented a self-ordered heatmap (a) with super-clusters annotated by visual identification of marker expression. The average frequency of each cluster (within each condition) was plotted as a bar graph (b).

Uniform Manifold Approximation and Projection (UMAP) is a method of reducing high-dimension data sets that can then be visualised as a 2-dimensional plot [162]. This method was applied to the same set of multi-parametric cytometry data to produce a visual map of the myeloid compartment with the expression of various surface antigens of interest. The data set was filtered on FlowSOM clusters of interest (as identified in Figure 46) from IL-12 LV mice, and all major myeloid populations (including interstitial macrophages) as described in Figure 44 were identified on a UMAP plot (Figure 47a). Expression of MHC-II (Figure 47b), f4/80 (Figure 47c), CD64 (Figure 47d), CD11c (Figure 47e), CD24 (Figure 47f) and CD11b (Figure 47g) were then projected onto the UMAP plot and coloured as mean fluorescent intensity (MFI). The cluster of cells identified as interstitial macrophages were found to express CD11b, MHC-II, f4/80, CD64 and CD11c; but not CD24. The MFI of all markers listed in Figure 46b was also projected onto this UMAP plot (Appendix Figure 66) and confirms the phenotype of interstitial macrophages as $CD11b^{+}MHC\text{-}II^{+}CD11c^{+}f4/80^{int}CD64^{+}CD24^{-}$ cells. This data recapitulates results produced via manual gating/FACS analysis.

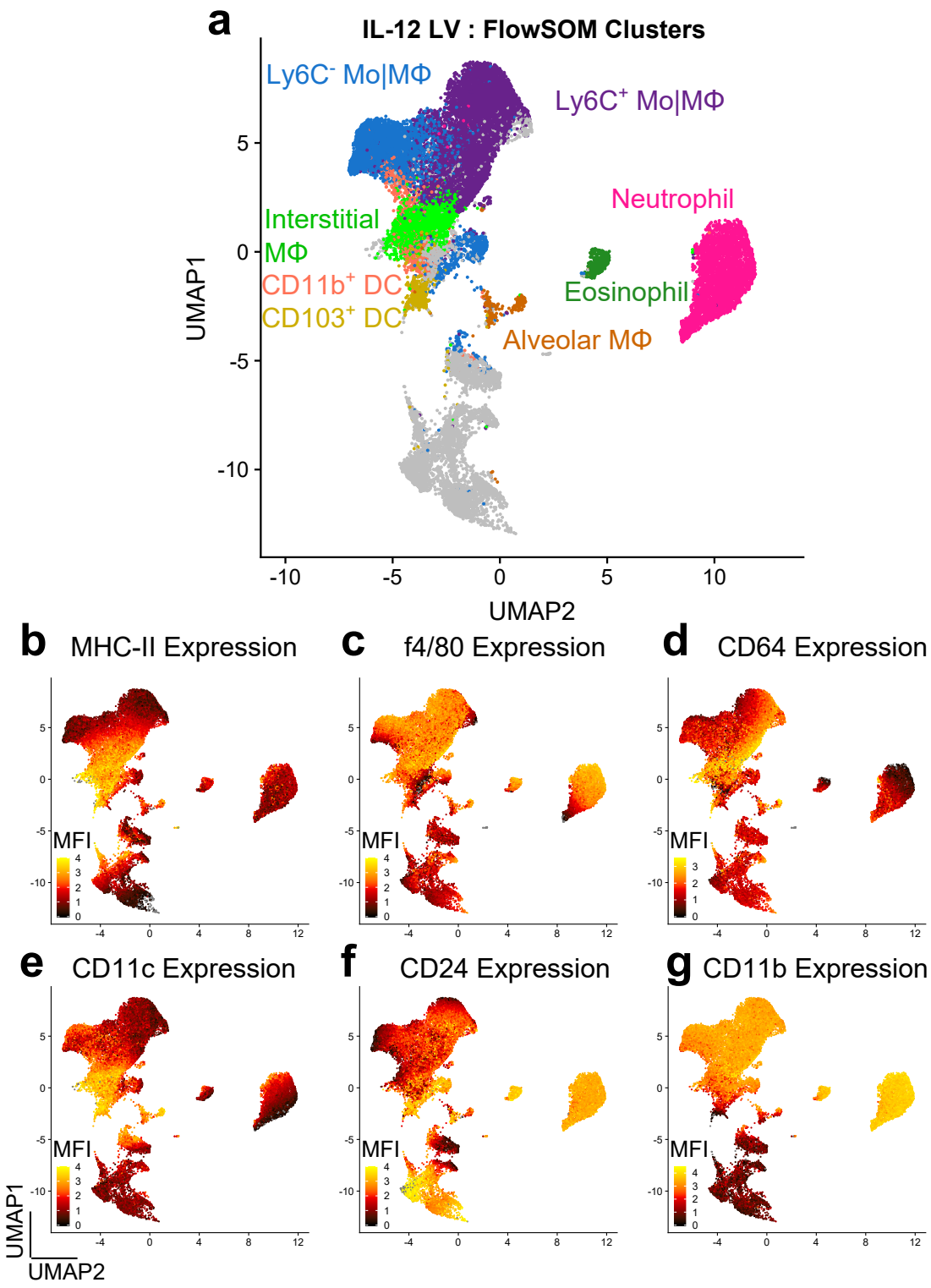

Figure 47: UMAP dimension reduced visualisation of the myeloid compartment UMAP dimension reduction visualisation was applied to flow cytometry data from IL-12 LV treated mice. UMAP plots were annotated with FlowSOM clusters (a) as per Figure 46. Expression (MFI) of MHC-II (b), f4/80 (c), CD64 (d), CD11c (e), CD24 (f) and CD11b (g) was expressed as heat on UMAP plotted data.

5.2 MHC-II^{+}iNOS^{+} macrophages are induced by IL-12 LV therapy

Results presented in the section 5.1 identified expansion of MHC-II^{+} interstitial macrophages in response to IL-12 LV therapy. As co-expression of MHC-II and iNOS is considered a key indicator of M1-like function in macrophages [156], we next sought to verify potential M1-like polarisation of interstitial macrophages in this model. Inducible nitric oxide synthase (iNOS) is an enzyme that catalyses the conversion of L-arginine into nitric oxide (NO) [118], it is strongly associated with M1 function [156]. iNOS is a key molecule involved in NO mediated oxidative burst that may be responsible for observed cytotoxicity directed against established metastases [38].

Lungs were harvested from tumour bearing untreated and IL-12 LV mice, leukocytes were isolated and FACS analysis defined a population as CD45^{+}CD3^{-}NK1.1^{-} Ly6G^{+}CD11b^{+} containing macrophages and dendritic cells (Figure 48a). M1 polarisation of the macrophage compartment was measured by expression of MHC-II (I-Ab) and co-expression of iNOS (Figure 48b). Co-expression of Ly6C and f4/80 was observed on I-Ab^{+}iNOS^{+} cells, verifying their identity as interstitial macrophages (Figure 48c). IL-12 LV was found to significantly increase expression of I-Ab (Figure 48d) and iNOS (Figure 48e) on CD11b^{+}Ly6G^{-} macrophages.

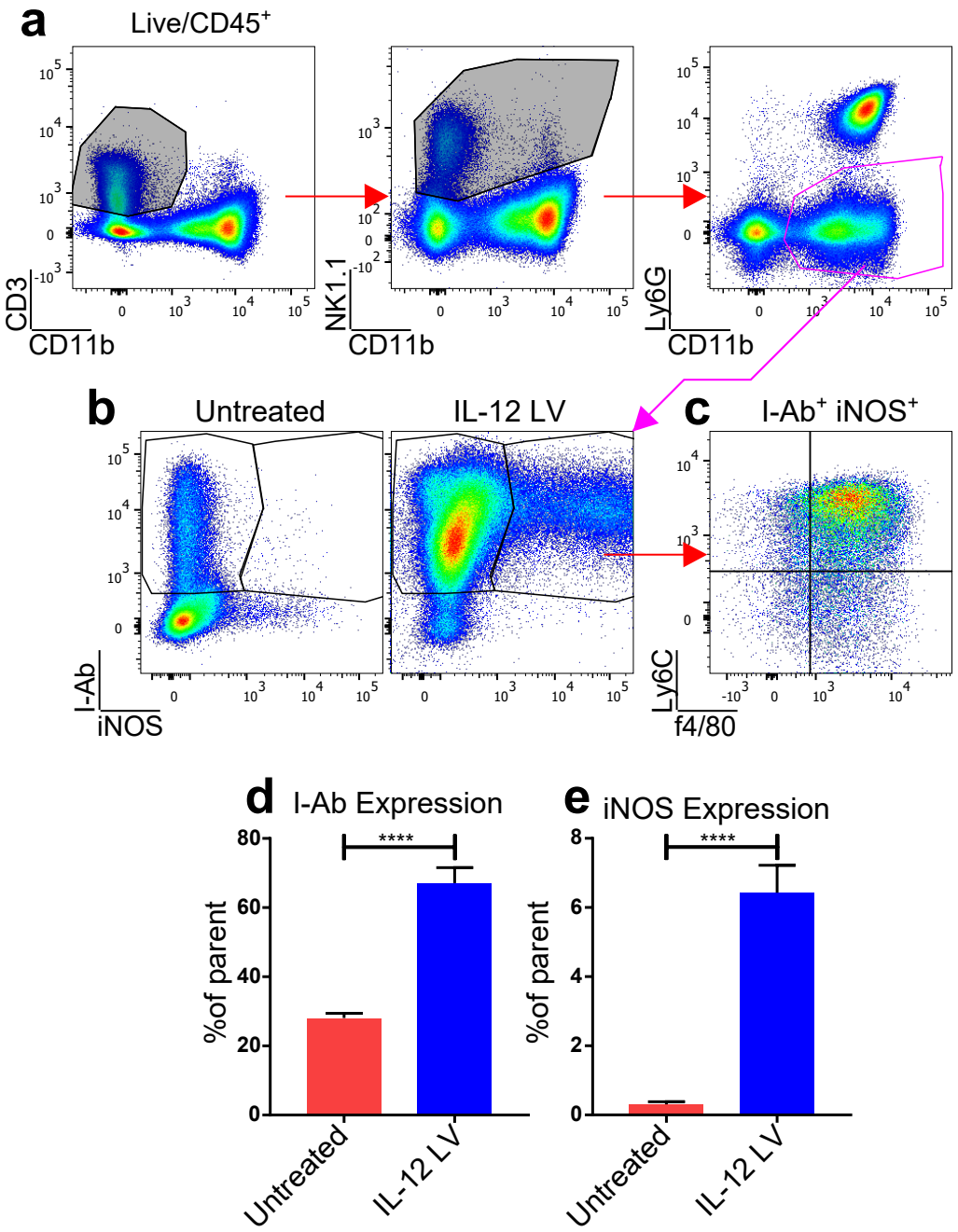

Figure 48: M1-like polarisation of macrophages in response to IL-12 LV therapy Mixed macrophage/DC populations were identified by FACS analysis as $CD45^{+}NK1.1^{-}Ly6G^{-}$ cells (a,b,c). Bar plots present MHC-II (I-Ab) (d) and iNOS (e) expression (± S.E.M) on $Ly6G^{-}$ gated cells. ****P<0.0001, unpaired 2-tailed t-test. n=25 from 5 independent experiments.

5.3 IL-12 LV induced tumouricidal activity is not mediated via CCR2^{+} circulating inflammatory macrophages

It was hypothesized that the M1-like macrophage population that is induced by IL-12 therapy may be a subset of macrophages known as inflammatory macrophages. So called as they play a central role in initiating and mediating inflammatory processes [18], these inflammatory macrophages are recruited from the periphery and circulate toward sites of inflammation by attraction to inflammation associated chemokine (c-c motif) ligand 2 (CCL2) expression, sensed by c-c chemokine receptor type 2 (CCR2) [267]. To test this hypothesis, we tested the efficacy of IL-12 LV therapy in wild type mice and *CCR2*$^{-/-}$ mice, the latter of which do not possess inflammatory macrophages capable of homing to sites of inflammation.

IL-12 LV therapy was repeated in wild type and *CCR2*$^{-/-}$ mice, lungs were harvested for cytometric analysis (Figure 49a). FACS analysis of eGFP^{+} tumour cells (Figure 49b) revealed significantly decreased tumour burden in IL-12 LV treated wild type and *CCR2*$^{-/-}$ mice (Figure 49c). Analysis of the myeloid compartment (Figure 50a) revealed significantly increased expression of I-Ab (Figure 50b,c) and iNOS (Figure 50b,d) whilst the absolute numbers of MHC-II^{+}iNOS^{+} M1-like macrophages were significantly increased in IL-12 LV treated wild type and *CCR2*$^{-/-}$ mice (Figure 50f). This data appears to exclude the role of inflammatory macrophages in the mechanism of IFNγ dependent IL-12 LV mediated tumour cytotoxicity.

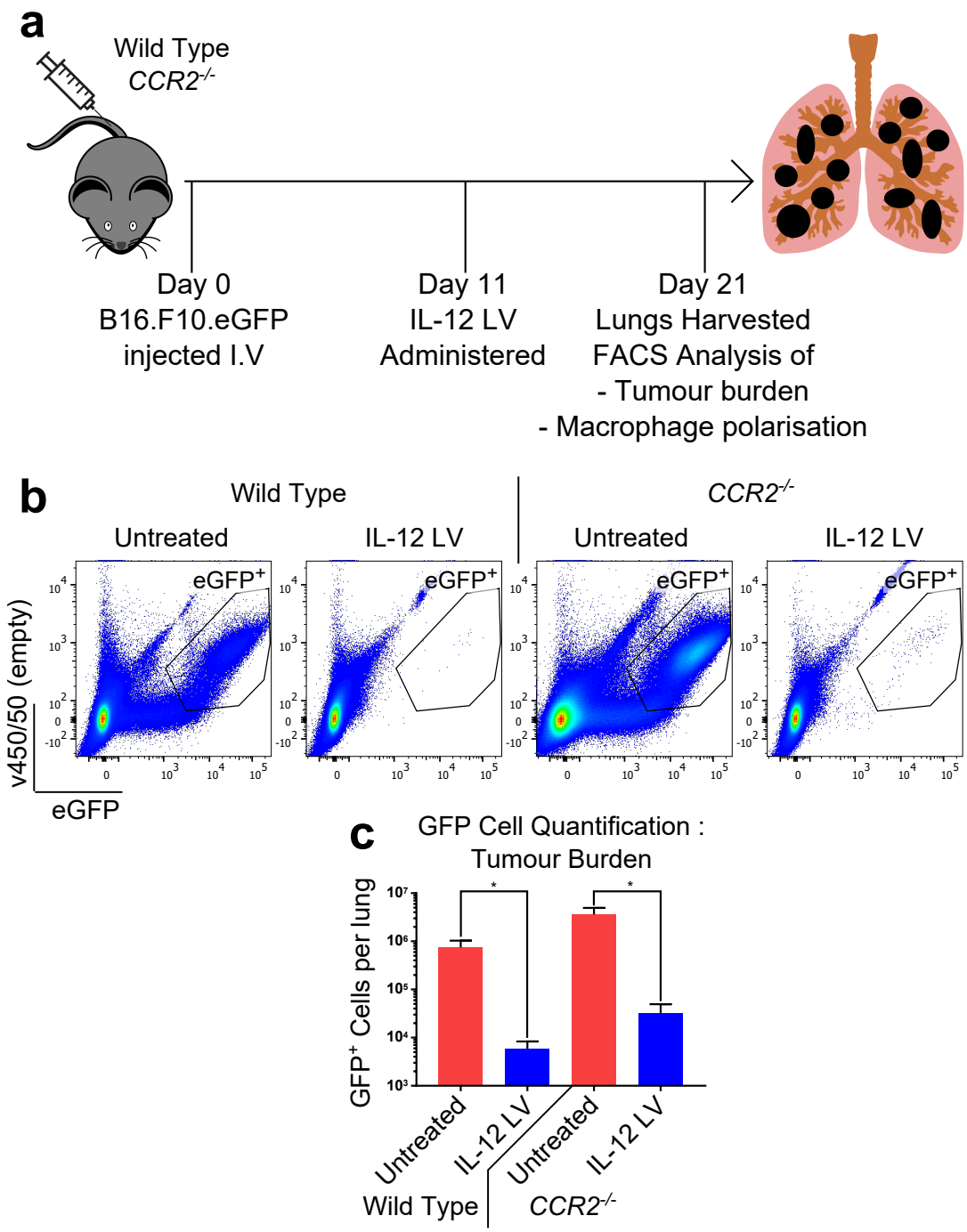

Figure 49: *CCR2*+ inflammatory macrophages do not mediate IL-12 LV induced cytotoxicity
Tumour bearing wild type and *CCR2*-/- mice were treated with IL-12 LV 11 days post tumour challenge. On the 21st day post challenge (10 days after IL-12 LV was administered), lungs were harvested for cytometric study (a). Tumour burden was measured by cytometric (b) quantification (c) of eGFP+ tumour cells. Error bars present S.E.M. *p<0.05, 1-Way ANOVA with Tukey's multiple comparison test. n=10 from 3 independent experiments.

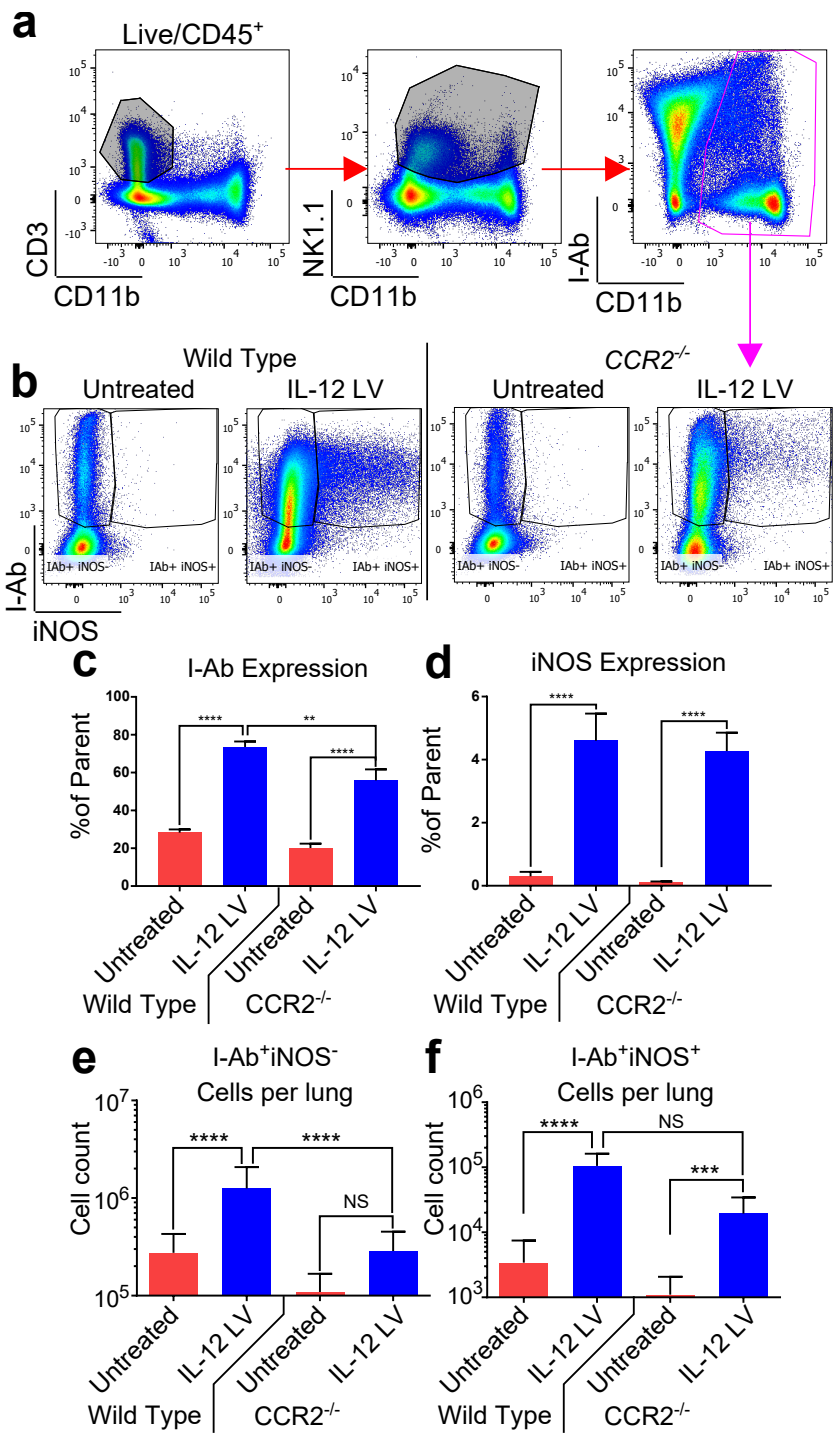

Figure 50: M1 polarisation in retained in IL-12 LV treated *CCR2*$^{-/-}$mice
The CD11b^{+} myeloid compartment was identified by FACS (a), wherein co-expression of MHC-II (I-Ab) and iNOS was measured (b). Absolute numbers of MHC-II^{+}iNOS^{-} (e) and MHC-II^{+}iNOS^{+} (f) cells were calculated per lung. Bar plots present (± S.E.M) expression and qauntification of I-Ab and iNOS expressing cells in untreated and IL-12 LV treated wild type and *CCR2*$^{-/-}$ mice. NS not signficant, **p<0.01, ****p<0.0001, 1-Way ANOVA, n=10 from 3 independent experiments.

5.4 IFNγ is a mediator of IL-12 LV induced M1 macrophage polarisation

We have demonstrated that IFNγ is a key mediator of IL-12 LV induced cytotoxicity. Subsequent neutralisation of IFNγ proved to effectively abrogate tumouricidal activity in this model. As we have hypothesised that IL-12 LV induced IFNγ is polarising interstitial macrophages into an M1-like phenotype (potentially with cytotoxic capacity), it should follow that IFNγ neutralisation in IL-12 LV treated mice will prevent macrophages from acquiring an M1-like phenotype that has been associated with tumouricidal activity.

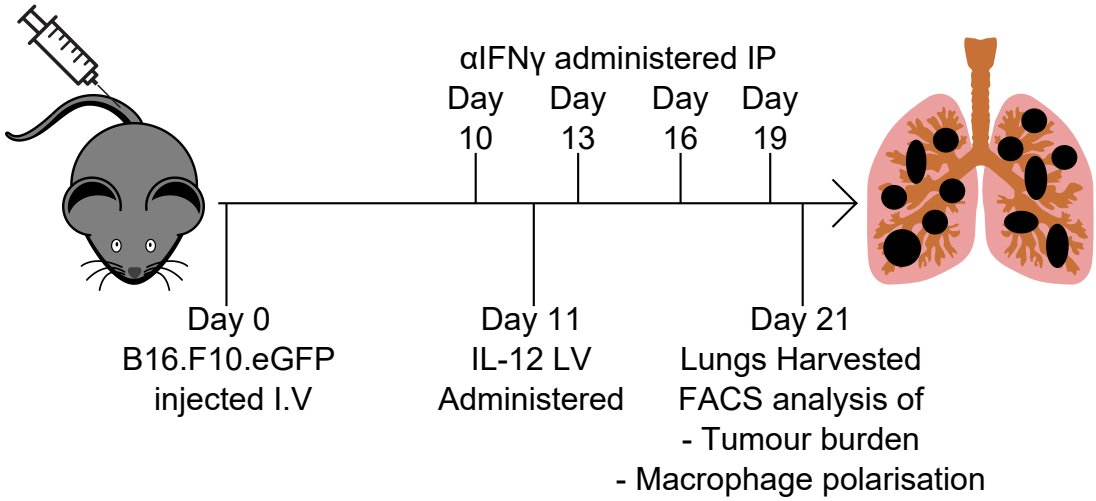

Figure 51: IFNγ neutralisation experimental design

IL-12 LV was administered to tumour bearing mice 11 days after tumour challenge. The IFNγ neutralising antibody (αIFNγ, XMG1.2 clone) was administered 1 day before IL-12 LV therapy and re-administered every 3 days until termination of the experiment. Mice were culled 21 days post tumour challenge, lungs were harvested and cytometric evaluation of lung tumour microenvironment was performed (Figure 51). FACS analysis of macrophages ($CD3^{-}CD49b^{-}CD11b^{+}Ly6G^{-}$) (Figure 52a) revealed significantly up-regulated expression of I-Ab (Figure 52b,c) and iNOS (Figure 52b,d) in IL-12 LV mice that was abrogated in IL-12 LV αIFNγ treated mice. These results were inversely associated with decreased tumour burden in IL-12 LV treated mice, abrogated by the addition of IFNγ neutralisation.

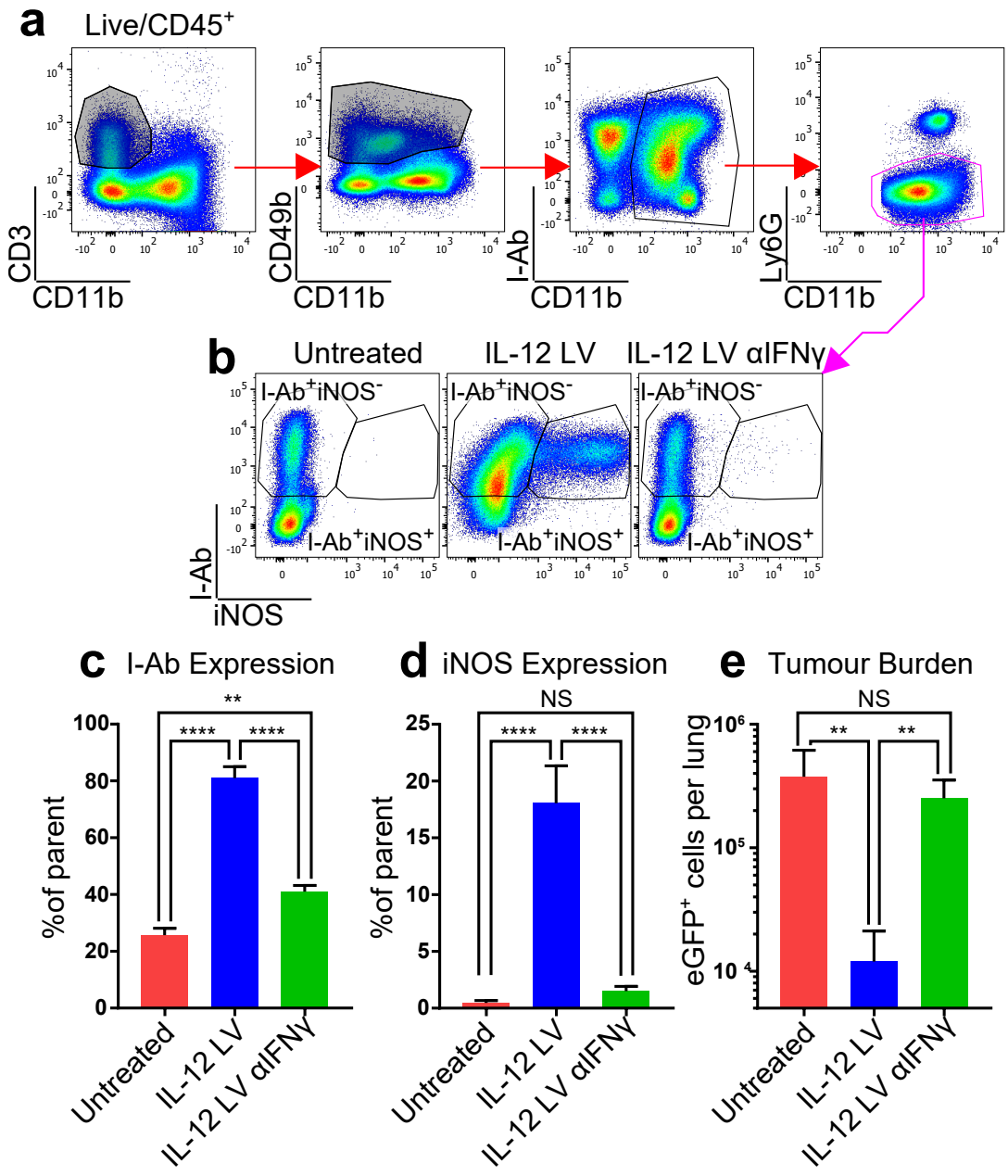

Figure 52: IL-12 LV mediated M1 macrophage polarization is IFNγ dependent FACS plots identify the macrophage containing compartment (defined as $CD45^+CD3^-CD49b^-CD11b^+Ly6G^-$) (a) wherein co-expression of MHC-II (I-Ab) and iNOS was measured (b). Bar plots represent expression of I-Ab (c) and iNOS (d) on gated cells as well as $eGFP^+$ tumour burden (e). Error bars present S.E.M. NS $p>0.05$, $^{**}p<0.01$, $^{****}p<0.0001$. 1-Way ANOVA, Tukey post test parametric I-Ab and iNOS analysis. Kruskal-Wallis with Dunn's post test for non-parametric $eGFP^+$ tumour burden analysis. n=10 from 3 independent experiments

5.5 Macrophage restricted IFNγ restricted receptor dysfunction impairs IL-12 LV mediated macrophage activation and tumouricidal activity

Having confirmed the key role of IFNγ in tumouricidal activity and M1 macrophage polarisation, we finally sought to investigate whether IFNγ mediated cytotoxicity was restricted to, or incidental to, IFNγ induced M1 macrophage polarisation.

We tested this hypotheses using the Macrophage Insensitive to Interferon Gamma (MIIG) transgenic mouse model [151]. This model has a knock-in transgene that expresses a CD68-restricted dominant-negative IFNγ receptor that renders $CD68^+$ macrophages insensitive to IFNγ. IL-12 LV was administered to tumour bearing wild type and MIIG mice 11 days post tumour challenge. Lungs were harvested 10 days post therapy (21 days post tumour challenge) and flow cytometry was used to quantify tumour burden and macrophage activity (Figure 53).

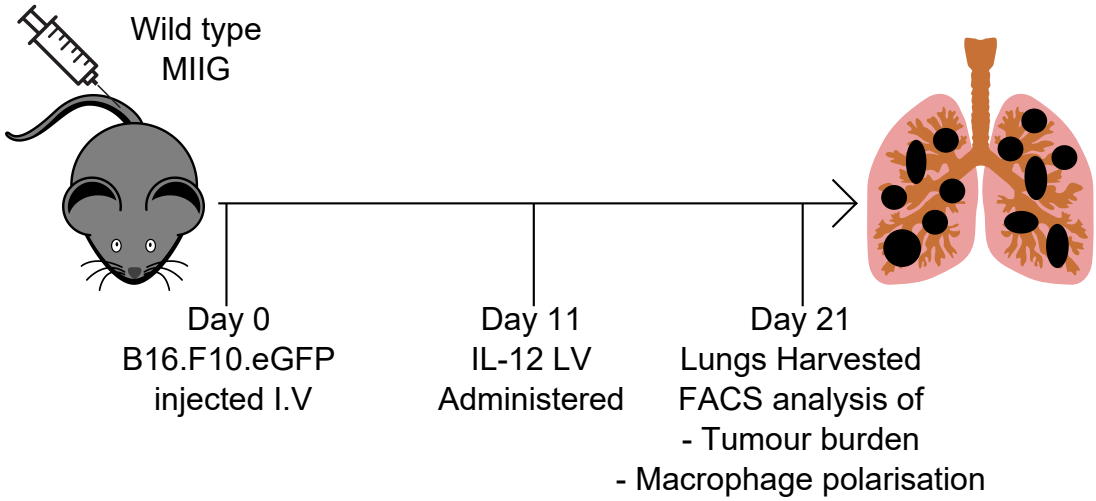

Figure 53: MIIG transgenic experimental design

FACS analysis of the $CD45^+$ pulmonary leukocytes identified macrophages ($CD3^-$ $NK1.1^-CD11b^+Ly6G^-$) (Figure 54a) and expression of I-Ab (Figure 54b,c) was up-regulated in both IL-12 LV wild type and MIIG mice (an increase of 28% and 14% respectively). iNOS (Figure 54b,d) significantly up-regulated by IL-12 LV therapy in wild type mice (increased by 5%); but not MIIG mice. Quantification of pulmonary metastases by measurement of $eGFP^+$ cells reveals significantly lower tumour burden in wild type mice treated with IL-12 LV (Figure 55a,b). This data was not replicated in MIIG mice, whose lungs presented no significant difference in tumour burden (e,f).

Concurrent analysis of T cell & NK cytotoxic potential (Figure 56a) revealed that $CD8^+$ T cells and NK cells upregulated expression of the cytotoxic molecule

Granzyme B (Figure 56b) in IL-12 LV treated wild type and MIIG mice with corresponding increases in T cell and NK proliferation as indicated by upregulated expression of Ki-67 (Figure 56c). This data indicates that NK and T cells retain IL-12 mediated cytotoxic function in the absence of a functional macrophage response to IFNγ.

Together, these data confirm that CD68^{+} M1 polarised macrophages are specifically activated by IFNγ in the model of IL-12 LV therapy, the absence of which correlates with tumouricidal activity regardless of NK & T cell cytotoxic function.

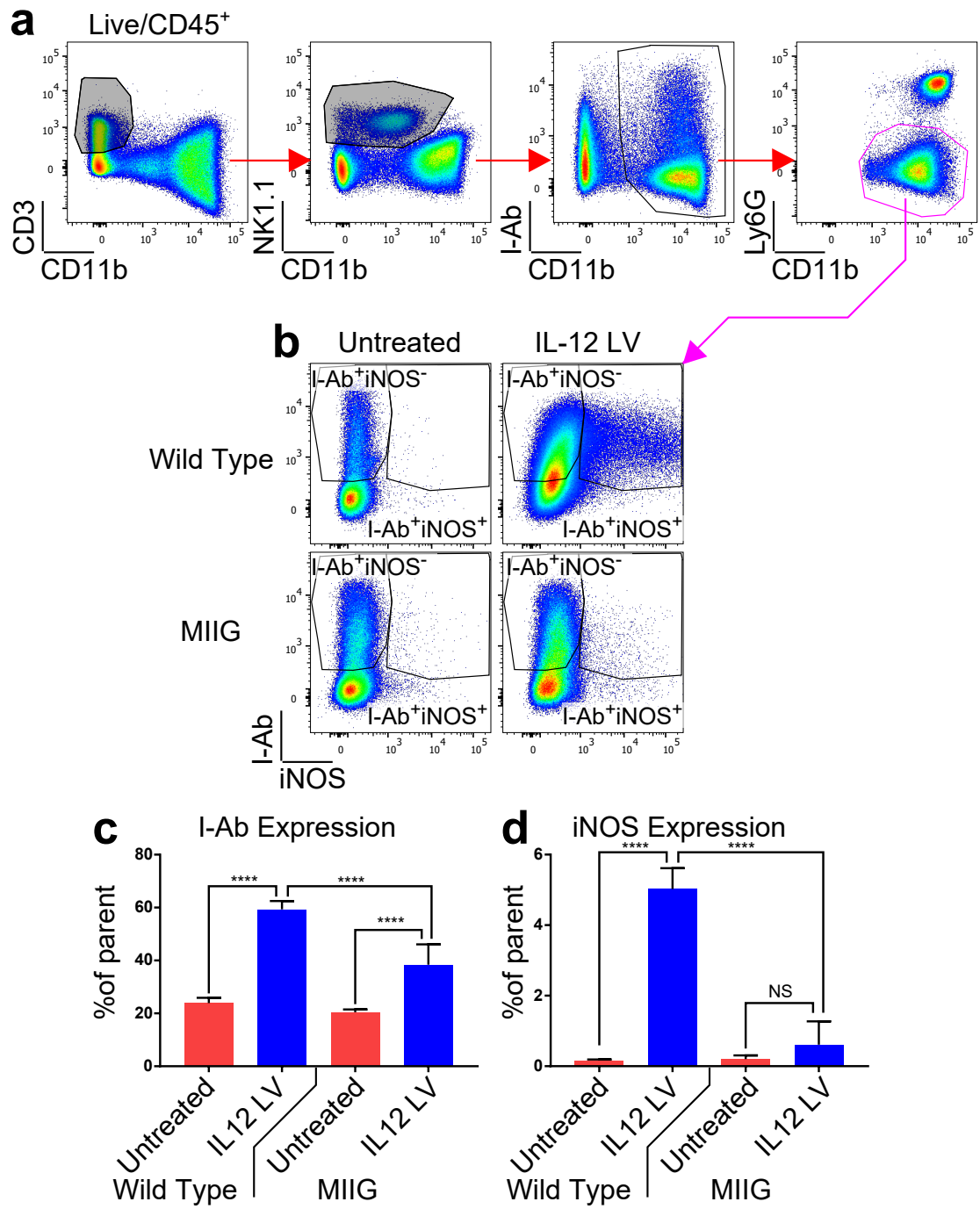

Figure 54: IFNγ insensitive macrophages do not undergo M1 polarisation in response to IL-12 LV

The CD45$^+$CD3$^-$NK1.1$^-$CD11b$^+$Ly6G$^-$ macrophage/DC compartment was identified by FACS (a) and co-expression of MHC-II (I-Ab) and iNOS (b) were measured in untreated and IL-12 LV wild type and MIIG mice. Bar plots present expression of I-Ab (c) and iNOS (d) on gated cells from untreated and IL-12 LV treated wild type and MIIG mice. Error bars present S.E.M. NS $p>0.05$, ****$p<0.0001$. 1-Way ANOVA with Tukey post test, n=10 from 3 independent experiments.

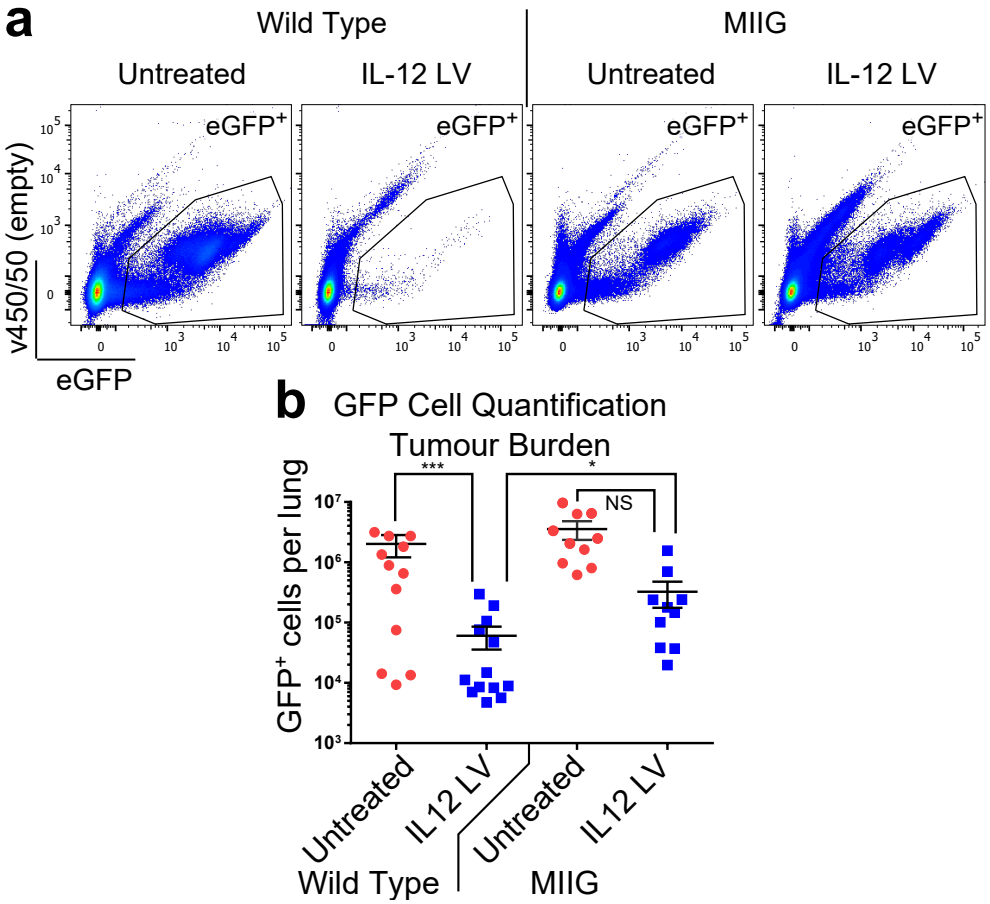

Figure 55: IFNγ sensitive macrophages are required to mediate IL-12 LV induced cytotoxicity

FACS plots (a) represent cytometric measurement of eGFP$^+$ tumour cells from untreated and IL-12 LV treated wild type and MIIG mice. Scatter plots (± S.E.M) present cytometric quantification of eGFP$^+$ tumour burden. NS $p>0.05$, *$p<0.05$, ***$p<0.001$, ****$p<0.0001$. Kruskal-Wallis with Dunn's post test for non-parametric eGFP tumour burden analysis (n=10) from the 3 independent experiments as presented in Figure 54.

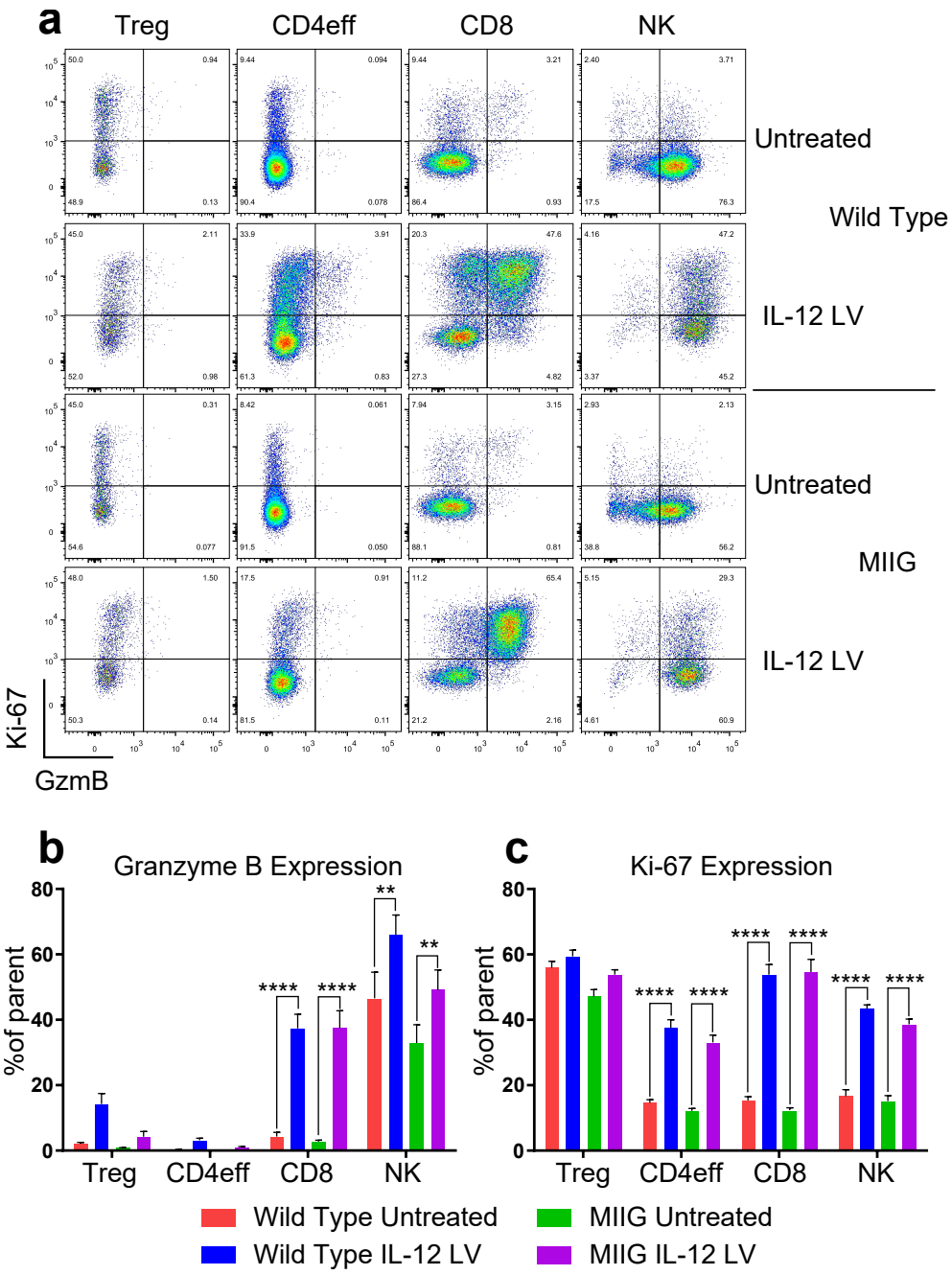

Figure 56: NK & T cell responses are retained in MIIG mice
Cytometric analysis (a) of the Granzyme B (GzmB) and Ki-67 expression in NK and T cells from IL-12 LV treated wild type and MIIG mice. Bar plots (± S.E.M) present expression of Granzyme B (b) and Ki-67 (c) measured from cytometry data. **p<0.01, ****p<0.0001. 2-Way ANOVA with Tukey post test, n=15 from 3 indepenent experiments.

5.6 Results section 5 discussion

The data presented in this final results chapter attempts to study the effect of IL-12 LV therapy on the pulmonary myeloid compartment in mice bearing pulmonary metastatic disease.

Initial experiments focused on measuring expansion of myeloid populations in IL-12 LV treated mice and by application of the pulmonary myeloid cytometry panel previously published by Alexander Misharin [171], we were able to resolve populations of CD103^{+} DC (cDC1), CD11b^{+}DC (cDC2), eosinophils, neutrophils, alveolar macrophages, MHC-II^{-} monocyte/macrophages (both Ly6C^{+} and Ly6C^{-}) and MHC-II^{+} interstitial macrophages with bi-modal expression of Ly6C.

Ratio-metric quantification of these populations revealed expansion of interstitial macrophages and Ly6C^{-} monocyte/macrophages with a non-significant decrease in alveolar macrophages in response to IL-12 LV therapy. This result may indicate that the Ly6C^{-} embryonically derived tissue resident macrophage population proliferates and matures into expanded MHC-II^{+} M1-like macrophages in response to IL-12.

Importantly, it is difficult to distinguish MHC-II^{+} TAM from MHC-II^{+} M1-like macrophages in this model as analysis is made of whole lung suspensions, and not of lung tumours specifically. Histopathological examination of IL-12 LV treated lungs (Figure 27a) present lungs almost devoid of tumour lesions and by extension such samples would therefore also present very few TAM for cytometric analysis. A refinement of FACS panels that may be applied to repeat experiments could include IL-10 and VEGF, as these two proteins may allow resolution of TAM (otherwise known as M2d [55]) against other MHC-II^{+} macrophages (including M1-like).

Further, experiments may be performed wherein lungs of untreated and IL-12 LV treated mice are collected shortly after IL-12 LV inoculation and fixed for immunofluorescent examination. High parameter immunofluorescence (IF) may allow labelling with up to 7 fluorescent antibodies [188] and could provide TAM/M1 phenotypic and functional insights into macrophages associated with tumour lesions. Such IF panels may include CD68, iNOS, IL-10, MHC-II and could focus on eGFP^{+} tumour lesions.

Interestingly, alveolar macrophages in IL-12 LV treated mice not only appeared to decrease in numbers but also upregulated surface expression of CD11b, an observation previously described in models of lung inflammation [52]. Functionally, this increased expression of CD11b (otherwise known as intergrin M) may indicate greater motility (as described in other CD11b^{+} cells [139]) and the possibility of an increased cytotoxic capacity (as previously observed in LPS stimulated alveolar macrophages [212]) in response to an IL-12 mediated inflammatory milieu.

Additionally, we do not believe that these changes in alveolar macrophage frequency and phenotype are indicators of an attenuated capacity to express IL-12 as we observe long term survival benefits with mice with persistent low tumour burdens (indicative of an ongoing response) and posit that this question could be answered by further analysis of IL-12 LV transduced alveolar macrophages by intracellular detection of IL-12 in a time-course experiment.

The upregulation of CD11b may additionally explain the apparent decrease in alveolar macrophage quantification as these SiglecF^{+} cells are masked in our gating strategy by SiglecF^{+}CD11b^{high} eosinophils. An argument against this interpretation may be that no corresponding increase in eosinophil count was recorded and that alternatively, alveolar macrophages may be dying in direct response to lentiviral transduction or by over stimulation and FAS related apoptosis (a phenomenon previously reported in silicosis patients [276]).

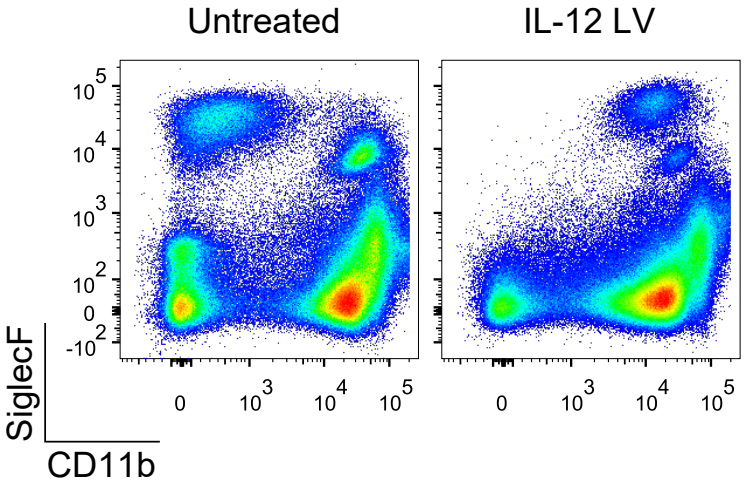

Figure 57: IL-12 LV upregulates CD11b expression on alveolar macrophages

Given the relatively complex gating strategy employed in our application of the Misharin phenotyping panel, we sought confirmation that our gating strategy was accurately capturing all significant myeloid populations and to this end, two unbiased automated analysis methods were applied to the set of cytometry data.

FlowSOM uses a self-organizing map (SOM) approach to generate unsupervised clustering of cytometric data [247] and is commonly applied to down-sampled (sub-sampled) data sets to alleviate the heavy strain this analysis exerts on computing resources. FlowSOM analysis was applied to randomly down-sampled cohorts from our data set on the UCL Legion computing cluster. This analysis was then repeated 50 times (a process referred to as “multiple iterations”) in order to capture the breadth of data that may be missed in the process of down-sampling.

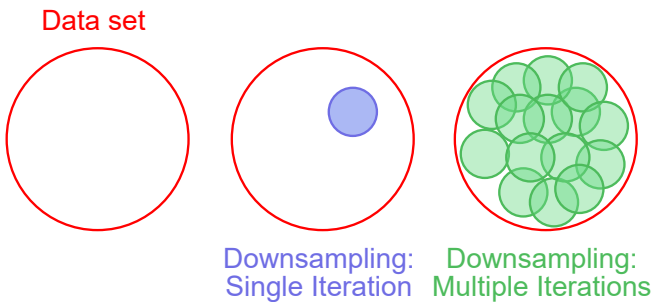

Figure 58: Multiple iteration sampling is used to increase coverage in downsampled data sets

The resultant clusters contain phenotypic and frequency data that was reconstituted into Figure 46 as a self-organising heatmap (Figure 46a) and bar graph (Figure 46b) respectively. Not only did this analysis recapitulate all manually gated populations, it also correctly identified populations of $CD64^{+}Ly6C^{-}$ and $CD64^{+}Ly6C^{+}$ interstitial macrophages not included in the original gating strategy, both of which appeared to expand (as a proportion of all myeloid cells) under IL-12 LV therapy.

Uniform approximation and projection (UMAP) [162] is a dimension reduction method that, when applied to cytometry data [17], attempts to construct a binomial plot of all analysed cells that retains the spatial relationship between all cells based on their phenotype from n-dimensional expression data. Resultant plots generally group phenotypically similar populations close to each and un-related populations further apart. Dimension reduced plots generated from UMAP or other methods such as t-stochastic neighbour embedding (tSNE) [1] and principal component analysis (PCA) [150] are generally combined with clustering data where clusters are mapped onto dimension-reduced plots.

The application of UMAP to our data set, combined with FlowSOM clusters, generated a single plot (Figure 47a) that effectively displayed a phenotypically close relationship between $Ly6C^{-}$ monocytes, $Ly6C^{+}$ monocytes, insterstital macrophages and DC while neutrophils, eosinophils and alveolar macrophages are phenotypically distinct. Although this data may have less value than manual gating or the unbiased clustering component of this analysis, it remains a useful tool to distill the information contained in 10 plots (Figure 44a) into a single plot (Figure 47a).

The *CCR2*$^{-/-}$ experiments sought to dissect the contribution of HSC derived $CCR2^{+}$ $Ly6C^{+}$ monocytes to the $iNOS^{+}$ interstitial macrophage pool in IL-12 LV treated mice. These experiments appear to rule out $CCR2^{+}$ monocyte involvement, however they cannot be discounted as sources of $iNOS^{+}$ macrophages as iNOS expression is observed on both $Ly6^{+}$ and $Ly6C^{-}$ macrophages in wild type mice. Without parallel experiments depleting $CCR2^{-}Ly6C^{-}$ macrophages we cannot rule out a role of $Ly6C^{+}$ monocytes as a reservoir to complement and supplant embry-

onically derived Ly6C$^-$ interstitial macrophages and it may well be that the Ly6C$^-$ compartment expands in *CCR2$^{-/-}$* mice to fill a niche that is usually bolstered by Ly6C$^+$ cells in the wild type condition.

The BD FACS Fortessa used in this study was limited to a maximum of 12 analytes, and a consequence of this limitation FACS panels were designed with some concessions made to panel design. Prominent concessions and errors made in design of iNOS functional panels left this panel underpowered to accurately discriminate M1-like macrophages from CD11b$^+$ DC (cDC2) and MHC-II$^+$ TAM.

Although we believe that the CD45$^+$CD3$^-$NK1.1$^-$CD11b$^+$Ly6G-MHC-II$^+$iNOS$^+$ gated population presented in this study represents a population of M1-like polarised interstitial macrophages, an improved panel to assess function would involve identification of CD45$^+$CD11b$^+$NK1.1$^-$Ly6G$^-$Zbtb46$^-$CD24$^-$CD64$^+$SiglecF$^-$ interstitial macrophages wherein Ly6C, CCR2, MerTK, MHC-II, iNOS, IL-12, CD206, IL-10, TGFβ and VEGF would be used to identify functional polarisation and ontology of these gated interstitial macrophages.

The role of IFNγ sensitive macrophages in IL-12 LV mediated tumour rejection was explored by replication of experimental conditions in MIIG transgenic mice. This transgenic model forces expression of a non-functional IFNγR (dnIFNγR) in all CD68$^+$ macrophages including alveolar macrophages. Using this model, we demonstrate that IL-12 LV induced tumouricidal activity is mediated via IFNγ sensitive macrophages as the tumour burden in IL-12 LV treated MIIG mice was not significantly different from the untreated control and is significantly greater than the wild type IL-12 LV treated condition. There does however appear to be a non-significant decreased tumour burden in IL-12 LV treated mice (cf. untreated control), we posit the following explanations for this observation.

Although presence of the MIIG transgene was confirmed in every mouse used in these experiments via PCR, it should be noted the wild type IFNγR has not been ablated and that we did not assay expression of the dnIFNγR in these mice to confirm presence of the dnIFNγR and the ratio of its expression against the wild type receptor. Given a great enough reservoir of IFNγ, there is a possibility that the sequestering capacity of the dnIFNγR becomes saturated and normal IFNγ signalling may occur through the wild type receptor with associated restoration of tumouricidal activity (Figure 59). A refinement of this model would involved conditional ablation of the wild type receptor.

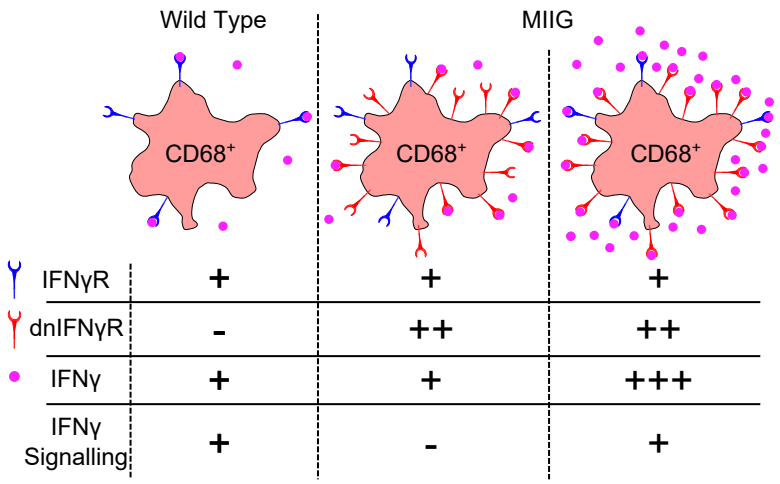

Figure 59: IFNγ saturation may restore sensitivity in MIIG mice

Additionally, the cytotoxic contribution of NK and T cells to IL-12 LV therapy has not been explored in this model where depletion of $CD8^+$ T cells and NK cells may further diminish the any residual cytotoxic functions still at play in the MIIG model.

The possibility of alveolar macrophage paracrine signalling may also be explored as IL-12 induced IFNγ may in turn drive alveolar macrophage cytotoxicity much as we have described in interstitial macrophages. An evolution of the MIIG experiments may expand this concept where the ideal model would restrict expression of the dnIFNγR to $SiglecF^+$ alveolar macrophages and not all macrophages as is the case in the current MIIG model.

Having demonstrated the critical requirement of IFNγ sensitive macrophages in the described mechanism of IL-12 mediated tumour rejection, we have yet to established a mechanism of action by which macrophages mediate tumour directed cytotoxicity. In order to investigate this question, nitric oxide mediated cytoxicity and phagocytic activity may be explored in several models.

The expression of nitric oxide (NO) by M1 polarised macrophages at high concentration has been shown to effectively kill tumour cells in vitro [144, 224]. We hypothesise that the application of iNOS inhibiting agents such as L-nil or 1400W to IL-12 LV treated mice may abrogate tumour lysis and elucidate the potential mechanism of macrophage cytotoxicity in this model. Pilot experiments were performed using 1400W, however dosage and schedule was not optimised and meaningful data was not collected.

Macrophages may also remove tumour cells directly via phagocytosis and we hypothesise that this process may be observed in IL-12 LV treated mice by imaging of macrophage/tumour interactions. MacBlue transgenic mice are an ideal model in which to study IL-12 LV activity as all *Csf1r* dependant macrophages

express cyan fluorescent protein (CFP) [210]. Intravenous challenge of MacBlue mice with red fluorescent protein (RFP) expressing B16.F10 tumour cells would allow *in vivo* imaging of tumour phagocytosis via multi-photon microscopy [202]. The application of DAF-2/DA in this model would allow the additional observation of nitric oxide activity in macrophage/tumour interactions as this non-fluorescent compound is reduced to fluorescein by NO [193].

Finally, the exploitation of the CD47/SIRPα suppression pathway may identify phagocytosis as a mechanism of action. Previous studies [280] have reported that tumours expressing CD47 can mediate signal-regulatory protein alpha (SIRPα) receptor signaling in macrophages, and an inhibition of macrophage-mediated tumour cell phagocytosis. We therefore hypothesise that if the IFNγ sensitive macrophages observed in our study were capable of direct tumour lysis, then the phagocytic activity of such cells would be abrogated in a model of CD47 over-expression on B16.F10 tumour cells, leading to uncontrolled tumour growth as seen in untreated mice.

6 Final Discussion

Biological model and context in previously published works

Given the data available, we propose a model wherein intranasal application of an IL-12 encoding lentivirus to lung tumour bearing mice transduces alveolar macrophages that in turn express IL-12.

Elevated pulmonary IL-12 promotes two distinct lymphocytic functions: $CD8^+$ T cell / NK cell mediated cytotoxicity and T cell / NK / ILC mediated IFNγ expression. The expression of IFNγ by lymphocytes stimulates expansion of $Ly6C^-$ interstitial macrophages, possibly supplemented by recruitment and differentiation of $Ly6C^+$ monocyte derived macrophages from the periphery.

IFNγ additionally polarises tumour associated macrophages, tumour adjacent M2-like macrophages and possibly alveolar macrophages toward an M1-like functional state that facilitates tumour clearance by iNOS mediated expression of NO and increased phagocytic function.

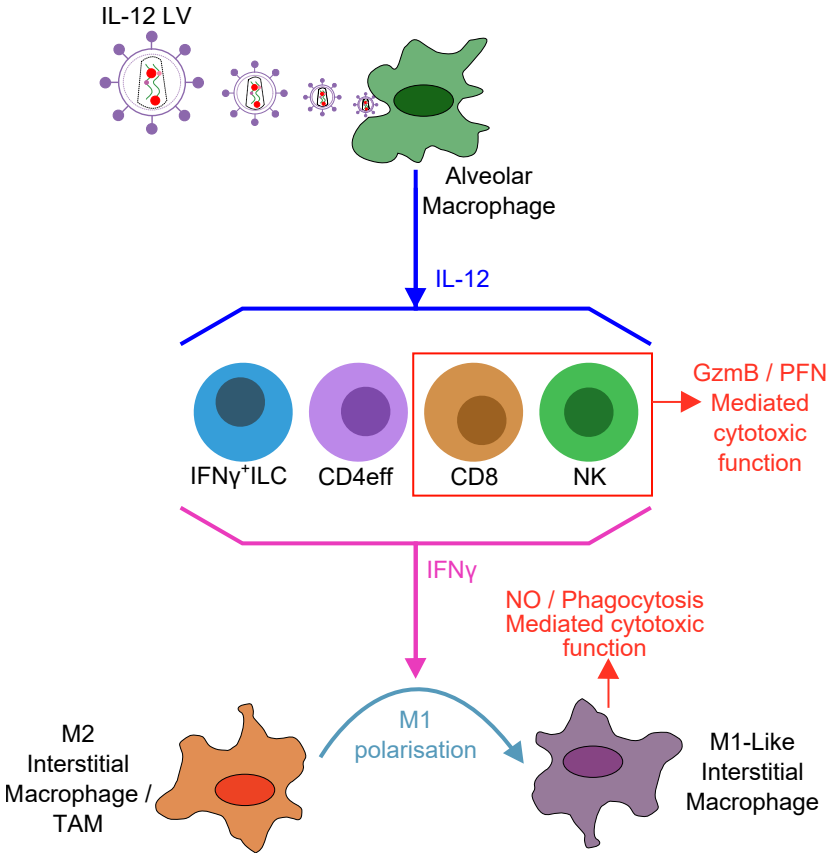

Figure 60: Proposed IL-12 LV biological model

Like macrophages, ILCs appear to seed lung tissue both as early tissue resident cells and later as HSC derived lymphocytes recruited from the periphery in response to inflammatory signals.

A study from the Rudensky group [76] utilised parabiosis models to identify that the majority of ILCs observed in lymphoid and non-lymphoid organs were tissue resident cells. Interestingly, this study found pulmonary ILC1 cells were derived from both parabionts and that donor derived ILC1 were restricted to the pulmonary vasculature and not the parenchyma.

A later study from the Di Santo group, found that ILC may also expand and infiltrate sites of inflammation through a process dubbed “ILC-poeisis” in which CD117^{+} ILC precursor (ILCP) cells were isolated from peripheral blood and readily differentiated into the broad spectrum of ILC subsets when stimulated with IL-2, IL7, IL-1β and IL-23 [136] while the addition of IL-12 skewed ILCP differentiation toward an IFNγ^{+} NK phenotype. Subsequent *in vivo* experiments further demonstrated migration of these cells from the periphery to sites of inflammation where they differentiated into ILCs.

In the context of these two studies we hypothesise that expression of IL-12 in the pulmonary compartment by transduced alveolar macrophages leads to rapid expansion of tissue resident ILC as well as recruitment and differentiation of ILCP from the periphery into infiltrating IFNγ^{+} ILC. Without the need for cognate antigen, these cells may be able to respond to IL-12 faster than T cells, mediating early IFNγ dependent processes. The relative scarcity of ILCs in comparison to T cells may be a function of the time point this data was collected, where ILC numbers may decrease after initial influx and are supplanted by T cells. This hypothesis may be supported by our observation that T cell deficient *Rag*$^{-/-}$ mice respond to IL-12 LV therapy with relatively higher numbers of IFNγ^{+} ILCs as they expand to fill the niche usually occupied by T cells at the later stage that these tissues are collected.

Imaging of ILCP, ILC, T cells and macrophages in lung sections taken at regular timepoints throughout the experimental schedule, or imaged directly in live tissue via intravital imaging would allow a full characterisation of the kinetics and temporo-spatial relationship between these cells during tumourigenesis and subsequent IL-12 LV mediated resolution of metastatic disease while single-cell analysis (cytometry or sequencing) may give greater insight into the function and phenotypic changes in these cells over time.

As described in section 5, high expression of IFNγ by ILCs, T cells and NK cells induced both the accumulation and activation of interstitial macrophages, leading to clearance of established B16.F10 melanoma pulmonary metastases in a model that is classically resistant to monotherapeutic approaches. This mechanism contrasts with those described in two other recent reports [61, 114].

The first study utilized an IL-12 transduced B16.F10 tumour cell line to investigate the tumouricidal activity of IL-12 in a prophylaxis rather than treatment setting [61].

Previous studies have shown that NKp46^{+} ILCs express IL-12 receptor [117] and are sensitive to IL-12 stimulation [21]. Adoptive transfer of NKp46^{+}ILCs into IL-12 receptor knockout mice (*IL-12RB2*$^{-/-}$) bearing IL-12-expressing subcutaneous B16.F10 tumors led to effective control of tumour growth, identifying a critical role for an intra-tumoural IL-12 sensitive ILC population (referred to as NKp46^{+} LTi cells) in this model. This function was, however, shown to be IFNγ independent, and cytotoxic activity was ascribed to the up-regulation of adhesion molecules in the tumour vasculature leading to increased leukocyte infiltration.

In contrast, the second study identified an IFNγ dependent mechanism of IL-12 activity, which was independent of NKp46^{+} ILC involvement [114]. T cells reactive to tumour antigen were transduced to express IL-12 and then transferred into mice bearing subcutaneous B16.F10 tumors, resulting in tumor rejection. The mechanism through which IL-12 mediated tumour rejection was dependent both on IFNγ and also on cross presentation of tumour antigens by a mixed myeloid population, characterized by increased intra-tumoural macrophages, dendritic cells and myeloid derived suppressor cells (MDSCs).

We propose a mechanism, which reconciles elements of both of these previous studies, whilst advancing our understanding of the clinical applications of IL-12 based therapies. The elimination of T cells through the use of *Rag*$^{-/-}$ mice, and the subsequent depletion of NK cells, highlights the key role of ILCs within the pulmonary niche. In the absence of both T cells and NK cells, ILCs become the principle source of IFNγ within the lung TME, which acts upon the interstitial macrophage population to mediate tumour destruction. We demonstrate that this population of IFNγ-sensitive macrophages are responsible for tumor clearance, even in NK and T cell replete mice (results section 5.5), and that both ILC and myeloid cells are required for activity, unifying the critical role of both of these populations as described individually in the previous studies [61, 114].

Clinical Relevance

Clinical application of lentivirus has largely been relegated to ex vivo manipulation of autologous cells for adoptive transfer (as described in section 1.7). This is in part due to challenges in scaling lentiviral production for clinical use and historical safety considerations [100].

Given these challenges, it may be prudent to consider an alternative vector for delivery of IL-12. Adeno-associated virus (AAV) is a well characterised non-integrating viral vector system that has been used extensively in Phase I and II trials to treat genetic defects in vivo (as per Table 5 in section 1.7).

Of particular note is a Phase I trial [63] that sought to treat cystic fibrosis by in-

tranasal delivery of cystic fibrosis transmembrane conductance regulator (CFTR) encoding AAV (serotype 2, AAV2). This study establishes that aerosol delivery of AAV2 can lead to relatively stable expression of CFTR where vector genome copies were detectable by PCR up to 30 days post therapy.

Although this may appear a viable alternative to lentivirus, further studies would need to be completed to assess whether AAV2 can package the ~2kb IL-12Fc transgene as would be predicted by it's reported 4.3kb limit [87] and whether or not this construct can transduce macrophages as efficiently as IL-12 LV.

The application of targeted IL-12 therapy has potential clinical relevance not only has a monotherapy, but also as a combination partner with immune checkpoint blockade.

A plethora of data has been generated recently in clinical application of immune checkpoint blockade (ICB) in a variety of solid cancers. The most well studied ICB therapies involve blockade of PD-1 (nivolumab & pembrolizumab) and CTLA-4 (ipilimumab) where objective clinical responses have been greatly improved over previous gold standard radiation and chemotherapies [166]. These responses are far from universal and do not show activity in many patients.

One concept that partially explains the failure of ICB in some patients involves a general lack of effector lymphocyte infiltration into the tumour microenvironment as these therapies are meaningless without tumour infiltrating lymphocytes (TILs) to stimulate and clear established tumour. Such poorly infiltrated tumours having recently been described as "cold tumours" are a focus of a great deal of research where various interventions are assessed in order to turn a "cold tumour" into a "hot tumour" that contains a high number of TILs to be affected by ICB therapy [22].

As a potent, pleiotropic immune stimulatory cytokine IL-12 is well placed as a potential ICB combination partner that may increase TIL infiltration and activity. Two recent pre-clinical studies have studied the synergistic combination of PD-1 blockade [75] or CTLA-4 blockade [256] with IL-12 where the former study identifies a role of IL-12 expressing DC that synergises with blockade of PD-1 on infiltrating T cells and the latter study demonstrates effective combination of IL-12 and aCTLA-4 in a pre-clinical model of glioblastoma that is resistant to either of these therapies applied alone.

We posit that local application of IL-12 to the lung tumour microenvironment via a viral vector delivery system holds potential for translation into a clinical setting not only has a monotherapy but as a synergistic partner with current gold standard immunotherapies.

Conclusions

We believe that our data support further evaluation of targeted approaches to the delivery of IL-12 for therapeutic application. The critical role of ILCs and myeloid cells in our model potentially offers new opportunities for clinical exploitation. Determining whether the lung TME is unique in this capacity, and the significance of each of these populations in other tumor models/cancer types, coupled to evaluation in human samples, will establish whether similar mechanisms underpin IL-12 responsiveness more broadly outside of the lung.

References

[1] Nicole V. Acuff and Joel Linden. Using Visualization of t-Distributed Stochastic Neighbor Embedding To Identify Immune Cell Subsets in Mouse Tumors. *Journal of Immunology (Baltimore, Md.: 1950)*, 198(11):4539–4546, 2017.

[2] Maryam Afkarian, John R. Sedy, Jianfei Yang, Nils G. Jacobson, Nezih Cereb, Soo Y. Yang, Theresa L. Murphy, and Kenneth M. Murphy. T-bet is a STAT1-induced regulator of IL-12r expression in naïve CD4+ T cells. *Nature Immunology*, 3(6):549–557, June 2002.

[3] Inna S. Afonina, Sean P. Cullen, and Seamus J. Martin. Cytotoxic and non-cytotoxic roles of the CTL/NK protease granzyme B. *Immunological Reviews*, 235(1):105–116, May 2010.

[4] C. Albanesi, C. Scarponi, A. Cavani, M. Federici, F. Nasorri, and G. Girolomoni. Interleukin-17 is produced by both Th1 and Th2 lymphocytes, and modulates interferon-gamma- and interleukin-4-induced activation of human keratinocytes. *The Journal of Investigative Dermatology*, 115(1):81–87, July 2000.

[5] W. K. Alderton, C. E. Cooper, and R. G. Knowles. Nitric oxide synthases: structure, function and inhibition. *The Biochemical Journal*, 357(Pt 3):593–615, August 2001.

[6] Ghalib Alkhatib. The biology of CCR5 and CXCR4. *Current opinion in HIV and AIDS*, 4(2):96–103, March 2009.

[7] Frederick Arce, Helen M. Rowe, Benjamin Chain, Luciene Lopes, and Mary K. Collins. Lentiviral vectors transduce proliferating dendritic cell precursors leading to persistent antigen presentation and immunization. *Molecular Therapy: The Journal of the American Society of Gene Therapy*, 17(9):1643–1650, September 2009.

[8] Frederick Arce Vargas, Andrew J. S. Furness, Kevin Litchfield, Kroopa Joshi, Rachel Rosenthal, Ehsan Ghorani, Isabelle Solomon, Marta H. Lesko, Nora Ruef, Claire Roddie, Jake Y. Henry, Lavinia Spain, Assma Ben Aissa, Andrew Georgiou, Yien Ning Sophia Wong, Myles Smith, Dirk Strauss, Andrew Hayes, David Nicol, Tim O'Brien, Linda Mårtensson, Anne Ljungars, Ingrid Teige, Björn Frendéus, TRACERx Melanoma, TRACERx Renal, TRACERx Lung consortia, Martin Pule, Teresa Marafioti, Martin Gore, James Larkin, Samra Turajlic, Charles Swanton, Karl S. Peggs, and

Sergio A. Quezada. Fc Effector Function Contributes to the Activity of Human Anti-CTLA-4 Antibodies. *Cancer Cell*, 33(4):649–663.e4, 2018.

[9] Frederick Arce Vargas, Andrew J. S. Furness, Isabelle Solomon, Kroopa Joshi, Leila Mekkaoui, Marta H. Lesko, Enrique Miranda Rota, Rony Dahan, Andrew Georgiou, Anna Sledzinska, Assma Ben Aissa, Dafne Franz, Mariana Werner Sunderland, Yien Ning Sophia Wong, Jake Y. Henry, Tim O'Brien, David Nicol, Ben Challacombe, Stephen A. Beers, Melanoma TRACERx Consortium, Renal TRACERx Consortium, Lung TRACERx Consortium, Samra Turajlic, Martin Gore, James Larkin, Charles Swanton, Kerry A. Chester, Martin Pule, Jeffrey V. Ravetch, Teresa Marafioti, Karl S. Peggs, and Sergio A. Quezada. Fc-Optimized Anti-CD25 Depletes Tumor-Infiltrating Regulatory T Cells and Synergizes with PD-1 Blockade to Eradicate Established Tumors. *Immunity*, 46(4):577–586, 2017.

[10] C. Asselin-Paturel, N. Lassau, J. M. Guinebretière, J. Zhang, F. Gay, F. Bex, S. Hallez, J. Leclere, P. Peronneau, F. Mami-Chouaib, and S. Chouaib. Transfer of the murine interleukin-12 gene in vivo by a Semliki Forest virus vector induces B16 tumor regression through inhibition of tumor blood vessel formation monitored by Doppler ultrasonography. *Gene Therapy*, 6(4):606–615, April 1999.

[11] M. B. Atkins, M. T. Lotze, J. P. Dutcher, R. I. Fisher, G. Weiss, K. Margolin, J. Abrams, M. Sznol, D. Parkinson, M. Hawkins, C. Paradise, L. Kunkel, and S. A. Rosenberg. High-dose recombinant interleukin 2 therapy for patients with metastatic melanoma: analysis of 270 patients treated between 1985 and 1993. *Journal of Clinical Oncology: Official Journal of the American Society of Clinical Oncology*, 17(7):2105–2116, July 1999.

[12] M. B. Atkins, M. J. Robertson, M. Gordon, M. T. Lotze, M. DeCoste, J. S. DuBois, J. Ritz, A. B. Sandler, H. D. Edington, P. D. Garzone, J. W. Mier, C. M. Canning, L. Battiato, H. Tahara, and M. L. Sherman. Phase I evaluation of intravenous recombinant human interleukin 12 in patients with advanced malignancies. *Clinical Cancer Research: An Official Journal of the American Association for Cancer Research*, 3(3):409–417, March 1997.

[13] Chiraz Atri, Fatma Z. Guerfali, and Dhafer Laouini. Role of Human Macrophage Polarization in Inflammation during Infectious Diseases. *International Journal of Molecular Sciences*, 19(6), 2018.

[14] C. M. Bacon, D. W. McVicar, J. R. Ortaldo, R. C. Rees, J. J. O'Shea, and J. A. Johnston. Interleukin 12 (IL-12) induces tyrosine phosphorylation of JAK2 and TYK2: differential use of Janus family tyrosine kinases by IL-2

and IL-12. *The Journal of Experimental Medicine*, 181(1):399–404, January 1995.

[15] C. M. Bacon, E. F. Petricoin, J. R. Ortaldo, R. C. Rees, A. C. Larner, J. A. Johnston, and J. J. O'Shea. Interleukin 12 induces tyrosine phosphorylation and activation of STAT4 in human lymphocytes. *Proceedings of the National Academy of Sciences of the United States of America*, 92(16):7307–7311, August 1995.

[16] Stefanie R. Bailey, Michelle H. Nelson, Richard A. Himes, Zihai Li, Shikhar Mehrotra, and Chrystal M. Paulos. Th17 cells in cancer: the ultimate identity crisis. *Frontiers in Immunology*, 5:276, 2014.

[17] Etienne Becht, Charles-Antoine Dutertre, Immanuel W.H. Kwok, Lai Guan Ng, Florent Ginhoux, and Evan W Newell. Evaluation of UMAP as an alternative to t-SNE for single-cell data. *bioRxiv*, page 298430, January 2018.

[18] G. J. Bellingan, H. Caldwell, S. E. Howie, I. Dransfield, and C. Haslett. In vivo fate of the inflammatory macrophage during the resolution of inflammation: inflammatory macrophages do not die locally, but emigrate to the draining lymph nodes. *Journal of Immunology (Baltimore, Md.: 1950)*, 157(6):2577–2585, September 1996.

[19] Nadège Bercovici, Marion V. Guérin, Alain Trautmann, and Emmanuel Donnadieu. The Remarkable Plasticity of Macrophages: A Chance to Fight Cancer. *Frontiers in Immunology*, 10:1563, 2019.

[20] Caroline A. Bernhard, Christine Ried, Stefan Kochanek, and Thomas Brocker. CD169+ macrophages are sufficient for priming of CTLs with specificities left out by cross-priming dendritic cells. *Proceedings of the National Academy of Sciences of the United States of America*, 112(17):5461–5466, April 2015.

[21] Jochem H. Bernink, Lisette Krabbendam, Kristine Germar, Esther de Jong, Konrad Gronke, Michael Kofoed-Nielsen, J. Marius Munneke, Mette D. Hazenberg, Julien Villaudy, Christianne J. Buskens, Willem A. Bemelman, Andreas Diefenbach, Bianca Blom, and Hergen Spits. Interleukin-12 and -23 Control Plasticity of CD127(+) Group 1 and Group 3 Innate Lymphoid Cells in the Intestinal Lamina Propria. *Immunity*, 43(1):146–160, July 2015.

[22] Paola Bonaventura, Tala Shekarian, Vincent Alcazer, Jenny Valladeau-Guilemond, Sandrine Valsesia-Wittmann, Sebastian Amigorena, Christophe Caux, and Stéphane Depil. Cold Tumors: A Therapeutic Challenge for Immunotherapy. *Frontiers in Immunology*, 10, February 2019.

[23] Houcine Bougherara, Fariba Némati, André Nicolas, Gérald Massonnet, Martine Pugnière, Charlotte Ngô, Marie-Aude Le Frère-Belda, Alexandra Leary, Jérôme Alexandre, Didier Meseure, Jean-Marc Barret, Isabelle Navarro-Teulon, André Pèlegrin, Sergio Roman-Roman, Jean-François Prost, Emmanuel Donnadieu, and Didier Decaudin. The humanized anti-human AMHRII mAb 3c23k exerts an anti-tumor activity against human ovarian cancer through tumor-associated macrophages. *Oncotarget*, 8(59), November 2017.

[24] Robert V. Bruggner, Bernd Bodenmiller, David L. Dill, Robert J. Tibshirani, and Garry P. Nolan. Automated identification of stratifying signatures in cellular subpopulations. *Proceedings of the National Academy of Sciences of the United States of America*, 111(26):E2770–2777, July 2014.

[25] M. J. Brunda, L. Luistro, R. R. Warrier, R. B. Wright, B. R. Hubbard, M. Murphy, S. F. Wolf, and M. K. Gately. Antitumor and antimetastatic activity of interleukin 12 against murine tumors. *The Journal of Experimental Medicine*, 178(4):1223–1230, October 1993.

[26] Bernhard Brüne, Andreas von Knethen, and Katrin B Sandau. Nitric oxide and its role in apoptosis. *European Journal of Pharmacology*, 351(3):261–272, June 1998.

[27] J. F. Brunet, F. Denizot, M. F. Luciani, M. Roux-Dosseto, M. Suzan, M. G. Mattei, and P. Golstein. A new member of the immunoglobulin superfamily–CTLA-4. *Nature*, 328(6127):267–270, July 1987.

[28] Veronika Caisová, Ondřej Uher, Pavla Nedbalová, Ivana Jochmanová, Karolína Kvardová, Kamila Masáková, Gabriela Krejčová, Lucie Paďouková, Jindřich Chmelař, Jan Kopecký, and Jan Ženka. Effective cancer immunotherapy based on combination of TLR agonists with stimulation of phagocytosis. *International Immunopharmacology*, 59:86–96, June 2018.

[29] Flávia Castro, Ana Patrícia Cardoso, Raquel Madeira Gonçalves, Karine Serre, and Maria José Oliveira. Interferon-Gamma at the Crossroads of Tumor Immune Surveillance or Evasion. *Frontiers in Immunology*, 9:847, 2018.

[30] Ann F. Chambers, Alan C. Groom, and Ian C. MacDonald. Dissemination and growth of cancer cells in metastatic sites. *Nature Reviews. Cancer*, 2(8):563–572, August 2002.

[31] D. C. Chan, D. Fass, J. M. Berger, and P. S. Kim. Core structure of gp41 from the HIV envelope glycoprotein. *Cell*, 89(2):263–273, April 1997.

[32] Jason R. Chan, Wendy Blumenschein, Erin Murphy, Caroline Diveu, Maria Wiekowski, Susan Abbondanzo, Linda Lucian, Richard Geissler, Scott Brodie, Alexa B. Kimball, Daniel M. Gorman, Kathleen Smith, Rene de Waal Malefyt, Robert A. Kastelein, Terrill K. McClanahan, and Edward P. Bowman. IL-23 stimulates epidermal hyperplasia via TNF and IL-20r2-dependent mechanisms with implications for psoriasis pathogenesis. *The Journal of Experimental Medicine*, 203(12):2577–2587, November 2006.

[33] M.-C. Chang, Y.-L. Chen, Y.-C. Chiang, T.-C. Chen, Y.-C. Tang, C.-A. Chen, W.-Z. Sun, and W.-F. Cheng. Mesothelin-specific cell-based vaccine generates antigen-specific immunity and potent antitumor effects by combining with IL-12 immunomodulator. *Gene Therapy*, 23(1):38–49, January 2016.

[34] Stéphane Chappaz and Daniela Finke. The IL-7 signaling pathway regulates lymph node development independent of peripheral lymphocytes. *Journal of Immunology (Baltimore, Md.: 1950)*, 184(7):3562–3569, April 2010.

[35] Hao Chen, Mai Chan Lau, Michael Thomas Wong, Evan W. Newell, Michael Poidinger, and Jinmiao Chen. Cytofkit: A Bioconductor Package for an Integrated Mass Cytometry Data Analysis Pipeline. *PLoS computational biology*, 12(9):e1005112, September 2016.

[36] Takatoshi Chinen, Arun K. Kannan, Andrew G. Levine, Xiying Fan, Ulf Klein, Ye Zheng, Georg Gasteiger, Yongqiang Feng, Jason D. Fontenot, and Alexander Y. Rudensky. An essential role for the IL-2 receptor in Treg cell function. *Nature Immunology*, 17(11):1322–1333, November 2016.

[37] K.-J. Choi, S.-N. Zhang, I.-K. Choi, J.-S. Kim, and C.-O. Yun. Strengthening of antitumor immune memory and prevention of thymic atrophy mediated by adenovirus expressing IL-12 and GM-CSF. *Gene Therapy*, 19(7):711–723, July 2012.

[38] Sheetal Korde Choudhari, Minal Chaudhary, Sachin Bagde, Amol R. Gadbail, and Vaishali Joshi. Nitric oxide and cancer: a review. *World Journal of Surgical Oncology*, 11:118, May 2013.

[39] Eoin Coakley, Christos J. Petropoulos, and Jeannette M. Whitcomb. Assessing chemokine co-receptor usage in HIV. *Current Opinion in Infectious Diseases*, 18(1):9–15, February 2005.

[40] J. Cohen. IL-12 deaths: explanation and a puzzle. *Science (New York, N.Y.)*, 270(5238):908, November 1995.

[41] W. B. Coley. The Treatment of Inoperable Sarcoma by Bacterial Toxins (the Mixed Toxins of the Streptococcus erysipelas and the Bacillus prodigiosus). *Proceedings of the Royal Society of Medicine*, 3(Surg Sect):1–48, 1910.

[42] Lucia Conde. Stand-alone version of cytofpipe. Contribute to UCL-BLIC/cytofpipe development by creating an account on GitHub, July 2018. original-date: 2018-03-08T10:16:57Z.

[43] Michael G. Constantinides, Benjamin D. McDonald, Philip A. Verhoef, and Albert Bendelac. A committed precursor to innate lymphoid cells. *Nature*, 508(7496):397–401, April 2014.

[44] Filippo Cortesi, Gloria Delfanti, Andrea Grilli, Arianna Calcinotto, Francesca Gorini, Ferdinando Pucci, Roberta Lucianò, Matteo Grioni, Alessandra Recchia, Fabio Benigni, Alberto Briganti, Andrea Salonia, Michele De Palma, Silvio Bicciato, Claudio Doglioni, Matteo Bellone, Giulia Casorati, and Paolo Dellabona. Bimodal CD40/Fas-Dependent Crosstalk between iNKT Cells and Tumor-Associated Macrophages Impairs Prostate Cancer Progression. *Cell Reports*, 22(11):3006–3020, March 2018.

[45] Virna Cortez-Retamozo, Martin Etzrodt, Andita Newton, Philipp J. Rauch, Aleksey Chudnovskiy, Cedric Berger, Russell J. H. Ryan, Yoshiko Iwamoto, Brett Marinelli, Rostic Gorbatov, Reza Forghani, Tatiana I. Novobrantseva, Victor Koteliansky, Jose-Luiz Figueiredo, John W. Chen, Daniel G. Anderson, Matthias Nahrendorf, Filip K. Swirski, Ralph Weissleder, and Mikael J. Pittet. Origins of tumor-associated macrophages and neutrophils. *Proceedings of the National Academy of Sciences of the United States of America*, 109(7):2491–2496, February 2012.

[46] Michael A. Curran. Preclinical Data Supporting Antitumor Activity of PD-1 Blockade. *Cancer Journal (Sudbury, Mass.)*, 24(1):2–6, February 2018.

[47] A. G. Dalgleish, P. C. Beverley, P. R. Clapham, D. H. Crawford, M. F. Greaves, and R. A. Weiss. The CD4 (T4) antigen is an essential component of the receptor for the AIDS retrovirus. *Nature*, 312(5996):763–767, January 1984.

[48] B. B. Desai, P. M. Quinn, A. G. Wolitzky, P. K. Mongini, R. Chizzonite, and M. K. Gately. IL-12 receptor. II. Distribution and regulation of receptor expression. *Journal of Immunology (Baltimore, Md.: 1950)*, 148(10):3125–3132, May 1992.

[49] A. S. Dighe, M. A. Farrar, and R. D. Schreiber. Inhibition of cellular responsiveness to interferon-gamma (IFN gamma) induced by overexpression of

inactive forms of the IFN gamma receptor. *Journal of Biological Chemistry*, 268(14):10645–10653, May 1993.

[50] C. A. Dinarello. Proinflammatory cytokines. *Chest*, 118(2):503–508, August 2000.

[51] A. G. Doyle, G. Herbein, L. J. Montaner, A. J. Minty, D. Caput, P. Ferrara, and S. Gordon. Interleukin-13 alters the activation state of murine macrophages in vitro: comparison with interleukin-4 and interferon-gamma. *European Journal of Immunology*, 24(6):1441–1445, June 1994.

[52] M Duan, D P Steinfort, D Smallwood, M Hew, W Chen, M Ernst, L B Irving, G P Anderson, and M L Hibbs. CD11b immunophenotyping identifies inflammatory profiles in the mouse and human lungs. *Mucosal Immunology*, 9(2):550–563, March 2016.

[53] Darryll D. Dudley, Jayanta Chaudhuri, Craig H. Bassing, and Frederick W. Alt. Mechanism and control of V(D)J recombination versus class switch recombination: similarities and differences. *Advances in Immunology*, 86:43–112, 2005.

[54] T. Dull, R. Zufferey, M. Kelly, R. J. Mandel, M. Nguyen, D. Trono, and L. Naldini. A third-generation lentivirus vector with a conditional packaging system. *Journal of Virology*, 72(11):8463–8471, November 1998.

[55] Dorothée Duluc, Yves Delneste, Fang Tan, Marie-Pierre Moles, Linda Grimaud, Julien Lenoir, Laurence Preisser, Ignacio Anegon, Laurent Catala, Norbert Ifrah, Philippe Descamps, Erick Gamelin, Hugues Gascan, Mohamed Hebbar, and Pascale Jeannin. Tumor-associated leukemia inhibitory factor and IL-6 skew monocyte differentiation into tumor-associated macrophage-like cells. *Blood*, 110(13):4319–4330, December 2007.

[56] Michel DuPage, Alison L. Dooley, and Tyler Jacks. Conditional mouse lung cancer models using adenoviral or lentiviral delivery of Cre recombinase. *Nature protocols*, 4(7):1064–1072, 2009.

[57] Aurélie Durgeau, Yasemin Virk, Stéphanie Corgnac, and Fathia Mami-Chouaib. Recent Advances in Targeting CD8 T-Cell Immunity for More Effective Cancer Immunotherapy. *Frontiers in Immunology*, 9:14, 2018.

[58] Gérard Eberl, Marco Colonna, James P. Di Santo, and Andrew N. J. McKenzie. Innate lymphoid cells. Innate lymphoid cells: a new paradigm in immunology. *Science (New York, N.Y.)*, 348(6237):aaa6566, May 2015.

[59] Gérard Eberl, Shana Marmon, Mary-Jean Sunshine, Paul D. Rennert, Yongwon Choi, and Dan R. Littman. An essential function for the nuclear receptor RORgamma(t) in the generation of fetal lymphoid tissue inducer cells. *Nature Immunology*, 5(1):64–73, January 2004.

[60] Nejat K. Egilmez, Mehmet O. Kilinc, Tao Gu, and Thomas F. Conway. Controlled-release particulate cytokine adjuvants for cancer therapy. *Endocrine, Metabolic & Immune Disorders Drug Targets*, 7(4):266–270, December 2007.

[61] Maya Eisenring, Johannes vom Berg, Glen Kristiansen, Elisabeth Saller, and Burkhard Becher. IL-12 initiates tumor rejection via lymphoid tissue-inducer cells bearing the natural cytotoxicity receptor NKp46. *Nature Immunology*, 11(11):1030–1038, November 2010.

[62] Catherine A. Evans, Tao Liu, André Lescarbeau, Somarajan J. Nair, Louis Grenier, Johan A. Pradeilles, Quentin Glenadel, Thomas Tibbitts, Ann M. Rowley, Jonathan P. DiNitto, Erin E. Brophy, Erin L. O'Hearn, Janid A. Ali, David G. Winkler, Stanley I. Goldstein, Patrick O'Hearn, Christian M. Martin, Jennifer G. Hoyt, John R. Soglia, Culver Cheung, Melissa M. Pink, Jennifer L. Proctor, Vito J. Palombella, Martin R. Tremblay, and Alfredo C. Castro. Discovery of a Selective Phosphoinositide-3-Kinase (PI3k)-γ Inhibitor (IPI-549) as an Immuno-Oncology Clinical Candidate. *ACS Medicinal Chemistry Letters*, 7(9):862–867, September 2016.

[63] Terence R. Flotte, Pamela L. Zeitlin, Thomas C. Reynolds, Alison E. Heald, Patty Pedersen, Suzanne Beck, Carol K. Conrad, Lois Brass-Ernst, Margaret Humphries, Kevin Sullivan, Randall Wetzel, George Taylor, Barrie J. Carter, and William B. Guggino. Phase I trial of intranasal and endobronchial administration of a recombinant adeno-associated virus serotype 2 (rAAV2)-CFTR vector in adult cystic fibrosis patients: a two-part clinical study. *Human Gene Therapy*, 14(11):1079–1088, July 2003.

[64] Darin K. Fogg, Claire Sibon, Chaouki Miled, Steffen Jung, Pierre Aucouturier, Dan R. Littman, Ana Cumano, and Frederic Geissmann. A clonogenic bone marrow progenitor specific for macrophages and dendritic cells. *Science (New York, N.Y.)*, 311(5757):83–87, January 2006.

[65] Marion M. France and Jerrold R. Turner. The mucosal barrier at a glance. *Journal of Cell Science*, 130(2):307–314, 2017.

[66] Ruth A. Franklin, Will Liao, Abira Sarkar, Myoungjoo V. Kim, Michael R. Bivona, Kang Liu, Eric G. Pamer, and Ming O. Li. The cellular and molec-

ular origin of tumor-associated macrophages. *Science (New York, N.Y.)*, 344(6186):921–925, May 2014.

[67] G. J. Freeman, A. J. Long, Y. Iwai, K. Bourque, T. Chernova, H. Nishimura, L. J. Fitz, N. Malenkovich, T. Okazaki, M. C. Byrne, H. F. Horton, L. Fouser, L. Carter, V. Ling, M. R. Bowman, B. M. Carreno, M. Collins, C. R. Wood, and T. Honjo. Engagement of the PD-1 immunoinhibitory receptor by a novel B7 family member leads to negative regulation of lymphocyte activation. *The Journal of Experimental Medicine*, 192(7):1027–1034, October 2000.

[68] S. O. Freytag, K. N. Barton, and Y. Zhang. Efficacy of oncolytic adenovirus expressing suicide genes and interleukin-12 in preclinical model of prostate cancer. *Gene Therapy*, 20(12):1131–1139, December 2013.

[69] Michael Fricker and Peter G. Gibson. Macrophage dysfunction in the pathogenesis and treatment of asthma. *European Respiratory Journal*, 50(3):1700196, September 2017.

[70] Anja Fuchs, William Vermi, Jacob S. Lee, Silvia Lonardi, Susan Gilfillan, Rodney D. Newberry, Marina Cella, and Marco Colonna. Intraepithelial type 1 innate lymphoid cells are a unique subset of IL-12- and IL-15-responsive IFN-γ-producing cells. *Immunity*, 38(4):769–781, April 2013.

[71] D. Fulton, J. P. Gratton, and W. C. Sessa. Post-translational control of endothelial nitric oxide synthase: why isn't calcium/calmodulin enough? *The Journal of Pharmacology and Experimental Therapeutics*, 299(3):818–824, December 2001.

[72] A. Gambotto, G. Dworacki, V. Cicinnati, T. Kenniston, J. Steitz, T. Tüting, P. D. Robbins, and A. B. DeLeo. Immunogenicity of enhanced green fluorescent protein (EGFP) in BALB/c mice: identification of an H2-Kd-restricted CTL epitope. *Gene Therapy*, 7(23):2036–2040, December 2000.

[73] Yan Gao, Simone A. Nish, Ruoyi Jiang, Lin Hou, Paula Licona-Limón, Jason S. Weinstein, Hongyu Zhao, and Ruslan Medzhitov. Control of T helper 2 responses by transcription factor IRF4-dependent dendritic cells. *Immunity*, 39(4):722–732, October 2013.

[74] Edward B. Garon, Naiyer A. Rizvi, Rina Hui, Natasha Leighl, Ani S. Balmanoukian, Joseph Paul Eder, Amita Patnaik, Charu Aggarwal, Matthew Gubens, Leora Horn, Enric Carcereny, Myung-Ju Ahn, Enriqueta Felip, Jong-Seok Lee, Matthew D. Hellmann, Omid Hamid, Jonathan W. Goldman, Jean-Charles Soria, Marisa Dolled-Filhart, Ruth Z. Rutledge, Jin

Zhang, Jared K. Lunceford, Reshma Rangwala, Gregory M. Lubiniecki, Charlotte Roach, Kenneth Emancipator, Leena Gandhi, and KEYNOTE-001 Investigators. Pembrolizumab for the treatment of non-small-cell lung cancer. *The New England Journal of Medicine*, 372(21):2018–2028, May 2015.

[75] Christopher S. Garris, Sean P. Arlauckas, Rainer H. Kohler, Marcel P. Trefny, Seth Garren, Cécile Piot, Camilla Engblom, Christina Pfirschke, Marie Siwicki, Jeremy Gungabeesoon, Gordon J. Freeman, Sarah E. Warren, SuFey Ong, Erica Browning, Christopher G. Twitty, Robert H. Pierce, Mai H. Le, Alain P. Algazi, Adil I. Daud, Sara I. Pai, Alfred Zippelius, Ralph Weissleder, and Mikael J. Pittet. Successful Anti-PD-1 Cancer Immunotherapy Requires T Cell-Dendritic Cell Crosstalk Involving the Cytokines IFN-γ and IL-12. *Immunity*, 49(6):1148–1161.e7, December 2018.

[76] G. Gasteiger, X. Fan, S. Dikiy, S. Y. Lee, and A. Y. Rudensky. Tissue residency of innate lymphoid cells in lymphoid and nonlymphoid organs. *Science*, 350(6263):981–985, November 2015.

[77] Stephen J. Gaudino and Pawan Kumar. Cross-Talk Between Antigen Presenting Cells and T Cells Impacts Intestinal Homeostasis, Bacterial Infections, and Tumorigenesis. *Frontiers in Immunology*, 10:360, 2019.

[78] Barbara Geering, Christina Stoeckle, Sébastien Conus, and Hans-Uwe Simon. Living and dying for inflammation: neutrophils, eosinophils, basophils. *Trends in Immunology*, 34(8):398–409, August 2013.

[79] Marco Gerlinger, Andrew J. Rowan, Stuart Horswell, M. Math, James Larkin, David Endesfelder, Eva Gronroos, Pierre Martinez, Nicholas Matthews, Aengus Stewart, Patrick Tarpey, Ignacio Varela, Benjamin Phillimore, Sharmin Begum, Neil Q. McDonald, Adam Butler, David Jones, Keiran Raine, Calli Latimer, Claudio R. Santos, Mahrokh Nohadani, Aron C. Eklund, Bradley Spencer-Dene, Graham Clark, Lisa Pickering, Gordon Stamp, Martin Gore, Zoltan Szallasi, Julian Downward, P. Andrew Futreal, and Charles Swanton. Intratumor heterogeneity and branched evolution revealed by multiregion sequencing. *The New England Journal of Medicine*, 366(10):883–892, March 2012.

[80] Florent Ginhoux and Martin Guilliams. Tissue-Resident Macrophage Ontogeny and Homeostasis. *Immunity*, 44(3):439–449, March 2016.

[81] Wendy Glenisson, Vincent Castronovo, and David Waltregny. Histone deacetylase 4 is required for TGFbeta1-induced myofibroblastic differentiation. *Biochimica Et Biophysica Acta*, 1773(10):1572–1582, October 2007.

[82] Elisa Gomez Perdiguero, Kay Klapproth, Christian Schulz, Katrin Busch, Emanuele Azzoni, Lucile Crozet, Hannah Garner, Celine Trouillet, Marella F. de Bruijn, Frederic Geissmann, and Hans-Reimer Rodewald. Tissue-resident macrophages originate from yolk-sac-derived erythro-myeloid progenitors. *Nature*, 518(7540):547–551, February 2015.

[83] Hugh D. Goold, David Escors, Thomas J. Conlan, Ronjon Chakraverty, and Clare L. Bennett. Conventional dendritic cells are required for the activation of helper-dependent CD8 T cell responses to a model antigen after cutaneous vaccination with lentiviral vectors. *Journal of Immunology (Baltimore, Md.: 1950)*, 186(8):4565–4572, April 2011.

[84] L. Gorelik and R. A. Flavell. Immune-mediated eradication of tumors through the blockade of transforming growth factor-beta signaling in T cells. *Nature Medicine*, 7(10):1118–1122, October 2001.

[85] Yoshiyuki Goto, Takashi Obata, Jun Kunisawa, Shintaro Sato, Ivaylo I. Ivanov, Aayam Lamichhane, Natsumi Takeyama, Mariko Kamioka, Mitsuo Sakamoto, Takahiro Matsuki, Hiromi Setoyama, Akemi Imaoka, Satoshi Uematsu, Shizuo Akira, Steven E. Domino, Paulina Kulig, Burkhard Becher, Jean-Christophe Renauld, Chihiro Sasakawa, Yoshinori Umesaki, Yoshimi Benno, and Hiroshi Kiyono. Innate lymphoid cells regulate intestinal epithelial cell glycosylation. *Science (New York, N.Y.)*, 345(6202):1254009, September 2014.

[86] Robert J. Gray. A Class of K-Sample Tests for Comparing the Cumulative Incidence of a Competing Risk. *The Annals of Statistics*, 16(3):1141–1154, September 1988.

[87] Joshua C. Grieger and Richard J. Samulski. Packaging capacity of adeno-associated virus serotypes: impact of larger genomes on infectivity and postentry steps. *Journal of Virology*, 79(15):9933–9944, August 2005.

[88] U. Grohmann, M. L. Belladonna, R. Bianchi, C. Orabona, E. Ayroldi, M. C. Fioretti, and P. Puccetti. IL-12 acts directly on DC to promote nuclear localization of NF-kappaB and primes DC for IL-12 production. *Immunity*, 9(3):315–323, September 1998.

[89] U. Gubler, A. O. Chua, D. S. Schoenhaut, C. M. Dwyer, W. McComas, R. Motyka, N. Nabavi, A. G. Wolitzky, P. M. Quinn, and P. C. Familletti. Coexpression of two distinct genes is required to generate secreted bioactive cytotoxic lymphocyte maturation factor. *Proceedings of the National Academy of Sciences of the United States of America*, 88(10):4143–4147, May 1991.

[90] Marion V. Guerin, Fabienne Regnier, Vincent Feuillet, Lene Vimeux, Julia M. Weiss, Georges Bismuth, Gregoire Altan-Bonnet, Thomas Guilbert, Maxime Thoreau, Veronica Finisguerra, Emmanuel Donnadieu, Alain Trautmann, and Nadège Bercovici. TGFβ blocks IFNα/β release and tumor rejection in spontaneous mammary tumors. *bioRxiv*, July 2019.

[91] Pierre Guermonprez and Sebastian Amigorena. Pathways for antigen cross presentation. *Springer Seminars in Immunopathology*, 26(3):257–271, January 2005.

[92] Jennifer L. Guerriero, Alaba Sotayo, Holly E. Ponichtera, Jessica A. Castrillon, Alexandra L. Pourzia, Sara Schad, Shawn F. Johnson, Ruben D. Carrasco, Suzan Lazo, Roderick T. Bronson, Scott P. Davis, Mercedes Lobera, Michael A. Nolan, and Anthony Letai. Class IIa HDAC inhibition reduces breast tumours and metastases through anti-tumour macrophages. *Nature*, 543(7645):428–432, March 2017.

[93] Martin Guilliams, Florent Ginhoux, Claudia Jakubzick, Shalin H. Naik, Nobuyuki Onai, Barbara U. Schraml, Elodie Segura, Roxane Tussiwand, and Simon Yona. Dendritic cells, monocytes and macrophages: a unified nomenclature based on ontogeny. *Nature Reviews. Immunology*, 14(8):571–578, 2014.

[94] S. M. Mansour Haeryfar and David W. Hoskin. Thy-1: more than a mouse pan-T cell marker. *Journal of Immunology (Baltimore, Md.: 1950)*, 173(6):3581–3588, September 2004.

[95] Therwa Hamza, John B. Barnett, and Bingyun Li. Interleukin 12 a key immunoregulatory cytokine in infection applications. *International Journal of Molecular Sciences*, 11(3):789–806, 2010.

[96] Douglas Hanahan and Robert A. Weinberg. Hallmarks of cancer: the next generation. *Cell*, 144(5):646–674, March 2011.

[97] Laurie E. Harrington, Robin D. Hatton, Paul R. Mangan, Henrietta Turner, Theresa L. Murphy, Kenneth M. Murphy, and Casey T. Weaver. Interleukin 17-producing CD4+ effector T cells develop via a lineage distinct from the T helper type 1 and 2 lineages. *Nature Immunology*, 6(11):1123–1132, November 2005.

[98] B. L. Harvat, P. Seth, and A. M. Jetten. The role of p27kip1 in gamma interferon-mediated growth arrest of mammary epithelial cells and related defects in mammary carcinoma cells. *Oncogene*, 14(17):2111–2122, May 1997.

[99] Jiabei He, Ying Hu, Mingming Hu, and Baolan Li. Development of PD-1/PD-L1 Pathway in Tumor Immune Microenvironment and Treatment for Non-Small Cell Lung Cancer. *Scientific Reports*, 5:13110, August 2015.

[100] Katherine A. High and Maria G. Roncarolo. Gene Therapy. *The New England Journal of Medicine*, 381(5):455–464, 2019.

[101] Shohei Hori, Takashi Nomura, and Shimon Sakaguchi. Control of regulatory T cell development by the transcription factor Foxp3. *Science (New York, N.Y.)*, 299(5609):1057–1061, February 2003.

[102] Alastair Hotblack, Sara Seshadri, Lei Zhang, Sahar Hamrang-Yousefi, Ronjon Chakraverty, David Escors, and Clare L. Bennett. Dendritic Cells Cross-Present Immunogenic Lentivector-Encoded Antigen from Transduced Cells to Prime Functional T Cell Immunity. *Molecular Therapy: The Journal of the American Society of Gene Therapy*, 25(2):504–511, 2017.

[103] Hiroaki Ikeda, Lloyd J. Old, and Robert D. Schreiber. The roles of IFN gamma in protection against tumor development and cancer immunoediting. *Cytokine & Growth Factor Reviews*, 13(2):95–109, April 2002.

[104] T. Jacks, M. D. Power, F. R. Masiarz, P. A. Luciw, P. J. Barr, and H. E. Varmus. Characterization of ribosomal frameshifting in HIV-1 gag-pol expression. *Nature*, 331(6153):280–283, January 1988.

[105] Sten Eirik W. Jacobsen and Claus Nerlov. Haematopoiesis in the era of advanced single-cell technologies. *Nature Cell Biology*, 21(1):2–8, 2019.

[106] N. G. Jacobson, S. J. Szabo, R. M. Weber-Nordt, Z. Zhong, R. D. Schreiber, J. E. Darnell, and K. M. Murphy. Interleukin 12 signaling in T helper type 1 (Th1) cells involves tyrosine phosphorylation of signal transducer and activator of transcription (Stat)3 and Stat4. *The Journal of Experimental Medicine*, 181(5):1755–1762, May 1995.

[107] S. Jenks. After initial setback, IL-12 regaining popularity. *Journal of the National Cancer Institute*, 88(9):576–577, May 1996.

[108] D. E. Jenne and J. Tschopp. Granzymes, a family of serine proteases released from granules of cytolytic T lymphocytes upon T cell receptor stimulation. *Immunological Reviews*, 103:53–71, March 1988.

[109] J. L. Jensen, A. Rakhmilevich, E. Heninger, A. T. Broman, C. Hope, F. Phan, S. Miyamoto, I. Maroulakou, N. Callander, P. Hematti, M. Chesi, P. L. Bergsagel, P. Sondel, and F. Asimakopoulos. Tumoricidal Effects of Macrophage-Activating Immunotherapy in a Murine Model of

Relapsed/Refractory Multiple Myeloma. *Cancer Immunology Research*, 3(8):881–890, August 2015.

[110] H. Jiang, C. A. Stewart, D. J. Fast, and R. W. Leu. Tumor target-derived soluble factor synergizes with IFN-gamma and IL-2 to activate macrophages for tumor necrosis factor and nitric oxide production to mediate cytotoxicity of the same target. *Journal of Immunology (Baltimore, Md.: 1950)*, 149(6):2137–2146, September 1992.

[111] Carl H. June and Michel Sadelain. Chimeric Antigen Receptor Therapy. *The New England Journal of Medicine*, 379(1):64–73, 2018.

[112] Thomas Kammertoens, Christian Friese, Ainhoa Arina, Christian Idel, Dana Briesemeister, Michael Rothe, Andranik Ivanov, Anna Szymborska, Giannino Patone, Severine Kunz, Daniel Sommermeyer, Boris Engels, Matthias Leisegang, Ana Textor, Hans Joerg Fehling, Marcus Fruttiger, Michael Lohoff, Andreas Herrmann, Hua Yu, Ralph Weichselbaum, Wolfgang Uckert, Norbert Hübner, Holger Gerhardt, Dieter Beule, Hans Schreiber, and Thomas Blankenstein. Tumour ischaemia by interferon-γ resembles physiological blood vessel regression. *Nature*, 545(7652):98–102, 2017.

[113] W. K. Kang, C. Park, H. L. Yoon, W. S. Kim, S. S. Yoon, M. H. Lee, K. Park, K. Kim, H. S. Jeong, J. A. Kim, S. J. Nam, J. H. Yang, Y. I. Son, C. H. Baek, J. Han, H. J. Ree, E. S. Lee, S. H. Kim, D. W. Kim, Y. C. Ahn, S. J. Huh, Y. H. Choe, J. H. Lee, M. H. Park, G. S. Kong, E. Y. Park, Y. K. Kang, Y. J. Bang, N. S. Paik, S. N. Lee, S. H. Kim, S. Kim, P. D. Robbins, H. Tahara, M. T. Lotze, and C. H. Park. Interleukin 12 gene therapy of cancer by peritumoral injection of transduced autologous fibroblasts: outcome of a phase I study. *Human Gene Therapy*, 12(6):671–684, April 2001.

[114] Sid P. Kerkar, Romina S. Goldszmid, Pawel Muranski, Dhanalakshmi Chinnasamy, Zhiya Yu, Robert N. Reger, Anthony J. Leonardi, Richard A. Morgan, Ena Wang, Francesco M. Marincola, Giorgio Trinchieri, Steven A. Rosenberg, and Nicholas P. Restifo. IL-12 triggers a programmatic change in dysfunctional myeloid-derived cells within mouse tumors. *The Journal of Clinical Investigation*, 121(12):4746–4757, December 2011.

[115] Stefanie Kirchberger, Daniel J. Royston, Olivier Boulard, Emily Thornton, Fanny Franchini, Rose L. Szabady, Oliver Harrison, and Fiona Powrie. Innate lymphoid cells sustain colon cancer through production of interleukin-22 in a mouse model. *The Journal of Experimental Medicine*, 210(5):917–931, May 2013.

[116] Christoph S. N. Klose, Melanie Flach, Luisa Möhle, Leif Rogell, Thomas Hoyler, Karolina Ebert, Carola Fabiunke, Dietmar Pfeifer, Veronika Sexl, Diogo Fonseca-Pereira, Rita G. Domingues, Henrique Veiga-Fernandes, Sebastian J. Arnold, Meinrad Busslinger, Ildiko R. Dunay, Yakup Tanriver, and Andreas Diefenbach. Differentiation of type 1 ILCs from a common progenitor to all helper-like innate lymphoid cell lineages. *Cell*, 157(2):340–356, April 2014.

[117] Christoph S. N. Klose, Elina A. Kiss, Vera Schwierzeck, Karolina Ebert, Thomas Hoyler, Yannick d'Hargues, Nathalie Göppert, Andrew L. Croxford, Ari Waisman, Yakup Tanriver, and Andreas Diefenbach. A T-bet gradient controls the fate and function of CCR6-RORγt+ innate lymphoid cells. *Nature*, 494(7436):261–265, February 2013.

[118] R. G. Knowles and S. Moncada. Nitric oxide synthases in mammals. *The Biochemical Journal*, 298 (Pt 2):249–258, March 1994.

[119] Hajime Kono and Kenneth L. Rock. How dying cells alert the immune system to danger. *Nature Reviews. Immunology*, 8(4):279–289, April 2008.

[120] L. L. Korn, H. L. Thomas, H. G. Hubbeling, S. P. Spencer, R. Sinha, H. Ma Simkins, N. H. Salzman, F. D. Bushman, and T. M. Laufer. Conventional CD4+ T cells regulate IL-22-producing intestinal innate lymphoid cells. *Mucosal Immunology*, 7(5):1045–1057, September 2014.

[121] Melissa A. Kotterman, Thomas W. Chalberg, and David V. Schaffer. Viral Vectors for Gene Therapy: Translational and Clinical Outlook. *Annual Review of Biomedical Engineering*, 17(1):63–89, December 2015.

[122] M. F. Krummel and J. P. Allison. CD28 and CTLA-4 have opposing effects on the response of T cells to stimulation. *The Journal of Experimental Medicine*, 182(2):459–465, August 1995.

[123] Tomohiro Kurosaki, Kohei Kometani, and Wataru Ise. Memory B cells. *Nature Reviews. Immunology*, 15(3):149–159, March 2015.

[124] M. Alper Kursunel and Gunes Esendagli. The untold story of IFN-γ in cancer biology. *Cytokine & Growth Factor Reviews*, 31:73–81, 2016.

[125] Matthew Scott Lalonde and Wesley I. Sundquist. How HIV finds the door. *Proceedings of the National Academy of Sciences of the United States of America*, 109(46):18631–18632, November 2012.

[126] A. G. Lamont and L. Adorini. IL-12: a key cytokine in immune regulation. *Immunology Today*, 17(5):214–217, May 1996.

[127] Witold Lasek, Radosław Zagożdżon, and Marek Jakobisiak. Interleukin 12: still a promising candidate for tumor immunotherapy? *Cancer immunology, immunotherapy: CII*, 63(5):419–435, May 2014.

[128] Henning Lauterbach, Barbara Bathke, Stefanie Gilles, Claudia Traidl-Hoffmann, Christian A. Luber, György Fejer, Marina A. Freudenberg, Gayle M. Davey, David Vremec, Axel Kallies, Li Wu, Ken Shortman, Paul Chaplin, Mark Suter, Meredith O'Keeffe, and Hubertus Hochrein. Mouse CD8alpha+ DCs and human BDCA3+ DCs are major producers of IFN-lambda in response to poly IC. *The Journal of Experimental Medicine*, 207(12):2703–2717, November 2010.

[129] Matthias Lechner, Philipp Lirk, and Josef Rieder. Inducible nitric oxide synthase (iNOS) in tumor biology: the two sides of the same coin. *Seminars in Cancer Biology*, 15(4):277–289, August 2005.

[130] R. D. Leek, C. E. Lewis, R. Whitehouse, M. Greenall, J. Clarke, and A. L. Harris. Association of macrophage infiltration with angiogenesis and prognosis in invasive breast carcinoma. *Cancer Research*, 56(20):4625–4629, October 1996.

[131] Maria P. Lemos, Lian Fan, David Lo, and Terri M. Laufer. CD8alpha+ and CD11b+ dendritic cell-restricted MHC class II controls Th1 CD4+ T cell immunity. *Journal of Immunology (Baltimore, Md.: 1950)*, 171(10):5077–5084, November 2003.

[132] Renato Lenzi, Robert Edwards, Carl June, Michael V. Seiden, Michael E. Garcia, Michael Rosenblum, and Ralph S. Freedman. Phase II study of intraperitoneal recombinant interleukin-12 (rhIL-12) in patients with peritoneal carcinomatosis (residual disease < 1 cm) associated with ovarian cancer or primary peritoneal carcinoma. *Journal of Translational Medicine*, 5:66, December 2007.

[133] John P. Leonard, Matthew L. Sherman, Gerald L. Fisher, Lynn J. Buchanan, Glenn Larsen, Michael B. Atkins, Jeffrey A. Sosman, Janice P. Dutcher, Nicholas J. Vogelzang, and John L. Ryan. Effects of Single-Dose Interleukin-12 Exposure on Interleukin-12–Associated Toxicity and Interferon-γ Production. *Blood*, 90(7):2541–2548, October 1997.

[134] J. S. Lewis, R. J. Landers, J. C. Underwood, A. L. Harris, and C. E. Lewis. Expression of vascular endothelial growth factor by macrophages is up-regulated in poorly vascularized areas of breast carcinomas. *The Journal of Pathology*, 192(2):150–158, October 2000.

[135] Spencer C. Liang, Xiang-Yang Tan, Deborah P. Luxenberg, Riyez Karim, Kyriaki Dunussi-Joannopoulos, Mary Collins, and Lynette A. Fouser. Interleukin (IL)-22 and IL-17 are coexpressed by Th17 cells and cooperatively enhance expression of antimicrobial peptides. *The Journal of Experimental Medicine*, 203(10):2271–2279, October 2006.

[136] Ai Ing Lim, Yan Li, Silvia Lopez-Lastra, Ralph Stadhouders, Franziska Paul, Armanda Casrouge, Nicolas Serafini, Anne Puel, Jacinta Bustamante, Laura Surace, Guillemette Masse-Ranson, Eyal David, Helene Strick-Marchand, Lionel Le Bourhis, Roberto Cocchi, Davide Topazio, Paolo Graziano, Lucia Anna Muscarella, Lars Rogge, Xavier Norel, Jean-Michel Sallenave, Matthieu Allez, Thomas Graf, Rudi W. Hendriks, Jean-Laurent Casanova, Ido Amit, Hans Yssel, and James P. Di Santo. Systemic Human ILC Precursors Provide a Substrate for Tissue ILC Differentiation. *Cell*, 168(6):1086–1100.e10, 2017.

[137] Adora A. Lin, Pulak K. Tripathi, Allyson Sholl, Michael B. Jordan, and David A. Hildeman. Gamma interferon signaling in macrophage lineage cells regulates central nervous system inflammation and chemokine production. *Journal of Virology*, 83(17):8604–8615, September 2009.

[138] Elaine Y. Lin, Valerie Gouon-Evans, Andrew V. Nguyen, and Jeffrey W. Pollard. The macrophage growth factor CSF-1 in mammary gland development and tumor progression. *Journal of Mammary Gland Biology and Neoplasia*, 7(2):147–162, April 2002.

[139] Ling Lin, Yang Jin, Wendy M. Mars, W. Brian Reeves, and Kebin Hu. Myeloid-derived tissue-type plasminogen activator promotes macrophage motility through FAK, Rac1, and NF-κB pathways. *The American Journal of Pathology*, 184(10):2757–2767, October 2014.

[140] Thomas M. Lincoln, Trudy L. Cornwell, Padmini Komalavilas, Lee Ann Macmillan-Crow, and Nancy Boerth. The Nitric Oxide–Cyclic GMP Signaling System. In *Biochemistry of Smooth Muscle Contraction*, pages 257–268. Elsevier, 1996.

[141] P. S. Linsley, W. Brady, M. Urnes, L. S. Grosmaire, N. K. Damle, and J. A. Ledbetter. CTLA-4 is a second receptor for the B cell activation antigen B7. *The Journal of Experimental Medicine*, 174(3):561–569, September 1991.

[142] Evan J. Lipson and Charles G. Drake. Ipilimumab: an anti-CTLA-4 antibody for metastatic melanoma. *Clinical Cancer Research: An Official Journal of the American Association for Cancer Research*, 17(22):6958–6962, November 2011.

[143] Jianguo Liu, Shanjin Cao, Sunjung Kim, Elaine Y. Chung, Yoichiro Homma, Xiuqin Guan, Violeta Jimenez, and Xiaojing Ma. Interleukin-12: an update on its immunological activities, signaling and regulation of gene expression. *Current Immunology Reviews*, 1(2):119–137, June 2005.

[144] Patrick H. Lizotte, Jason R. Baird, Cynthia A. Stevens, Peter Lauer, William R. Green, Dirk G. Brockstedt, and Steven N. Fiering. Attenuated Listeria monocytogenes reprograms M2-polarized tumor-associated macrophages in ovarian cancer leading to iNOS-mediated tumor cell lysis. *Oncoimmunology*, 3:e28926, 2014.

[145] F. Lohr, D. Y. Lo, D. A. Zaharoff, K. Hu, X. Zhang, Y. Li, Y. Zhao, M. W. Dewhirst, F. Yuan, and C. Y. Li. Effective tumor therapy with plasmid-encoded cytokines combined with in vivo electroporation. *Cancer Research*, 61(8):3281–3284, April 2001.

[146] Seila Lorenzo-Herrero, Christian Sordo-Bahamonde, Segundo Gonzalez, and Alejandro López-Soto. CD107a Degranulation Assay to Evaluate Immune Cell Antitumor Activity. *Methods in Molecular Biology (Clifton, N.J.)*, 1884:119–130, 2019.

[147] M. T. Lotze, L. Zitvogel, R. Campbell, P. D. Robbins, E. Elder, C. Haluszczak, D. Martin, T. L. Whiteside, W. J. Storkus, and H. Tahara. Cytokine gene therapy of cancer using interleukin-12: murine and clinical trials. *Annals of the New York Academy of Sciences*, 795:440–454, October 1996.

[148] B. Lowin, O. Krähenbühl, C. Müller, M. Dupuis, and J. Tschopp. Perforin and its role in T lymphocyte-mediated cytolysis. *Experientia*, 48(10):911–920, October 1992.

[149] Pierre-Louis Loyher, Pauline Hamon, Marie Laviron, Aïda Meghraoui-Kheddar, Elena Goncalves, Zihou Deng, Sara Torstensson, Nadège Bercovici, Camille Baudesson de Chanville, Béhazine Combadière, Frederic Geissmann, Ariel Savina, Christophe Combadière, and Alexandre Boissonnas. Macrophages of distinct origins contribute to tumor development in the lung. *The Journal of Experimental Medicine*, 215(10):2536–2553, October 2018.

[150] Enrico Lugli, Marcello Pinti, Milena Nasi, Leonarda Troiano, Roberta Ferraresi, Chiara Mussi, Gianfranco Salvioli, Valeri Patsekin, J. Paul Robinson, Caterina Durante, Marina Cocchi, and Andrea Cossarizza. Subject classification obtained by cluster analysis and principal component analy-

sis applied to flow cytometric data. *Cytometry. Part A: The Journal of the International Society for Analytical Cytology*, 71(5):334–344, May 2007.

[151] Jennifer E. Lykens, Catherine E. Terrell, Erin E. Zoller, Senad Divanovic, Aurelien Trompette, Christopher L. Karp, Julio Aliberti, Matthew J. Flick, and Michael B. Jordan. Mice with a selective impairment of IFN-gamma signaling in macrophage lineage cells demonstrate the critical role of IFN-gamma-activated macrophages for the control of protozoan parasitic infections in vivo. *Journal of Immunology (Baltimore, Md.: 1950)*, 184(2):877–885, January 2010.

[152] D. C. Macdonald, H. Singh, M. A. Whelan, D. Escors, F. Arce, S. E. Bottoms, W. S. Barclay, M. Maini, M. K. Collins, and W. M. C. Rosenberg. Harnessing alveolar macrophages for sustained mucosal T-cell recall confers long-term protection to mice against lethal influenza challenge without clinical disease. *Mucosal Immunology*, 7(1):89–100, January 2014.

[153] G. B. Mackaness. Cellular resistance to infection. *The Journal of Experimental Medicine*, 116:381–406, September 1962.

[154] Michael H. Malim and Michael Emerman. HIV-1 Accessory Proteins—Ensuring Viral Survival in a Hostile Environment. *Cell Host & Microbe*, 3(6):388–398, June 2008.

[155] A. Mantovani, B. Bottazzi, F. Colotta, S. Sozzani, and L. Ruco. The origin and function of tumor-associated macrophages. *Immunology Today*, 13(7):265–270, July 1992.

[156] Alberto Mantovani, Antonio Sica, Silvano Sozzani, Paola Allavena, Annunciata Vecchi, and Massimo Locati. The chemokine system in diverse forms of macrophage activation and polarization. *Trends in Immunology*, 25(12):677–686, December 2004.

[157] Markus G. Manz, Toshihiro Miyamoto, Koichi Akashi, and Irving L. Weissman. Prospective isolation of human clonogenic common myeloid progenitors. *Proceedings of the National Academy of Sciences of the United States of America*, 99(18):11872–11877, September 2002.

[158] Shannon L. Maude. Future directions in chimeric antigen receptor T cell therapy. *Current Opinion in Pediatrics*, 29(1):27–33, 2017.

[159] G. Mazzolini, C. Qian, X. Xie, Y. Sun, J. J. Lasarte, M. Drozdzik, and J. Prieto. Regression of colon cancer and induction of antitumor immunity by intratumoral injection of adenovirus expressing interleukin-12. *Cancer Gene Therapy*, 6(6):514–522, December 1999.

[160] Edward F. McCarthy. The toxins of William B. Coley and the treatment of bone and soft-tissue sarcomas. *The Iowa Orthopaedic Journal*, 26:154–158, 2006.

[161] Nicholas McGranahan, Andrew J. S. Furness, Rachel Rosenthal, Sofie Ramskov, Rikke Lyngaa, Sunil Kumar Saini, Mariam Jamal-Hanjani, Gareth A. Wilson, Nicolai J. Birkbak, Crispin T. Hiley, Thomas B. K. Watkins, Seema Shafi, Nirupa Murugaesu, Richard Mitter, Ayse U. Akarca, Joseph Linares, Teresa Marafioti, Jake Y. Henry, Eliezer M. Van Allen, Diana Miao, Bastian Schilling, Dirk Schadendorf, Levi A. Garraway, Vladimir Makarov, Naiyer A. Rizvi, Alexandra Snyder, Matthew D. Hellmann, Taha Merghoub, Jedd D. Wolchok, Sachet A. Shukla, Catherine J. Wu, Karl S. Peggs, Timothy A. Chan, Sine R. Hadrup, Sergio A. Quezada, and Charles Swanton. Clonal neoantigens elicit T cell immunoreactivity and sensitivity to immune checkpoint blockade. *Science (New York, N.Y.)*, 351(6280):1463–1469, March 2016.

[162] Leland McInnes, John Healy, and James Melville. UMAP: Uniform Manifold Approximation and Projection for Dimension Reduction. *arXiv:1802.03426 [cs, stat]*, February 2018. arXiv: 1802.03426.

[163] Laura McKinley, John F. Alcorn, Alanna Peterson, Rachel B. Dupont, Shernaaz Kapadia, Alison Logar, Adam Henry, Charles G. Irvin, Jon D. Piganelli, Anuradha Ray, and Jay K. Kolls. TH17 cells mediate steroid-resistant airway inflammation and airway hyperresponsiveness in mice. *Journal of Immunology (Baltimore, Md.: 1950)*, 181(6):4089–4097, September 2008.

[164] R. E. Mebius, P. Rennert, and I. L. Weissman. Developing lymph nodes collect CD4+CD3- LTbeta+ cells that can differentiate to APC, NK cells, and follicular cells but not T or B cells. *Immunity*, 7(4):493–504, October 1997.

[165] José Medina-Echeverz, Lydia A. Haile, Fei Zhao, Jaba Gamrekelashvili, Chi Ma, Jean-Yves Métais, Cynthia E. Dunbar, Veena Kapoor, Michael P. Manns, Firouzeh Korangy, and Tim F. Greten. IFN-γ regulates survival and function of tumor-induced CD11b+ Gr-1high myeloid derived suppressor cells by modulating the anti-apoptotic molecule Bcl2a1. *European Journal of Immunology*, 44(8):2457–2467, August 2014.

[166] Humera Memon and Bhoomika M. Patel. Immune checkpoint inhibitors in non-small cell lung cancer: A bird's eye view. *Life Sciences*, 233:116713, September 2019.

[167] C. Menetrier-Caux, G. Montmain, M. C. Dieu, C. Bain, M. C. Favrot, C. Caux, and J. Y. Blay. Inhibition of the differentiation of dendritic cells from CD34(+) progenitors by tumor cells: role of interleukin-6 and macrophage colony-stimulating factor. *Blood*, 92(12):4778–4791, December 1998.

[168] Otto-Wilhelm Merten, Matthias Hebben, and Chiara Bovolenta. Production of lentiviral vectors. *Molecular Therapy. Methods & Clinical Development*, 3:16017, 2016.

[169] Rodolfo D. Vicetti Miguel, Thomas L. Cherpes, Leah J. Watson, and Kyle C. McKenna. CTL Induction of Tumoricidal Nitric Oxide Production by Intratumoral Macrophages Is Critical for Tumor Elimination. *The Journal of Immunology*, 185(11):6706–6718, December 2010.

[170] C. D. Mills, K. Kincaid, J. M. Alt, M. J. Heilman, and A. M. Hill. M-1/M-2 macrophages and the Th1/Th2 paradigm. *Journal of Immunology (Baltimore, Md.: 1950)*, 164(12):6166–6173, June 2000.

[171] Alexander V. Misharin, Luisa Morales-Nebreda, Gökhan M. Mutlu, G. R. Scott Budinger, and Harris Perlman. Flow Cytometric Analysis of Macrophages and Dendritic Cell Subsets in the Mouse Lung. *American Journal of Respiratory Cell and Molecular Biology*, 49(4):503–510, May 2013.

[172] Martin Montes, Elin A. Jaensson, Aaron F. Orozco, Dorothy E. Lewis, and David B. Corry. A general method for bead-enhanced quantitation by flow cytometry. *Journal of Immunological Methods*, 317(1-2):45–55, December 2006.

[173] T. R. Mosmann, H. Cherwinski, M. W. Bond, M. A. Giedlin, and R. L. Coffman. Two types of murine helper T cell clone. I. Definition according to profiles of lymphokine activities and secreted proteins. *Journal of Immunology (Baltimore, Md.: 1950)*, 136(7):2348–2357, April 1986.

[174] L. Naldini, U. Blomer, F. H. Gage, D. Trono, and I. M. Verma. Efficient transfer, integration, and sustained long-term expression of the transgene in adult rat brains injected with a lentiviral vector. *Proceedings of the National Academy of Sciences*, 93(21):11382–11388, October 1996.

[175] C. L. Nastala, H. D. Edington, T. G. McKinney, H. Tahara, M. A. Nalesnik, M. J. Brunda, M. K. Gately, S. F. Wolf, R. D. Schreiber, and W. J. Storkus. Recombinant IL-12 administration induces tumor regression in association with IFN-gamma production. *Journal of Immunology (Baltimore, Md.: 1950)*, 153(4):1697–1706, August 1994.

[176] C. F. Nathan, H. W. Murray, M. E. Wiebe, and B. Y. Rubin. Identification of interferon-gamma as the lymphokine that activates human macrophage oxidative metabolism and antimicrobial activity. *The Journal of Experimental Medicine*, 158(3):670–689, September 1983.

[177] Natalie J. Neubert, Martina Schmittnaegel, Natacha Bordry, Sina Nassiri, Noémie Wald, Christophe Martignier, Laure Tillé, Krisztian Homicsko, William Damsky, Hélène Maby-El Hajjami, Irina Klaman, Esther Danenberg, Kalliopi Ioannidou, Lana Kandalaft, George Coukos, Sabine Hoves, Carola H. Ries, Silvia A. Fuertes Marraco, Periklis G. Foukas, Michele De Palma, and Daniel E. Speiser. T cell–induced CSF1 promotes melanoma resistance to PD1 blockade. *Science Translational Medicine*, 10(436):eaan3311, April 2018.

[178] J. Newson, M. Stables, E. Karra, F. Arce-Vargas, S. Quezada, M. Motwani, M. Mack, S. Yona, T. Audzevich, and D. W. Gilroy. Resolution of acute inflammation bridges the gap between innate and adaptive immunity. *Blood*, 124(11):1748–1764, September 2014.

[179] Masa-aki Nishitani, Tohru Sakai, Kazunari Ishii, Manxin Zhang, Yoko Nakano, Yoshio Nitta, Jun-ichi Miyazaki, Hiro-omi Kanayama, Susumu Kagawa, and Kunisuke Himeno. A convenient cancer vaccine therapy with in vivo transfer of interleukin 12 expression plasmid using gene gun technology after priming with irradiated carcinoma cells. *Cancer Gene Therapy*, 9(2):156–163, February 2002.

[180] K. E. Nograles, L. C. Zaba, E. Guttman-Yassky, J. Fuentes-Duculan, M. Suárez-Fariñas, I. Cardinale, A. Khatcherian, J. Gonzalez, K. C. Pierson, T. R. White, C. Pensabene, I. Coats, I. Novitskaya, M. A. Lowes, and J. G. Krueger. Th17 cytokines interleukin (IL)-17 and IL-22 modulate distinct inflammatory and keratinocyte-response pathways. *The British Journal of Dermatology*, 159(5):1092–1102, November 2008.

[181] Margherita Norelli, Barbara Camisa, Giulia Barbiera, Laura Falcone, Ayurzana Purevdorj, Marco Genua, Francesca Sanvito, Maurilio Ponzoni, Claudio Doglioni, Patrizia Cristofori, Catia Traversari, Claudio Bordignon, Fabio Ciceri, Renato Ostuni, Chiara Bonini, Monica Casucci, and Attilio Bondanza. Monocyte-derived IL-1 and IL-6 are differentially required for cytokine-release syndrome and neurotoxicity due to CAR T cells. *Nature Medicine*, 24(6):739–748, 2018.

[182] Jesse C. Nussbaum, Steven J. Van Dyken, Jakob von Moltke, Laurence E. Cheng, Alexander Mohapatra, Ari B. Molofsky, Emily E. Thornton,

Matthew F. Krummel, Ajay Chawla, Hong-Erh Liang, and Richard M. Locksley. Type 2 innate lymphoid cells control eosinophil homeostasis. *Nature*, 502(7470):245–248, October 2013.

[183] Kathrin Nussbaum, Sara H. Burkhard, Isabel Ohs, Florian Mair, Christoph S. N. Klose, Sebastian J. Arnold, Andreas Diefenbach, Sonia Tugues, and Burkhard Becher. Tissue microenvironment dictates the fate and tumor-suppressive function of type 3 ILCs. *The Journal of Experimental Medicine*, 214(8):2331–2347, August 2017.

[184] Stephen L. Nutt, Philip D. Hodgkin, David M. Tarlinton, and Lynn M. Corcoran. The generation of antibody-secreting plasma cells. *Nature Reviews. Immunology*, 15(3):160–171, March 2015.

[185] Timothy M Nywening, Andrea Wang-Gillam, Dominic E Sanford, Brian A Belt, Roheena Z Panni, Brian M Cusworth, Adetunji T Toriola, Rebecca K Nieman, Lori A Worley, Motoyo Yano, Kathryn J Fowler, A Craig Lockhart, Rama Suresh, Benjamin R Tan, Kian-Huat Lim, Ryan C Fields, Steven M Strasberg, William G Hawkins, David G DeNardo, S Peter Goedegebuure, and David C Linehan. Targeting tumour-associated macrophages with CCR2 inhibition in combination with FOLFIRINOX in patients with borderline resectable and locally advanced pancreatic cancer: a single-centre, open-label, dose-finding, non-randomised, phase 1b trial. *The Lancet Oncology*, 17(5):651–662, May 2016.

[186] Naoki Okada, Sayaka Iiyama, Yuka Okada, Hiroyuki Mizuguchi, Takao Hayakawa, Shinsaku Nakagawa, Tadanori Mayumi, Takuya Fujita, and Akira Yamamoto. Immunological properties and vaccine efficacy of murine dendritic cells simultaneously expressing melanoma-associated antigen and interleukin-12. *Cancer Gene Therapy*, 12(1):72–83, January 2005.

[187] Abigail E. Overacre-Delgoffe, Maria Chikina, Rebekah E. Dadey, Hiroshi Yano, Erin A. Brunazzi, Gulidanna Shayan, William Horne, Jessica M. Moskovitz, Jay K. Kolls, Cindy Sander, Yongli Shuai, Daniel P. Normolle, John M. Kirkwood, Robert L. Ferris, Greg M. Delgoffe, Tullia C. Bruno, Creg J. Workman, and Dario A. A. Vignali. Interferon-γ Drives Treg Fragility to Promote Anti-tumor Immunity. *Cell*, 169(6):1130–1141.e11, June 2017.

[188] Edwin R. Parra, Naohiro Uraoka, Mei Jiang, Pamela Cook, Don Gibbons, Marie-Andrée Forget, Chantale Bernatchez, Cara Haymaker, Ignacio I. Wistuba, and Jaime Rodriguez-Canales. Validation of multiplex immunofluorescence panels using multispectral microscopy for immune-profiling of formalin-fixed and paraffin-embedded human tumor tissues. *Scientific Reports*, 7(1):13380, 2017.

[189] Elisa Peranzoni, Jean Lemoine, Lene Vimeux, Vincent Feuillet, Sarah Barrin, Chahrazade Kantari-Mimoun, Nadège Bercovici, Marion Guérin, Jérôme Biton, Hanane Ouakrim, Fabienne Régnier, Audrey Lupo, Marco Alifano, Diane Damotte, and Emmanuel Donnadieu. Macrophages impede CD8 T cells from reaching tumor cells and limit the efficacy of anti–PD-1 treatment. *Proceedings of the National Academy of Sciences*, 115(17):E4041–E4050, April 2018.

[190] Emma K. Persson, Heli Uronen-Hansson, Monika Semmrich, Aymeric Rivollier, Karin Hägerbrand, Jan Marsal, Sigurdur Gudjonsson, Ulf Håkansson, Boris Reizis, Knut Kotarsky, and William W. Agace. IRF4 transcription-factor-dependent CD103(+)CD11b(+) dendritic cells drive mucosal T helper 17 cell differentiation. *Immunity*, 38(5):958–969, May 2013.

[191] Joseph M. Pickard, Corinne F. Maurice, Melissa A. Kinnebrew, Michael C. Abt, Dominik Schenten, Tatyana V. Golovkina, Said R. Bogatyrev, Rustem F. Ismagilov, Eric G. Pamer, Peter J. Turnbaugh, and Alexander V. Chervonsky. Rapid fucosylation of intestinal epithelium sustains host-commensal symbiosis in sickness. *Nature*, 514(7524):638–641, October 2014.

[192] Lubna Pinky and Hana M. Dobrovolny. Coinfections of the Respiratory Tract: Viral Competition for Resources. *PloS One*, 11(5):e0155589, 2016.

[193] E. Planchet. Nitric oxide (NO) detection by DAF fluorescence and chemiluminescence: a comparison using abiotic and biotic NO sources. *Journal of Experimental Botany*, 57(12):3043–3055, August 2006.

[194] J. E. Portielje, W. H. Kruit, M. Schuler, J. Beck, C. H. Lamers, G. Stoter, C. Huber, M. de Boer-Dennert, A. Rakhit, R. L. Bolhuis, and W. E. Aulitzky. Phase I study of subcutaneously administered recombinant human interleukin 12 in patients with advanced renal cell cancer. *Clinical Cancer Research: An Official Journal of the American Association for Cancer Research*, 5(12):3983–3989, December 1999.

[195] Johanna E. A. Portielje, Cor H. J. Lamers, Wim H. J. Kruit, Alex Sparreboom, Reinder L. H. Bolhuis, Gerrit Stoter, Christoph Huber, and Jan W. Gratama. Repeated administrations of interleukin (IL)-12 are associated with persistently elevated plasma levels of IL-10 and declining IFN-gamma, tumor necrosis factor-alpha, IL-6, and IL-8 responses. *Clinical Cancer Research: An Official Journal of the American Association for Cancer Research*, 9(1):76–83, January 2003.

[196] G. Poste, J. Doll, and I. J. Fidler. Interactions among clonal subpopulations affect stability of the metastatic phenotype in polyclonal populations of B16 melanoma cells. *Proceedings of the National Academy of Sciences of the United States of America*, 78(10):6226–6230, October 1981.

[197] Ivan Presta, Marco Vismara, Fabiana Novellino, Annalidia Donato, Paolo Zaffino, Elisabetta Scali, Krizia Caterina Pirrone, Maria Francesca Spadea, Natalia Malara, and Giuseppe Donato. Innate Immunity Cells and the Neurovascular Unit. *International Journal of Molecular Sciences*, 19(12), December 2018.

[198] David J. Propper, David Chao, Jeremy P. Braybrooke, Pru Bahl, Parames Thavasu, Frances Balkwill, Helen Turley, Nicola Dobbs, Kevin Gatter, Denis C. Talbot, Adrian L. Harris, and Trivadi S. Ganesan. Low-dose IFN-gamma induces tumor MHC expression in metastatic malignant melanoma. *Clinical Cancer Research: An Official Journal of the American Association for Cancer Research*, 9(1):84–92, January 2003.

[199] Binzhi Qian, Yan Deng, Jae Hong Im, Ruth J. Muschel, Yiyu Zou, Jiufeng Li, Richard A. Lang, and Jeffrey W. Pollard. A distinct macrophage population mediates metastatic breast cancer cell extravasation, establishment and growth. *PloS One*, 4(8):e6562, August 2009.

[200] Benjamin J. C. Quah, Danushka K. Wijesundara, Charani Ranasinghe, and Christopher R. Parish. Fluorescent target array killing assay: a multiplex cytotoxic T-cell assay to measure detailed T-cell antigen specificity and avidity in vivo. *Cytometry. Part A: The Journal of the International Society for Analytical Cytology*, 81(8):679–690, August 2012.

[201] Virginie M. Renoux, Alya Zriwil, Claudia Peitzsch, Jakob Michaëlsson, Danielle Friberg, Shamit Soneji, and Ewa Sitnicka. Identification of a Human Natural Killer Cell Lineage-Restricted Progenitor in Fetal and Adult Tissues. *Immunity*, 43(2):394–407, August 2015.

[202] Mathieu P. Rodero, Fabrice Licata, Lucie Poupel, Pauline Hamon, Kiarash Khosrotehrani, Christophe Combadiere, and Alexandre Boissonnas. In vivo imaging reveals a pioneer wave of monocyte recruitment into mouse skin wounds. *PloS One*, 9(10):e108212, 2014.

[203] S. Ruben, A. Perkins, R. Purcell, K. Joung, R. Sia, R. Burghoff, W. A. Haseltine, and C. A. Rosen. Structural and functional characterization of human immunodeficiency virus tat protein. *Journal of Virology*, 63(1):1–8, January 1989.

[204] Mark P. Rubinstein, Ee Wern Su, Samantha Suriano, Colleen A. Cloud, Kristina Andrijauskaite, Pravin Kesarwani, Kristina M. Schwartz, Katelyn M. Williams, C. Bryce Johnson, Mingli Li, Gina M. Scurti, Mohamed L. Salem, Chrystal M. Paulos, Elizabeth Garrett-Mayer, Shikhar Mehrotra, and David J. Cole. Interleukin-12 enhances the function and anti-tumor activity in murine and human CD8(+) T cells. *Cancer immunology, immunotherapy: CII*, 64(5):539–549, May 2015.

[205] Levi J. Rupp, Kathrin Schumann, Kole T. Roybal, Rachel E. Gate, Chun J. Ye, Wendell A. Lim, and Alexander Marson. CRISPR/Cas9-mediated PD-1 disruption enhances anti-tumor efficacy of human chimeric antigen receptor T cells. *Scientific Reports*, 7(1):737, 2017.

[206] Stephanie L. Sanos, Viet L. Bui, Arthur Mortha, Karin Oberle, Charlotte Heners, Caroline Johner, and Andreas Diefenbach. RORgammat and commensal microflora are required for the differentiation of mucosal interleukin 22-producing NKp46+ cells. *Nature Immunology*, 10(1):83–91, January 2009.

[207] D. M. Sansom. CD28, CTLA-4 and their ligands: who does what and to whom? *Immunology*, 101(2):169–177, October 2000.

[208] Jordy Saravia, Nicole M. Chapman, and Hongbo Chi. Helper T cell differentiation. *Cellular & Molecular Immunology*, March 2019.

[209] Naoko Satoh-Takayama. Heterogeneity and diversity of group 3 innate lymphoid cells: new cells on the block. *International Immunology*, 28(1):29–34, January 2016.

[210] Kristin A. Sauter, Clare Pridans, Anuj Sehgal, Calum C. Bain, Charlotte Scott, Lindsey Moffat, Rocío Rojo, Ben M. Stutchfield, Claire L. Davies, David S. Donaldson, Kathleen Renault, Barry W. McColl, Alan M. Mowat, Alan Serrels, Margaret C. Frame, Neil A. Mabbott, and David A. Hume. The MacBlue Binary Transgene (csf1r-gal4vp16/UAS-ECFP) Provides a Novel Marker for Visualisation of Subsets of Monocytes, Macrophages and Dendritic Cells and Responsiveness to CSF1 Administration. *PLoS ONE*, 9(8):e105429, August 2014.

[211] Shinichiro Sawa, Matthias Lochner, Naoko Satoh-Takayama, Sophie Dulauroy, Marion Bérard, Melanie Kleinschek, Daniel Cua, James P. Di Santo, and Gérard Eberl. RORγt+ innate lymphoid cells regulate intestinal homeostasis by integrating negative signals from the symbiotic microbiota. *Nature Immunology*, 12(4):320–326, April 2011.

[212] Keiichi Sawachi, Yasuteru Shimada, Hiroaki Taniguchi, Keiji Hirota, Hiroyuki Inagawa, Chie Kohchi, Gen-Ichiro Soma, Kimiko Makino, and Hiroshi Terada. Cytotoxic effects of activated alveolar macrophages on lung carcinoma cells via cell-to-cell contact and nitric oxide. *Anticancer Research*, 30(8):3135–3141, August 2010.

[213] Andreas Schlitzer, Naomi McGovern, and Florent Ginhoux. Dendritic cells and monocyte-derived cells: Two complementary and integrated functional systems. *Seminars in Cell & Developmental Biology*, 41:9–22, May 2015.

[214] Christian Schulz, Elisa Gomez Perdiguero, Laurent Chorro, Heather Szabo-Rogers, Nicolas Cagnard, Katrin Kierdorf, Marco Prinz, Bishan Wu, Sten Eirik W. Jacobsen, Jeffrey W. Pollard, Jon Frampton, Karen J. Liu, and Frederic Geissmann. A lineage of myeloid cells independent of Myb and hematopoietic stem cells. *Science (New York, N.Y.)*, 336(6077):86–90, April 2012.

[215] Joey Schyns, Fabrice Bureau, and Thomas Marichal. Lung Interstitial Macrophages: Past, Present, and Future. *Journal of Immunology Research*, 2018:5160794, 2018.

[216] L. Scrucca, A. Santucci, and F. Aversa. Competing risk analysis using R: an easy guide for clinicians. *Bone Marrow Transplantation*, 40(4):381–387, August 2007.

[217] Elodie Segura and Sebastian Amigorena. Cross-presentation by human dendritic cell subsets. *Immunology Letters*, 158(1-2):73–78, April 2014.

[218] Kimberly Shafer-Weaver, Thomas Sayers, Susan Strobl, Eric Derby, Tracy Ulderich, Michael Baseler, and Anatoli Malyguine. The Granzyme B ELISPOT assay: an alternative to the 51cr-release assay for monitoring cell-mediated cytotoxicity. *Journal of Translational Medicine*, 1(1):14, December 2003.

[219] Abbas Shapouri-Moghaddam, Saeed Mohammadian, Hossein Vazini, Mahdi Taghadosi, Seyed-Alireza Esmaeili, Fatemeh Mardani, Bita Seifi, Asadollah Mohammadi, Jalil T. Afshari, and Amirhossein Sahebkar. Macrophage plasticity, polarization, and function in health and disease. *Journal of Cellular Physiology*, 233(9):6425–6440, September 2018.

[220] Antonio Sica and Alberto Mantovani. Macrophage plasticity and polarization: in vivo veritas. *Journal of Clinical Investigation*, 122(3):787–795, March 2012.

[221] Tyler R. Simpson, Fubin Li, Welby Montalvo-Ortiz, Manuel A. Sepulveda, Katharina Bergerhoff, Frederick Arce, Claire Roddie, Jake Y. Henry, Hideo Yagita, Jedd D. Wolchok, Karl S. Peggs, Jeffrey V. Ravetch, James P. Allison, and Sergio A. Quezada. Fc-dependent depletion of tumor-infiltrating regulatory T cells co-defines the efficacy of anti-CTLA-4 therapy against melanoma. *The Journal of Experimental Medicine*, 210(9):1695–1710, August 2013.

[222] D. Skelton, N. Satake, and D. B. Kohn. The enhanced green fluorescent protein (eGFP) is minimally immunogenic in C57bl/6 mice. *Gene Therapy*, 8(23):1813–1814, December 2001.

[223] Johanna A. Smith and René Daniel. Following the path of the virus: the exploitation of host DNA repair mechanisms by retroviruses. *ACS chemical biology*, 1(4):217–226, May 2006.

[224] Paul Spear, Amorette Barber, Agnieszka Rynda-Apple, and Charles L. Sentman. Chimeric antigen receptor T cells shape myeloid cell function within the tumor microenvironment through IFN-γ and GM-CSF. *Journal of Immunology (Baltimore, Md.: 1950)*, 188(12):6389–6398, June 2012.

[225] Hergen Spits, David Artis, Marco Colonna, Andreas Diefenbach, James P. Di Santo, Gerard Eberl, Shigeo Koyasu, Richard M. Locksley, Andrew N. J. McKenzie, Reina E. Mebius, Fiona Powrie, and Eric Vivier. Innate lymphoid cells–a proposal for uniform nomenclature. *Nature Reviews. Immunology*, 13(2):145–149, February 2013.

[226] Matthew H. Spitzer, Pier Federico Gherardini, Gabriela K. Fragiadakis, Nupur Bhattacharya, Robert T. Yuan, Andrew N. Hotson, Rachel Finck, Yaron Carmi, Eli R. Zunder, Wendy J. Fantl, Sean C. Bendall, Edgar G. Engleman, and Garry P. Nolan. IMMUNOLOGY. An interactive reference framework for modeling a dynamic immune system. *Science (New York, N.Y.)*, 349(6244):1259425, July 2015.

[227] B. Starcich, L. Ratner, S. F. Josephs, T. Okamoto, R. C. Gallo, and F. Wong-Staal. Characterization of long terminal repeat sequences of HTLV-III. *Science (New York, N.Y.)*, 227(4686):538–540, February 1985.

[228] Richard Stebbings, Stephen Poole, and Robin Thorpe. Safety of biologics, lessons learnt from TGN1412. *Current Opinion in Biotechnology*, 20(6):673–677, December 2009.

[229] M. Stein, S. Keshav, N. Harris, and S. Gordon. Interleukin 4 potently enhances murine macrophage mannose receptor activity: a marker of alter-

native immunologic macrophage activation. *The Journal of Experimental Medicine*, 176(1):287–292, July 1992.

[230] Antonius Steven, Scott A. Fisher, and Bruce W. Robinson. Immunotherapy for lung cancer. *Respirology (Carlton, Vic.)*, April 2016.

[231] R. Stripecke, M. Carmen Villacres, D. Skelton, N. Satake, S. Halene, and D. Kohn. Immune response to green fluorescent protein: implications for gene therapy. *Gene Therapy*, 6(7):1305–1312, July 1999.

[232] Fan Sun, Gutian Xiao, and Zhaoxia Qu. Murine Bronchoalveolar Lavage. *Bio-Protocol*, 7(10), May 2017.

[233] Y. Sun, K. Jurgovsky, P. Möller, S. Alijagic, T. Dorbic, J. Georgieva, B. Wittig, and D. Schadendorf. Vaccination with IL-12 gene-modified autologous melanoma cells: preclinical results and a first clinical phase I study. *Gene Therapy*, 5(4):481–490, April 1998.

[234] Rajasekhar N V S Suragani, Samuel M Cadena, Sharon M Cawley, Dianne Sako, Dianne Mitchell, Robert Li, Monique V Davies, Mark J Alexander, Matthew Devine, Kenneth S Loveday, Kathryn W Underwood, Asya V Grinberg, John D Quisel, Rajesh Chopra, R Scott Pearsall, Jasbir Seehra, and Ravindra Kumar. Transforming growth factor-β superfamily ligand trap ACE-536 corrects anemia by promoting late-stage erythropoiesis. *Nature Medicine*, 20(4):408–414, April 2014.

[235] J. E. Talmadge and I. J. Fidler. Cancer metastasis is selective or random depending on the parent tumour population. *Nature*, 297(5867):593–594, June 1982.

[236] Janis M. Taube, Robert A. Anders, Geoffrey D. Young, Haiying Xu, Rajni Sharma, Tracee L. McMiller, Shuming Chen, Alison P. Klein, Drew M. Pardoll, Suzanne L. Topalian, and Lieping Chen. Colocalization of inflammatory response with B7-h1 expression in human melanocytic lesions supports an adaptive resistance mechanism of immune escape. *Science Translational Medicine*, 4(127):127ra37, March 2012.

[237] Cosmin A. Tegla, Cornelia Cudrici, Snehal Patel, Richard Trippe, Violeta Rus, Florin Niculescu, and Horea Rus. Membrane attack by complement: the assembly and biology of terminal complement complexes. *Immunologic Research*, 51(1):45–60, October 2011.

[238] B. Thaci, A. U. Ahmed, I. V. Ulasov, D. A. Wainwright, P. Nigam, B. Auffinger, A. L. Tobias, Y. Han, L. Zhang, K.-S. Moon, and M. S. Lesniak. Depletion of myeloid-derived suppressor cells during interleukin-12 immunogene

therapy does not confer a survival advantage in experimental malignant glioma. *Cancer Gene Therapy*, 21(1):38–44, January 2014.

[239] Joseph A. Trapani and Mark J. Smyth. Functional significance of the perforin/granzyme cell death pathway. *Nature Reviews Immunology*, 2(10):735–747, October 2002.

[240] G. Trinchieri and F. Gerosa. Immunoregulation by interleukin-12. *Journal of Leukocyte Biology*, 59(4):505–511, April 1996.

[241] G. Trinchieri, M. Rengaraju, A. D'Andrea, N. M. Valiante, M. Kubin, M. Aste, and J. Chehimi. Producer cells of interleukin-12. *Immunology Today*, 14(5):237–238, May 1993.

[242] Diane Tseng, Jens-Peter Volkmer, Stephen B. Willingham, Humberto Contreras-Trujillo, John W. Fathman, Nathaniel B. Fernhoff, Jun Seita, Matthew A. Inlay, Kipp Weiskopf, Masanori Miyanishi, and Irving L. Weissman. Anti-CD47 antibody-mediated phagocytosis of cancer by macrophages primes an effective antitumor T-cell response. *Proceedings of the National Academy of Sciences of the United States of America*, 110(27):11103–11108, July 2013.

[243] Kangla Tsung and Jeffrey A. Norton. Lessons from Coley's Toxin. *Surgical Oncology*, 15(1):25–28, July 2006.

[244] T. Ueno, M. Toi, H. Saji, M. Muta, H. Bando, K. Kuroi, M. Koike, H. Inadera, and K. Matsushima. Significance of macrophage chemoattractant protein-1 in macrophage recruitment, angiogenesis, and survival in human breast cancer. *Clinical Cancer Research: An Official Journal of the American Association for Cancer Research*, 6(8):3282–3289, August 2000.

[245] A. Untergasser, H. Nijveen, X. Rao, T. Bisseling, R. Geurts, and J. A.M. Leunissen. Primer3plus, an enhanced web interface to Primer3. *Nucleic Acids Research*, 35(Web Server):W71–W74, May 2007.

[246] R. van Furth, Z. A. Cohn, J. G. Hirsch, J. H. Humphrey, W. G. Spector, and H. L. Langevoort. The mononuclear phagocyte system: a new classification of macrophages, monocytes, and their precursor cells. *Bulletin of the World Health Organization*, 46(6):845–852, 1972.

[247] Sofie Van Gassen, Britt Callebaut, Mary J. Van Helden, Bart N. Lambrecht, Piet Demeester, Tom Dhaene, and Yvan Saeys. FlowSOM: Using self-organizing maps for visualization and interpretation of cytometry data. *Cytometry. Part A: The Journal of the International Society for Analytical Cytology*, 87(7):636–645, July 2015.

[248] J. P. van Netten, E. J. George, B. J. Ashmead, C. Fletcher, I. G. Thornton, and P. Coy. Macrophage-tumour cell associations in breast cancer. *Lancet (London, England)*, 342(8875):872–873, October 1993.

[249] Federica Vannini, Khosrow Kashfi, and Niharika Nath. The dual role of iNOS in cancer. *Redox Biology*, 6:334–343, December 2015.

[250] Lucia Vanrell, Marianna Di Scala, Laura Blanco, Itziar Otano, Irene Gil-Farina, Victor Baldim, Astrid Paneda, Pedro Berraondo, Stuart G. Beattie, Abdelwahed Chtarto, Lilianne Tenenbaum, Jesús Prieto, and Gloria Gonzalez-Aseguinolaza. Development of a liver-specific Tet-on inducible system for AAV vectors and its application in the treatment of liver cancer. *Molecular Therapy: The Journal of the American Society of Gene Therapy*, 19(7):1245–1253, July 2011.

[251] Els Verhoeyen, Valerie Dardalhon, Odile Ducrey-Rundquist, Didier Trono, Naomi Taylor, and François-Loïc Cosset. IL-7 surface-engineered lentiviral vectors promote survival and efficient gene transfer in resting primary T lymphocytes. *Blood*, 101(6):2167–2174, March 2003.

[252] Kirstin Veugelers, Bruce Motyka, Christine Frantz, Irene Shostak, Tracy Sawchuk, and R. Chris Bleackley. The granzyme B-serglycin complex from cytotoxic granules requires dynamin for endocytosis. *Blood*, 103(10):3845–3853, May 2004.

[253] R. Visconti, M. Gadina, M. Chiariello, E. H. Chen, L. F. Stancato, J. S. Gutkind, and J. J. O'Shea. Importance of the MKK6/p38 pathway for interleukin-12-induced STAT4 serine phosphorylation and transcriptional activity. *Blood*, 96(5):1844–1852, September 2000.

[254] Eric Vivier, David Artis, Marco Colonna, Andreas Diefenbach, James P. Di Santo, Gérard Eberl, Shigeo Koyasu, Richard M. Locksley, Andrew N. J. McKenzie, Reina E. Mebius, Fiona Powrie, and Hergen Spits. Innate Lymphoid Cells: 10 Years On. *Cell*, 174(5):1054–1066, August 2018.

[255] Eric Vivier, Elena Tomasello, Myriam Baratin, Thierry Walzer, and Sophie Ugolini. Functions of natural killer cells. *Nature Immunology*, 9(5):503–510, May 2008.

[256] Johannes Vom Berg, Melissa Vrohlings, Sergio Haller, Aladin Haimovici, Paulina Kulig, Anna Sledzinska, Michael Weller, and Burkhard Becher. Intratumoral IL-12 combined with CTLA-4 blockade elicits T cell-mediated glioma rejection. *The Journal of Experimental Medicine*, 210(13):2803–2811, December 2013.

[257] Cedric Vonarbourg, Arthur Mortha, Viet L. Bui, Pedro P. Hernandez, Elina A. Kiss, Thomas Hoyler, Melanie Flach, Bertram Bengsch, Robert Thimme, Christoph Hölscher, Manfred Hönig, Ulrich Pannicke, Klaus Schwarz, Carl F. Ware, Daniela Finke, and Andreas Diefenbach. Regulated expression of nuclear receptor RORγt confers distinct functional fates to NK cell receptor-expressing RORγt(+) innate lymphocytes. *Immunity*, 33(5):736–751, November 2010.

[258] Jennifer A. Walker, Jillian L. Barlow, and Andrew N. J. McKenzie. Innate lymphoid cells–how did we miss them? *Nature Reviews. Immunology*, 13(2):75–87, February 2013.

[259] Fang Wang, Zhiping Wang, Hongwei Tian, Meijiao Qi, Zhenxing Zhai, Shuwen Li, Renju Li, Hongjuan Zhang, Wenyun Wang, Shenjun Fu, Jianzhong Lu, Ronald Rodriguez, Yinglu Guo, and Liqun Zhou. Biodistribution and safety assessment of bladder cancer specific recombinant oncolytic adenovirus in subcutaneous xenografts tumor model in nude mice. *Current Gene Therapy*, 12(2):67–76, April 2012.

[260] Qiu-Shuang Wang, Shi-Qiang Shen, Hua-Wen Sun, Zhi-Xiang Xing, and Hou-Lai Yang. Interferon-gamma induces autophagy-associated apoptosis through induction of cPLA2-dependent mitochondrial ROS generation in colorectal cancer cells. *Biochemical and Biophysical Research Communications*, 498(4):1058–1065, 2018.

[261] Rui Wang, Jie Zhang, Sufeng Chen, Meng Lu, Xiaoyang Luo, Shihua Yao, Shilei Liu, Ying Qin, and Haiquan Chen. Tumor-associated macrophages provide a suitable microenvironment for non-small lung cancer invasion and progression. *Lung Cancer (Amsterdam, Netherlands)*, 74(2):188–196, November 2011.

[262] P. Waterhouse, J. M. Penninger, E. Timms, A. Wakeham, A. Shahinian, K. P. Lee, C. B. Thompson, H. Griesser, and T. W. Mak. Lymphoproliferative disorders with early lethality in mice deficient in Ctla-4. *Science (New York, N.Y.)*, 270(5238):985–988, November 1995.

[263] Jeffrey S. Weber, Steven O'Day, Walter Urba, John Powderly, Geoff Nichol, Michael Yellin, Jolie Snively, and Evan Hersh. Phase I/II study of ipilimumab for patients with metastatic melanoma. *Journal of Clinical Oncology: Official Journal of the American Society of Clinical Oncology*, 26(36):5950–5956, December 2008.

[264] Julia M. Weiss, Marion V. Guérin, Fabienne Regnier, Gilles Renault, Isabelle Galy-Fauroux, Lene Vimeux, Vincent Feuillet, Elisa Peranzoni,

Maxime Thoreau, Alain Trautmann, and Nadège Bercovici. The STING agonist DMXAA triggers a cooperation between T lymphocytes and myeloid cells that leads to tumor regression. *OncoImmunology*, 6(10):e1346765, October 2017.

[265] R. A. Weiss. How does HIV cause AIDS? *Science (New York, N.Y.)*, 260(5112):1273–1279, May 1993.

[266] B. Wiemann and C. O. Starnes. Coley's toxins, tumor necrosis factor and cancer research: a historical perspective. *Pharmacology & Therapeutics*, 64(3):529–564, 1994.

[267] Sebastian Willenborg, Tina Lucas, Geert van Loo, Johanna A. Knipper, Thomas Krieg, Ingo Haase, Bent Brachvogel, Matthias Hammerschmidt, Andras Nagy, Napoleone Ferrara, Manolis Pasparakis, and Sabine A. Eming. CCR2 recruits an inflammatory macrophage subpopulation critical for angiogenesis in tissue repair. *Blood*, 120(3):613–625, July 2012.

[268] Christopher T. Winkelmann, Said Daibes Figueroa, Tammy L. Rold, Wynn A. Volkert, and Timothy J. Hoffman. Microimaging characterization of a B16-F10 melanoma metastasis mouse model. *Molecular Imaging*, 5(2):105–114, June 2006.

[269] David R. Withers and Matthew R. Hepworth. Group 3 Innate Lymphoid Cells: Communications Hubs of the Intestinal Immune System. *Frontiers in Immunology*, 8:1298, 2017.

[270] Kerstin Wolk, Ellen Witte, Ute Hoffmann, Wolf-Dietrich Doecke, Stefanie Endesfelder, Khusru Asadullah, Wolfram Sterry, Hans-Dieter Volk, Bianca Maria Wittig, and Robert Sabat. IL-22 induces lipopolysaccharide-binding protein in hepatocytes: a potential systemic role of IL-22 in Crohn's disease. *Journal of Immunology (Baltimore, Md.: 1950)*, 178(9):5973–5981, May 2007.

[271] Jeffrey B. Wyckoff, Yarong Wang, Elaine Y. Lin, Jiu-feng Li, Sumanta Goswami, E. Richard Stanley, Jeffrey E. Segall, Jeffrey W. Pollard, and John Condeelis. Direct visualization of macrophage-assisted tumor cell intravasation in mammary tumors. *Cancer Research*, 67(6):2649–2656, March 2007.

[272] Wei Xu, Rita G. Domingues, Diogo Fonseca-Pereira, Manuela Ferreira, Hélder Ribeiro, Silvia Lopez-Lastra, Yasutaka Motomura, Lara Moreira-Santos, Franck Bihl, Véronique Braud, Barbara Kee, Hugh Brady, Mark C. Coles, Christian Vosshenrich, Masato Kubo, James P. Di Santo, and Henrique Veiga-Fernandes. NFIL3 orchestrates the emergence of common

helper innate lymphoid cell precursors. *Cell Reports*, 10(12):2043–2054, March 2015.

[273] R. Yamanaka, S. A. Zullo, R. Tanaka, J. Ramsey, M. Blaese, and K. G. Xanthopoulos. Induction of a therapeutic antitumor immunological response by intratumoral injection of genetically engineered Semliki Forest virus to produce interleukin-12. *Neurosurgical Focus*, 9(6):e7, December 2000.

[274] Qi Yang, Fengyin Li, Christelle Harly, Shaojun Xing, Longyun Ye, Xuefeng Xia, Haikun Wang, Xinxin Wang, Shuyang Yu, Xinyuan Zhou, Maggie Cam, Hai-Hui Xue, and Avinash Bhandoola. TCF-1 upregulation identifies early innate lymphoid progenitors in the bone marrow. *Nature Immunology*, 16(10):1044–1050, October 2015.

[275] Shengyu Yang, J. Jillian Zhang, and Xin-Yun Huang. Mouse models for tumor metastasis. *Methods in Molecular Biology (Clifton, N.J.)*, 928:221–228, 2012.

[276] San-qiao Yao, Liying Wang Rojanasakul, Zhi-yuan Chen, Ying-jun Xu, Yu-ping Bai, Gang Chen, Xi-ying Zhang, Chun-min Zhang, Yan-qin Yu, Fu-hai Shen, Ju-xiang Yuan, Jie Chen, and Qin-cheng He. Fas/FasL pathway-mediated alveolar macrophage apoptosis involved in human silicosis. *Apoptosis*, 16(12):1195–1204, December 2011.

[277] Mariko Yokouchi and Akiharu Kubo. Maintenance of tight junction barrier integrity in cell turnover and skin diseases. *Experimental Dermatology*, 27(8):876–883, 2018.

[278] Jae Kwang Yoo, Jae Ho Cho, Seung Woo Lee, and Young Chul Sung. IL-12 provides proliferation and survival signals to murine CD4+ T cells through phosphatidylinositol 3-kinase/Akt signaling pathway. *Journal of Immunology (Baltimore, Md.: 1950)*, 169(7):3637–3643, October 2002.

[279] M. L. Zapp and M. R. Green. Sequence-specific RNA binding by the HIV-1 Rev protein. *Nature*, 342(6250):714–716, December 1989.

[280] Ke Zen, Yalan Guo, Zhen Bian, Zhiyuan Lv, Dihan Zhu, Hiroshi Ohnishi, Takashi Matozaki, and Yuan Liu. Inflammation-induced proteolytic processing of the SIRPα cytoplasmic ITIM in neutrophils propagates a proinflammatory state. *Nature Communications*, 4:2436, 2013.

[281] Boning Zeng, Shengnan Shi, Gareth Ashworth, Changjiang Dong, Jing Liu, and Feiyue Xing. ILC3 function as a double-edged sword in inflammatory bowel diseases. *Cell Death & Disease*, 10(4):315, April 2019.

[282] Bin Zhang, Theodore Karrison, Donald A. Rowley, and Hans Schreiber. IFN-γ– and TNF-dependent bystander eradication of antigen-loss variants in established mouse cancers. *Journal of Clinical Investigation*, 118(4):1398–1404, April 2008.

[283] Cai Zhang, Jianhua Zhang, Jiafeng Niu, Zhixia Zhou, Jian Zhang, and Zhigang Tian. Interleukin-12 improves cytotoxicity of natural killer cells via upregulated expression of NKG2d. *Human Immunology*, 69(8):490–500, August 2008.

[284] Jingxian Zhao, Jincun Zhao, and Stanley Perlman. Differential effects of IL-12 on Tregs and non-Treg T cells: roles of IFN-γ, IL-2 and IL-2r. *PloS One*, 7(9):e46241, 2012.

[285] Yan Zheng, Patricia A. Valdez, Dimitry M. Danilenko, Yan Hu, Susan M. Sa, Qian Gong, Alexander R. Abbas, Zora Modrusan, Nico Ghilardi, Frederic J. de Sauvage, and Wenjun Ouyang. Interleukin-22 mediates early host defense against attaching and effacing bacterial pathogens. *Nature Medicine*, 14(3):282–289, March 2008.

[286] R. Zufferey, T. Dull, R. J. Mandel, A. Bukovsky, D. Quiroz, L. Naldini, and D. Trono. Self-inactivating lentivirus vector for safe and efficient in vivo gene delivery. *Journal of Virology*, 72(12):9873–9880, December 1998.

[287] R. Zufferey, D. Nagy, R. J. Mandel, L. Naldini, and D. Trono. Multiply attenuated lentiviral vector achieves efficient gene delivery in vivo. *Nature Biotechnology*, 15(9):871–875, September 1997.

7 Appendix

7.1 Reagents used for flow cytometry

Reagent	Component	Concentration
FACS Buffer	FCS	2%
	EDTA	2mM
	PBS	
FoxP3 Perm Buffer	FoxP3 Fix/Perm concentrate (Thermo)	25%
	FoxP3 Fix/Perm diluent (Thermo)	75%
FoxP3 Wash	10X FoxP3 Permeabilization buffer (Thermo)	10%
	De-ionised water	90%
BD Perm Buffer	Fixation/Permeabilization solution (BD)	100%
BD Perm Wash	10x Perm/Wash Buffer (BD)	10%
	De-ionised water	90%
Extracellular Master-mix buffer	Normal Mouse Serum	20%
	Normal Rat Serum	20%
	FCS	8%
	anti-CD16/32 antibody (clone 2.4G2, 1mg/ml stock concentration)	8%
	Sodium Azide	1%
	PBS	43%
Intracellular Master-mix buffer	FCS	5%
	BD Perm Wash	95%
Intranuclear Master-mix buffer	FCS	5%
	FoxP3 Wash	95%
Extracellular Master-mix	Extracellular Master-mix Buffer	
	Monoclonal antibodies as per section 2.7.3	
Intracellular Master-mix	Intracellular Master-mix Buffer	
	Monoclonal antibodies as per section 2.7.3	
Intranuclear Master-mix	Intranuclear Master-mix buffer	
	Monoclonal antibodies as per section 2.7.3	

Table 13: FACS Buffers & Reagents

Marker	Clone	Supplier	Fluorophore	Extracellular	Intranuclear
CCR2	475301	R&D Systems	APC	X	
CD11c	N418	BioLegend	BV785	X	
CD19	6D5	BioLegend	BV605	X	
CD3	17A2	BioLegend	PerCP-Cy5.5	X	
CD3	145-2C11	Thermo	PE-Cy7	X	
CD4	RM4-5	BD	v500	X	
CD49b	DX5	BioLegend	Pacific Blue	X	
CD64	X54-5/7.1	BioLegend	BV711	X	
CD8	53-6.7	Thermo	eFluor 450	X	
CD8	53-6.7	BioLegend	BV650	X	
EOMES	Dan11mag	Thermo	PE		X
FoxP3	FJK-16s	Thermo	PE		X
FoxP3	FJK-16s	Thermo	Alexa Fluor 700		X
Granzyme B	GB11	BD	PE		X
Granzyme B	GB11	BD	APC		X
ICOS	C398.4A	BioLegend	PE-Cy7	X	
Ki67	SolA15	Thermo	FITC		X
Ki67	SolA15	Thermo	PerCP-eFluor 710		X
NK1.1	PK136	Thermo	eFluor 450	X	
NK1.1	PK136	BioLegend	BV 650	X	
NK1.1	PK136	Thermo	Alexa Fluor 700	X	
NKp46	29A1.4	BioLegend	BV605	X	
NKp46	29A1.4	BioLegend	APC	X	
T-bet	4B10	BioLegend	BV711		X
Viability Dye	n/a	Thermo	APC eFluor 780	X	

Table 14: T cell / NK Panel Antibodies

Marker	Clone	Supplier	Fluorophore	Extracellular	Intra-
B220	RA3-6B2	BD	BUV661	X	
CD117	ACK2	BioLegend	BV510	X	
CD117	2B8	BD	BB700	X	
CD11b	M1/70	BD	BUV661	X	
CD11b	M1/70	BioLegend	BV711	X	
CD11b	M1/70	Thermo	APC	X	
CD127	SB/199	BD	BUV737	X	
CD127	A7R34	Thermo	APC	X	
CD19	eBio1D3	Thermo	Alexa Fluor 700	X	
CD27	LG.3A10	BD	BUV395	X	
CD3	17A2	Thermo	Alexa Fluor 700	X	
CD4	RM4-5	BioLegend	BV785	X	
CD4	GK1.5	Thermo	APC	X	
CD45	30-F11	BD	BUV563	X	
CD49b	DX5	BioLegend	BV650	X	
CD5	53-7.3	Thermo	eFluor 450	X	
EOMES	Dan11mag	Thermo	PE		Intranuclear
IFNγ	XMG1.2	BD	BV480		Intracellular
IFNγ	XMG1.2	BioLegend	Alexa Fluor 488		Intracellular
NK1.1	PK136	BioLegend	BV650	X	
NK1.1	PK136	BD	BUV395	X	
NKp46	29A1.4	BioLegend	BV605	X	
NKp46	29A1.4	BioLegend	BV650	X	
NKp46	29A1.4	BioLegend	APC	X	
RORγt	Q31-378	BD	BV421		Intracellular
RORγT	B2D	eBio	PerCP-eFluor 710		Intranuclear
T-bet	4B10	BioLegend	BV711		Intranuclear
T-bet	O4-46	BD	BV786		Intranuclear
T-bet	4B10	BioLegend	PE		Intranuclear
Viability	n/a	Thermo	APC eFluor 780	X	

Table 15: IFNγ / ILC Panel Antibodies

Marker	Clone	Supplier	Fluorophore	Extracellular
CD103	M290	BD	BV421	X
CD11b	M1/70	BD	PerCP-Cy5.5	X
CD11b	M1/70	Thermo	APC	X
CD11c	N418	BioLegend	BV785	X
CD11c	N418	BioLegend	APC	X
CD16/32	93	Thermo	FITC	X
CD19	eBio1D3	Thermo	Alexa Fluor 700	X
CD24	M1/69	Thermo	FITC	X
CD3	17A2	Thermo	Alexa Fluor 700	X
CD45	30-F11	BioLegend	BV421	X
CD45	30-F11	BD	BV480	X
CD45.2	104	BD	v500	X
CD64 (FcgRI)	X54-5/7.1	BioLegend	BV711	X
f4/80	BM8	BioLegend	BV650	X
f4/80	BM8	BioLegend	Alexa Fluor 700	X
GR-1	RB6-8C5	BioLegend	PE-Cy7	X
I-Ab	25-9-17	BioLegend	Alexa Fluor 488	X
Ly6C	AL-21	BD	BV605	X
Ly6G	1A8	BioLegend	PE-Cy7	X
NK1.1	PK136	BioLegend	BV650	X
NK1.1	PK136	Thermo	Alexa Fluor 700	X
PD-L1	MIH5	Thermo	PE	X
Siglec F	E50-2440	BD	PE	X
Viability	n/a	Thermo	APC eFluor 780	X

Table 16: Myeloid Phenotype Panel Antibodies

Marker	Clone	Supplier	Fluorophore	Extracellular	Intra-
CD103	M290	BD	BV421	X	
CD11b	M1/70	BioLegend	BV711	X	
CD11b	M1/70	BD	PerCP-Cy5.5	X	
CD11c	N418	BioLegend	BV785	X	
CD11c	HL3	BD	FiTC	X	
CD11c	N418	BioLegend	APC	X	
CD3	17A2	BD	BV785	X	
CD3	17A2	BioLegend	PerCP-Cy5.5	X	
CD3	17A2	Thermo	Alexa Fluor 700	X	
CD45	30-F11	BD	v500	X	
CD49b	DX5	BioLegend	Pacific Blue	X	
f4/80	BM8	Thermo	eFluor450	X	
f4/80	BM8	BioLegend	BV605	X	
f4/80	BM8	BioLegend	BV650	X	
GR-1	RB6-8C5	BioLegend	PE-Cy7	X	
I-Ab	AF6-210.1	Thermo	eFluor450	X	
I-Ab	25-9-17	BioLegend	Alexa Fluor 488	X	
IFNγ	XMG1.2	BioLegend	Alexa Fluor 488		Intracellular
iNOS	CXNFT	Thermo	PE		Intracellular
Ki67	SolA15	Thermo	eFluor450		Intranuclear
Ki67	SolA15	Thermo	FiTC		Intranuclear
Ly6C	AL-21	BD	Alexa Fluor 700	X	
Ly6G	1A8	BioLegend	PE-Cy7	X	
NK1.1	PK136	BioLegend	BV650	X	
NK1.1	PK136	Thermo	eFluor450	X	
NKp46	29A1.4	BioLegend	BV605	X	
viability	n/a	Thermo		X	

Table 17: Myeloid Function Panel Antibodies

7.2 Additional Molecular Biology Figures

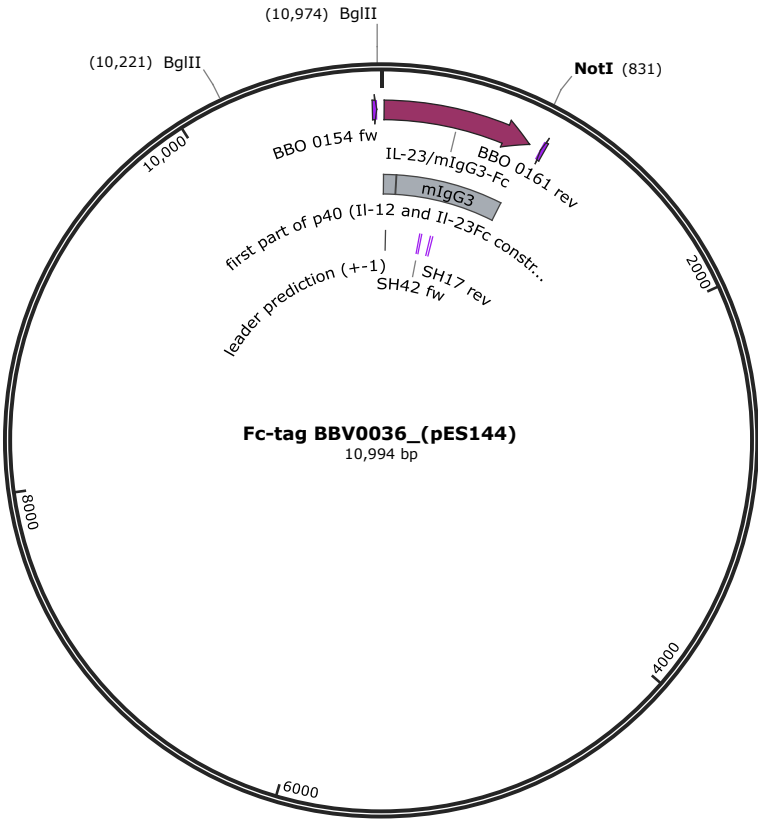

Figure 61: FcTag Vector Map

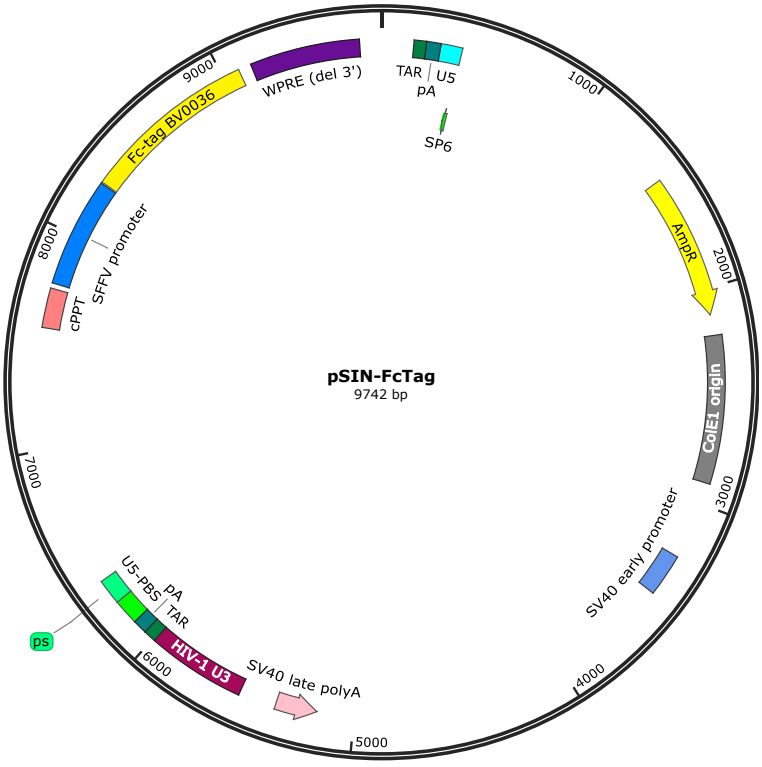

Figure 62: pSIN-FcTag (FcTag LV) Vector Map

p40_FW_SalI SalI

5' GTCGACgccaccatgtgtcctcagaagctaaccatctc 3'

Fc_RV_MluI MluI

5' ACGCGTtcatttaccaggggagcgagacagg 3'

p40_FW_BglII BglII

5' GTCGCCCGGGGGagatctGCCACCATGTGTCCTCAGAAGCTAACCATCTC 3'

Fc_RV_NotI NotI

5' GACTCTAGAGTCgcggccgcTCATTTACCAGGGGAGCGAGACAGG 3'

Figure 63: Primers used for PCR

7.3 Additional Flow Cytometry Figures

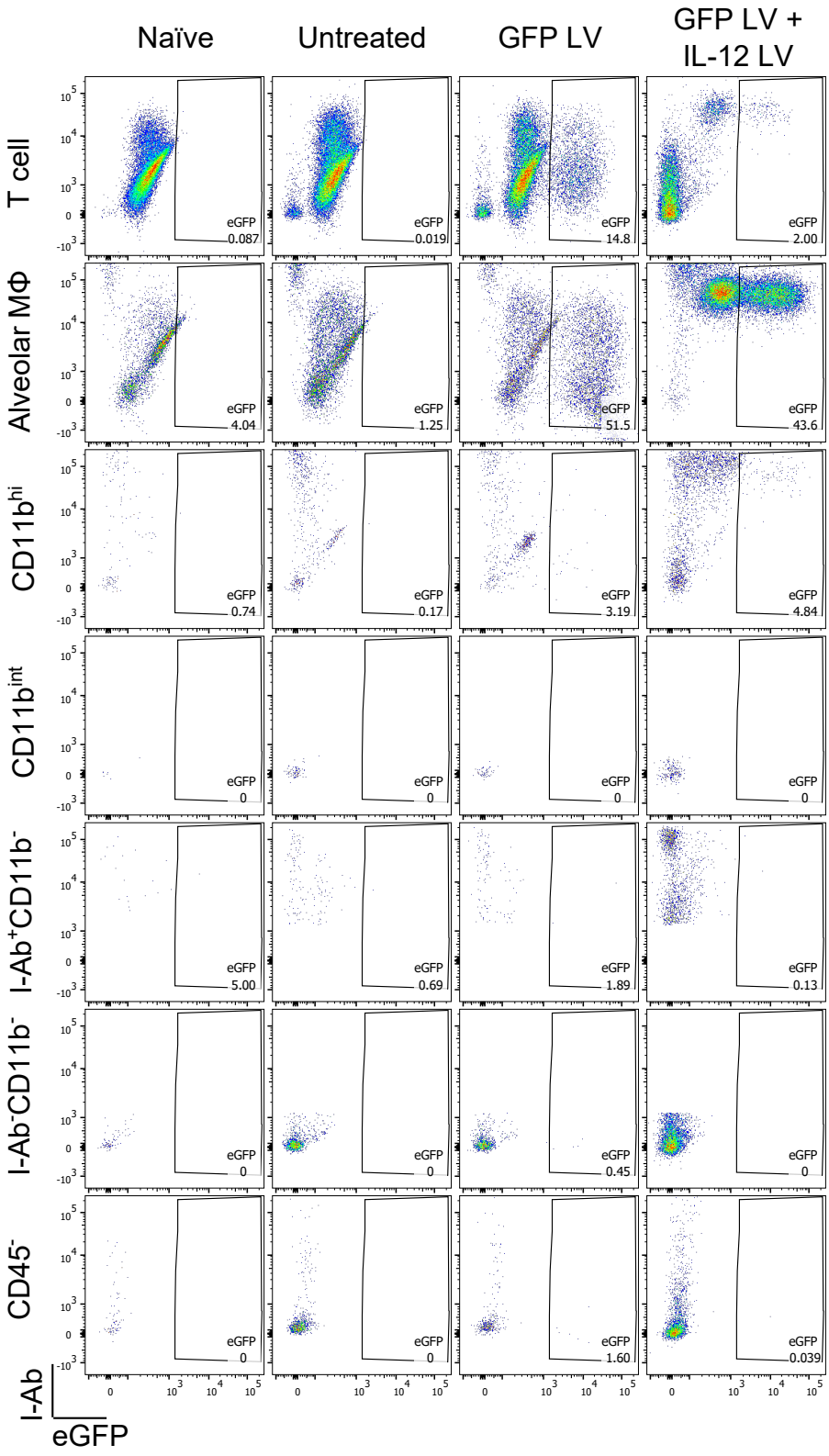

Figure 64: *In Vivo* transduction of leukocytes isolated from BAL

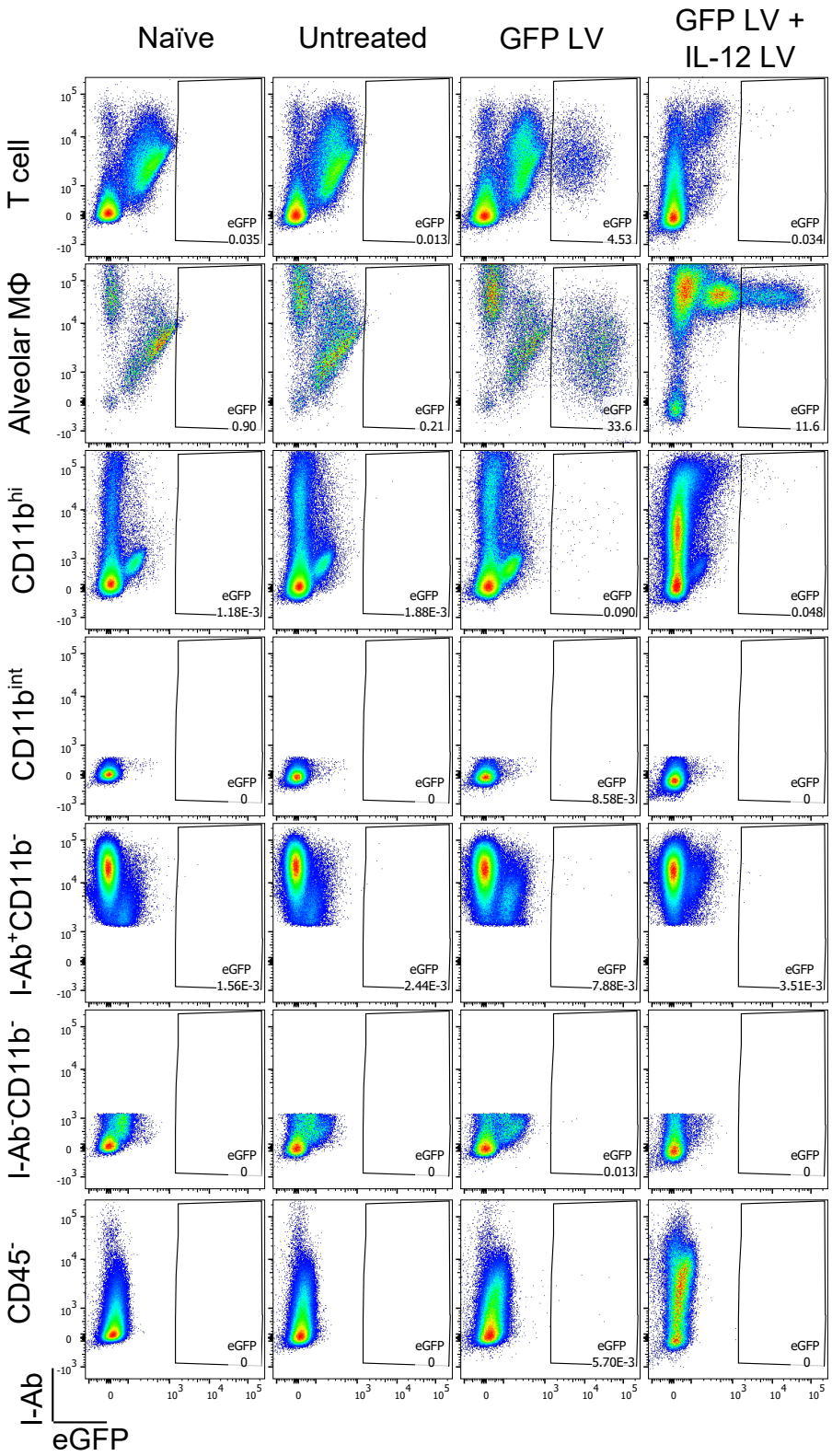

Figure 65: *In Vivo* transduction of leukocytes isolated from Lung

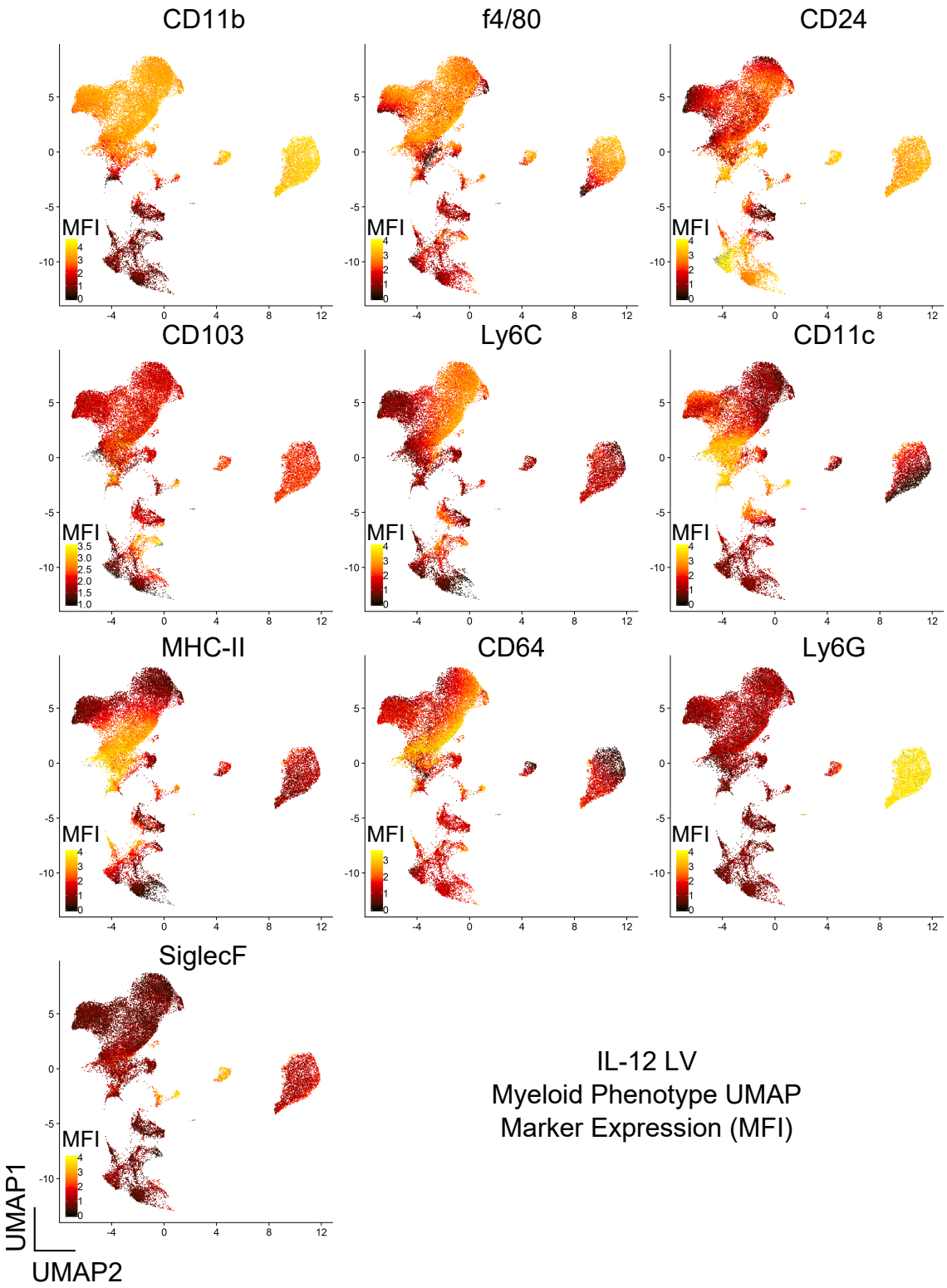

Figure 66: Myeloid population UMAP : Marker expression (MFI)